ISSN 2409-9074

Міністерство освіти і науки України
Національний університет
«Полтавська політехніка імені Юрія Кондратюка»

Ministry of Education and Science of Ukraine
National University
«Yuri Kondratyuk Poltava Polytechnic»

ЗБІРНИК НАУКОВИХ ПРАЦЬ

ГАЛУЗЕВЕ МАШИНОБУДУВАННЯ, БУДІВНИЦТВО

Випуск 2 (61)’ 2023

ACADEMIC JOURNAL

INDUSTRIAL MACHINE BUILDING, CIVIL ENGINEERING

Issue 2 (61)’ 2023

Міністерство освіти і науки України

Національний університет
«Полтавська політехніка імені Юрія Кондратюка»

Ministry of Education and Science of Ukraine

National University «Yuri Kondratyuk Poltava Polytechnic»

ЗБІРНИК НАУКОВИХ ПРАЦЬ

ГАЛУЗЕВЕ МАШИНОБУДУВАННЯ,
БУДІВНИЦТВО

Випуск 2 (61)′ 2023

ACADEMIC JOURNAL

INDUSTRIAL MACHINE BUILDING,
CIVIL ENGINEERING

Issue 2 (61)′ 2023

Полтава – 2023

Poltava – 2023











www.znp.nupp.edu.ua
http://journals.nupp.edu.ua/znp

**Збірник наукових праць. Галузеве машинобудування, будівництво /
Національний університет «Полтавська політехніка імені Юрія Кондратюка»**

Збірник наукових праць видається з 1999 р., періодичність – двічі на рік.

Засновник і видавець – Національний університет «Полтавська політехніка імені Юрія Кондратюка».

Свідоцтво про державну реєстрацію КВ 24621-14561ПР від 14.12.2020 р.

Збірник наукових праць уключений до переліку наукових фахових видань (категорія Б), у яких можуть публікуватися результати дисертаційних робіт (Наказ МОН України №1218 від 07.11.2018 року).

Збірник наукових праць рекомендовано до опублікування вченою радою Національного університету «Полтавська політехніка імені Юрія Кондратюка» протокол №13 від 12.12.2023 р.

У збірнику представлені результати наукових і науково-технічних розробок у галузі машинобудування, автомобільного транспорту та механізації будівельних робіт; із проектування, зведення, експлуатації та реконструкції будівельних конструкцій, будівель і споруд; їх основ та фундаментів; будівельної фізики та енергоефективності будівель і споруд; а також у галузях гірництва, нафтогазової інженерії та технологій, екології.

Призначений для наукових й інженерно-технічних працівників, аспірантів і магістрів.

Адреса видавця та редакції – Національний університет «Полтавська політехніка імені Юрія Кондратюка»
Науково-дослідницька частина, к. 320Ф, Першотравневий проспект, 24, м. Полтава, 36011.
Тел.: (05322) 29875; e-mail: v171@pntu.edu.ua; www.pntu.edu.ua
Макет та тиражування виконано у поліграфічному центрі Національного університету «Полтавська політехніка імені Юрія Кондратюка», Першотравневий проспект, 24, м. Полтава, 36011.
Свідоцтво про внесення суб'єкта видавничої справи до державного реєстру видавців, виготівників і розповсюджувачів видавничої продукції (ДК № 3130 від 06.03.2008 р.).
Комп'ютерна верстка – В.В. Ільченко.
Підписано до друку 21.12.2023 р.
Папір ксерокс. Друк різограф. Формат 60x80 1/8. Ум. Друк. Арк. – 13,25.
Тираж 300 прим.

Academic journal. Industrial Machine Building, Civil Engineering / National University «Yuri Kondratyuk Poltava Polytechnic»

Academic journal was founded in 1999, the publication frequency of the journal is twice a year.
Founder and Publisher is National University «Yuri Kondratyuk Poltava Polytechnic».
State Registration Certificate КВ 24621-14561ПР dated 14.12.2020.
Academic journal is included into the list of specialized academic publications where graduated thesis results could be presented (Order of Department of Education and Science of Ukraine № 1218 dated 07.11.2018).
Academic journal was recommended for publication by the Academic Board of National University «Yuri Kondratyuk Poltava Polytechnic», transactions №13 of 12.12.2023.

The results of scientific and scientific-technical developments in the sphere of mechanical engineering, automobile transport and mechanization of construction works; designing, erection, operation and reconstruction of structural steels, buildings and structures; its bases and foundations; building physics and energy efficiency of buildings and structures are presented in the collection; as well as in the fields of mining, oil and gas engineering and technology; ecology.

Academic journal is designed for researchers and technologists, postgraduates and senior students.

Address of Publisher and Editorial Board − National University «Yuri Kondratyuk Poltava Polytechnic»,
Research Centre, room 320-F, Pershotravnevyi Avenue, 24, Poltava, 36011, Ukraine.
tel.: (05322) 29875; e-mail: v171@pntu.edu.ua; www.pntu.edu.ua
Layout and printing made in the printing center of National University «Yuri Kondratyuk Poltava Polytechnic»,
Pershotravnevyi Avenue, 24, Poltava, 36011, Ukraine.
Registration certificate of publishing subject in the State Register of Publishers Manufacturers and Distributors of publishing products (ДК № 3130 from 06.03.2008).
Desktop Publishing – V. Ilchenko.
Authorize for printing 21.12.2023.
Paper copier. Print rizograf. Format 60x80 1/8. Conventionally printed sheets – 13,25.
Circulation 300 copies.

Збірник наукових праць. Галузеве машинобудування, будівництво
Academic journal. Industrial Machine Building, Civil Engineering
http://journals.nupp.edu.ua/znp
https://doi.org/10.26906/znp.2023.61.3848

UDC 624.04 (091)

Consideration of the structures working conditions in the method of limit states

Sergii Pichugin [1*]

[1] National University «Yuri Kondratyuk Poltava Polytechnic» https://orcid.org/0000-0001-8505-2130
*Corresponding author E-mail: pichugin.sf@gmail.com

In the method of limit states, the coefficient of working conditions must take into account all the features of the work and operation of structures. In the code editions, the scale of these coefficients was regularly reviewed and supplemented. Probabilistic aspects of substantiating the coefficients of the working conditions were developed by researchers of the building structure's reliability. The interpretation of the constructive correction as an experimental analog of the coefficient of working conditions was achieved by full-scale tests of industrial buildings structures. The analysis of the reliability of compressed-bent elements and statically uncertain systems determined the additional coefficients of the working conditions. The article contains a systematic analytical review of normative documents and scientific publications with an analysis of the evolution of steel structure design codes in terms of changes in the coefficient of working conditions and the involvement of research, experimental and statistical data.

Keywords: design codes, reliability, limit states, coefficient of working conditions, constructive correction

Врахування умов роботи конструкцій в методиці граничних станів

Пічугін С.Ф.[1*]

[1] Національний університет «Полтавська політехніка імені Юрія Кондратюка»
*Адреса для листування E-mail: pichugin.sf@gmail.com

У загальній методиці розрахунку конструкцій за граничними станами коефіцієнт умов роботи повинен враховувати всі особливості роботи й експлуатації конструкцій, що не враховані в явному вигляді іншими коефіцієнтами методики. Можна вважати, що цей коефіцієнт покриває всі неточності розрахункової моделі, що виникають внаслідок її спрощення і ідеалізації, для того, щоб розрахунок можна виконати з необхідною точністю та з розумними працевтратами. Відомо, що у будь-якому розрахунку вводять спрощуючі положення, зокрема, основні гіпотези опору матеріалів та будівельної механіки. Унаслідок цього в будь-якому розрахунку виникають неминучі відхилення, обумовлені неточністю розрахункової моделі, котрі мають або систематичний, або випадковий характер. Для того щоб врахувати (або компенсувати) ці похибки і забезпечити необхідну надійність конструкції, що проєктується, вводять коефіцієнт умов роботи. Очевидно, що він має статистичну природу, в окремих випадках він детально вивчений і обґрунтований. Однак у деяких випадках його значення встановлені експертним методом на основі досвіду проектування та експлуатації і потребують подальшого вивчення й уточнення. Дані стосовно розрахункових коефіцієнтів методики граничних станів, зокрема коефіцієнта умов роботи, вміщено в численних випусках нормативних документів, затверджених у різні роки. Таким чином створено значний масив інформації, котрий не проаналізовано у достатній мірі. Не систематизовано результати натурних випробувань будівель і конструкцій як основи нормування коефіцієнта умов роботи. Маловідомими залишаються наробки дослідників надійності будівельних конструкцій, які можна залучити до обґрунтування нових коефіцієнтів умов роботи різних конструкцій. Тому метою і задачами статті є систематизований аналітичний огляд нормативних документів і наукових публікацій, починаючи з 1950-х років, з аналізом еволюції норм проектування сталевих конструкцій у частині змін коефіцієнта умов роботи та залученням до цього дослідних експериментальних і статистичних даних.

Ключові слова: норми проєктування, надійність, граничні стани, коефіцієнт умов роботи, конструктивна поправка

Introduction

In the general method of calculating structures according to limit states, the coefficient of working conditions γ_c (preliminary designation m) must take into account all the features of the work and operation of structures, which are not explicitly taken into account by other coefficients of the method. Therefore, this coefficient is the most loaded by purpose and the least determined by content and value. The value $\gamma_c < 1$ takes into account

the unfavorable operating conditions of the structure, the value $\gamma_c < 1$ – favorable operating conditions.

It can be assumed that this coefficient covers all the inaccuracies of the calculation model, which arise as a result of its simplification and idealization, so that the calculation can be performed with the necessary accuracy and with reasonable labor costs. It is known that in any calculation, simplifying provisions are introduced, in particular, the main hypotheses of resistance of materials and construction mechanics. Let us name here as examples assumptions about the operation of the material (for example, the Prandtl diagram), elements (hypothesis of flat sections), structures (hinged nodes of steel trusses), constructive systems (simplified schemes of the industrial buildings frames). As a result, in any calculation there are inevitable deviations caused by the inaccuracy of the calculation model, which are either systematic or random in nature.

In order to take into account (or compensate) these errors and ensure the necessary reliability of the designed structure, the coefficient of working conditions γ_c is entered. It can be considered that it has a statistical nature, in some cases it is studied in detail and substantiated. However, in some cases, its values are established by an expert method based on design and operation experience and require further study and clarification.

Review of research sources and publications

Some aspects of the substantiation of the future coefficient of working conditions were developed even within the framework of the methodology for calculating building structures according to allowable stresses, which prevailed in design until the middle of the 20th century [1, 2]. The initial values of the working conditions coefficients were included in the first limit state design codes introduced in the 1950s. In subsequent editions of the codes, the scale of these coefficients was regularly reviewed and supplemented. With additional changes, the coefficients of working conditions were transferred to the codes of Ukraine, in particular, in DBN B.2.6-198:2014 "Steel structures. Design codes" [3]. Probabilistic aspects of substantiating the coefficients of the working conditions of structures of various purposes were developed by researchers of the building structures reliability [4, 5] and representatives of the scientific school "Reliability of Building Structures" of the National University "Yury Kondratyuk Poltava Polytechnic" [6, 7]. A significant contribution to the interpretation of the structural correction as an experimental analog of the coefficient of working conditions was achieved by full-scale tests of steel structures of industrial buildings [8]. The analysis of the reliability of compressed-bent elements determined the additional coefficient of the working conditions of stepped steel columns of shops equipped with overhead cranes [9, 10]. The result of the successful application of the probabilistic method of limit equilibrium to the reliability assessment of statically uncertain systems was the development of a scale of their working conditions coefficients [11-13]. The substantiation of the calculated coefficients of the limit state method, in particular the coefficient of working conditions, was in the field of view of leading foreign researchers of reliability [14-18]. The national codes of recent years outline the prospects for the development of the general methodology for calculating building structures and the scale of calculation coefficients [19-20].

Definition of unsolved aspects of the problem

Data regarding the calculation coefficients of the limit state methodology, in particular the coefficient of working conditions, are included in numerous issues of normative documents approved in different years. In this way, a significant mass of information was created, which has not been analyzed to a sufficient extent. The results of field tests of buildings and structures have not been systematized as a basis for normalizing the coefficient of working conditions. Little is known about the achievements of researchers of the building structures reliability, which can be involved in justifying new coefficients of the working conditions of various structures.

Problem statement

Carrying out a systematic analytical review of normative documents and scientific publications, starting from the 1950s, with an analysis of the evolution of steel structure design codes in terms of changes in the coefficient of working conditions and the involvement of research, experimental and statistical data.

Basic material and results

Evolution of the coefficient of working conditions in codes.

The initial values of the working conditions coefficient were included in the first design codes for limit states. In particular, in NITU 121-55 "Codes and technical conditions for the design of steel structures" a rather extensive scale of the values of this coefficient was included, we will give an explanation for some of them.

• For tank hulls and bottoms, a reduced coefficient of working conditions of $m = 0.8$ was introduced, which takes into account the increased risk of tank collapse and the complex stress state of the sheet structure of the tank, in particular, the connection of the hull with the bottom, where the edge effect is created.

• The coefficient of working conditions, less than the unit $m = 0.9$, is regulated for columns, trusses and beams of public buildings, that is, in relation to structures under the action of a mainly constant load (with a small reliability coefficient for the load). This is justified by the fact that these responsible structures can collapse from any minor accidental overload. It should also be noted that the listed structures work on a low-variable load, and their limit state can occur when the value of the resistance of the material of the structure is the smallest. For comparison, if the structure works on a load with significant variability, the limit state occurs when the smallest values of material resistance are combined with the largest values of loads, which happens much less often and is less dangerous.

• The coefficient $m = 0.9$ is attributed to compressed elements of roof trusses, the possible destruction of which occurs suddenly and is particularly dangerous.
• It is taken into account that rods made of single corners transmit forces with an eccentricity, which reduces their load-bearing capacity, in the places where they join one of the shelves, which is taken into account by the coefficient of working conditions $m = 0.75$.
• The reduced operating conditions coefficients of riveted and bolted connections $m = 0.6 – 0.8$ take into account their specifics of operation and are associated with transition coefficients for the allowable resistances of the same connections [1].
• Significantly reduced coefficient of working conditions of anchor bolts $m = 0.65$ takes into account their increased responsibility, since they ensure the stability of the building as a whole, being at the same time in a hidden concreted state; in addition, they have a thread and can be loaded unevenly. This approach became the method of limit states from calculations based on allowable stresses [1].
In the following codes of SNiP II-V.3-72 "Steel structures. Design codes" from the table of coefficients of working conditions, the items regarding structures of tanks, roof trusses and purlins loaded with snow load, and connections of structures were removed from the table, and the following additional coefficients of working conditions were introduced.
• Reduced coefficient $m = 0.8$ in relation to the compressed elements of the truss lattice. This was due to the fact that the compressed rods, which were usually located in the middle parts of the trusses, were picked up with little effort, had small sections and were too flexible; they were easily damaged during transportation, installation and operation, could prematurely lose stability and lead to truss accidents (such cases really happened in the 1960s-1970s of the last century). The introduction of this coefficient removed the specified problem.
• The coefficients $m = 0.75...0.9$ regulated the specific features of the rods work of the of spatial lattice structures from single corners.
• The reduced coefficient of working conditions $m = 0.9$ was intended to increase the reliability of steel crane beams, which suffered frequent damage in difficult operating conditions.
In the codes of SNiP II-23-81 "Steel structures. Design codes"), the table of coefficients of working conditions, from which the reduced coefficient for crane beams was removed, was significantly supplemented with new items.
• Reducing coefficient $\gamma_c = 0.95$ for checks of the overall stability of solid beams, which takes into account the nature of this type of destruction, which occurs suddenly and dangerously.
• Reduced coefficient $\gamma_c = 0.9$, which takes into account the presence of threads in stretched elements in the calculation of the main section.
• Coefficients for the rod structures elements: reduced $\gamma_c = 0.95$ for compressed elements during stability testing and stretched elements in welded structures; at the same time, for the same structures with bolted connections, an increased factor $\gamma_c = 1.05$ is regulated in strength calculations.
• Increased coefficients $\gamma_c = 1.05 – 1.1$ for structures connected by bolts, which takes into account the more favorable nature of work and possible destruction of such structures compared to welded structures.
In addition to the given coefficients γ_c, which can be considered "basic", the codes of SNiP II-23-81 contained the scales of the working conditions coefficients of connections $\gamma_b = 0.75 – 1.0$; elements of power transmission line supports $\gamma_c = 0.75 – 0.95$; structures of communication antenna structures $\gamma_c = 0.55 – 1.10$ and separately – determination of coefficients of working conditions for a stretched single corner, which is fastened to one shelf with bolts.
With additional changes, the scale of coefficients of working conditions was transferred to the codes of Ukraine DBN V.2.6-198:2014 "Steel structures. Design codes" [3]. From the previous version of the codes, a reduced coefficient for calculating solid beams for overall stability and an increased coefficient for checking the strength of solid beams and columns with bolted connections under static load were removed.
At the same time, new items of the table of coefficients of working conditions were entered into the DBN.
• Coefficient $\gamma_c = 1.05$ for the columns of industrial structures with bridge cranes, which partially takes into account the increased level of reliability of the columns compared to other structures due to the combined action of several random loads on them (information on this issue is given below and in more detail in the monograph [4]).
• A group of increased coefficients of working conditions $\gamma_c = 1.10 – 1.20$ in relation to support plates of different thicknesses under the action of static load, taking into account, obviously, the relatively favorable working conditions under the load of these structural elements.
As in the previous version of the code for the design of steel structures, DBN B.2.6-198:2014, in addition to the general coefficients of working conditions, regulates the corresponding coefficients for specific types of steel structures:
• for bolted connections – in the form of an expanded table;
• for structures of supports of overhead power lines, structures of open devices and contact lines of electrical transport networks - $\gamma_c = 0.75 – 0.95$;
• for structures of communication antenna structures up to 500 m high –$\gamma_c = 0.55 – 1.10$;
• for structures of river hydrotechnical structures - $\gamma_c = 0.55 – 1.10$ in the main combinations of loads; $\gamma_c = 0.70 – 1.50$ in special combinations of loads.

Constructive correction as an experimental assessment of the coefficient of working conditions.

The constructive correction k is the ratio of the actual stress or deflection from the selected load to the conditional calculated stress (or deflection) from the same load:

$$k_\sigma = \frac{\sigma_{експер}}{\sigma_{теор}}; \quad k_f = \frac{f_{експер}}{f_{теор}}. \tag{1}$$

The size of the constructive correction is a characteristic of the approximation of the accepted calculation assumptions to the actual operating conditions of the structure, it shows how close the conditional calculation scheme is to its actual scheme. This interpretation of the constructive correction practically coincides with the above definition of the content of the coefficient of working conditions, so it can be considered that the constructive correction is an experimental assessment of the coefficient of working conditions. Considering the limit inequality of the limit states of the first group, the operating conditions coefficient is the inverse of the constructive correction, i.e.

$$\gamma_c = 1/k_\sigma; \quad k_\sigma = 1/\gamma_c. \tag{2}$$

Therefore, constructive corrections, smaller units, correspond to the values of the operating conditions coefficient, larger units, which indicates favorable features of work and possible reserves of the structure's bearing capacity. On the contrary, constructive corrections, larger units, indicate an underestimation by the selected calculation models of real stresses, which requires the introduction of coefficients of working conditions, smaller units and corresponding strengthening of the structure.

The experience of field tests of real structures, in particular steel structures, convincingly shows that the constructive corrections in most cases are not equal to unity. DSc. G.A. Shapiro, who conducted large-scale studies of the actual operation of steel structures in industrial workshops in 1936...1951 [8], developed the approximate structure of constructive correction of steel structures as follows:

$$k = \alpha_1\alpha_2\alpha_3\alpha_4\alpha_5\alpha_6\alpha_7\alpha_8, \tag{3}$$

where α_1 is a general correction to the calculation scheme;

α_2 – correction to the geometric scheme;

α_3 – correction to structural elements;

α_4 – correction for cross-sections of working elements;

α_5 – correction for spatial work;

α_6 – correction for draft and rotation of supports;

α_7 – load correction: its magnitude, relative position and change;

α_8 – correction for stiffness of nodes.

As we can see, this still incomplete list of components clearly shows the rather complex structure and content of the constructive correction and, accordingly, the coefficient of working conditions.

In the years preceding the Second World War, TsNIPS and Gynstalmost performed tests of 300 light roof trusses [8], which made it possible to construct an experimental distribution curve of the constructive correction by stresses with numerical characteristics: average value $\bar{k} = 0,90$, standard $\hat{k} = 0,11$. The experimental curve was approximated by normal distribution.

In order to understand the nature of the constructive correction of steel roof trusses, let us remind you that for determining the forces, the trusses are represented by an idealized system with rectilinear rods converging at one point (the center of the nodes) and connected by hinges. It is usually believed that the rods are made of perfectly elastic material, and the circuit itself does not deform. Therefore, the constructive corrections for the deflections are less than one unit (Table 1) due to the influence of the nodes stiffness and the indistinctness of the belts. These features have less effect on the values of axial forces in the rods: the design correction for stresses is equal to $k = 0.96$ for light-type welded trusses (Table 1). This tendency appears to a lesser extent for heavy trusses with H-shaped bar sections, as well as for riveted trusses.

Table 1 – Constructive corrections of steel trusses of various types

Truss tape	Constructive corrections	
	by deflections	by stresses in the middle of the truss belts
Welded light type	0,89	0,96
Welded heavier type	0,79	0,79
Riveted light type	0,76	0,68
Riveted heavier type	0,59	0,55

It is obvious that the calculation model of the trusses must correspond to their general static scheme (split, non-split, freely supported, clamped). This provision is clearly illustrated by the data in the Table 2.

Table 2 – Constructive corrections of steel multi-span uncut truss (with different calculation methods)

Calculation scheme	Constructive corrections	
	by stresses in the middle of the truss in the lower and upper belts	by deflections in the middle of truss
Inseparable system	0,96	0,89
Split system	0,71	0,75
Truss freely supported on two supports	0,88	0,86

During the above-mentioned studies, G.A. Shapiro [8] investigated the actual operation of some steel crane beams, the resulting constructive corrections are listed in the Table 3. Rather unusual values of corrections exceeding unity are the result of rather complex work of crane beams. This was explained by the presence of a biaxial stress state in the wall of the beams, the early appearance of plasticity, and the influence of the curvature of the beam wall. In fact, there are many other factors affecting the operation of crane beams, which at the time of the tests (1936...1951) were insufficiently investigated. So, this is an example of how the values of the constructive correction reflected the level of structural research.

Table 3 – Constructive corrections of crane beams by stresses

	Crane beams			
	1	2	3	4
Constructive corrections	1,29	1,26…1,33	0,955…1,070	1,18…1,47

During the period of transition from the method of allowable stresses to the method of limit states (50s...60s of the 20th century), full-scale experimental studies of structures were intensified to clarify their actual operation and identify constructive corrections. Tests of steel structures of several metallurgical plants gave the following values of constructive corrections:

• crane trusses (by deflections) $k = 0.67...1.00$;
• crane beams (by deflections) $k = 0.53...1.07$;
• crane beams (according to stresses) $k = 0.51...0.87$.

At the same time, the great difficulties of field research in operating workshops, especially metallurgical ones with their exceptionally intensive mode of operation and highly aggressive internal environment (high temperatures, gassing, dynamic crane effects, etc.) are obvious. It should be noted that the majority of the received constructive corrections turned out to be less than one, that is, they had the opposite character to the data of G.A. Shapiro. It is possible that this indicated the available reserves in the studied beams and the possibility of some increase in the coefficient of working conditions. According to data obtained experimentally in the 1960s, the constructive correction for deflections of welded crane beams is in the range of 0.85...1.00.

The most complete data on constructive corrections of transverse frames was obtained by G.A. Shapiro during large-scale field tests of production buildings (OVB) in the 30s...50s of the last century [8]. Some of the obtained results are shown in the Table 4. Workshop No. 1 – Marteniv shop, built at the beginning of the 20th century, with a hinged connection of crossbars with columns and riveted steel structures. Workshop No. 4 is also Marteniv shop, designed in the 1940s, with rigid transverse frames and lattice crossbars. As can be seen from the Table. 4, constructive corrections for transverse displacements were found to be very small compared to the calculation of a flat free-standing frame, which clearly indicates the significant approximation of this calculation model. After taking into account the spatial calculation model, the constructive correction was significantly increased, although it still does not reach unity, which indicates the incomplete perfection of the spatial model of the OVB of the 1940s..1950s.

Table 4 – Constructive corrections of OVB frames according to transverse displacements

No workshop	Marking the place of displacement measurement, m	Transverse braking of a bridge crane		Horizontal force on the marks of the trusses bottom or the head of the rail	
		Flat frame	Spatial system	Flat frame	Spatial system
№1	25,7	0,12	0,60	0,21	0,80
	18,5	0,16	0,80	0,15	0,58
№4	15,2	0,09	1,00	0,08	0,51
	12,4	0,06	0,90	0,10	0,57

As field tests of OVB steel columns have shown, theoretical and experimental values of normal forces differ slightly, constructive corrections are close to unity (Table 5). Constructive corrections of columns in terms of moments are much smaller due to their more complex nature (uncertainty of lateral forces of cranes, eccentricity of crane beams support, complex construction of trusses and work platforms, etc.).

Table 5 – Constructive corrections of steel columns

Column type		Constructive corrections	
		by normal forces	by bending moments
Heavy (with branches from folded I-beams)	Extreme row	0,91…1,01	0,66…0,74
	Average row	0,76…1,00	0,44…0,67
Light (with branches from rolled corners)		0,87…1,03	0,64…0,74

Probabilistic estimates of the coefficient of working conditions of steel structures. The substantiation of the coefficients of working conditions, in addition to the assessment of constructive corrections, can also be based on probabilistic studies and assessments of the structures reliability.

Let's consider the justification of the coefficient of the working conditions of steel stepped columns. The peculiarity of column structures is, in particular, that several random loads of different probabilistic nature (permanent, atmospheric, crane) act on them. Therefore, the assessment of the reliability of such structures is quite difficult, it was obtained in studies conducted at the department of KMDiP PoltNTU over several years [9, 10]. These studies made it possible, in particular, to estimate the reserves of the bearing capacity of OVB steel columns, which did not take into account the current codes, and to propose a new coefficient of working conditions.

To obtain specific results, a number of characteristic stepped columns of industrial buildings, designed according to codes [3], were tested, part of the obtained results is illustrated in *Table 6*, in which the following designations are adopted: L – span of the transverse frame of the industrial building; B – pitch of columns; l_2, l_1 – lengths of the upper and lower parts of the column, respectively; $Q_2(t)$, $Q_1(t)$ are the failure probabilities, respectively, of the upper and lower parts of the column for the service life of t = 50 years, which were determined approximately by the number of emissions $N_+(t) \leq 1$.

As can be seen from Table 6, columns were considered in a wide range of parameters: with rigid and hinged connections of columns with crossbars, for frames with spans of 24...36 *m* and pitchs of 6 and 12 *m*, with warm and cold roofs with profiled flooring and reinforced concrete panels, with overhead cranes with a load capacity of 30/5...125/20 *t* of modes 4K-6K and 7K, with snow and wind loads of I, II and III districts; all columns are selected according to the calculation without reserve.

Information of the Table 6 show that the upper parts of stepped columns have the same failure probabilities as columns of constant section and rafter beams with a heavy roof, so we can speak for approximately equal security of this group of steel structures. At the same time, systematically, both with a rigid and with a hinged connection of the crossbars with the columns, the reliability of the lower parts turned out to be significantly greater than the upper ones. This is a consequence of applying to the lower part a greater number of random loads, in particular, a vertical crane load.

This provision made it possible to estimate the reliability reserves of the lower parts of the columns and from the condition $Q_1(t) \approx Q_2(t)$ to find the reduced cross-sectional area and the coefficient of the working condition, which was equal to γ_c = 1,15…1,53 for the tested versions of the columns. This coefficient, determined on the basis of the criterion of equal reliability of parts, can be recommended to be introduced into the calculation formulas for the columns of OVB equipped with bridge cranes. The obtained data made it possible to assign, in the first approximation, the coefficient of working conditions γ_C = 1.15 for the lower parts of steel stepped columns with a margin of the lower calculated values and to recommend it in the codes of design and reinforcement of steel structures. When developing DBN V.2.6-198:2014 "Steel structures. Design codes" [3] this recommendation is carefully considered in the form γ_C = 1.05 for OVB columns equipped with bridge cranes.

Let's proceed to the justification of the coefficient of the working conditions of statically indeterminate frames. In the theory of building structures reliability, the calculation of statically indeterminate systems (beams and frames, multi-story and multi-span buildings) is considered one of the most difficult problems. The reason for this is the complex nature of the destruction of statically indeterminate systems (SIS), which differs from the nature of the destruction of a statically determined system. After the failure of one or even several elements of the SIS, it can maintain an operational state. Therefore, the destruction of a statically indeterminate system can occur, as individual elements fail, by transitioning through different operational states corresponding to different schemes and probability parameters of the system. As a result, the assessment of SIS reliability is a rather cumbersome task, the degree of complexity of which increases rapidly in accordance with the complexity of the system. The researches conducted at the department of KMDiP PoltNTU [11 – 13] managed to overcome the indicated difficulties and to develop methods for assessing the reliability of SIS, suitable for practical use, and to propose a new scale of coefficients of working conditions for such systems.

Table 6 – Reliability assessment of stepped columns of industrial buildings

Variant	Connection of the crossbars with the columns	Geometric parameters		Loads					Failure probabilities		Coefficient of working conditions
		$\frac{L}{B}$	$\frac{l_2}{l_1}$	Roof	Cranes		Districts		Upper part	Lower part	
					Q, t	Mode	Snow	Wind	Q_2(t)	Q_1(t)	γ_c
1	rigid	$\frac{24}{12}$	$\frac{3,97}{16,4}$	warm concrete panels	15/3	7K	III	I	0,48	$0,96\times10^{-2}$	1,15
2	rigid	$\frac{36}{12}$	$\frac{6,6}{12,4}$	warm concrete panels	125/20	4K-6K	III	II	0,023	$4,15\times10^{-4}$	1,15
3	hinged	$\frac{30}{12}$	$\frac{6,1}{11,0}$	warm profiled flooring	100/20	4K-6K	III	II	$9,83\times10^{-4}$	$2,24\times10^{-7}$	1,32
4	rigid	$\frac{30}{12}$	$\frac{6,4}{14,2}$	warm concrete panels	100/20	4K-6K	III	II	0,054	$6,5\times10^{-5}$	1,25
5	hinged	$\frac{36}{12}$	$\frac{6,02}{14,4}$	warm concrete panels	80/20	7K	III	II	0,213	$1,71\times10^{-6}$	1,18
6	hinged	$\frac{24}{12}$	$\frac{5,23}{17,0}$	warm concrete panels	50/10	4K-6K	I	III	0,54	$5,0\times10^{-8}$	1,19
7	hinged	$\frac{24}{6}$	$\frac{3,25}{9,75}$	cold concrete panels	30/5	7K	II	I	0,71	$2,78\times10^{-12}$	1,32

The researches conducted at the department of KMDiP PoltNTU [11 – 13] managed to overcome the indicated difficulties and to develop methods for assessing the reliability of SIS, suitable for practical use, and to propose a new scale of coefficients of working conditions for such systems.

A comparative analysis of SIS reliability calculation methods was carried out: state method, logical-probabilistic method, limit equilibrium method. On this basis, the probabilistic limit equilibrium method (PLEM) was developed. A full assessment of the probability of failure of the SIS with random strength and load was obtained as a result of the development of the PLEM variant, which is based on the kinematic method of limit equilibrium. A variant of this method was used, called the "method of combined mechanisms", which consists of the main mechanisms of SIS destruction: beam, floor (sliding) and nodal. The method is implemented in the form of an algorithm and a computer program, during the calculation of which combined mechanisms with a different number of plasticity hinges are formed, statically unacceptable (excessive) and unlikely mechanisms are rejected. The assessment of the probability of failure of the SIS as a whole was defined as the disjunction of the correlated failure conditions of the main mechanisms, corresponding to the increased probability of destruction.

Using the developed methods and programs, a numerical experiment was performed to determine the reliability of 140 statically indeterminate frames of various purposes and configurations, with the number of floors varying from one to three, the number of spans also from one to three. It has been quantitatively confirmed that the elastic-plastic calculation of the considered SIS leads to material savings of 10...15% compared to the elastic calculation.

In addition, for the first time, the SIS reliability reserve was quantified compared to individual elements and statically determined systems. This reserve is proposed to be taken into account by the newly introduced "schematic reliability coefficient γ_S", similar to the coefficient of the working conditions of the current codes. The justification of the values of this coefficient is based on taking into account its probabilistic nature and the condition of equal reliability of the SIS, according to which the probability of the system failure as a whole is equal to the probability of failure of individual elements.

The analysis showed that as the mechanism of SIS destruction approaches the beam mechanism, the coefficient γ_S decreases, and increases to the shear mechanism; the maximum values of the coefficient γ_S are obtained for the complete destruction mechanisms, the partial mechanism leads to a decrease in the coefficient γ_S. The obtained schematic reliability coefficients are in the interval γ_S = 1.18...1.27 (Table 7), they indicate significant reserves of the SIS's carrying capacity, which do not take into account the

current codes. This coefficient of SIS working conditions is intended for use in calculations of the load-bearing capacity of of SIS elements sections, taking into account the plastic stage of operation.

Table 7 – Calculated values of the working conditions coefficient γ_S of statically indeterminate steel frames

Number of spans	Number of floors		
	1 floor	2 floors	3 floors
1 span	1,18	1,21	1,21
2 spans	1,19	1,26…1,27	–
3 spans	1,24	–	–

Conclusions

The article is devoted to issues of substantiation and normalization of the coefficient of working conditions - an important factor in the methodology of calculation of building structures according to limit states. A systematic analysis of changes in the normalization of this coefficient in the design codes of steel structures, starting from the 1950s to the present time, was carried out. Emphasis is placed on the constructive correction - the experimental basis of the coefficient of working conditions, the results of the relevant field tests of steel structures of the operating workshops are given. The perspective of probabilistic methods for substantiating the coefficients of the working conditions of stepped columns and statically indeterminate systems is shown.

References

1. Pichugin S. (2022). The allowable stress method is the basis of the modern method of calculating building structures according to limit states. *Industrial Machine Building, Civil Engineering,* 1(58), 17-32 https://doi.org/10.26906/znp.2022.58.3078.
2. Баженов В.А. Ворона Ю.В., Перельмутер А.В. (2016). *Будівельна механіка і теорія споруд. Нариси з історії.* К.: Каравела. ISBN 978-966-222-968-8
3. ДБН В.2.6-198:2014.(2010). *Сталеві конструкції. Норми проектування*. К.: Мінрегіонбуд України
4. Пічугін С.Ф. (2016). *Розрахунок надійності будівельних конструкцій*. Полтава: ТОВ «АСМІ»
5. Pichugin S.F. (2018). Reliability Estimation of Industrial Building Structures. *Magazine of Civil Engineering.* 83(7). 24-37. DOI: 10.18720/MCE.83.3
6. Пічугін С.Ф. (2015). Наукова школа «Надійність будівельних конструкцій»: досягнення і перспективи *Industrial Machine Building, Civil Engineering,* 1(43), 3-16.
7. Pichugin S. (2019). Scientific School «Reliability of Building structures»: new results and perspectives. *Industrial Machine Building, Civil Engineering,* 2(53). 5-12. https://doi.org/10.26906/znp.2019.53.1880.
8. Перельмутер А.В., Пічугін С.Ф. (2024). *Метод граничних станів. Загальні положення та застосування в нормах проєктування.* К.: «Софія-А»
9. Пічугін С.Ф., Пащенко А.М. (2000). Імовірнісний розрахунок сталевих колон методом статистичного моделювання. *Industrial Machine Building, Civil Engineering,* 6 (2), 115-118
10. Пічугін С.Ф, Харченко Ю.А. (2000). Алгоритм імовірнісного розрахунку сталевих стиснуто-зігнутих елементів на ПЕОМ. *Industrial Machine Building, Civil Engineering,* 6 (2), 90-93.
11. Pichugin S.F. (1996). Probabilistic Analysis of Redundant Steel Structures. *XLII Konferencia Naukowa KILIW PAN i KN PZITB «Krynica 1996». Krakow-Krynica.* 8, 85-92.
12. Пічугін С.Ф., Гнітько О.В. (1998). Дослідження пластичного руйнування статично невизначених сталевих рам методом граничної рівноваги. *Механіка і фізика руйнування будівельних матеріалів і конструкцій.* Львів: «Каменяр», 3, 181-186.

1. Pichugin S. (2022). The allowable stress method is the basis of the modern method of calculating building structures according to limit states. *Industrial Machine Building, Civil Engineering,* 1(58), 17-32 https://doi.org/10.26906/znp.2022.58.3078.
2. Bazhenov V.A. Vorona Y.V., Perelmuter A.V. (2016). *Construction mechanics and theory of buildings*. *Essays on history*. K.:Caravela. ISBN 978-966-222-968-8
3. DBN V.2.6-198:2014. (2010*). Steel structures. Design codes*. K.: Ministry of Regional Construction of Ukraine
4. Pichugin S.F. *Reliability calculation of building structures*. Poltava: TOV “ASMI”
5. Pichugin S.F. (2018). Reliability Estimation of Industrial Building Structures. *Magazine of Civil Engineering.* 83(7). 24-37. DOI: 10.18720/MCE.83.3
6. Pichugin S. (2019). Scientific School «Reliability of Building structures»: achievement and perspectives. *Industrial Machine Building, Civil Engineering,* 1(43). 3-16. .
7. Pichugin S. (2019). Scientific School «Reliability of Building structures»: new results and perspectives. *Industrial Machine Building, Civil Engineering,* 2(53). 5-12. https://doi.org/10.26906/znp.2019.53.1880.
8. Perelmuter A.V., Pichugin S.F. (2024). *Method of limit states. General provisions and application in design codes*. K.: "Sofia-A"
9. Pichugin S.F., Pashchenko A.M. (2000). Probabilistic calculation of steel columns by the method of statistical modeling. *Industrial Machine Building, Civil Engineering,* 6 (2), 115-118
10. Pichugin S.F, Kharchenko Yu.A. (2000). Algorithm of probabilistic calculation of steel compressed-bent elements on PC. *Industrial Machine Building, Civil Engineering,* 6 (2), 90-93.
11. Pichugin S.F. (1996). Probabilistic Analysis of Redundant Steel Structures. *XLII Konferencia Naukowa KILIW PAN i KN PZITB «Krynica 1996». Krakow-Krynica.* 8, 85-92.
12. Pichugin S.F., Gnytko O.V. (1998). Study of plastic failure of statically indeterminate steel frames by the limit equilibrium method. *Mechanics and physics of destruction of building materials and structures*. Lviv: "Kamenyar", 3, 181-186.

13. Пічугін С.Ф., Гнітько О.В. (2000). Імовірнісна оцінка резервів несучої здатності статично невизначених сталевих рам. *Механіка і фізика руйнування будівельних матеріалів і конструкцій.* Львів: «Каменяр»,.4, 167-170.
14. Lemaire M. (2009). *Structural Reliability*. London: ISTE-Wiley
15. Elishakoff I. (2012). *Safety Factors and Reliability: Friends or Foes?* Berlin: Springer Science & Buisness Media
DOI: 10.1007/978-1-4020-2131-216
16. Elishakoff I. (2017). *Probabilistic Methods in the Theory of Structures.* Singapore: World Scientific
17. Doorn N., Hansson S.O. (2018). Factors and Margins of Safety. *Handbook of Safety Principles*. New York: Wiley, 87-114
DOI: 10.1002/9781119443070
18. Raizer V., Elishakoff I. (2022). *Philosophies of Structural Safety and Reliability.* London, New York: CRC Press of Taylor & Francis Group
DOI: 10.1201/9781003265993
19. ДБН В.1.2.-14:2018. (2018). *Загальні принципи забезпечення надійності та конструктивної безпеки будівель і споруд*. К.: Мінрегіон України
20. ДБН В.1.2-6:2022. (2022). *Основні вимоги до будівель і споруд. Механічний опір та стійкість.* К.: Міністерство розвитку громад та територій України

13. Pichugin S.F., Hnytko O.V. (2000). Probabilistic assessment of reserves of bearing capacity of statically indeterminate steel frames. *Mechanics and physics of destruction of building materials and structures*. Lviv: "Kamenyar", 4, 167-170
14. Lemaire M. (2009). *Structural Reliability*. London: ISTE-Wiley
15. Elishakoff I. (2012). *Safety Factors and Reliability: Friends or Foes?* Berlin: Springer Science & Buisness Media

16. Elishakoff I. (2017). *Probabilistic Methods in the Theory of Structures.* Singapore: World Scientific
17. Doorn N., Hansson S.O. (2018). Factors and Margins of Safety. *Handbook of Safety Principles*. New York: Wiley, 87-114

18. Raizer V., Elishakoff I. (2022). *Philosophies of Structural Safety and Reliability.* London, New York: CRC Press of Taylor & Francis Group

19. DBN V.1.2.-14:2018. (2018*). General principles of ensuring the reliability and structural safety of buildings and structures*. K.: Ministry of the Region of Ukraine
20. DBN V.1.2-6:2022. (2022). *Basic requirements for buildings and structures. Mechanical resistance and stability.* K.: Ministry of Development of Communities and Territories of Ukraine

Збірник наукових праць. Галузеве машинобудування, будівництво
Academic journal. Industrial Machine Building, Civil Engineering

http://journals.nupp.edu.ua/znp
https://doi.org/10.26906/znp.2023.61.3777

UDC 533.068.2:622.1011.4

Approbation of the express penetration method for assessing the strength of sedimentary cohesive rocks

Yuriy Vynnykov [1*], Andrii Bondar [2], Anna Liashenko [3], Valeriy Novokhatniy [4], Maryna Rybalko [5]

[1] National University «Yuri Kondratyuk Poltava polytechnic» https://orcid.org/0000-0003-2164-9936
[2] National University «Yuri Kondratyuk Poltava polytechnic» https://orcid.org/0000-0002-1624-6975
[3] National University «Yuri Kondratyuk Poltava polytechnic» https://orcid.org/0000-0001-6560-9931
[4] National University «Yuri Kondratyuk Poltava polytechnic» https://orcid.org/0000-0001-8107-7912
[5] National University «Yuri Kondratyuk Poltava polytechnic» https://orcid.org/0009-0002-9813-5175
*Corresponding author E-mail: vynnykov@ukr.net

The advantages of express methods of penetration and probing for evaluating the mechanical parameters of cohesive sedimentary rocks over traditional methods of testing them in single-plane displacement devices, odometers, and stabilometers are analyzed, such as: complete independence from the applied force and cone immersion depth; simplicity and reliability of the equipment; high reliability of results, etc. The methodology and results of 185 sets of penetration-shear tests of various clay rocks, from sandy loams to clays, are presented. Their results were used to determine the strength indicators of cohesive rocks (angle of internal friction and specific adhesion). Through statistical processing of experimental data, it was confirmed that for the water-saturated state of clay rocks there is an almost functional relationship between the penetration index and the porosity coefficient.

Keywords: well, sedimentary cohesive rock, strength, express method of penetration, specific penetration resistance, uniplanar displacement, internal friction angle, specific adhesion, the equation of interrelation.

Апробація експрес-методу пенетрації для оцінювання міцності осадових зв'язних гірських порід

Винников Ю.Л.[1*], Бондар А.В. [2], Ляшенко А.В. [3], Новохатній В.Г. [4], Рибалко М.О. [5]

[1,2,3,4,5] Національний університет «Полтавська політехніка імені Юрія Кондратюка»,
*Адреса для листування E-mail: vynnykov@ukr.net

Проаналізовано переваги експрес-методів пенетрації та зондування для оцінювання механічних параметрів зв'язних осадових порід перед традиційними способами їх випробувань у приладах одноплощинного зрушення, одометрах і стабілометрах, як-то: повну незалежність від прикладеного зусилля та глибини занурення конуса; простоту й надійність обладнання; високу достовірність результатів і т. ін. Виділено галузі їх раціонального використання, у т. ч.: лабораторні та польові методи визначення параметрів міцності й стисливості різновидів осадових, а особливо зв'язних, гірських порід; обґрунтування рівнянь взаємозв'язку між фізичними і механічними властивостями різновидів порід, які мають постійні індикаційні характеристики за узагальненням дослідних даних та ін. Відзначено, що результати пенетраційних випробувань відповідно до рішень вісесиметричної задачі теорії граничної рівноваги оцінюють за питомим опором пенетрації. Подано методику і підсумки 185 комплексів пенетраційно-зрушувальних випробувань різних глинистих порід, від супісків до глин. Їх результати використано для визначення показників міцності зв'язних порід (кута внутрішнього тертя й питомого зчеплення). Шляхом статистичної обробки дослідних даних підтверджено, що для водонасиченого стану глинистих порід існує майже функціональний зв'язок між показником пенетрації і коефіцієнтом пористості. Встановлено, що питомі опори зрушенню глинистих порід за умови однакового фізичного стану лінійно взаємопов'язані з відповідними середніми величинами питомого опору пенетрації при коефіцієнті кореляції близько 0,80. Проведення вишукувань за рекомендованою методикою суттєво зменшує обсяг нормативних випробувань на одноплощинне зрушення, а також дає можливість одержати достатньо достовірні результати з меншою трудомісткістю та тривалістю робіт.

Ключові слова: свердловина, осадова зв'язна гірська порода, міцність, експрес-метод пенетрації, питомий опір пенетрації, одноплощинне зрушення, кут внутрішнього тертя, питоме зчеплення, рівняння взаємозв'язку.

Introduction

The level of technical reliability and cost-effectiveness of innovative design and technological solutions for underground components of modern mining facilities, in particular, various types of oil and gas wells [1, 2], etc., significantly depends on the correct determination of the physical and mechanical characteristics of sedimentary rocks of natural massifs.

Typically, cylindrical samples of sedimentary rocks of natural structure, pre-selected during field surveys, are tested in the laboratory in a relatively simple compression device (odometer) to assess their deformation properties, and then to determine the strength parameters in a uniaxial shear device.

However, the most realistic stress-strain state (SSS) of the rock in the massif corresponds to the study of its cylindrical (sometimes cubic) samples in much more complex three-axis compression devices (stabilometers). The results of such tests can be used to determine both compressibility and strength characteristics [3-5].

Various types of stamp tests are used in field studies. However, these well-tested and reliable methods are quite labor-intensive, and for large volumes of the same type of tests, they are also time-consuming.

Therefore, in rock mechanics, the so-called express methods of studying the physical and mechanical properties of sedimentary rocks, such as penetration and probing, have become quite widespread.

This method of penetration is based on the slow immersion of a conical tip (indenter, cone) into the rock to a depth h, which does not exceed the height of the cone itself h_k. During penetration tests in the laboratory, the load is usually transferred in stages, while simultaneously recording the depth of the indenter. The duration of the load steps is kept constant (most often 1-2 minutes).

The generalized parameters of penetration tests were obtained on the basis of known solutions to the axisymmetric problem of the theory of limiting equilibrium. In particular, for cohesive sedimentary rocks (sandy loam, loam, clay), the ratio of the penetration force P to the square of the tip immersion depth - the specific penetration resistance R, MPa - is taken as such an indicator.

Practice has proven the main advantage of penetration tests of homogeneous sedimentary rocks, the so-called invariance condition of their results, i.e., complete independence from the applied force and the corresponding depth of the indenter immersion, and, taking into account the constants of the cones used, also independence from the angle of their opening. Thus, the results of the research do not depend on the means of recording the penetration resistance and the design of the penetrometers.

In addition, the penetration method is distinguished by: simplicity and reliability of the equipment; high reliability of test results; effective control over their probability; the ability to set up numerous experiments both in the field and in the laboratory; the ability to determine the mechanical parameters (mainly strength) of any natural and artificial materials, from gelled systems to rocks [6-8].

Thus, further development of high-speed penetration and sensing methods is relevant to reduce the labour intensity and duration of work to determine the mechanical properties, primarily strength parameters, of sedimentary rocks for the subsequent correct design of underground components of modern mining facilities.

Review of the research sources and publications

The express method of penetration in rock mechanics has been gaining some popularity gradually.

In particular, it is advisable to highlight the following most important stages of its development, in the authors' opinion.

1. Use of penetration testing to assess the condition of clayey rocks by consistency (or flowability).
2. Comprehensive substantiation of theoretical schemes of interaction of conical dies (indenters) with non-cohesive (sand) and cohesive (clay) rock.
3. Substantiation of the interaction between conical indenters and sedimentary rock from the standpoint of the theory of limit equilibrium, which was already approved at that time.
4. Introduction of research on sedimentary rocks by means of their ball tests.
5. Proposals for the use of resistivity and penetration index, as well as their use to establish the relationship between the physical and mechanical properties of cohesive (clay) rocks.
6. Further spreading of penetration tests for quantitative assessment of mechanical properties of sedimentary rocks, mainly their strength parameters and to a lesser extent - their deformability properties.

The most commonly used method for testing sedimentary rocks is with a tapered tip with a taper angle of $\alpha = 30°$.

In the modern practice of penetration testing of sedimentary rocks, it makes sense to highlight a number of popular areas. First of all, the equipment for penetration and static rock sounding, as well as the methods of processing and interpreting the results of these studies, continue to be improved [9, 10].

In recent years, the theoretical foundations of the penetration method have been improved by mathematical modelling using the solution of an axisymmetric problem by the finite element method in a physically and geometrically nonlinear formulation of the stress-strain state of a continuous medium around conical indenters (tips) when they are immersed in a certain volume of sedimentary rocks [11-14].

Mining practice has shown that various variations of the method of penetration testing of sedimentary rocks have been successfully tested for:

– classification of sedimentary rocks [15];

– quantitative assessment of changes in the state and mechanical properties of various sedimentary rocks under any type of external impact on them (compaction, moistening, drying, freezing, thawing, etc.) [16], as well as under dynamic (e.g., seismic) impact [17]. The

quantitative effect of the impact on rock properties is usually assessed as the ratio of the values of the specific resistivity R/R_0 for cohesive rocks (or the penetration indices U/U_0 for non-cohesive rocks) obtained before and after the impact;

– control of the results of mechanical tests of rocks performed by traditional methods [18];

– laboratory and field methods for determining strength parameters [19-21] and sometimes deformability (compressibility) [22] of dispersed sedimentary rocks;

– identification of a certain relationship between the physical state indicators and strength characteristics of genetically homogeneous sedimentary rocks [23];

– substantiation of generalising equations of the relationship between the physical and mechanical properties of individual rock types that have constant, so-called, indicative characteristics (e.g., ductility number, mineralogical composition, structural features, etc.) based on the results of generalising numerical experimental data [24];

– interpretation of the results of penetration tests of sedimentary rocks in certain characteristic regions, in particular, on the sea shelf [25-27];

– evaluation of anisotropic mechanical properties of sedimentary rocks, in particular, determination of the anisotropy coefficient of mechanical characteristics of the rock as a ratio of the values of the specific resistance to penetration at a certain angle to the isotropy plane to the same parameter, but at zero angle [28];

– comprehensive geophysical, geomorphological and geotechnical studies to identify risk zones in landslide massifs composed of clayey rocks (such data are useful for understanding the mechanisms of landslide triggering, its depth, shape and condition of the material in the landslide body) [29];

– to assess the degree of heterogeneity of artificial massifs of sedimentary rocks [30];

– to assess the hydraulic conductivity of marine and deltaic sediments based on piezocone testing [31].

Definition of unsolved aspects of the problem

However, despite the noted advantages of rapid penetration and sensing methods for assessing the mechanical parameters of cohesive sedimentary rocks over traditional methods of testing them in single-plane displacement devices, odometers and stabilisers, these high-speed methods have not yet been widely tested and are almost not reflected in regulatory sources.

Problem statement

Therefore, the aim of the work is to test the penetration method for rapid but reliable determination of the strength of sedimentary cohesive rocks.

The objective of the study is to establish possible quantitative relationships in sedimentary cohesive (clay) rocks in a water-saturated state between the penetration index and the porosity coefficient, as well as between the specific shear resistance and the corresponding average values of the specific penetration resistance.

The object of the study is the interaction of conical indenters (stamps) and sedimentary cohesive rocks.

The subject of the study is the strength parameters of sedimentary cohesive rocks determined using the rapid penetration method.

Basic material and results

Theoretical justification of research methodology.

First of all, it should be noted that the presence in the theoretical expression of the resistance of a cohesive (clay) rock to shear of two conditional, but generally accepted, parameters of its strength, namely the angle of internal friction φ and the specific cohesion c, somewhat complicates the practical application of the penetration method.

The methodology for calculating the angle of internal friction φ of clay rocks of disturbed and natural structures is based on the known condition of proportionality between the specific cohesion c and the specific resistance to penetration R, which is based on the basic theory of the limiting equilibrium of the medium from the immersion of a conical tip

$$c = K_\varphi \cdot R, \quad (1)$$

where K_φ – is the proportionality function, which depends on the taper angle α and the dimensionless coefficient M_φ, which in turn is a function of the internal friction angle φ, or

$$K_\varphi = 1/(D_0 \cdot \pi \cdot tg^2\alpha/2), \quad (2)$$

Theoretically, the coefficients M_φ and K_φ were calculated for a certain range of values of the rock internal friction angle $\varphi = 0 \div 20°$ and a tip with a taper angle $\alpha = 30°$, in particular for:

$\varphi = 0°,\ M_\varphi = 16,0$ *and* $K_\varphi = 0,87;$

$\varphi = 10°,\ M_\varphi = 21,5$ *and* $K_\varphi = 0,646;$

$\varphi = 20°,\ M_\varphi = 37,0$ *and* $K_\varphi = 0,376.$

At the same time, however, the genesis of the sedimentary rock itself and the peculiarities of experimental methods for determining the angle φ were not taken into account.

Subsequently, the Geotechnical School of National University "Yuri Kondratyuk Poltava Polytechnic" determined the values based on the data of combined tests of lake-glacial clay (with the plasticity number $I_p = 20,4\%$ and the moisture content at the yield point $W_L = 41,7\%$).

The experiments were conducted using a well-tested laboratory penetrometer LP-1 with a rotational shear attachment and a combined tip with a taper angle of $\alpha = 30°$, which had mutually perpendicular wings.

This made it possible to obtain the specific penetration resistance in each experiment, and, after rotational displacement, the maximum torque $M_{\max}$.

Then, using the tip constant K_τ, the specific resistance to rotational displacement τ was determined,

and identifying τ and c, the coefficient $K_\varphi = c / R$ and the value of the internal friction angle φ were determined.

The results of numerous field experiments of this clay were summarised in the graph $c = f(R)$, from which the value of K_φ as the tangent of the angle of inclination of the line drawn from the origin to the axis of the coordinates was derived. For a certain number of experiments, the average values of R, c, and K_φ were determined under conditions of similarity of rock moisture and density.

It turned out that the values of K_φ give angles φ very close to those theoretically obtained for the values of the internal friction angle of the rock $\varphi = 0 \div 20°$ and a tip with a taper angle $\alpha = 30°$.

Methodology of penetration-shear tests of clay rocks

At 60 sites in the Poltava region, 185 sets of penetration and shear tests were performed on various quaternary clay rocks, from sandy loam to light clay (with a plasticity index of I_P = 1-18 %).

Their results became the research basis for identifying the relationship between the specific resistances to shear τ and penetration R of these rocks.

The algorithm of laboratory tests, in particular, included the following blocks.

1. Cutting out samples from the cores taken from the boreholes using cutting rings 33-35 mm high and 70-71 mm in diameter, and determining the parameters of the initial physical state of the rock (moisture content, porosity coefficient *e*, etc.).

2. Preliminary compaction of the samples with their soaking.

3. Penetration tests of samples on both sides with 4-7 degrees of loading for each geological element (rock layer) and determination of the average value of its specific resistance to penetration $\overline{R}$.

By the way, the property of invariance of the resistivity of penetration with respect to a certain initial value of the cone immersion was also confirmed, which depends on a number of factors related, in particular, to the quality of preparation of the sample surface for penetration, the state of the cohesive rock under the tip, etc. The influence of these factors can be excluded if the first one or two degrees of loading on the tip are not taken into account.

Fig. 1 shows the test of a clay rock sample using the laboratory penetrometer LP-1, which was improved (by including a clock-type indicator in the process of fixing the indenter's immersion value in the rock) at Poltava Polytechnic.

4. Testing of these samples for rapid uniaxial shear according to the consolidated-drained scheme, determination of the specific shear resistance τ and the corresponding strength indicators φ_{II}, c_{II}. It should be noted that in the experiments, the actual height of the specimens allowed the shear plane to be created below the penetration mark.

5. Determination of the final values of moisture content and density of clay rock samples.

6. Determination of the coefficient $K_\varphi = c_{II} / \overline{R}$ for each geological element.

7. Comparison of the values of K_φ from penetration-shear experiments and φ_{II} from the results of consolidated-drained shear, i.e: $K_\varphi = f(\varphi)$.

Figure 1 – Testing a clay rock sample with an advanced laboratory penetrometer

The range of variability of the strength properties of clay rocks was as follows: $\overline{R}$ = 60-600 kPa; c_{II} = 8-65 kPa; φ_{II} = 9-36°; K_φ = 0,061-0,329.

The penetration and one-plane shear indices of water-saturated and pre-compacted clay samples of the same physical condition obtained from the comprehensive penetration and shear tests allowed us to make the following generalisations of the results.

Results of penetration-shear tests of clay rocks

The processing of the results of shear and penetration showed that it should be carried out in a differentiated manner, separating a group of experiments related to sandy loam and a group of experiments that included loams and clays.

It turned out that the most effective relationship between the penetration and uniaxial displacement indicators exists between the average specific resistance to penetration $\overline{R}$ and the specific resistance to displacement τ under conditions of constant vertical pressure σ=*const*.

Both parameters characterise the strength of the rock and, after statistical processing, make it possible to establish the relationship between R and τ.

Thus, it is advisable to develop one of the possible methods of using the penetration index $\bar{R}$ for practical calculations of rock strength parameters φ and c.

In Fig. 2 shows the test points and the corresponding approximated graph of the dependence of $K_\varphi = f(\varphi)$.

Fig. 3 shows the experimental points and the corresponding graph of the dependence between $\bar{R}$ and τ at a vertical pressure of σ=*const=100 kPa* for sandy loam (50 complexes were statistically processed).

Fig. 4 shows similar dependences between $\bar{R}$ and τ at a pressure of σ=*const=100 kPa* for loams and clays (more than 130 complexes were statistically processed).

In all cases, the correlation coefficients of these empirical dependencies were about 0.80, which for rocks indicates a close connection.

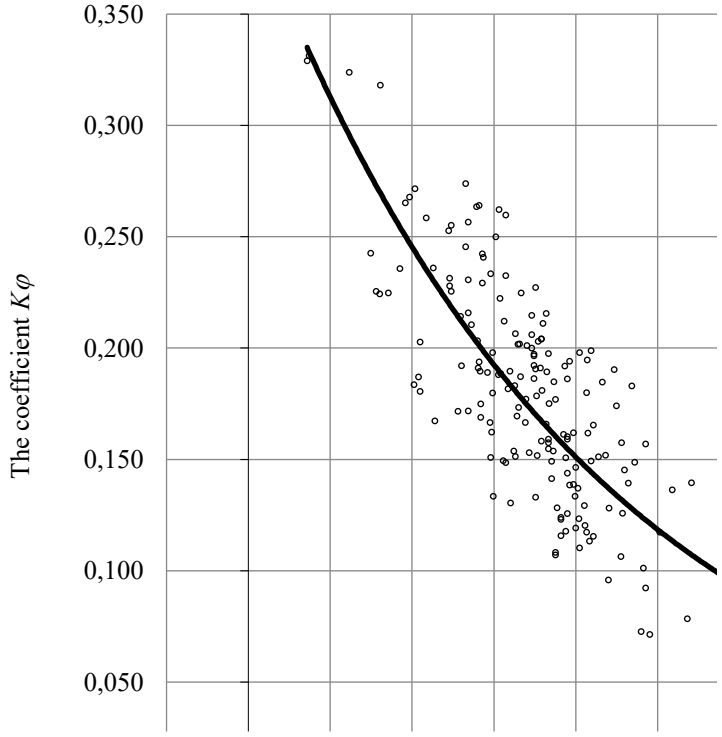

Figure 2 – Dependence of the coefficient K_φ on the angle of internal friction φ

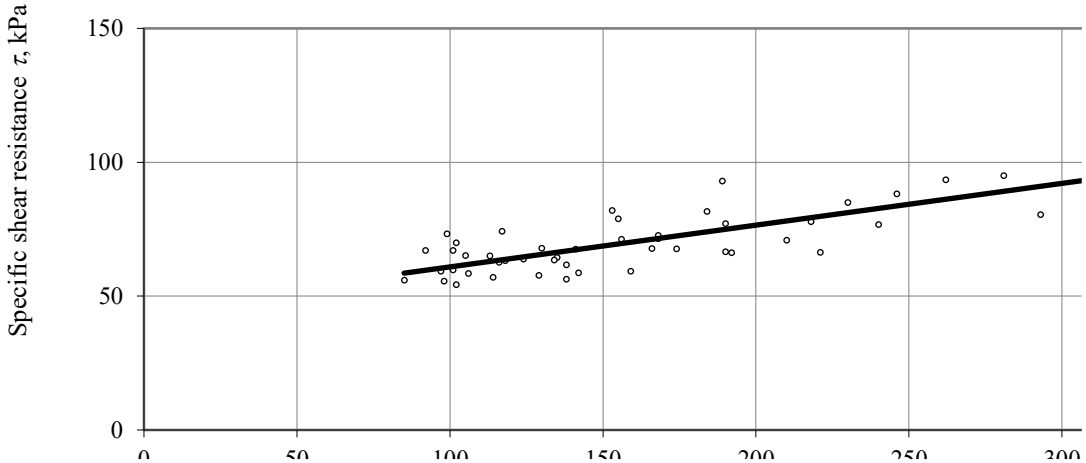

Figure 3 – Dependence between the specific resistance to penetration $\bar{R}$ and the specific shear resistance τ at a pressure of σ=*const=100 kPa* for sandy loams

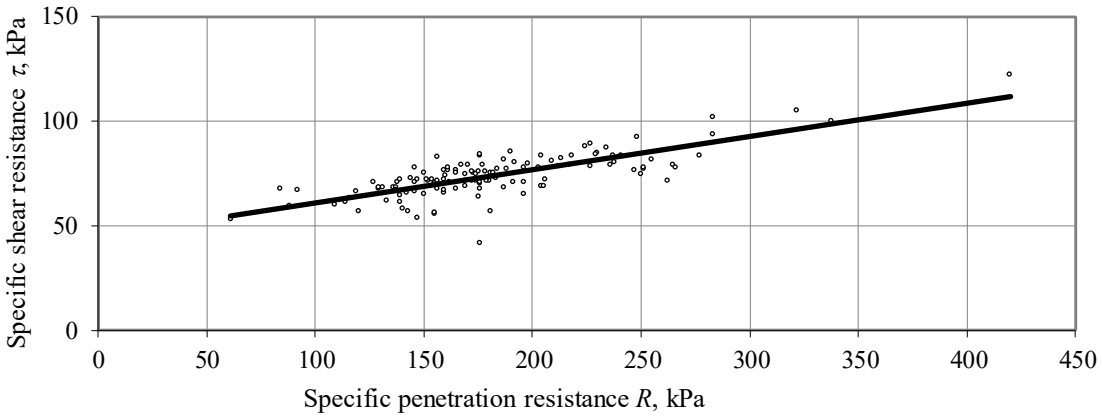

Figure 4 – Dependence between the specific resistance to penetration $\bar{R}$ and the specific shear resistance τ at a pressure of *σ=const=100 kPa* for loams and clays

The equation of the relationship between the penetration indicators and the strength of sedimentary cohesive rocks

Based on the results of determining the relationship between the specific resistances of penetration $\bar{R}$ and one-plane displacement τ under the condition *σ=const*, we have

$$\sigma = 100\ kPa,\ \tau = 0,2156 \cdot \bar{R} + 36,86; \quad (3)$$

$$\sigma = 200\ kPa,\ \tau = 0,5378 \cdot \bar{R} + 15,03. \quad (4)$$

Then

$$tg\varphi_{II} = \frac{0,5378 \cdot \bar{R} + 15,03 - (0,2156 \cdot \bar{R} + 36,86)}{200 - 100} = 0,003 \cdot \bar{R} - 0,1883$$

and the specific adhesion (from the expression $c_{II} = \tau - \sigma \cdot tg\varphi_{II}$) is

$$c_{II} = (0,5378 \cdot \bar{R} + 15,03) - 200 \cdot (0,003 \cdot \bar{R} - 0,18) = -0,1062 \cdot \bar{R} + 32,68$$

Let's look at an example of such a calculation.

The average value of the specific resistance to penetration $\bar{R}$ =152,2 kPa was obtained on the clay rock samples of the site after their compaction and water saturation.

It was determined after 12 tests of 6 samples on both sides of the ring to the cone immersion depth *h*>10 mm.

Based on the results of one-plane shear of the same samples, 12 values of the specific shear resistance τ were obtained, and after their statistical processing, the values of the internal friction angle φ_{II}*=16°* and the specific adhesion c_{II}*=36,4* kPa were calculated.

According to the above dependences $\tau = f(\bar{R})$, we have $\tau_{100} = 66,67\ kPa$ and $\tau_{200} = 96,89\ kPa$, respectively, at a vertical pressure of $\sigma = 100\ kPa$ and $\sigma = 200\ kPa$.

Then $tg\varphi_{II} = (96,89 - 66,67) / (200 - 100) = 0,302$; the angle of internal friction is equal to $\varphi_{II} = 16,8°$; and the specific adhesion $c_{II} = -0,1062 \cdot 152,2 + 52,69 = -16,16 + 52,69 = 36,5 kPa$. Thus, the results of the established relationship between the parameters *R* and τ made it possible to determine the strength of the experimental heavy dusty loam (with a plasticity number $I_p = 14,5\%$), which practically coincided with the data of its tests for uniaxial shear.

The validity of these generalisations can be easily checked by looking at the porosity coefficient *e*, the flowability (consistency) index I_L and the water saturation coefficient S_r for clayey rocks.

As an example, for semi-hard clays, Table 1 shows the calculated values of K_φ and $\bar{R}$.

The final equation for the dependence of $\tau = f(\bar{R})$, which does not depend on the porosity coefficient *e*, is as follows

$$\tau = (11,75 + 0,206 \cdot \sigma) + (0,166 + 0,00047 \cdot \sigma) \cdot \bar{R} \quad (5)$$

Thus, it is possible to determine the strength parameters of clay rock (internal friction angle φ_{II} and specific adhesion c_{II}) from the average value of the specific penetration resistance $\bar{R}$ of compacted samples after their water saturation (usually reduced to the water saturation coefficient $S_r \geq 0,80$).

Of course, similar calculations and tables can be drawn up for other clay consistency values, as well as for loams or sandy loams.

It makes sense to establish the final equations of the relation $\tau = f(\bar{R})$ for a sufficiently wide range of variability of the clay rock yield factor, for example, $0 \leq I_L \leq 0,75$, in the form

$$\tau = A + B \cdot \sigma + (C + D \cdot \sigma) \cdot \bar{R} \quad (6)$$

where *A, B, C, D* – are the empirical coefficients of the equation.

Table 1 - Estimated values of the coefficient K_φ, depending on the rock strength parameters φ_{II} and $\bar{R}$

	Clay porosity coefficient e					
	0,55	0,65	0,75	0,85	0,95	1,05
$K_\varphi = f(\varphi)$	0,196	0,204	0,211	0,219	0,235	0,250
$\bar{R} = c_{II} / K_\varphi$	413	333	255,1	214,2	174,6	143,9
Specific shear resistance τ, kPa, at vertical pressure σ, kPa						
σ=100 kPa	119,0	104,0	88,4	79,5	69,7	60,9
σ=200 kPa	157,7	140,8	122,9	112,0	98,3	85,8
σ=300 kPa	190,2	177,2	157,2	144,8	127,0	110,8

Conclusions

1. It has been experimentally confirmed that for the water-saturated state of a cohesive (clay) rock, there is a practically functional relationship between the penetration index and the porosity coefficient. The specific shear resistances of clayey rocks, under the condition of the same physical state, are linearly interrelated with the corresponding average values of the specific resistance to penetration.

2. From the interrelation equations of the type (8), it is easy to determine the specific resistance to penetration obtained in the experiment from the average value of the specific resistance to shear of clay rocks at least at two values of vertical pressure, and then - the strength of the cohesive rock and (and, if necessary, taking into account the reliability factors, their calculated values).

3. The use of the expressions $K_\varphi = f(\varphi)$ and $K_\varphi = c / \bar{R}$ gives grounds for the use of simplified tests of cohesive rock for uniaxial shear, which consist in the penetration of pre-compacted water-saturated samples with the determination of the specific resistance to penetration, the performance of uniaxial shear at the minimum possible pressure and the establishment of the corresponding value of the specific cohesion.

4. Conducting surveys according to the recommended methodology significantly reduces the volume of regulatory tests for single-plane displacement, and also makes it possible to obtain sufficiently reliable results with less labour intensity and duration of work. Further testing of the penetration method for determining the strength of cohesive rocks opens up prospects for a wider reflection of this express method in regulatory sources.

References

1. Asad M.M. (2019). Oil and Gas Disasters and Industrial Hazards Associated with Drilling Operation. An Extensive Literature Review. *2nd Intern. Conf. on Computing, Mathematics and Engineering Technologies (ICoMET)*, March, 1–6.
https://doi.org/10.1109/ICOMET.2019.8673516

2. Onyshchenko V., Vynnykov Y., Shchurov I. & Kharchenko M. (2023). Case Study: Sites for the Drilling and Repair of Oil and Gas Wells. *Lecture Notes in Civil Engineering*, 299, 367-389.
https://link.springer.com/book/10.1007/978-3-031-17385-1

3. Jaeger J.C., Cook N.G.W. & Zimmerman R. (2007). *Fundamentals of Rock Mechanics*. Wiley-Blackwell.
https://doi.org/:10.1017/CBO9780511735349

4. Schnaid F. (2009). *In-situ testing in geomechanics – the main tests*. Taylor & Francis Group, London.
https://doi.org/10.1201/9781482266054

5. Das B.M. (2019). *Advanced Soil Mechanics*. London: CRC Press.
https://doi.org/10.1201/9781351215183

6. Meigh A.C. (1987). *Cone Penetration Testing: Methods and Interpretation*. Butterworths, London.

7. Mayne P.W., Saftner D. & Dagger R. (2018). *Cone Penetration Testing Manual for Highway Geotechnical Engineers*. Report.
https://www.dot.state.mn.us/research/reports/2018/201832.pdf

8. Zotsenko M., Vynnykov Yu., Lartseva I. & Sivitska S. (2018). Ground base deformation by circular plate peculiarities. *MATEC Web of Conferences 230, 02040. 7th Intern. Scientific Conf. "Reliability and Durability of Railway Transport Engineering Structures and Buildings" (Transbud-2018)*.
https://doi.org/10.1051/matecconf/201823002040

1. Asad M.M. (2019). Oil and Gas Disasters and Industrial Hazards Associated with Drilling Operation. An Extensive Literature Review. *2nd Intern. Conf. on Computing, Mathematics and Engineering Technologies (ICoMET)*, March, 1–6.
https://doi.org/10.1109/ICOMET.2019.8673516

2. Onyshchenko V., Vynnykov Y., Shchurov I. & Kharchenko M. (2023). Case Study: Sites for the Drilling and Repair of Oil and Gas Wells. *Lecture Notes in Civil Engineering*, 299, 367-389.
https://link.springer.com/book/10.1007/978-3-031-17385-1

3. Jaeger J.C., Cook N.G.W. & Zimmerman R. (2007). *Fundamentals of Rock Mechanics*. Wiley-Blackwell.
https://doi.org/:10.1017/CBO9780511735349

4. Schnaid F. (2009). *In-situ testing in geomechanics – the main tests*. Taylor & Francis Group, London.
https://doi.org/10.1201/9781482266054

5. Das B.M. (2019). *Advanced Soil Mechanics*. London: CRC Press.
https://doi.org/10.1201/9781351215183

6. Meigh A.C. (1987). *Cone Penetration Testing: Methods and Interpretation*. Butterworths, London.

7. Mayne P.W., Saftner D. & Dagger R. (2018). *Cone Penetration Testing Manual for Highway Geotechnical Engineers*. Report.
https://www.dot.state.mn.us/research/reports/2018/201832.pdf

8. Zotsenko M., Vynnykov Yu., Lartseva I. & Sivitska S. (2018). Ground base deformation by circular plate peculiarities. *MATEC Web of Conferences 230, 02040. 7th Intern. Scientific Conf. "Reliability and Durability of Railway Transport Engineering Structures and Buildings" (Transbud-2018)*.
https://doi.org/10.1051/matecconf/201823002040

9. Powell J.J.M., Shields C.H. & Wallace C.F. (2015). Liquid Limit testing – only use the Cone Penetrometer! *Proc. of the XVI ECSMGE Geotechnical Eng. for Infrastructure and Development*. Edinburg, 3305-3310.

10. Uhlig M. & Herle I. (2015). Advanced analysis of cone penetration tests**.** *Proc. of the XVI ECSMGE Geotechnical Eng. for Infrastructure and Development*. Edinburg, 3073-3078.
https://doi:10.1680/ecsmge.60678

11. Kryvosheiev P., Farenyuk G., Tytarenko V., Boyko I., Kornienko M., Zotsenko M., Vynnykov Yu., Siedin V., Shokarev V. & Krysan V. (2017). Innovative projects in difficult soil conditions using artificial foundation and base, arranged without soil excavation. *Proc. of 19th Intern. Conf. on Soil Mechanics and Geotechnical Engineering*. Seoul, 3007-3010.
https://doi.org/10.1680/geot.1997.47.3.693

12. Ahmadi M.M. & Golestani Dariani A.A. (2017). Cone penetration test in sand: A numerical-analytical approach. *Computers and Geotechnic*s. Vol. 90, 176-189.
https://doi.org/10.1016/j.compgeo.2017.06.010

13. Golestani Dariani A.A. & Ahmadi M.M. (2019). CPT Cone Factor: Numerical-Analytical Approach**.** *Intern. Journal of Geomechanics*, 19(12).
https://ascelibrary.org/doi/abs/10.1061/%28ASCE%29GM.1943-5622.0001521

14. Liyanapathirana S. (2022). Large deformation finite element analysis to predict penetration resistance of offshore pipelines. *Proc. of the 20th Intern. Conf. on Soil Mechanics and Geotechnical Engineering.* Sydney: Australian Geomechanics Society. Vol. 2, 821-826.

15. Robertson P.K. (2016). CPT-based Soil Behaviour Type (SBT) Classification System – an update. *Canadian Geotechnical Journal*. 53(12),
https://doi.org/10.1139/cgj-2016-0044

16. Xing Y., Kulatilake P. & Sandbak L. (2019). *Rock Mass Stability Around Underground Excavations in a Mine*. London. CRC Press.
https://doi.org/10.1201/9780429343230

17. Golestani Dariani A.A. & Naserifar A. (2024). Effects of Seismic Waves on the Segmental Lining of Shiraz Subway Line 2: A Case Study. *Geotechnical and Geological Engineering*. Vol. 42, 1089-1104.
https://link.springer.com/article/10.1007/s10706-023-02606-2

18. Briaud J.-L. (2013). *Geotechnical Engineering: Unsaturated and Saturated Soils*. Wiley.
https://doi.org/:10.1002/9781118686195

19. Zein A.K.M. (2017). Estimation of undrained shear strength of fine grained soils from cone penetration resistance. *Intern. Journal of Geo-Engineering*, 8(1).
https://link.springer.com/article/10.1186/s40703-017-0046-y

20. Liu L., Cai G., Liu X., Li X., Liu S., Puppala A.J. (2021). Estimation of Undrained Shear Strength of Overconsolidated Clay Using a Maximum Excess Pore Pressure Method Based on Piezocone Penetration Test (CPTU). *Geotech. Test. J.* 44(4), 1153-1162.
https://doi.org/10.1520/GTJ20190248

21. Yang Z., Liu X., Guo L., Cui Y., Su X., Jia C. & Ling X. (2022). CPT-Based estimation of undrained shear strength of fine-grained soils in the Huanghe River Delta. *J. Acta Oceanologica Sinica*, 41(5): 136-146.
http://www.aosocean.com/article/doi/10.1007/s13131-021-1946-4

22. Equihua-Anguiano L.N., Orozco-Calderon M. & Foray P. (2013). Estimation of undrained shear strength of soft obtained by cylinder vertical penetration. *Proc. of the 18th Intern. Conf. on Soil Mechanics and Geotechnical Engineering*.

9. Powell J.J.M., Shields C.H. & Wallace C.F. (2015). Liquid Limit testing – only use the Cone Penetrometer! *Proc. of the XVI ECSMGE Geotechnical Eng. for Infrastructure and Development*. Edinburg, 3305-3310.

10. Uhlig M. & Herle I. (2015). Advanced analysis of cone penetration tests**.** *Proc. of the XVI ECSMGE Geotechnical Eng. for Infrastructure and Development*. Edinburg, 3073-3078.
https://doi:10.1680/ecsmge.60678

11. Kryvosheiev P., Farenyuk G., Tytarenko V., Boyko I., Kornienko M., Zotsenko M., Vynnykov Yu., Siedin V., Shokarev V. & Krysan V. (2017). Innovative projects in difficult soil conditions using artificial foundation and base, arranged without soil excavation. *Proc. of 19th Intern. Conf. on Soil Mechanics and Geotechnical Engineering*. Seoul, 3007-3010.
https://doi.org/10.1680/geot.1997.47.3.693

12. Ahmadi M.M. & Golestani Dariani A.A. (2017). Cone penetration test in sand: A numerical-analytical approach. *Computers and Geotechnic*s. Vol. 90, 176-189.
https://doi.org/10.1016/j.compgeo.2017.06.010

13. Golestani Dariani A.A. & Ahmadi M.M. (2019). CPT Cone Factor: Numerical-Analytical Approach**.** *Intern. Journal of Geomechanics*, 19(12).
https://ascelibrary.org/doi/abs/10.1061/%28ASCE%29GM.1943-5622.0001521

14. Liyanapathirana S. (2022). Large deformation finite element analysis to predict penetration resistance of offshore pipelines. *Proc. of the 20th Intern. Conf. on Soil Mechanics and Geotechnical Engineering.* Sydney: Australian Geomechanics Society. Vol. 2, 821-826.

15. Robertson P.K. (2016). CPT-based Soil Behaviour Type (SBT) Classification System – an update. *Canadian Geotechnical Journal*. 53(12),
https://doi.org/10.1139/cgj-2016-0044

16. Xing Y., Kulatilake P. & Sandbak L. (2019). *Rock Mass Stability Around Underground Excavations in a Mine*. London. CRC Press.
https://doi.org/10.1201/9780429343230

17. Golestani Dariani A.A. & Naserifar A. (2024). Effects of Seismic Waves on the Segmental Lining of Shiraz Subway Line 2: A Case Study. *Geotechnical and Geological Engineering*. Vol. 42, 1089-1104.
https://link.springer.com/article/10.1007/s10706-023-02606-2

18. Briaud J.-L. (2013). *Geotechnical Engineering: Unsaturated and Saturated Soils*. Wiley.
https://doi.org/:10.1002/9781118686195

19. Zein A.K.M. (2017). Estimation of undrained shear strength of fine grained soils from cone penetration resistance. *Intern. Journal of Geo-Engineering*, 8(1).
https://link.springer.com/article/10.1186/s40703-017-0046-y

20. Liu L., Cai G., Liu X., Li X., Liu S., Puppala A.J. (2021). Estimation of Undrained Shear Strength of Overconsolidated Clay Using a Maximum Excess Pore Pressure Method Based on Piezocone Penetration Test (CPTU). *Geotech. Test. J.* 44(4), 1153-1162.
https://doi.org/10.1520/GTJ20190248

21. Yang Z., Liu X., Guo L., Cui Y., Su X., Jia C. & Ling X. (2022). CPT-Based estimation of undrained shear strength of fine-grained soils in the Huanghe River Delta. *J. Acta Oceanologica Sinica*, 41(5): 136-146.
http://www.aosocean.com/article/doi/10.1007/s13131-021-1946-4

22. Equihua-Anguiano L.N., Orozco-Calderon M. & Foray P. (2013). Estimation of undrained shear strength of soft obtained by cylinder vertical penetration. *Proc. of the 18th Intern. Conf. on Soil Mechanics and Geotechnical Engineering*.

Paris. 2933-2936.
https://www.cfms-sols.org/sites/default/files/Actes/2933-2936.pdf
23. Chang C., Zoback M.D. & Khaksar A. (2006). Empirical relations between rock strength and physical properties in sedimentary rocks. *Journal of Petroleum Science and Engineering*. Vol. 51, Is. 3–4, 223-237.
https://doi.org/10.1016/j.petrol.2006.01.003
24. Zotsenko M.L., Vynnykov Yu., Pinchuk N.M. & Manzhalii S.M. (2019). Research of "influence area" parameters of the foundations arranged without soil. *IOP Conf. Series Materials Science and Engineering*. 708(1):012076.
https://doi:10.1088/1757-899X/708/1/012076
25. Lu Y., Duan Z., Zheng J., Zhang H., Liu X. & Luo S. (2020). Offshore Cone Penetration Test and Its Application in FullWater-Depth Geological Surveys. *OP Conf. Series: Earth and Environmental Science* 570(4):042008
https://doi:10.1088/1755-1315/570/4/042008
26. Guo S.-Z. & Liu R. (2015). Application of cone penetration test in offshore engineering, *Chinese Journal of Geotechnical Engineering*, vol. 37, no. 1, 207-211.
https://doi:10.11779/CJGE2015S1039
27. Wu B., Wang G., Li J., Wang Y. & Liu B. (2018). Determination of the Engineering Properties of Submarine Soil Layers in the Bohai Sea Using the Piezocone Penetration Test. *Advances in Civil Engineering*. 6: 1-13. *Follow journal.*
https://doi:10.1155/2018/9651045
28. Ma H., Zhou M., Hu Y. & Hossain M.S. (2017). Effects of cone tip roughness, in-situ stress anisotropy and strength inhomogeneity on CPT data interpretation in layered marine clays: numerical study. *Engineering Geology*, Vol. 227, 12-22.
https://doi.org/1016/j.enggeo.2017.06.003
29. Solberg I-L., Long M., Baranwal V.C., Gylland A.S. & Rønning J.R. (2016). Geophysical and geotechnical studies of geology and sediment properties at a quick-clay landslide site at Esp, Trondheim, Norway. *Engineering Geology*. Vol. 208, 214-230.
https://doi.org/10.1016/j.enggeo.2016.04.031
30. Vynnykov Yu., Kharchenko M., Dmytrenko V. & Manhura A. (2020). Probabilistic calculation in terms of deformations of the formations consisting of compacted overburden of quarternary rocks. *Mining of Mineral Deposits*, 14(4), 122-129.
https://doi.org/10.33271/mining14.04.122
31. Shen S.L., Wang J.P., Wu H.N., Xu Y.S., Ye G.L. & Yin Z.Y. (2015). Evaluation of hydraulic conductivity for both marine and deltaic deposit based on piezocone test. *Ocean Eng*. Vol. 110, 174-182.
https://doi.org/10.1016/j.oceaneng.2015.10.011

Paris. 2933-2936.
https://www.cfms-sols.org/sites/default/files/Actes/2933-2936.pdf
23. Chang C., Zoback M.D. & Khaksar A. (2006). Empirical relations between rock strength and physical properties in sedimentary rocks. *Journal of Petroleum Science and Engineering*. Vol. 51, Is. 3–4, 223-237.
https://doi.org/10.1016/j.petrol.2006.01.003
24. Zotsenko M.L., Vynnykov Yu., Pinchuk N.M. & Manzhalii S.M. (2019). Research of "influence area" parameters of the foundations arranged without soil. *IOP Conf. Series Materials Science and Engineering*. 708(1):012076.
https://doi:10.1088/1757-899X/708/1/012076
25. Lu Y., Duan Z., Zheng J., Zhang H., Liu X. & Luo S. (2020). Offshore Cone Penetration Test and Its Application in FullWater-Depth Geological Surveys. *OP Conf. Series: Earth and Environmental Science* 570(4):042008
https://doi:10.1088/1755-1315/570/4/042008
26. Guo S.-Z. & Liu R. (2015). Application of cone penetration test in offshore engineering, *Chinese Journal of Geotechnical Engineering*, vol. 37, no. 1, 207-211.
https://doi:10.11779/CJGE2015S1039
27. Wu B., Wang G., Li J., Wang Y. & Liu B. (2018). Determination of the Engineering Properties of Submarine Soil Layers in the Bohai Sea Using the Piezocone Penetration Test. *Advances in Civil Engineering*. 6: 1-13. *Follow journal.*
https://doi:10.1155/2018/9651045
28. Ma H., Zhou M., Hu Y. & Hossain M.S. (2017). Effects of cone tip roughness, in-situ stress anisotropy and strength inhomogeneity on CPT data interpretation in layered marine clays: numerical study. *Engineering Geology*, Vol. 227, 12-22.
https://doi.org/1016/j.enggeo.2017.06.003
29. Solberg I-L., Long M., Baranwal V.C., Gylland A.S. & Rønning J.R. (2016). Geophysical and geotechnical studies of geology and sediment properties at a quick-clay landslide site at Esp, Trondheim, Norway. *Engineering Geology*. Vol. 208, 214-230.
https://doi.org/10.1016/j.enggeo.2016.04.031
30. Vynnykov Yu., Kharchenko M., Dmytrenko V. & Manhura A. (2020). Probabilistic calculation in terms of deformations of the formations consisting of compacted overburden of quarternary rocks. *Mining of Mineral Deposits*, 14(4), 122-129.
https://doi.org/10.33271/mining14.04.122
31. Shen S.L., Wang J.P., Wu H.N., Xu Y.S., Ye G.L. & Yin Z.Y. (2015). Evaluation of hydraulic conductivity for both marine and deltaic deposit based on piezocone test. *Ocean Eng*. Vol. 110, 174-182.
https://doi.org/10.1016/j.oceaneng.2015.10.011

Збірник наукових праць. Галузеве машинобудування, будівництво
Academic journal. Industrial Machine Building, Civil Engineering
http://journals.nupp.edu.ua/znp
https://doi.org/10.26906/znp.2023.61.3849

UDC 624.072.2.014.2-413

The limit state of steel beams research of damaged building elements

Serhii Hudz [1]*, Vitaliia Harkusha [2], Yuriy Sergienko [3], Tetiana Hodun [4]

[1] Priazovsky State Technical University https://orcid.org/0000-0002-4764-8635
[2] Priazovsky State Technical University https://orcid.org/0000-0002-5016-0737
[3] Priazovsky State Technical University https://orcid.org/0000-0002-3295-6280
[4] Priazovsky State Technical University https://orcid.org/0000-0003-1710-9099

*Corresponding author E-mail: goods_s_a@pstu.edu

The article is devoted to the study of the limit state of steel I-beams under buckling with operational geometric imperfections revealed during inspections of damaged elements of reconstructed buildings. The influence of damage in the form of initial curvature in the horizontal plane on the stability and bearing capacity of structures is analyzed. The possibility of using bearing capacity resources, namely lateral bracing restraint with the help of structures attached to a steel beam, is considered. The proposed approaches are aimed at optimizing the use of materials and increasing savings by detailing the verification calculations of damaged steel beams.

Keywords: buckling, I-beam, initial curvature, operational geometric imperfections, restraint.

Дослідження граничного стану сталевих балок пошкоджених елементів будівель

Гудзь С.А.[1]*, Гаркуша В.С. [2], Сергієнко Ю.В. [3], Годун Т.М.[4]

[1, 2, 3, 4] Державний вищий навчальний заклад «Приазовський державний технічний університет»
*Адреса для листування E-mail: goods_s_a@pstu.edu

У будівлях, які експлуатуються тривалий час і зазнали пошкоджень, прокатні балки є одними із найбільш поширених елементів, що потребують обстеження для точного визначення їх технічного стану та можливості відновлення. Основним способом оцінки технічного стану конструкцій є перевірочний розрахунок, у якому здійснюється врахування дефектів і пошкоджень. Під час його виконання використовуються дані, отримані в ході натурних оглядів, контролю характеристик міцності матеріалів, уточнення навантажень і впливів. Стаття присвячена вивченню граничного стану сталевих балок при втраті стійкості з експлуатаційними геометричними недосконалостями, виявленими під час обстежень пошкоджених елементів відновлюваних будівель. Проведено аналіз впливу пошкоджень у вигляді початкових викривлень у горизонтальній площині на стійкість та несучу здатність конструкцій. Основний акцент робиться на визначенні особливостей експлуатації балок. Зокрема, розглядається можливість застосування ресурсів несучої здатності, а саме бокового розкріплення за допомогою конструкцій, приєднаних до сталевої балки. При дотриманні нормативних вимог щодо забезпечення надійного з'єднання суцільного жорсткого настилу зі стиснутим поясом стійкість балки не перевіряється. Удосконалена теоретична модель враховує і усуває присутні у попередній моделі недоліки. Запропоновані підходи спрямовані на оптимізацію використання матеріалів та збільшення економії шляхом деталізації перевірочних розрахунків сталевих балок із пошкодженнями. Висвітлені та розглянуті підходи щодо визначення допустимих викривлень сталевих двотаврових балок у горизонтальній площині можуть бути використані з достатньою точністю при відновленні пошкоджених елементів будівель. Не зважаючи на певні недоліки, якими наділені ці методи, вони достатньо прості та відповідають нормам проєктування сталевих будівельних конструкцій.

Ключові слова: втрата стійкості, двотаврова балка, початкове викривлення, експлуатаційні геометричні недосконалості, розкріплення.

Introduction

Frame buildings in general, and one-story buildings in particular, are the most common use of steel structures in the world. Until recently, hot-rolled beam profiles were predominantly used for roof purlins in industrial buildings. Although solid section purlins are heavier than lattice girders, they are much easier to manufacture and install. This type of purlin was often used in combination with steel trusses with a spacing of 6

meters. Steel beams made from hot-rolled sections can still be used instead of cold-formed thin-walled sections for roof purlins. With large roof slopes, the channel section of the purlin works well for oblique bending. Under heavy loads, which are typical for flat roofs of large shopping malls, the cross-section of the purlins can be taken from rolled I-beams (Fig. 1). Hot-rolled purlins can be used in large-scale panel solutions, where they are particularly useful for providing intermediate support for decking that is not capable of spanning large spans on its own. However, with the advent of cold-formed purlins, which are significantly lighter and less expensive, the use of hot-rolled purlins has become unusual.

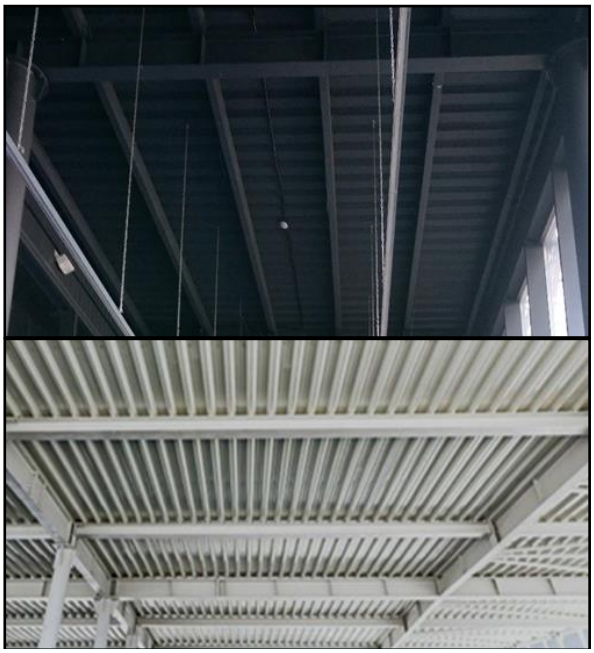

Figure 1 – View of the flat roof structures on I-beams in the transverse and longitudinal directions

Review of the latest research sources and publications

The effect of geometric imperfections (in particular, the initial curvature of the beam axis in the plane of least stiffness) is partially taken into account in the standards by introducing a working conditions factor. In compliance with the regulatory requirements for ensuring a reliable connection of a continuous rigid deck with a compressed flange, the stability of the beam is not checked. At the same time, the bracing should be designed to withstand the fictional load. In other cases, if the compression flange is insufficiently restrained, the stability of the beam should be calculated using the formula with a buckling factor. The fictional (conditional, equivalent, stabilizing) load is understood as the forces arising from geometric imperfections and deformations of the beam and acting between the structural elements. They create an dominate action on the bracing structures and a supporting action on the beam. Their determination in construction practice is often performed using approximate methods that consider the compressed beam flange separately from the rest of the section as a continuously supported compressed rod with a longitudinal force.

In recent years, much attention has been paid to the study of the stress-strain state of damaged steel beams. Numerous theoretical and experimental studies in this area consider both thin-walled steel beams without bracing and those with bracing [1, 2]. The multifactor spatial model for describing the fictional load, which is presented in the works of German scientists [3 – 5], is used under the condition of sufficient stiffness of bracing structures in the calculation of bracings and stiffening diaphragms. These papers reveal aspects of torsion and stability of beams, providing valuable theoretical conclusions. In particular, it is argued that for unbraced beams, the compressed rod model underestimates the maximum fictional load, which reduces the reliability of the structure, and in the case of sufficiently braced beams, it is shown by example that such a model leads to significant material overruns and is not economically feasible. In [6], the problems of developing a spatial model to describe the fictional loads on steel beams of asymmetric cross-section under the combined action of transverse bending and forced torsion were formulated and solved. In solving stability problems, the energy method is widely used, which is of interest and involves the automatic execution of cumbersome computer operations [7, 8]. These sources provide a snapshot and show the state of modern research on the stress-strain state of damaged steel beams, taking into account various aspects of stability and buckling.

Definition of unsolved aspects of the problem

An unresolved part of the general problem of analyzing and studying the condition of steel elements is to determine the permissible values of curvature of steel beams in the horizontal plane when restoring damaged parts of buildings. Attention should be focused on ensuring the stability and efficiency of further operation of the beams.

Problem statement

The aim of the study is to determine the effect of beam damage on their stress-strain state. As part of the study, it is planned to take into account the peculiarities of structures, adhering to the relevant regulatory documents in construction. In particular, the model for determining the load-bearing capacity of steel beams of the most common I-beam constant cross-section in length, taking into account strain and stresses resulting from damage, needs to be improved. Additionally, the causes and consequences of torsion in structures with curvature are considered. The results of this study will be useful for further improvements in the design and operation of steel structures with regard to possible and existing damage.

Basic material and results

In buildings that have been in operation for a long time and have suffered damage, rolled beams are among the most common elements that require inspection to accurately determine their technical condition and the possibility of restoration. The main method of assessing the technical condition of structures is a verification calculation that takes into account defects and

damages. It uses data obtained during on-site inspections, control of material strength characteristics, and specification of loads and impacts. Overloading of the roof, in particular by snow load, leads to damage and emergency conditions (Fig. 2).

Figure 2 – Damage to roof from overloading

Structures can also be unprotected from damage and become damaged in the event of accidental explosions. For example, in the event of a fire, the steel frame of an operated building quickly heats up to the temperature of the metal's transition to a plastic state, resulting in an increase in irreversible deformations and exhaustion of the load-bearing capacity until failure occurs (Fig. 3).

Figure 3 – Appearance of metal frame after a fire and design sketch of the beam by fire effect

The fire resistance of metal structures is insignificant because metal has a high thermal conductivity. In addition, thin-walled cross-sections of structural elements are more prone to buckling when heated, which is one of their disadvantages. If damaged beam elements are reused for further operation, they develop new initial geometric imperfections that lead to torsion, which can lead to a lateral-torsional buckling.

By buckling, in addition to deflection strain, the beam receives strain of curvature and rotation of the cross-section. The spatial model of the beam strain is shown in Fig. 4.

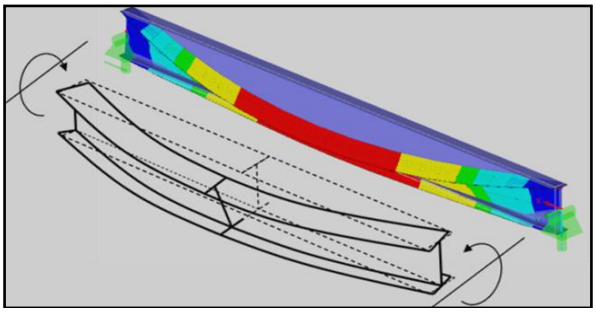

Figure 4a – Beam strain during buckling

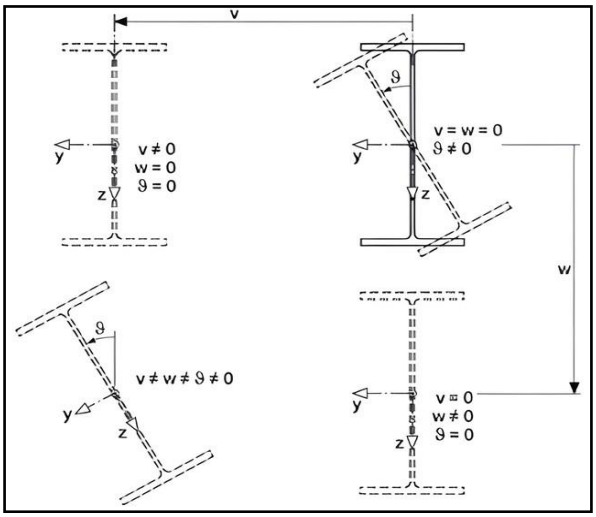

Figure 4b – Actual beam performance

To find the permissible value of the initial curvature of damaged beams in the horizontal plane, it is possible to use the formulas of DBN V.2.6-198:2014 [9] to determine the fictional transverse load and fictional transverse force used in the calculations of attachment of rigid decking, elements of longitudinal or transverse ties to the compressed beam flange. To calculate the fictional loads, the building codes [9] adopt a static model that can be considered flat, since it considers only the forces and strain in the plane of the upper flange. The effects of lateral deformation of the lower flange and spatial twisting of the cross-section are not taken into account in this model.

On the other hand, such a relatively simple representation of the beam operation in the standards allows describing the fictional load as a function of the longitudinal force and strain of the restrained flange, which is obtained in the static model as a result of solving the differential equation of a compressed rod from the condition of balanced forces in the flange. When laterally restrained, the upper flange will move due to the pliability of the attached structures. To take into account the deformation of the upper girder of the beam, its total total value should be used instead of the initial curvature. In this case, it is assumed that the initial curvature of the beam and the displacement of the upper girders are distributed along the length of the beam according to the same law. The maximum fictional transverse load will be determined in this model by the formula:

$$q_{fic} = \frac{\pi^2 N}{l^2}(v_0 + v) \quad (1)$$

where N is the value of the longitudinal compressive force in the beam flange determined in the plastic stage of operation ($N = N_{pl} = A_f R_{yf} + 0{,}25 A_w R_{yw}$, where A_f, A_w are the cross-sectional areas of the compressed flange and beam web; R_{yf}, R_{yw} are the calculated steel resistances of the compressed flange and web, respectively); l is the span of the beam; v_0 is the largest value of the initial curvature of the beam (in Table 5.1 of EN 1993-1-1 it corresponds to the value e_0, which is set depending on the type of curvature curve, cross-section and span of the beam, as well as the type of calculation); v is the largest value of the displacement strain of the compressed flange under load in the y-axis direction.

Next, we will use expression (9.34) of DBN V.2.6-198:2014 [9] for the fictional load:

$$q_{fic} = \frac{3Q_{fic}}{l} \quad (2)$$

The values of the fictional transverse force Q_{fic} in formula (2) can be determined by the approximate dependence (8.14) approximated in DBN V.2.6-198:2014 [9]:

$$Q_{fic} = 7{,}15 \cdot 10^{-6}\left(2330 - \frac{E}{R_y}\right)\frac{N}{\varphi}, \quad (3)$$

where E is the modulus of elasticity of steel; R_y is the calculated resistance of steel to tension, compression and bending beyond the yield strength; φ is the stability factor of under central compression, which is assumed to be equal to one when the compressed beam flange is continuously restrained by the supporting deck.

By equating formulas (1) and (2) with expression (3), we obtain a formula for determining the total allowable horizontal curvature, in which the flexibility of the upper flange fastening is taken into account by assuming an increased initial beam curvature, including strain of the upper flange under load:

$$v_{tot} = 7{,}15 \cdot 10^{-6}\left(2330 - \frac{E}{R_y}\right)\frac{3l}{\pi^2} = \frac{l}{\delta}. \quad (4)$$

Some values of the dimensionless parameter δ for different values of R_y and $E = 2{,}06 \cdot 10^5$ MPa are given in Table 1.

Table 1 – The value of the dimensionless parameter δ for determining the permissible curvature

R_y, МПа	δ	R_y, МПа	δ
220	330	300	280
230	321	310	276
240	313	320	273
250	306	330	270
260	299	340	267
270	294	350	264
280	289	360	262
290	284	370	259

Note. When determining the permissible value of the initial beam curvature in the elastic stage, the obtained values should be reduced by the value N_{el}/N_{pl}.

The total curvature of the loaded beam takes into account the influence of transverse displacements of the compliant restraint caused by the action of external and fictional loads. The increase in deformation for unbraced beams usually does not exceed 20% [5]. Therefore, when approximating the permissible value of the initial curvature of an unloaded beam, the values in the table should be increased by 20%.

The initial geometric imperfections that occur in a damaged beam in service can be determined during inspections of rehabilitated buildings by measuring the actual deviations using tools. In this way, the values of the initial curvature strain at the level of the weight center of the cross-section, as well as the initial angle of rotation, are determined in the first place. The total linear strain of the initial curvature at the level of the beam upper flange can be determined approximately from the second equation shown in Fig. 5. The initial deflection of the beam is practically absent due to its significant stiffness in the main plane.

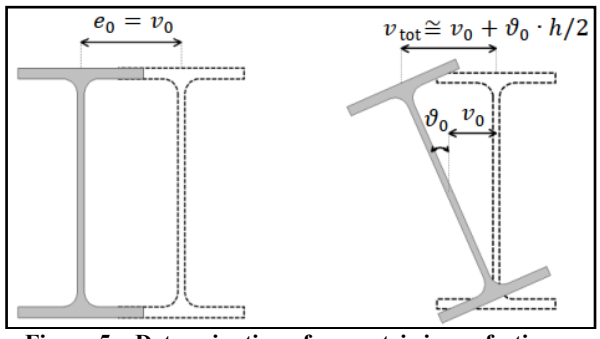

Figure 5 – Determination of geometric imperfections, occurring in the operated damaged beam

Separately, it is necessary to focus on the study of the interaction between damage and stresses in the restrained elements. If the actual curvature exceeds the permissible value established by formula (4) and Table 1, a more detailed analysis of the stress-strain state of the beam should be performed. It is already necessary to determine the additional normal stresses due to the initial curvature of the beam and compare them with the permissible stress increase, i.e., the difference between the value of the calculated resistance R_y, or the actual yield strength σ_y obtained as a result of the inspection tests, and the value of normal stresses in the uncurved beam σ. The methodology for determining additional stresses, which is given in [10], was implemented in the state standard for assessing the technical condition of steel building structures in operation [11]. Its prerequisite is to take the curve corresponding to the curvature function as a square parabola. It is worth noting that the disadvantages of the methodology are the failure to take into account the level of load application along the height of the beam and the existing eccentricities in

asymmetric cross-sections, which is not a safety factor. A refinement and comparison of this methodology are given in the scientific article [8]. The form of the formulas in Table 2 is slightly modified to take into account the flange displacement under load and is intended only for a symmetrical I-beam.

Table 2 – Additional normal stresses in a beam with a curvature

Concentrated force in the middle of the span
$\sigma_{ad} = \frac{2Fv_{tot}}{l} \cdot \frac{E\omega}{GI_t}\left(1 - \frac{\tanh\frac{kl}{2}}{\frac{kl}{2}}\right)$
Uniformly distributed load
$\sigma_{ad} = qv_{tot} \cdot \frac{E\omega}{GI_t}\left(1 - \frac{\tanh\frac{kl}{2}}{\frac{kl}{2}}\frac{\tanh\frac{kl}{4}}{\frac{kl}{4}}\right)$

Note. F is a concentrated force; q is uniformly distributed load; G is the shear modulus; $k = \sqrt{\frac{GI_t}{EI_\omega}}$ is elastic bending-torsional characteristic; I_t is the torsional constant; I_ω is the warping constant; ω is the warping area of the beam cross-section at the stress determination point; $\omega = bh/n$; b is the width of the beam flange; h is the height of the beam; $n = 4$ in the elastic stage of design, $n = 6$ in the plastic stage.

The design model laid down in the European design standards EN 1993-1-1 [12] allows for a variety of loading conditions and types of diagrams, as well as bracing conditions. The initial curvature of the beam is assumed to be the maximum permissible and is determined depending on the type of curvature curve, cross-sectional type, and span of the beam. The calculation method EN 1993-1-1 [12] is more open to the designer and is more intended for machine design. The solution of the corresponding differential equation for the fictional load can also be represented in accordance with the European approach in the form:

$$q_{fic} = \alpha \frac{\pi^2 N}{l^2} v_0, \qquad (5)$$

where α is a multiplying factor to account for the second-order effects, which in the compressed rod model is determined by equation:

$$\alpha = \left(1 - \frac{1}{\alpha_{cr}}\right)^{-1}, \qquad (6)$$

where α_{cr} is the coefficient of increase in the design load at which the buckling in the elastic stage occurs.

In equation (5), the longitudinal compressive force in the upper beam flange is defined in the elastic stage as the ratio of the bending moment that causes it to the distance h_f between the weight centers of the beam flanges, taking into account the longitudinal force arising in the beam from the external load:

$$N = N_{el} = \frac{M_{y,Ed}}{h_f} - \frac{N_{Ed}}{2}, \qquad (7)$$

where $M_{y,Ed}$, N_{Ed} are the design values of bending moment relative to the y-y axis and longitudinal force.

The critical load on the upper flange will be proportional to its bending stiffness according to the Euler's formula. Since, when taking into account the pliability, the critical force in the flange will be approximately equal to the shear stiffness of the structures attached to it [5], a simplified expression can be written to determine the total strain of the initial curvature at the level of the upper flange of the restrained beam:

$$v_{tot} \approx v_0\left(1 - \frac{N}{S}\right)^{-1} = v_0 + \frac{Nv_0}{S - N}, \qquad (8)$$

where S is the available shear stiffness of the bracing structures per beam, which must exceed the required stiffness according to formula (BB.2) of EN 1993-1-1 [12] to accept the translational restraint and ensure the beam stability.

If a profiled deck is rigidly attached to the upper flange of a steel beam in lightly roofed framework using self-tapping screws and riveted together at the longitudinal joints (Fig. 6), it can prevent torsion and be used to counteract the lateral-torsional buckling of the beam. This function can also be performed by cross bracings in purlinless buildings for frame rafters.

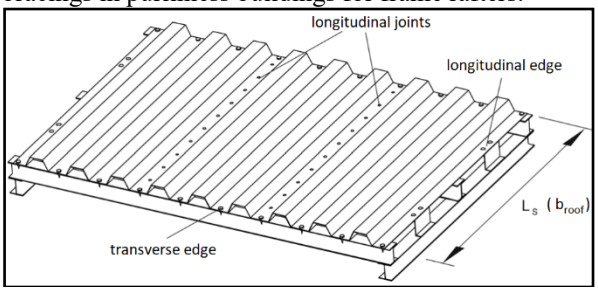

Figure 6 – An example of a roof panel with fastening of profiled deck to the purlins on all four edges

For an approximate determination of the shear stiffness of a profiled deck in newtons, EN 1993-1-3 [13] provides the expression (10.1b):

$$S = 1000\sqrt{t^3}\,(50 + 10\sqrt[3]{b_{roof}})\frac{s}{h_w}, \qquad (9)$$

where t is the thickness of the profiled deck in mm; b_{roof} is the width of the roof in mm (L_s); s is the distance between purlins in mm; h_w is the height of the profiled deck in mm.

The formula (9) slightly underestimates the stiffness value, but it is suitable for any profiled deck and does not require that the deck be fixed to the supporting structures with all four edges, but only with two. This method of fastening simplifies the process and reduces the erection cost. Some manufacturers (Hoesch, Fischer, Arcelor) have developed their own methods for determining the shear stiffness of profiled decking, which can be used only for this product and in the case of fastening with four edges (Fig. 6). For economic reasons, profiled deck is often fixed through a wave (mostly to channel purlins). Formula (9) is used when fixing the deck to the beam in each wave. If the profiled deck is fixed only every second wave, then its shear stiffness is assumed to be reduced by a factor of five compared to the initial stiffness.

Conclusions

The highlighted and considered approaches to determining the permissible curvature of steel I-beams in the horizontal plane can be used with sufficient accuracy in the restoration of damaged building elements. Despite certain drawbacks of these methods, they are quite simple and comply with the design standards for steel building structures.

References

1. Nagy Zs. Stressed skin effect on the elastic buckling of pitched roof portal frames / Zs. Nagy, A. Pop, I. Moiș, and R. Ballok // In Structures, vol. 8, Elsevier, 2016. – pp. 227 – 244. http://dx.doi.org/10.1016/j.istruc.2016.05.001

2. Wrzesien A.M. Effect of Stressed Skin Action on the Behaviour of Cold-Formed Steel Portal Frames / A.M. Wrzesien, J.B.P. Lim, Y. Xu, I.A. MacLeod, R.M. Lawson // Engineering Structures, 105, 2015. – pp. 123 – 136. http://dx.doi.org/10.1016/j.engstruct.2015.09.026

3. Kindmann R., Stahlbau, Teil 2: Stabilität und Theorie II. Ordnung. 5. Auflage, Berlin: Ernst & Sohn, 2021. – 579 p. https://doi.org/10.1002/9783433600030

4. Kindmann R. and Kraus M., Steel structures: Design using FEM, John Wiley & Sons, (2011), – 540 p. https://doi.org/10.1002/9783433600771.fmatter

5. Kindmann R. Bemessung stabilisierender Verbände und Schubfelder / R. Kindmann, M. Krahwinkel // Stahlbau 70, 2001. – pp. 885 – 899. https://doi.org/10.1002/stab.200102860

6. Krahwinkel, M.: Zur Beanspruchung stabilisierender Konstruktionen im Stahlbau. Fortschritt-Berichte VDI, Reihe 4 Bauingenieurwesen, Nr. 166. Düsseldorf: VDI-Verlag 2001. – 182 p.

7. Гудзь С.А. Розвинена модель розрахунку сталевих розкріплених елементів на стійкість при сумісній дії поперечного згину та кручення / С.А. Гудзь, Г.М. Гасій, В.В. Дарієнко // Сучасні будівельні конструкції з металу та деревини: Збірник наукових праць. – Одеса: ОДАБА, 2020. – вип. 24. – С. 43 – 52.

8. Гудзь С.А. Несуча здатність сталевих двотаврових балок, що експлуатуються з недосконалостями у вигляді початкових викривлень у площині найменшої жорсткості / С.А. Гудзь // Вісник Одеської державної академії будівництва та архітектури. Випуск № 61. – Одеса: Зовнішрекламсервіс, 2016. – С. 95 – 101.

9. ДБН В.2.6-198:2014. Конструкції будівель і споруд. Сталеві конструкції. Норми проектування / Остаточна редакція. Видання офіційне. – Надано чинності з 1 січня 2015 р. – К.: Мінрегіонбуд України, 2014. – 199 с.

10. Семко В.О. Розрахунок та експериментальні дослідження сталевих балок з викривленням в горизонтальній площині / В.О. Семко, С.А. Гудзь // Збірник наукових праць. Ресурсоекономні матеріали, конструкції, будівлі та споруди. – Випуск 14. – Рівне: Видавництво Національного університету водного господарства та природокористування, 2006. – С. 317 – 322.

11. Оцінка технічного стану сталевих будівельних конструкцій, що експлуатуються: ДСТУ Б.В.2.6–210:2016. – [Чинний з 2017-01-01]. – К. : Мінгеріонбуд України, 2016. – 45 с.

12. EN 1993-1-1:2003. Eurocode 3: Design of steel structures. Part 1-1: General rules and rules for buildings. – Brussels: CEN, 2003. – 90 p.

13. EN 1993-1-3:2006. Eurocode 3: Design of steel structures. Part 1-3: General rules. Supplementary rules for cold-formed members and sheeting. – Brussels: CEN, 2006. – 130 p.

1. Nagy Zs. Stressed skin effect on the elastic buckling of pitched roof portal frames / Zs. Nagy, A. Pop, I. Moiș, and R. Ballok // In Structures, vol. 8, Elsevier, 2016. – pp. 227 – 244. http://dx.doi.org/10.1016/j.istruc.2016.05.001

2. Wrzesien A.M. Effect of Stressed Skin Action on the Behavior of Cold-Formed Steel Portal Frames / A.M. Wrzesien, J.B.P. Lim, Y. Xu, I.A. MacLeod, R.M. Lawson // Engineering Structures, 105, 2015. – pp. 123 – 136. http://dx.doi.org/10.1016/j.engstruct.2015.09.026

3. Kindmann R., Steel construction, Part 2: Stability and the second order theory. 5th edition, Berlin: Ernst & Sohn, 2021. – 579 p. https://doi.org/10.1002/9783433600030

4. Kindmann R. and Kraus M., Steel structures: Design using FEM, John Wiley & Sons, (2011), – 540 p. https://doi.org/10.1002/9783433600771.fmatter

5. Kindmann R. Design of truss and diaphragm type bracing / R. Kindmann, M. Krahwinkel // Steel construction 70, 2001. – pp. 885 – 899. https://doi.org/10.1002/stab.200102860

6. Krahwinkel, M.: For stressing stabilizing structures in steel construction. VDI Progress Reports, Series 4 Civil Engineering, No. 166. Düsseldorf: VDI-Verlag 2001. – 182 p.

7. Hudz S.A. Developed model of steel restrained elements design for stability by the compatible action of transverse bending and torsion / S.A. Hudz, G.M. Gasii, V.V. Darienko // Modern building structures made of metal and wood: Collection of scientific papers – Odesa: Odesa State University of Architecture and Construction, 2020. – Issue 24. – pp. 43 – 52.

8. Hudz S. Bearing capacity of steel I-beams operated with imperfections in the form of initial curvature in the plane of least stiffness / S.A. Hudz // Bulletin of the Odesa State Academy of Civil Engineering and Architecture. Issue # 61 – Odesa: Zovnishreklamkarservis, 2016. – pp. 95 – 101.

9. DBN V.2.6-198: 2014. Buildings structures. Steel structures. Design standards / Final edition. Official edition. – Entered into force on January 1, 2015 – K.: Ministry of Regional Development of Ukraine, 2014. – 199 p.

10. Semko V.O. Calculation and experimental studies of steel beams with curvature in the horizontal plane / V.O. Semko, S.A. Hudz // Collection of scientific papers. Resource-efficient materials, buildings and structures. – Issue 14. – Rivne: Publishing House of the National University of Water and Environmental Engineering, 2006. – pp. 317 – 322.

11. Assessment of the technical condition of steel building structures in operation: DSTU B.V.2.6-210: 2016 – [Effective from 2017-01-01] – K. : Mingerionbud of Ukraine, 2016. – 45 p.

12. EN 1993-1-1:2003. Eurocode 3: Design of steel structures. Part 1-1: General rules and rules for buildings. – Brussels: CEN, 2003. – 90 p.

13. EN 1993-1-3:2006. Eurocode 3: Design of steel structures. Part 1-3: General rules. Supplementary rules for cold-formed members and sheeting. – Brussels: CEN, 2006. – 130 p.

Збірник наукових праць. Галузеве машинобудування, будівництво
Academic journal. Industrial Machine Building, Civil Engineering
http://journals.nupp.edu.ua/znp
https://doi.org/10.26906/znp.2023.61.3850

UDC 624.971:624.014.2

The mobile communication antenna structures classification

Anton Hasenko [1], Yurii Padun [2]*, Mykola Bibik [3]

[1] National University «Yuri Kondratyuk Poltava Polytechnic» https://orcid.org/0000-0003-1045-8077
[2] National University «Yuri Kondratyuk Poltava Polytechnic» https://orcid.org/0009-0007-5785-1454
[3] National University «Yuri Kondratyuk Poltava Polytechnic» https://orcid.org/0009-0001-8681-486X

*Corresponding author E-mail: jurij.padun@gmail.com

The article analyses the problem of mobile communication antenna structures classification, considers their main design features, advantages and disadvantages. Generalized classification of mobile communication antenna structures operated in Ukraine is proposed. The regular recurrence of accidents and destruction of antenna structures indicate that the existing methods of calculation and design of such structures do not always take into account all their structural features. Technical and constructive solutions, peculiarities of operation of structures under load, aspects of application and their requirements for safe operation are considered, strengths and weaknesses of each type of antenna structures are given. One of the most effective and widely used antenna structures are lattice towers and masts. The main advantage of lattice towers is a small building area, however, from the point of view of consumption, steel masts are more cost-effective with the same height of the structure and payload. However, the cost of building an antenna structure is not always the main criterion for choosing its design scheme. First of all, radio-technical, technological and architectural requirements are of great importance. In the absence of restrictions on geometric parameters, preference is given to towers with a minimum number of faces, for example, when going from a 3-faceted to a 4-faceted tower, its weight increases by 10%. For technical and economic efficiency, not only rational types of cross-sections of elements are selected, but also various combined structural systems are developed. A good example is introduction into mass construction of combined supports on the basis of a conical concrete monopole CK-26, on top of which a steel lattice extension is installed. The structural disadvantage of the combined supports based on the conical concrete monopole CK-26 is their limited bearing capacity at the +2,000...+3,000 m mark, which in a number of cases led to accidental destruction in this particular area.

Key words: antenna structures, classification, mast, tower, combined support.

Класифікація антенних споруд мобільного зв'язку

Гасенко А.В.[1], Падун Ю.О.[2]*, Бібік М.В.[3]

[1,2,3] Національний університет «Полтавська політехніка імені Юрія Кондратюка»
*Адреса для листування E-mail: jurij.padun@gmail.com

У статті проаналізовано класифікації антенних споруд мобільного зв'язку за конструктивною схемою, розміщенням, матеріалом, типом перерізу та просторовою формою стовбуру; розглянуто їх основні особливості, переваги та недоліки. Узагальнена класифікація антенних споруд складена для тих, що експлуатуються на території Україні. Регулярна повторюваність аварій та руйнувань антенних споруд вказує на те, що існуючі методи розрахунку і проектування таких конструкцій не завжди враховують їх усі конструктивні особливості. Розглянуто технічні та конструктивні рішення, особливості роботи споруд під навантаженням, аспекти застосування та їх вимоги до безпечної експлуатації. Одними з найбільш ефективних та масово використовуваних антенних споруд є решітчасті вежі та щогли. Основною перевагою решітчастих веж є невелика площа забудови, однак з точки зору витрати сталі щогли є більш економічно ефективними при однаковій висоті споруди та корисному навантаженню. Проте, вартість будівництва антенної споруди не завжди є основним критерієм вибору її конструктивної схеми. Передусім, велике значення мають радіотехнічні, технологічні й архітектурні вимоги. При відсутності обмежень на геометричні параметри перевагу віддають вежам з мінімальною кількістю граней, наприклад, при переході від 3-х до 4-х гранної вежі її вага збільшується на 10%. Для техніко-економічної ефективності не тільки підбираються раціональні типи поперечних перерізів елементів, а й розробляються різні комбіновані конструктивні системи. Яскравим прикладом є впровадження у масове будівництво комбінованих опор на базі конічної залізобетонної стійки СК-26, поверх якої встановлена сталева решітчаста надставка. Конструктивним недоліком комбінованих опор на базі конічної залізобетонної стійки СК-26 є їх обмежена несуча здатність на відмітці +2,000…+3,000 м, що в ряді випадків призводило до аварійних руйнувань саме на цій характерній ділянці.

Ключові слова: антенні споруди, класифікація, щогла, вежа, комбінована опора.

Introduction

At the beginning of the development of mobile communication in Ukraine, one of the main disadvantages was a drastic deterioration in the quality of communication due to insufficient coverage or the remoteness of the user from the base station. The solution to this problem was the rapid and massive expansion and densification of the network of base stations and the modernization of already existing antenna-feeder equipment at antenna facilities. This greatly contributed to bringing the quality and speed indicators of telecommunications to a qualitatively new level [1]. However, the fast, massive, sometimes chaotic and unregulated construction had negative consequences, which was primarily reflected in the reliability of antenna structures, the inefficiency of the adopted constructive decisions and noncompliance with the requirements of the current legislation [2]. Today, the use of modern computers and software complexes in static and dynamic calculations, analysis of the reliability of antenna structures allows solving complex problems with a high degree of static uncertainty [3; 4]. In the past, it was practically impossible to solve problems of this complexity, and we had to be satisfied with approximate results.

Review of the research sources and publications

A number of foreign and national scientists were engaged in the research of mobile communication antenna structures. Currently, researchers have proposed a number of classifications of antenna structures, many features of each type have been considered. Molchanov raises the problem of the emergency of mobile communication facilities. The author notes a number of the main causes of accidents and recommendations for their prevention [5]. In their publication, Holodonov and Doan investigate the main impacts on antenna-mast structures during their operation, proposing a methodology for determining a complex risk indicator [6]. Nielsen in his work raises the problem of effective selection of types of structures in accordance with operating conditions, principles of their operation, specifics of perception of wind and ice loads [7; 8].

Definition of unresolved aspects of the problem

The regular frequency of accidents and destruction of antenna structures [9] indicates that the existing methods of calculation and design of such structures do not always take into account all their design features [10-12]. In addition, the study of the condition of antenna structures, their classification will allow to solve a large number of problems related to the general characteristics of the existing fund and predict problems that may arise in the future [13-14]. Available information and research in the field of antenna structures of mobile communication requires a clear classification, structuring and generalization.

Problem statement

The purpose of this work is the analysis and classification of antenna structures according to their structural features and the systematization of information about them.

Basic material and results

Antenna structures are a wide class of structures that are designed for placing technological and radio equipment on them. According to the construction scheme, antenna structures are divided into towers, masts and combined supports (see Fig. 1) [15]. A distinctive feature of antenna structures is their high height compared to the dimensions of their cross-sections, so their designs are mainly designed for atmospheric loads (wind, ice, temperature) [16-17].

To a large extent, the technical condition of antenna structures depends on the features and stages of communication development in Ukraine. The process of determining the technical condition of an individual construction is greatly simplified when data on design features, operation, durability and reliability of similar buildings are known.

Based on the own statistics of the results of technical surveys for the period 2017-2023, among the total number of 1,600 mobile communication antenna structures, masts make up – 41%, towers – 27%, combined supports – 9%, tubular towers – 3%, masts and large pipe supports on the roof – 20% of the total number of network objects. Depending on the specifics of the region and the density of buildings, the ratios for the types of structures may differ slightly.

The placement of mobile communication antenna structures is primarily conditioned by urban planning restrictions, the existing high-rise buildings and the possibility of potential lease of the land plot. Based on the characteristics of the area and the request of radio planning engineers regarding the need to expand the network, a decision is made on the feasibility of using a certain type of structures. Antenna structures can be placed on their own free-standing foundations, on the roofs of buildings, on other high-rise structures (smokestacks, water towers, etc.), on a technological container with the help of a support frame. In the absence of land lease restrictions, in rural areas constructions on their own foundations are usually preferred. This makes it possible not to be limited in the choice of the structural scheme of the building and to adopt the most economically attractive option.

In conditions of high-rise urban buildings, it is more appropriate to use the existing height effectively to place antenna structures on the roofs of buildings, while minimizing the required height of antenna structures and solving the potential problem of radio shading of adjacent buildings (reduction of signal quality due to the density of buildings). In addition, in a dense urban development, it is sometimes extremely difficult to find a potential site for the construction of buildings on their own foundations, and if it is available, it may be economically impractical for construction. Placement on other high-rise structures (smokestacks, water towers) is rational in industrial buildings, using the existing structures to install the necessary equipment with practically no additional requirements for the maximum wind area or weight.

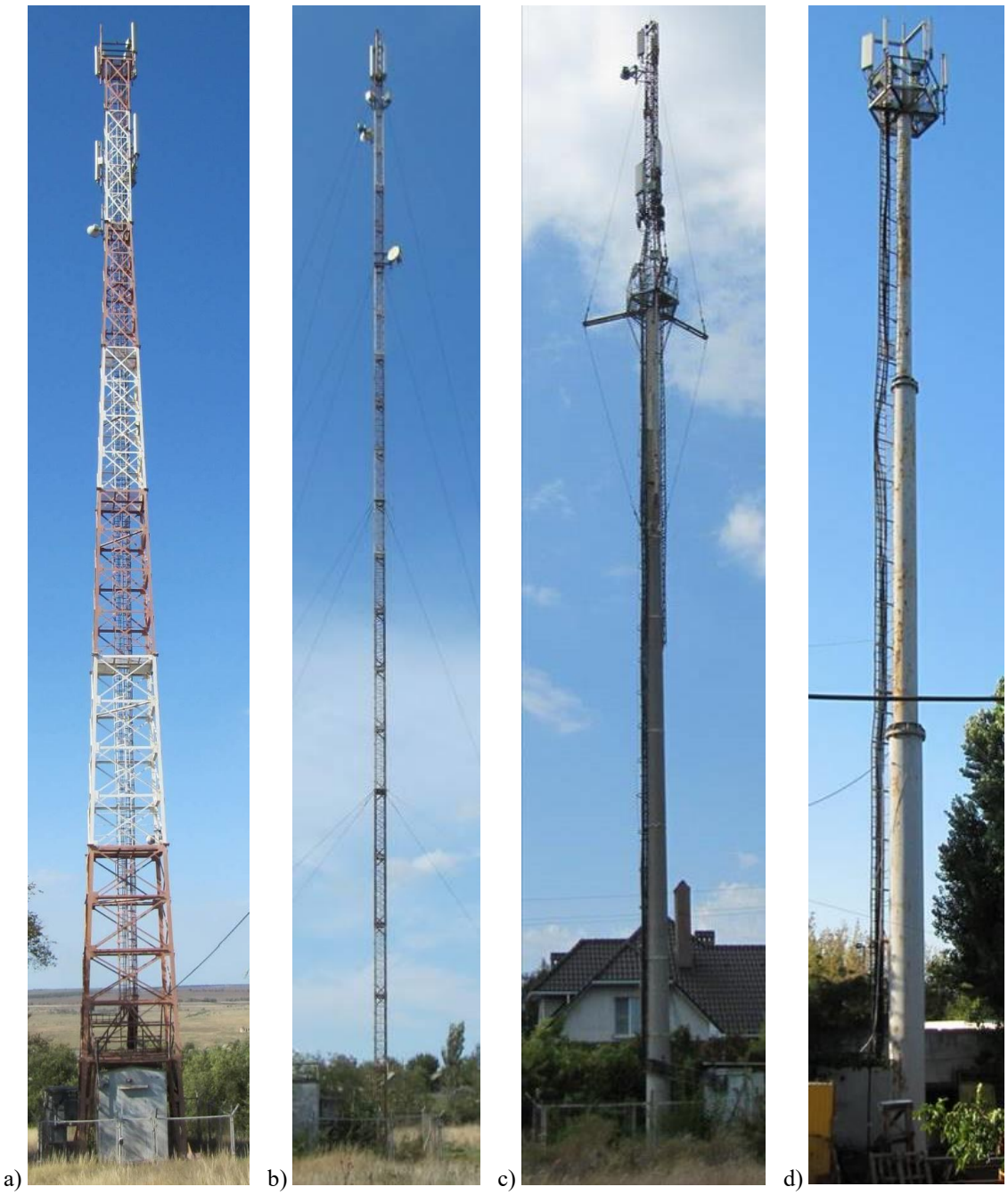

Figure 1 – General view of the tower (a), mast (b), combined support (c) and tubular tower (d)

Design schemes. Antenna structures are divided into towers, masts, combined supports, pipe supports on buildings and smokestacks.

A mast (see Fig. 1b) is a rigidly or hinged support installed on the foundation, which is unfastened in height by a system of elastic supports – braces – placed in one or more tiers. The cross-section of the trunk of the masts is most often lattice triangular or square, in some cases solid round. In the plan, the braces are placed in three or four directions. The number of tiers in height is from one to seven tiers. The optimal angle of inclination of the braces is 45-60°, with a further increase in the angle of inclination of the braces, the forces in the belts of the mast trunk increase. For each direction of braces, one foundation can be installed for all tiers, and separate foundations for each tier of braces.

The calculation scheme of the mast is a continuous multi-span beam, in which the elastic supports are the connecting nodes of the braces. Ties are flexible threads that are loaded with their own weight, the weight of ice and the force of the wind, the ends of which are fixed at different levels and have a preliminary tension. Such a cable-rod system has a complex operation under load and pre-tension of the ropes, which is related to the operation of the tensioners as flexible threads, and the calculation scheme may change when the load changes. Calculations of such a system are performed according to the deformed scheme by methods of gradual approximation.

The reliability of antenna-mast structures primarily depends on the technical condition of the ties, which are made of steel ropes. The situation is complicated by the

widespread use of ropes with an organic (hemp, sisal) or synthetic (polypropylene) core as tensioners, which have increased flexibility and are intended for use in pulleys, winches, elevators and are not intended for use in tensioners of antenna-mast structures, have significantly less (by 20-30%) breaking force in contrast to ropes with a steel core.

In the basic scenario, masts are more economical than towers, but a much larger area is required for their installation (for masts, the building area can be approximately 400-800 m^2, for towers of a similar height – 20-40 m^2). In addition, masts can perceive the useful antenna load much less than lattice towers.

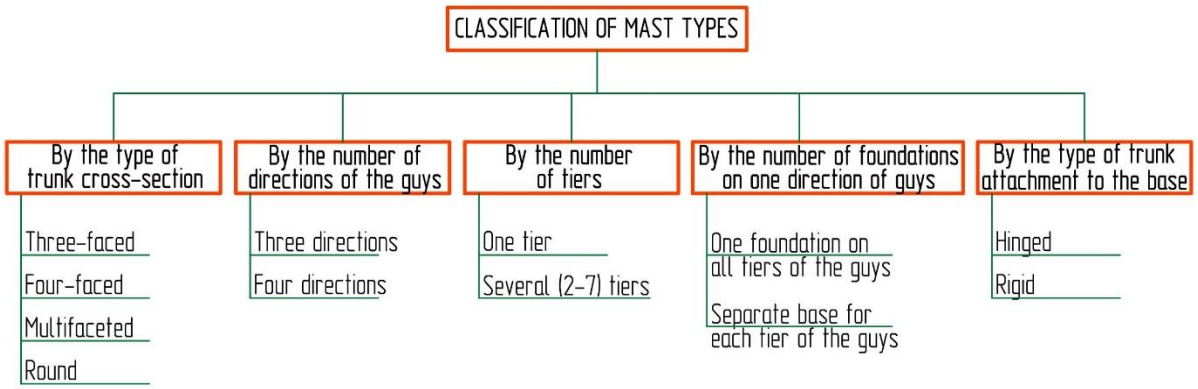

Figure 2 – Classification of mast types

Tower (see Fig. 1a) is a cantilever-type support rigidly installed on the foundation. According to the type of cross section, the towers are divided into through (lattice) and continuous (tubular, conical) towers.

According to their design features, the towers belong to complex engineering structures, this is due to their functional purpose and the nature of the force loads they perceive during operation. The use of towers has an advantage for construction in mountainous conditions when it is difficult to place anchor foundations for mast braces.

The most widespread is the design of the tower, the geometric scheme of which fits into the figure formed by the rotation of a broken line around a vertical axis. Due to belt breaks, the shape of the tower approaches the one that follows the shear of moments from wind load.

Lattice towers usually have a triangular or square, rarely polygonal cross-section. The tower consists of pyramidal or prismatic sections with combined bases. The main elements of the tower are belts, the axes of which coincide with the edges of the sections, struts and braces are placed in the plane of the faces. Rigid diaphragms are installed in part of the cross-sections (at a distance of no more than 3 cross-sections), which prevent the cross-section from changing.

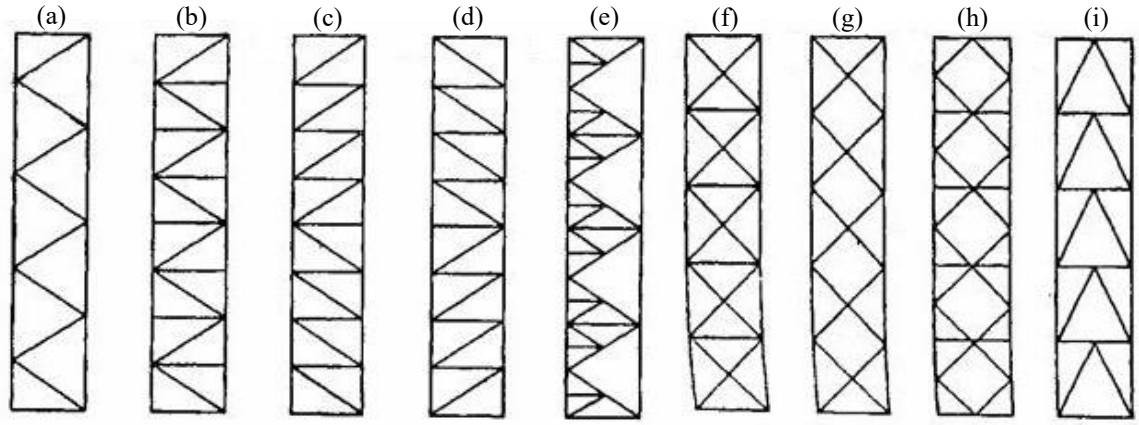

Figure 3 – Types of tower lattices: triangular (a), triangular with additional supports (b), canted with ascending braces (c), canted with descending braces (d), sprengel (e), cross (f), crosswise (g), rhombic (h), semi-canted (i)

Canted and triangular lattices (see Fig. 3a-d) consist of elements that work both in compression and tension. The cross-sectional area of the elements is selected according to the compressive strength. These grids have a relatively smaller number of elements and simple connection nodes. They are convenient for manufacturing and installation, but braced and triangular lattices are used for small panel sizes (relative to the cross-section of the element) in order to avoid increasing the

weight of braces and spacers due to limitations in their flexibility.

Cross lattice (see Fig. 3f) in towers usually it is used with braces, which are excluded from work in compression and work only in tension. At the same time, only compressive force occurs in the spacer, which connects the intersection nodes of the braces with the belts. An auxiliary spacer in the grid serves to unfasten the free length of the belt. The structure of the cross lattice allows pre-tensioning of its elements (braces made of round steel with tension couplings). Compared to the diagonal and triangular lattice, it has more complex nodes.

In the rhombic lattice (see Fig. 3h) the main struts are absent, and the braces work in compression and tension. As in the cross lattice, the additional strut serves to untie the free length of the belt.

Cross and rhombic lattices are most often used in the construction of mobile communication towers. They are very different from each other by the nature of work. Under equal conditions (the same magnitude of the transverse force, the size of the panels, the type of cross-section of the belt elements), the cross-sectional area in the braces of the rhombic lattice is selected for the force approximately two times less than in the braces of the cross. This circumstance often puts the rhombic lattice in a more favourable position compared to the cross lattice.

Semi-canted grid (see Fig. 3i) is used much less often, mainly in those cases when it is planned to place a large number of antenna-feeder equipment on technological sites and with increased requirements for the deformability of the tower. It is distinguished by the relative simplicity of nodes compared to other types of lattices, but under normal conditions it has a greater relative weight than the cross lattice.

In the absence of restrictions on geometric parameters, preference is given to towers with a minimum number of faces. The weight of the tower depends on the number of faces. For example, when moving from a 3-faced tower to a 4-faced tower, its weight increases by 10%, and the difference in the number of main elements can be up to 35%.

The height of lattice towers varies in a wide range - from 40 to 500 m. Lattice towers are usually made of corners or tubular elements. The belts of the tower rest on free-standing reinforced concrete foundations that act in compression, pull-out force and shear force.

Tower structures are more convenient for installation and operation of antenna-feeder equipment, as well as for maintenance of the structure itself, since there is no need for periodic adjustment of tension and replacement of ropes, unlike in masts.

Tubular tower (see Fig. 1d) is a cantilever support of a solid cross-section, consisting usually of several separate tubular sections 6-12 m high, the sections are connected on the flanges with the help of high-strength bolts. The height of tubular towers is most often in the range of 30–50 m. The construction of tubular towers of greater height is not implemented, because the design solution completely loses its economic feasibility. The main advantage of this type of construction is the minimum requirements for the building area and relative invisibility in the architectural ensemble of the city, however, the cost of construction is much higher than other structures of similar height.

Combined support (combination of tower and mast, see Fig. 1c) is a conical concrete monopole CK-26 rigidly buried in the ground, on top of which a lattice extension is installed, unfastened by additional elastic supports - braces, which are attached to horizontal elements (beams).

The appearance of combined supports is due to unification of structures with an economically acceptable price and with minimal requirements for land acquisition of the site for development. This type of construction generally met the above requirements and played a significant role in the rapid deployment of the cellular network throughout Ukraine. But it also had its design flaws, namely the limited bearing capacity of the conical concrete monopole CK-26, which in turn imposed rather strong restrictions on operation in various windy areas and the installation of the maximum possible number of antenna-feeder equipment. As a result, during operation with an increase in the number of antenna-feeder equipment on the antenna structure, the maximum moment in the rack may exceed the permissible moment in terms of bearing capacity. The failure of a reinforced concrete column occurs in a specific area at +2,000...+3,000m above ground level – a combination of close to the maximum moment and a decrease in the number of rods of prestressed reinforcement in the cross section of the column.

Types of connections. In the vast majority of cases, antenna structures are made prefabricated, in the form of starting marks – sections, 2-6 m high (for convenience of installation and transportation). Bolted connections are made through flanges or overlays made of rolled metal, usually using bolts of strength class not lower than 8.8 (see Fig. 4). Less often, sections are connected using welding or bushings (boltless, exclusively in masts).

The calculation of bolted connections, depending on their type, is performed both for tensile forces (flange connections) and shear forces (connections on pads). When determining the number of bolts in flange connections, they tend to reduce their diameter. This leads to a decrease in the diameter of the circle along the centers of the bolts and, as a result, to a decrease in the weight of the flanges. The calculation of the thickness of the flanges is performed taking into account the work of the pipe wall.

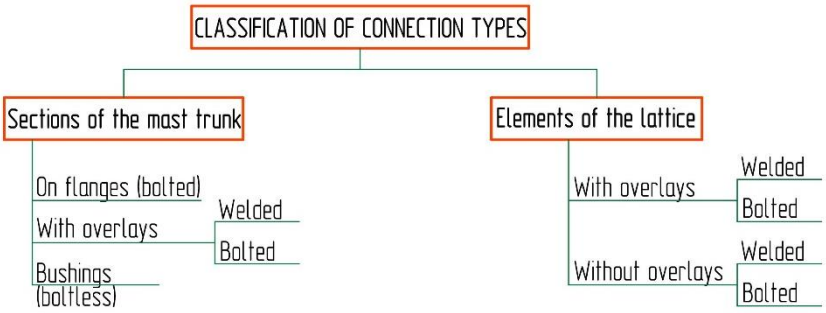

Figure 4 – Classification of connection types in antenna structures

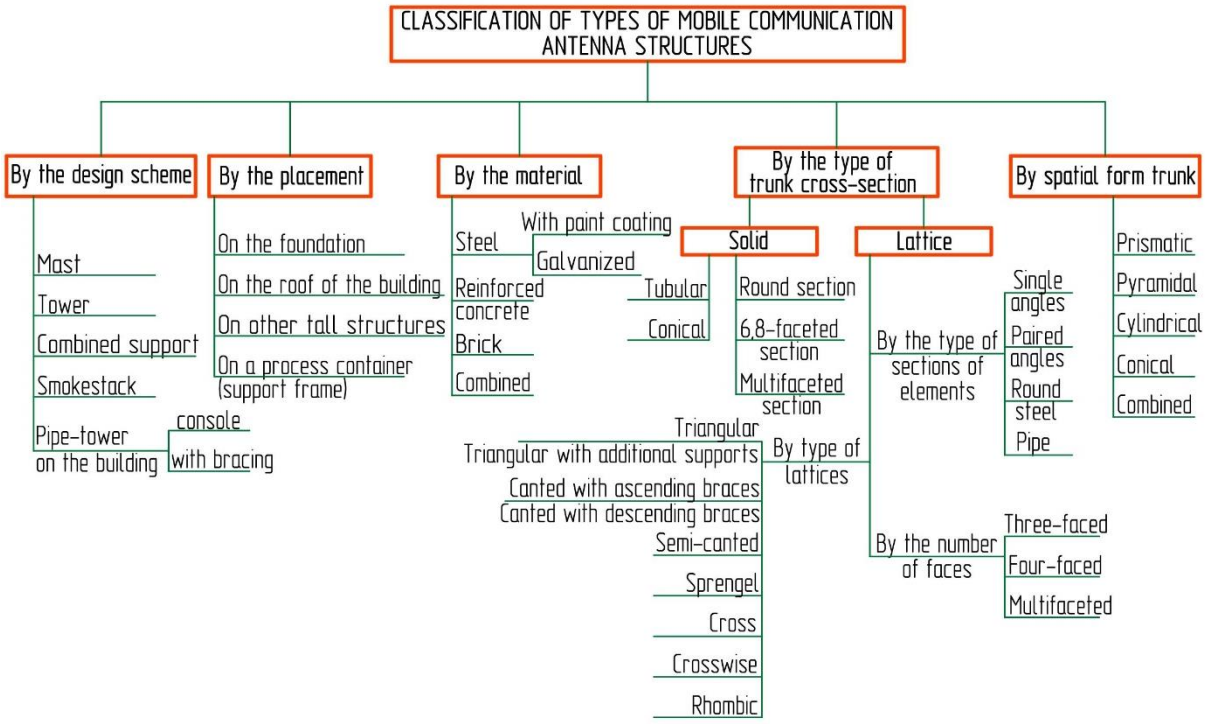

Figure 5 – Classification of types of mobile communication antenna structures

Conclusions

In the article a generalized classification of types of mobile communication antenna structures that are operated on the territory of Ukraine is provided (see Fig. 5).

The cost of building an antenna structure is not always the main criterion for choosing its design scheme. First of all, radio-technical, technological and architectural requirements are of great importance. In general, masts are more economical than lattice towers, but their installation requires a much larger area of land. In addition, masts perceive the useful antenna load less than lattice towers.

The use of lattice towers has an advantage for construction in mountainous conditions when it is difficult to place anchor foundations for mast braces. In the construction of lattice towers, cross and rhombic lattices are most often used. Under equal conditions (the same magnitude of the transverse force, the size of the panels, the type of cross-section of the belt elements), the cross-sectional area in the braces of the rhombic lattice is selected for the force approximately two times less than in the braces of the cross. This circumstance often puts the rhombic lattice in a more favourable position compared to the cross lattice.

In the absence of restrictions on geometric parameters, preference is given to towers with a minimum number of faces. The main advantage of tubular towers is the minimum requirements for the building area and relative invisibility in the architectural ensemble of the city, however, the cost of construction is much higher than other structures of similar height. When moving from a 3-faced to a 4-faced tower, its weight increases by 10%, and the difference in the number of elements can be up to 35%.

The appearance of combined supports solved the demand for fast and massive construction, for the unification of structures and for minimum requirements for the building area. But it also has its design flaws, namely the limited load-bearing capacity of the conical concrete monopole CK-26, which in a number of cases led to accidental destruction.

References

1. Smith, B.W. (2007). *Communication structures.* London: Thomas Telford. https://doi.org/10.1680/cs.34006
2. Murty, K.S. (Ed.). (2002). *Dynamic Response of Lattice Towers and Guyed Masts. Reston: ASCE.*
3. Павловський, В.Ф., Кондра, М.П., (1979). *Сталеві башти (проектування та монтаж)*. Київ: Будівельник.
4. Пічугін, С.Ф., (2018). *Металеві конструкції. Спеціальні металеві конструкції. Курс лекцій – частина 5.* Полтава: ПолтНТУ.
5. Молчанов, Д.С. (2013). Аварії опор мобільного зв'язку. *Сборник научных трудов ОГАСА «Современные строительные конструкции из металла и древесины», 17,* 152-157.
6. Голоднов, О.І., Доан, Н.Т. (2010). Дослідження основних впливів на технічний стан антенно-щоглових споруд. *Збірник наукових праць Українського науково-дослідного та проектного інституту сталевих конструкцій імені В.М. Шимановського, 5*, 237-245.
7. Mogens G. Nielsen. (2009). The Analysis of Masts and Towers. *International Journal of Space Structures,* 24(2), 97-102.
https://doi.org/10.1260/026635109789043269
8. Mogens G. Nielsen. (2019). *New Eurocode for Towers, Masts and Chimneys,* The 14thNordic Steel Construction Conference 2019. Berlin: Ernst&Sohn.
https://doi.org/10.1002/cepa.1094
9. Smith B. (2009). *50 years in the Design of Towers and Masts From IASS Recommendations to Current Procedures,* (IASS) Symposium 2009. Valencia: Editorial Universitat Politècnica de València.
10. DSTU - NB EN 1993-3-1. (2013). Eurocode 3. Design of steel structures. Part 3-1. Towers, masts and chimneys. Towers and masts. Kyiv: Ministry of the Regions of Ukraine.
11. DBN V.2.6-198:2014. (2014). *Steel structures. Design standards*. Kyiv: Ministry of the Region of Ukraine.
12. DSTU B V.2.6-125:2010. (2010). *Centrifuged conical reinforced concrete risers for supports of high-voltage power lines. Design and dimensions*. Kyiv: Ministry of Regional Construction of Ukraine.
13. Pezo, ML, Bakic, VV, Markovic, ZJ (2016). Structural analysis of guyed mast exposed to wind action. *Thermal Science,* 20(5), 1473-1483.
https://doi.org/10.2298/TSCI16S5473P
14. Juozapaitis, A., Jatulis, D., Šapalas, A. (2009). Design and analysis of combined plane steel guyed tower-mast. *Statybinės constructions and technologies,* 1(4), 157-165. https://doi.org/10.3846/skt.2009.19
15. Belevičius, R., Jatulis, D., Rusakevičius, D (2024). Optimal Schemes of Tall Pinned Masts. *KSCE Journal of Civil Engineering,* 28, 904–915.
https://doi.org/10.1007/s12205-023-1087-8
16. Ching Wen Chien. (2010). Wind - resistant design of high mast structures. *Journal of the Chinese Institute of Engineers*, 33(4), 597-615. https://doi.org/10.1080/02533839.2010.9671648
17. Gioffrè, M., Gusella, V., Materazzi, A., Venanzi, I., (2004). Removable guyed mast for mobile phone networks: wind load modeling and structural response. *Journal of Wind Engineering and Industrial Aerodynamics,* 92(6), 463–475. https://doi.org/10.1016/j.jweia.2004.01.006

1. Smith, B.W. (2007). *Communication structures.* London: Thomas Telford. https://doi.org/10.1680/cs.34006
2. Murty, K.S. (Ed.). (2002). *Dynamic Response of Lattice Towers and Guyed Masts. Reston: ASCE.*

3. Pavlovsky, V.F., Kondra, M.P., (1979). *Steel towers (design and installation).* Kyiv: Budivelnyk.
4. Pichugin, S.F., (2018). *Metal structures. Special metal structures. Course of lectures - part 5.* Poltava: Poltava National Technical University.
5. Molchanov, D.S. (2013). Accidents of mobile communication towers. *Collection of scientific works of OGASA "Modern building constructions of metal and wood", 17,* 152-157.
6. Holodnov, O.I., Doan, N.T. (2010). Study of the main influences on the technical condition of antenna-mast structures. *Collection of scientific works of the Ukrainian Research and Design Institute of Steel Structures named after V.M. Shymanovsky, 5*, 237-245.

7. Mogens G. Nielsen. (2009). The Analysis of Masts and Towers. *International Journal of Space Structures,* 24(2), 97-102.
https://doi.org/10.1260/026635109789043269
8. Mogens G. Nielsen. (2019). *New Eurocode for Towers, Masts and Chimneys,* The 14thNordic Steel Construction Conference 2019. Berlin: Ernst&Sohn.
https://doi.org/10.1002/cepa.1094
9. Smith B. (2009). *50 years in the Design of Towers and Masts From IASS Recommendations to Current Procedures,* (IASS) Symposium 2009. Valencia: Editorial Universitat Politècnica de València.
10. DSTU - NB EN 1993-3-1. (2013). Eurocode 3. Design of steel structures. Part 3-1. Towers, masts and chimneys. Towers and masts. Kyiv: Ministry of the Regions of Ukraine.
11. DBN V.2.6-198:2014. (2014). *Steel structures. Design standards*. Kyiv: Ministry of the Region of Ukraine.
12. DSTU B V.2.6-125:2010. (2010). *Centrifuged conical reinforced concrete risers for supports of high-voltage power lines. Design and dimensions*. Kyiv: Ministry of Regional Construction of Ukraine.
13. Pezo, ML, Bakic, VV, Markovic, ZJ (2016). Structural analysis of guyed mast exposed to wind action. *Thermal Science,* 20(5), 1473-1483.
https://doi.org/10.2298/TSCI16S5473P
14. Juozapaitis, A., Jatulis, D., Šapalas, A. (2009). Design and analysis of combined plane steel guyed tower-mast. *Statybinės constructions and technologies,* 1(4), 157-165. https://doi.org/10.3846/skt.2009.19
15. Belevičius, R., Jatulis, D., Rusakevičius, D (2024). Optimal Schemes of Tall Pinned Masts. *KSCE Journal of Civil Engineering,* 28, 904–915.
https://doi.org/10.1007/s12205-023-1087-8
16. Ching Wen Chien. (2010). Wind - resistant design of high mast structures. *Journal of the Chinese Institute of Engineers*, 33(4), 597-615. https://doi.org/10.1080/02533839.2010.9671648
17. Gioffrè, M., Gusella, V., Materazzi, A., Venanzi, I., (2004). Removable guyed mast for mobile phone networks: wind load modeling and structural response. *Journal of Wind Engineering and Industrial Aerodynamics,* 92(6), 463–475. https://doi.org/10.1016/j.jweia.2004.01.006

Збірник наукових праць. Галузеве машинобудування, будівництво
Academic journal. Industrial Machine Building, Civil Engineering
http://journals.nupp.edu.ua/znp
https://doi.org/10.26906/znp.2024.63.3883

UDC 624.012.4-183.2:624.94.012.45:624.042.65

Studies of multilayer bent reinforced concrete structures of rectangular cross section review

Dmytrii Romanenko [1]

[1] The Separated Structural Subdivision Rubizhne Professional College of State Institution «Luhansk Taras Shevchenko National University» https://orcid.org/0009-0004-1265-4535
*Corresponding author E-mail: alpintel@ukr.net

Reducing the use of cement and reducing the weight of concrete in bending reinforced concrete elements is an important task in modern construction. To solve this problem, various methods are being implemented, including the use of both removable and non-removable void formers, and the combination of several materials (e.g., heavy in the compressed zone and light in the tensile zone of concrete) for their mutually beneficial joint operation. The paper provides an overview of several experimental and theoretical studies in these areas, which substantiate the possibility and feasibility of reducing the strength of concrete in the tensile zone of bending reinforced concrete structures, and as a result, reducing the consumption of cement for the preparation of concrete mix for structures, without prestressing the latter. The use of two- and multi-layer elements reduces the dead weight of structures, improves sound and thermal insulation properties, which leads to savings in materials, labor and financial resources. The right choice of material for each layer allows for the creation of structures with high performance characteristics.

Keywords: test, experiment, reinforced concrete, bending, multilayer.

Огляд досліджень багатошарових згинаних залізобетонних конструкцій прямокутного поперечного перерізу

Романенко Д.Б.[1]

[1] Відокремлений структурний підрозділ «Рубіжанський фаховий коледж» Державного закладу «Луганський національний університет імені Тараса Шевченка»
*Адреса для листування E-mail: alpintel@ukr.net

Зменшення використання цементу та зниження ваги бетону у згинальних залізобетонних елементах є важливим завданням у сучасному будівництві. Для його вирішення впроваджуються різні методи, зокрема використання як знімних, так і незнімних пустото утворювачів, поєднання декількох матеріалів для взаємовигідної їх сумісної роботи. Хоча у нормативних документах зазначено, що бетон в розтягнутій зоні не працює, попри це, бетон у розтягнутій зоні традиційно приймають того ж класу міцності, що й у стиснутій зоні елемента. Однак систематизований огляд досліджень можливості заміни розтягнутого бетону у таких конструкціях на більш дешевий матеріал, наприклад бетон меншого класу по міцності чи із пористими заповнювачами, не виконаний. Метою роботи є огляд експериментальних і теоретичних досліджень, що обґрунтовують можливість та доцільність зменшення міцності бетону в розтягнутій зоні згинальних залізобетонних конструкцій, і як результат зменшення витрат цементу на приготування бетонної суміші для конструкцій, без попереднього напруження останніх. Глуховський В.Д. і Пахомов В.А. вперше науково обґрунтували застосування шлаколужного цементу замість портландцементу для виробництва розтягнутої частини залізобетонних конструкцій. Байков В.М. та Сігалов Е.Є. розробили ряд прикладів, в яких наведено економічне обґрунтування застосування бетонів меншого класу у розтягнутій зоні. Дослідники Національного університету «Львівська політехніка» Рутковська І.З., Рутковський З.М., Вознюк Л.І., Марущак А. провели експериментальні дослідження тришарових балок, виготовлених у двох серіях: у першій серії середній шар складався з керамзитобетону, у другій – із пінобетону. Науковці з В'єтнаму T.Q.K. Lam, T.M.D. Do, V.T. Ngo, T.T.N. Nguyen, D.Q. Pham експериментальним шляхом та методом чисельного моделювання дослідили зміну класу бетону у шарах тришарових сталефібробетонних балок. Слід відзначити, що багатошарові згинані залізобетонні конструкції із бетоном меншого класу утворюються також у під час підсилення. Так Мазурак А., Ковалик І. та інші наводять результати експериментальних випробувань залізобетонних конструкцій, підсилених торкретуванням.

Ключові слова: випробування, експеримент, залізобетон, згинання, багатошаровість.

Introduction

Reducing the use of cement and reducing the weight of concrete in bending reinforced concrete elements is an important task in modern construction [1]. Various methods are being implemented to solve this problem, including the use of both removable and non-removable void fillers made of cardboard-polyethylene, asbestos cement or plastics with various cross-sectional shapes: round, square, vertical, elliptical or oval [2]. Slag and fly ash concretes are also used, and optimising the size and ratio of crushed stone to sand helps to achieve this goal [3-4]. Another option is to replace stretched concrete in such structures with a cheaper material, such as concrete of a lower strength class or with porous aggregates. Therefore, the review and systematisation of the results of experimental studies of multilayer bent reinforced concrete structures is an urgent issue.

Review of the research sources and publications

The growing volume of reconstruction and modernisation of buildings requires efficient and cost-effective structural solutions. The idea of multilayered structures has a long history, but its development has been significantly accelerated by its use in aviation and aerospace, where lightweight and durable materials are required [5]. Today, multilayer reinforced concrete structures are becoming increasingly common in construction. The use of lightweight concrete with porous aggregates helps to create energy-efficient solutions. The use of two- and multi-layer elements with porous aggregates can significantly improve sound and thermal insulation characteristics, as well as reduce the dead weight of structures, which leads to savings in materials, labour and financial resources [6]. However, the right choice of material for each layer allows for the creation of structures with high performance characteristics.

In their research [7], scientists propose using ash, ground slag, metallurgical waste, slag-alkali concrete, chemical additives (potash, liquid glass, plasticisers), aggregates and void fillers, as well as improving the composition of concrete mixtures and their heat treatment to reduce concrete and cement consumption.

Publication [8] describes a method for the production of precast concrete slabs with oval cavities, which is aimed at reducing the consumption of concrete and cement during their manufacture. However, this method has not gained popularity in mass production due to the destruction of the walls of the oval holes when the punches are removed from the newly formed slab.

Baikov V.M. and Sigalov E.E. noted that with a nominal span of 6 m, the most economical in terms of concrete consumption are slabs with oval cavities, the thickness of the concrete layer of which is 92 mm, compared to 120 mm for slabs with round cavities. At the same time, the production of such panels is accompanied by technological difficulties: after the removal of the void formers, the walls of the channels in newly formed products sometimes collapse. For this reason, boards with round cavities are standardised for production. Further development of technologies allows us to move to more economical designs.

Glukhovsky V.D. and Pakhomov V.A. were the first to scientifically substantiate the use of slag cement instead of Portland cement for the production of concrete and reinforced concrete structures.

Current regulations [5] define cement consumption rates for the manufacture of concrete and reinforced concrete products. The regulated amount of cement per 1 m³ of concrete must ensure the design properties, such as compressive strength class, density grade, frost resistance and water resistance.

An interesting method of reducing concrete consumption in the production of floor slabs is the use of non-removable plastic void formers of various shapes (washer, spherical, box) [2; 9], as well as stone materials. This method can reduce concrete consumption by up to 30 % compared to solid slabs.

Definition of unsolved aspects of the problem

Thus, the creation of resource-saving reinforced concrete structures involves the search for new types of them from one material or in combination of several materials for their joint mutually beneficial operation, reduction of their cost while ensuring the same bearing capacity, increase of manufacturing manufacturability, etc. It should be noted that in calculations of the total bearing capacity of a structure, stretched concrete is not taken into account, but only increases its weight and, consequently, the cost of manufacturing. However, a systematic review of studies on the possibility of replacing stretched concrete in such structures with a cheaper material, such as concrete of a lower strength class or with porous aggregates, has not been carried out. Also, the impact of physical and mechanical characteristics of the layers, their thickness and the method of reinforcement on the strength and deformation properties of such structures remains insufficiently investigated. The design of such structures is difficult due to the imperfection of theoretical calculations for the limit states.

Problem statement

The purpose of the paper is to review experimental and theoretical studies that substantiate the possibility and feasibility of reducing the strength of concrete in the tensile zone of bending reinforced concrete structures, and as a result, reducing the consumption of cement for the preparation of concrete mix for structures without prestressing the latter.

Basic material and results

Baikov V.M. and Sigalov E.E. note that in sections perpendicular to the longitudinal axis of elements (under bending, off-centre compression or tension), at a stage close to destructive loads, the same stress-strain state is characteristic under conditions of a two-digit stress diagram. In calculating the strength of elements, the forces perceived by a section perpendicular to the longitudinal axis of the element are determined by the calculated material resistances, taking into account the coefficients of working conditions [10].

The following assumptions are used: concrete in the tensile zone is inactive, i.e., its resistance f_{ctk} is zero;

concrete in the compressed zone has a rectangular stress diagram with a design resistance f_{ck}; longitudinal reinforcement operates within the design stresses $\sigma_s \leq f_{yd}$, and in the compressed zone, reinforcement is subjected to stresses f_{ck}.

Nevertheless, concrete in the tensile zone is traditionally assumed to be of the same strength class as in the compressed zone of the element. The authors also note that the load-carrying capacity of the element is ensured by various combinations of cross-sectional dimensions and the number of reinforcement bars. The cost of reinforced concrete elements is close to the optimum under the conditions:

μ=1-2% at x/h_0=0.3-0.4 for beams;

μ=0.3-0.6% at x/h_0=0.1-0.15 for slabs.

To reduce cement consumption, it is proposed in [11] to use concrete of reduced strength in the lower (tensile) zone of the element.

Examples of calculations of the economic efficiency of using concrete of a lower strength class in the tensile zone of beams according to [11].

Example 1: Precast concrete beam without prestressing, dimensions 6(L)×0.5(h)×0.2(b) m. The concrete used was C16/20 class with cement grade 400, the cement consumption per beam was 340 kg/m³ with a yield strength of 80%. The volume of concrete in the beam was V_b=6×0.5×0.2=0.6 m^3, and the cement consumption was 0.6×340=204 kg. After replacing the concrete in the tensile zone with C8/10 concrete, the cement consumption is reduced to 0.446 m^3×235 = 104.9 kg. In the compressed zone, the cement consumption is 0.6 - 0.446 m^3 × 340 = 53.76 kg. The total cement consumption after the changes is 158.66 kg, which is 22.23% less.

Example 2: A monolithic reinforced concrete slab with a thickness of 24 cm. Concrete volume per 1 m^2: 0.24 m3. Initial cement consumption: 370 kg/m^3 × 0.24 = 88.8 kg. After replacing the concrete in the tensile zone with C8/10 class, the cement consumption is reduced to 49 + 11.66 = 60.66 kg, which is 31.7% less.

Example 3: Precast concrete slab with dimensions of 630×150×22 cm with voids. Initial cement consumption for C20/25 concrete: 547.83 kg. After replacing the concrete in the tensile zone with C8/10 class, the cement consumption decreased by 33.5%.

It should be noted that multilayer bent reinforced concrete structures with concrete of a lower class are also formed during reinforcement. Thus, A. Mazurak, I. Kovalyk, V. Mykhaylechko, P. Ambrozyak [12] describe the methodology for experimental studies of reinforced concrete elements reinforced with shotcrete at different levels of loading. The aim of the study is to evaluate the bearing capacity, deformability, and crack resistance of reinforced concrete elements reinforced by different methods, taking into account the technological features of reinforcement. Additionally, a methodology for experimental testing of reinforced concrete beams has been developed, taking into account the residual stresses before their reinforcement. The design and calculation of the experimental beams were based on the analysis of literature sources, current standards, and previous experience in conducting similar studies. To test the methodology, three series of reinforced concrete beams with dimensions of 2300 × 200 × 80 mm and a working span of 2100 mm were manufactured. The beams were reinforced using different technological schemes depending on the series (see Fig. 1): on one side, on both sides and with a U-shaped cage from below and on both sides simultaneously.

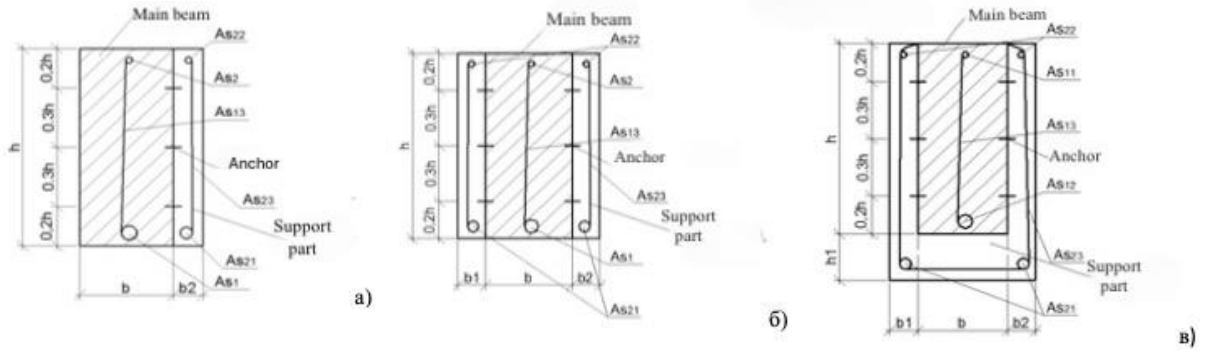

Figure 1 – Amplification schemes of prototypes: a) series 1; b) series 2; c) series 3

To determine the main characteristics, such as bearing capacity, deformability and crack resistance, as well as to assess the effect of the load level on the stress-strain state of the reinforced specimens, bending tests were carried out under short-term concentrated load. The prestressing load levels for the beams reinforced by the shotcrete method were 0, 0.32, 0.45, and 0.63 of the destructive load under conditions of reinforcement yield.

The loading process was carried out in two stages:

1. Before strengthening - the specimens were loaded on a bench in one-third of the section span using weights, springs and a threaded device. Load control was carried out using pre-calibrated springs, threaded tighteners and a lever wrench with a dynamometer. The load was increased gradually ($\Delta F < 0.05\ F_{max}$) with a holding time of 25 min at each step.

2. After strengthening, the beams were tested on a test bench using a hydraulic jack (250 kN) and a distribution beam. The forces were monitored using dynamometers located on the beam supports. The loading was also carried out gradually: before the appearance of cracks with an increase of $\Delta F < 0.05\ F_{max}$, and after

their appearance - by $\Delta F < 0.1\ F_{max}$, with a holding time of 20 min.

To record the deformations, we used:
- clock-type indicators (accuracy 0.01 mm) for measuring deflections of beams;
- micro-indicators (accuracy 0.001 mm) to determine the deformations of concrete and reinforcement;
- electric strain gauges (50 mm base) to measure stresses in the zone of maximum bending moment;
- MPB-2 microscope for recording the moment of crack formation and determining their width.

To improve visual control over the development of cracks, the surface of the beams was painted with water-based paint or putty. The test results were recorded in the relevant journals.

The authors A. Mazurak, I. Kovalyk, P. Ambrozyak, V. Mykhaylechko, [13] proposed methodology made it possible to evaluate the bearing capacity, crack resistance and deformability of reinforced concrete beams reinforced by shotcrete, i.e. two-layer reinforced concrete beams, taking into account the residual stresses before the moment of reinforcement.

Researchers of Lviv Polytechnic National University I.Z. Rutkovska, Z.M. Rutkovskyi, L.I. Vozniuk, A. Marushchak [14] conducted experimental studies of three-layer structures. A methodology for studying three-layer reinforced concrete beams manufactured in two series was proposed. In the first series, the middle layer consisted of expanded clay concrete, and in the second - of foam concrete. Control cubes and prisms were tested to assess the properties of the materials. The beams were mounted on two supports, one movable and one fixed, and the load was applied by two concentrated forces located on the upper face in one-third of the span. The loading process was carried out in gradual stages. To prevent deformations in the areas of concentrated load and supports, distributing steel plates were used on a layer of cement-sand mortar. During the experiment, the moment of crack formation and development were monitored.

The purpose of this experimental study was to improve the methodology for assessing the stress-strain state of three-layer reinforced concrete structures. For this purpose, two series of three-layer reinforced concrete beams (four in each), as well as 12 concrete prisms and 12 control cubes were manufactured (see Fig. 2). The test specimens had dimensions of 1200 × 90 × 120 mm. All beams were reinforced with longitudinal reinforcement of A400C class and transverse reinforcement of Bp1200 class, with a transverse reinforcement spacing of 50 mm. The middle layer of the first series consisted of expanded clay concrete, the second of foam concrete, while the outer layers were made of heavy concrete. The thickness of the inner layer was 40 mm, the upper layer was 30 mm, and the lower layer was 50 mm.

The spatial frame of the reinforcement was made by resistance welding. The concrete mix was made of M500 cement, quartz sand and granite crushed stone. The prismatic strength and initial elastic modulus were determined using a 2PG-100 press, with measurements made on specimens of different sizes. Concrete deformations were recorded with micro-indicators with an accuracy of 0.001 mm. The control tests confirmed that the average prismatic strength of expanded clay concrete was 4.88 MPa, foam concrete - 5.03 MPa, and heavy concrete - 15.28 MPa.

The beams were concreted in batches at the factory and underwent a standard manufacturing cycle, including moulding, compaction and heat treatment. After being transported to the laboratory, they were stored at a temperature of 8-10 °C until the test. The beams were loaded in gradual stages, with control measurements made at each stage of loading. To ensure the accuracy of deflection measurements, used clock-type indicators with a division price of 0.01 mm and for deformations used electric strain gauges.

The results of the experiments showed the effectiveness of the improved methodology for the study of three-layer reinforced concrete beams. The data obtained allow us to better understand the stress distribution, the process of crack formation and development, as well as the behaviour of structures under load. The research results open up new prospects for the further development of multilayer reinforced concrete structures in construction.

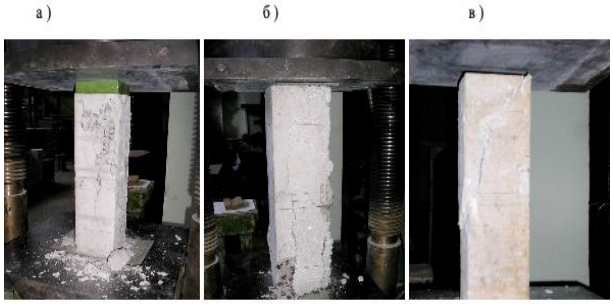

Figure 2 – Fracture pattern of prism samples: a) heavy concrete; b) foam concrete; c) expanded clay concrete

Other researchers - A.V. Mazurak, V.M. Kalitovsky, M.Y. Yukhym, T.A. Mazurak [15] - conducted experimental studies of reinforced concrete beams made and reinforced with shotcrete (see Fig. 3). The main objective of this study is to develop a methodology for assessing the parameters, deformation characteristics, crack resistance and bonding strength of new and old concrete when reinforcing bending reinforced concrete structures with shotcrete. The design and calculation of the experimental beams were performed in accordance with the current regulatory requirements for standard reinforced concrete elements.

The basic shotcrete mixture tested on the test specimens was prepared by dry mixing and had the following composition by weight: sand - 22%, screenings - 9%, crushed stone of 2-5 mm fraction - 20%, crushed stone of 5-10 mm fraction - 25%, cement - 24%. To improve the characteristics, a plasticising admixture silol latex was added in the amount of 0.15% by weight of cement.

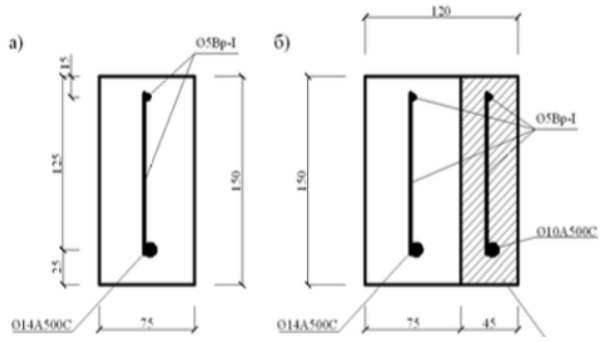

Figure 3 – Scheme of construction of experimental beams: a) beams B-1-1-1, B-1-1-2, B-1-2-1, B-1-2-2, B-1-2-1t, B-1-2-2t; b) reinforced beams with shotcrete B-1-1-1pt, B-1-1-2pt

The compressive and tensile strengths of the concrete specimens during bending were determined in accordance with the standard. The tests were carried out on 40×40×160 mm specimens and 600×600 mm shotcrete slabs. The experimental beams were manufactured in the laboratory of Lviv Regional Scientific and Technical Centre of 'DerzhdorNDI', and the materials were tested in the laboratories of 'DerzhdorNDI', Karpenko Physical Engineering Institute of the National Academy of Sciences of Ukraine and Lviv National Agricultural University.

The research series included eight experimental beams with dimensions of 1650×150×75(150) mm. Four of them (B-1-1-1, B-1-1-2, B-1-2-1, B-1-2-2) were manufactured in the traditional way, and two (B-1-1-1pt, B-1-1-2pt) were reinforced with shotcrete. Two more beams (B-1-2-1t, B-1-2-2t) were manufactured using shotcrete technology with subsequent cutting into separate elements.

To determine the parameters of strength, deformation capacity and crack resistance, the beams were tested in bending by applying two concentrated loads to the upper edge in one-third of the span. The tests were performed on the 220th day after concreting. The working span was 1500 mm, and the loads were applied in stages with a 15-minute dwell time at each stage to stabilise the deformations.

The force was applied using a 250 kN hydraulic jack and a distribution beam. The load was monitored using a reference dynamometer and two ring dynamometers located on the beam supports.

Deflections were recorded using three 0.01 mm precision clock-type indicators mounted on a special metal frame. Concrete deformations were determined by micro-indicators with a division price of 0.001 mm, mounted on the side faces of the beams. Reinforcement deformations were monitored using micro-indicators mounted on special holders attached to the reinforcing bars by resistance welding.

Crack formation was recorded using an MPB-2 microscope. The determination of the moment of crack formation was supplemented by the readings of strain gauges that recorded sudden changes in deformation.

Conclusions according to [16]. The developed methodology makes it possible to evaluate the strength characteristics of concrete, shotcrete, and reinforced concrete beams reinforced by the shotcrete method. It helped to determine the main parameters of strength, crack resistance and deformability of structures in the zones of maximum bending moment. However, further research and improvement of methods for analysing their stress-strain state are needed to gain a deeper understanding of the performance of multilayer structures.

Scientists from Vietnam (Faculty of Civil Engineering, Western Construction University (MTU) T.Q.K. Lam, T.M.D. Do, V.T. Ngo, T.T.N. Nguyen, D.Q. Pham [17] in a scientific article in an international scientific journal investigated the change in concrete class in the layers of three-layer steel fibre-reinforced concrete beams (see Fig. 4). Beams with a cross-section of 150×300 mm, a total span length of 2200 mm and a working length of 2000 mm were studied, where the middle layer consisted of ordinary concrete. All beam specimens were tested under two-point loads. The study modelled three-layer concrete beams with different concrete layers, with and without steel fibres, taking into account the nonlinearity of the material.

However, this study focuses only on the change in concrete class in the layers, but does not take into account parameters such as the number of reinforcing bars, reinforcement diameter, steel fibre content in concrete, changes in layer thickness, etc.

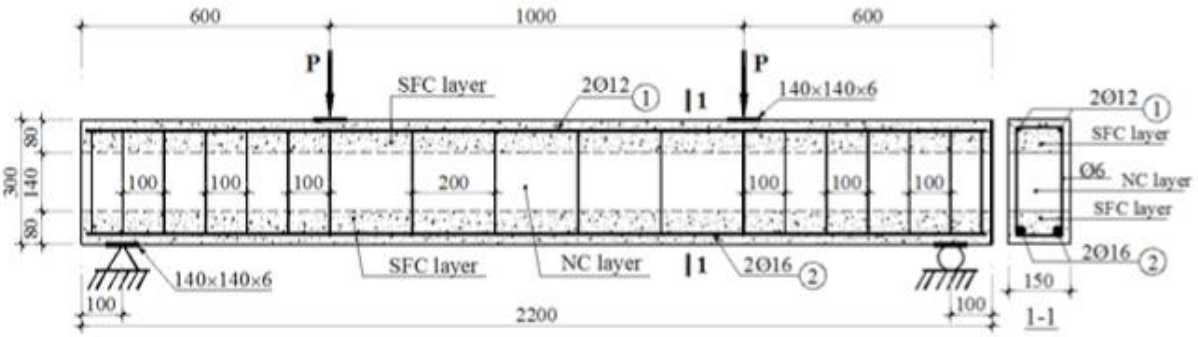

Figure 4 – Structural solution for a three-layer concrete beam model

The results of the study characterise the stress-strain state, crack formation and development, load-compression stress diagrams, load-tensile stress diagrams, and load-vertical displacement in three-layer beams with a change in concrete class. Also, the scheme of crack formation and development in three-layer concrete beams was determined, the load at which cracking begins and the load at which the beams collapse were determined. The relationships between the load, compressive stress, tensile stress, and vertical displacement in the middle of the three-layer beams were established. The study showed that these three-layer concrete beams crack earlier in cases 2 and 3, but the failure of the beams in case 3 occurs at 67 kN, which is the lowest value, and in case 6 - at 116 kN, which is the highest value.

Paper [18] also presents the results of numerical modelling in the ANSYS software package, which includes the analysis of the stress-strain state and crack formation of steel fibre-reinforced concrete layers of three-layer reinforced concrete beams. The advantage of the research is the use of a real concrete work diagram in the numerical modelling of structures (see Fig. 5). Figure 6 shows a diagram of crack formation between the finite elements of stretched concrete.

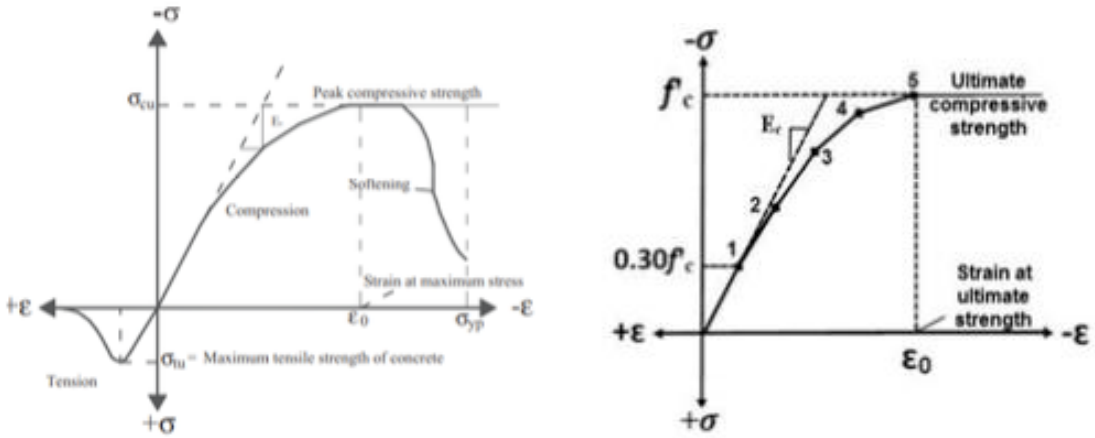

Figure 5 – Typical uniaxial compression and tension diagram for concrete

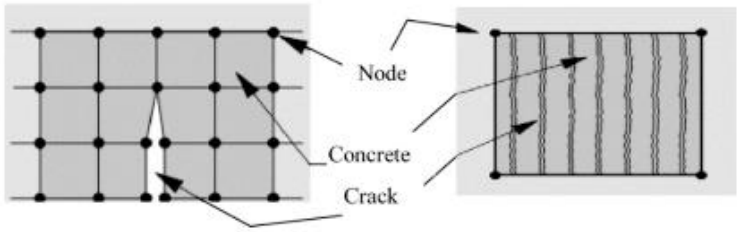

Figure 6 – Model of crack formation in concrete

Finite element model of a reinforced concrete beam with steel fiber reinforcement in ANSYS show in Fig. 9. Element types used in this model. *Concrete:* concrete modeling element: the SOLID65 element is a specialized material simulation for concrete. It can model concrete reinforcement, including cracking and compression effects, and allows the definition of nonlinear material properties. This is a 3D element with 8 nodes (see Fig. 7, a). In SOLID65, the content of steel fibers can be specified as a constant percentage of concrete reinforcement. *Steel reinforcement:* Steel bar element: the BEAM188 element is used for modeling beam reinforcement. It is based on Timoshenko beam theory and consists of 2 nodes, each having 6 degrees of freedom (Fig. 7, b and 8).

The analysis of multilayer steel fibre-reinforced concrete beams using experimental and numerical methods (see Figs. 9) shows the need for further study of other parameters that affect the performance of three-layer beams. Based on the results of the study [21-22], the following conclusions were drawn: the analysis of changes in the concrete grade in the layers shows that the value of the compressive stress is the lowest in case 1. Cases 3 and 6 have higher tensile stress values than the other cases considered. The change in vertical deflection in the centre of the span between the cases is very small. Bearing capacity of the beam: the earliest damage is observed in case 3, while the latest damage is observed in case 6. In cases 5 and 6, the effect of steel fibres on the change in concrete grade in the layers of three-layer concrete beams is very significant; the use of steel fibres in the layers of three-layer concrete beams is necessary. In cases 1 and 3, the effect of the presence or absence of steel fibres is minimal.

In the scientific article ‘Experimental study of prestressed two-layer reinforced concrete beams’, the authors: Yakov Iskhakov, Yuri Rybakov, Klaus Holschechmacher, Stefan Keseberg [23] discussed the issue of researching a series of experiments on the study of double-layer beams (DLB). As part of this series, the concept of the DBG was developed, high-strength concrete with metal fibres (HSCF) was tested as a material, and simple braced and double-span beams were tested.

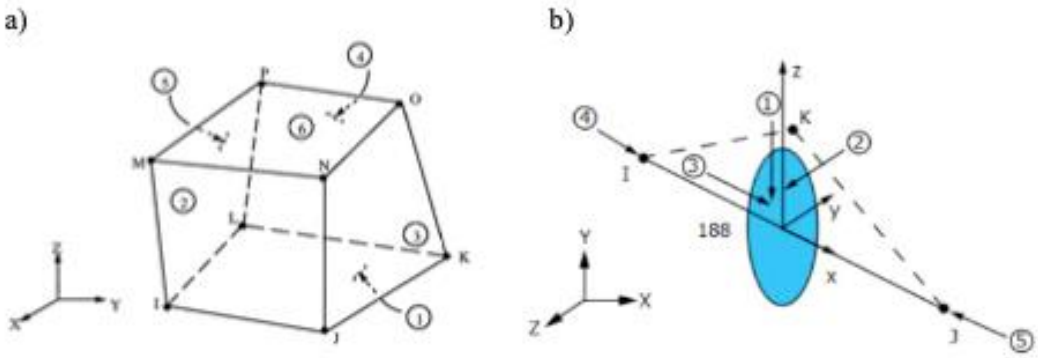

Figure 7 – Types of beam elements: a) Solid65 element, b) beam188 element

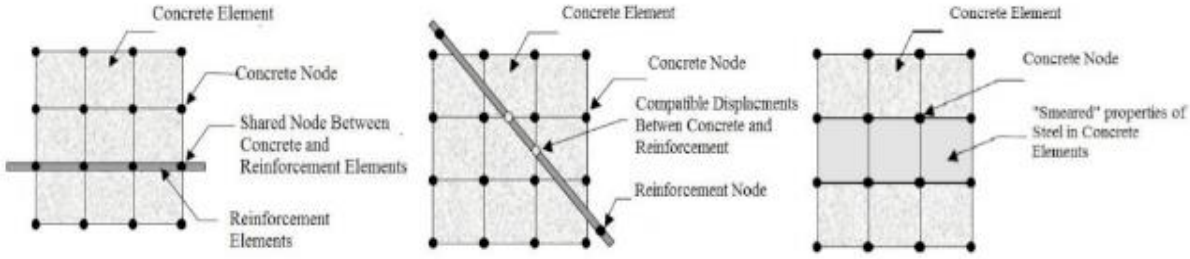

Figure 8 – Model of steel fibres in concrete

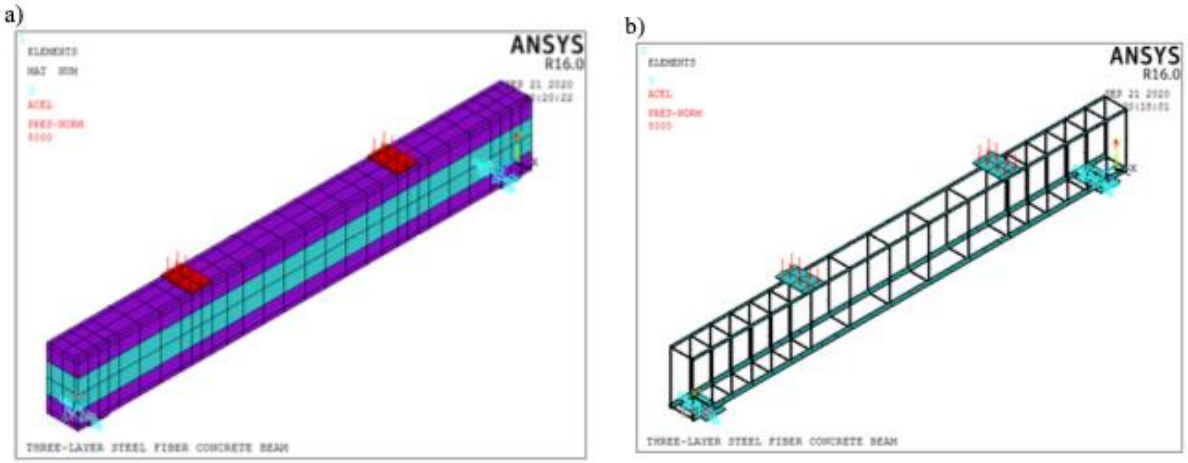

Figure 9 – Three-layer model of concrete beam in ANSYS: a) model of a three-layer concrete beam, b) modelling of steel bars in concrete beams.

In the scientific article 'Experimental study of prestressed two-layer reinforced concrete beams', the authors: Yakov Iskhakov, Yuri Rybakov, Klaus Holschechmacher, Stefan Keseberg [23] discussed the issue of researching a series of experiments on the study of double-layer beams (DLB). As part of this series, the concept of the DBG was developed, high-strength concrete with metal fibres (HSCF) was tested as a material, and simple braced and double-span beams were tested. The current study focuses on the testing of full-scale prestressed simple braced beams (SSBs). The aim of the study is to investigate the bending behaviour of the PPSSB under a four-point loading scheme and compare it with non-prestressed beams (see Figure 10).

As in the previous stages of the study, the interaction of concrete layers in the HFRPB was studied to confirm the effectiveness of such beams in real long-span reinforced concrete structures.

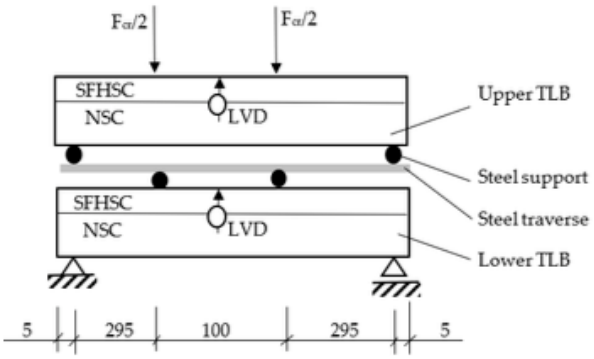

Figure 10 – Dimensions and loading pattern of the investigated double-layer reinforced concrete beams (DLRB)

No delamination between the HSMF and conventional concrete (CC) layers was observed up to the ultimate state, indicating a reliable interaction between the layers. The obtained results allow us to recommend the

HSCF for further research of full-scale reinforced concrete elements with larger spans (9-12 m) and their practical application as efficient and economical bending elements.

Conclusions from [15]: continuing the previous research on non-prestressed DLRBs, this work is devoted to the study of prestressed DLRBs (PPDLRBs). The study is aimed at testing simple support beams with an optimum steel fibre content under a four-point loading scheme from the initial stage to failure, and comparing the results with those of previous studies of non-prestressed beams. The interaction of the concrete layers in the prestressed concrete beams was studied to confirm the effectiveness of such beams in real structures.

The following aspects were considered for the studied PCSBs: crack initiation and development, vertical deflections, transverse deformations, vertical and horizontal shear deformations between layers, and the behaviour of prestressed ropes.

The appearance of bending cracks in the WB layer was observed at 75 kN, which is approximately twice the value for the unstressed SSBs. At subsequent loading stages, the cracks developed to the interface between the layers, but no cracks were observed in the HFBF layer. The bearing capacity of the prestressed beams is approximately 20% higher than that of the DSBs. Similar to the DSBs, the PPDSSBs showed good interaction between the HFBF and reinforced concrete layers. The maximum transverse strains in the HSMF layer of the PPDSS were twice as high as those in the DSB, which demonstrates the possibility of nonlinear deformation in concrete. This is especially important for DSBs with a compressed layer of high-strength concrete.

The maximum vertical shear strains in the linear range of the PPDSS and DSB are similar, but the ultimate shear strains in the PPDSS are about 70% higher and the bearing capacity is 20% higher compared to the DSB.

At the stages with insignificant cracking, the horizontal shear strains between the layers in the PPDSC are insignificant, which confirms the perfect interaction between the layers of the HMF and the concrete. The maximum horizontal shear strains between the layers in the PPDSC are approximately twice as high as in the DSB, which corresponds to the increase in transverse strains in the compressed layer of the PPDSC.

In all the studied PPDSCs, no cracks between the HFBF and WB layers were observed up to the limit state, which indicates proper interaction of the layers. The obtained results allow us to recommend the PPBF for further research of full-scale elements with a larger span (9-12 m) and their practical application as efficient and economical continuous bending elements.

The above-mentioned authors [11] also considered the issue and covered it in an article in an international scientific journal: Methodology and Experimental Investigation of Linear Creep in Double-Layer Reinforced Concrete Beams.

This article presents the first stage of the experimental study of creep in double-layer reinforced concrete beams. The main focus is on the methodology of testing beams under long-term loading in order to investigate the real effect of linear creep. The beams under study consisted of ordinary strength concrete (OSC) in the tensile zone and high strength steel fibre concrete (HSCF) in the compressed zone.

The specimens were subjected to bending under a four-point loading scheme at loads of 70% and 85% of their bearing capacity. The load was applied using special reinforcing devices. The experiment at this stage lasted 90 days. Deflections were measured in the middle of the span of each specimen. During the first 24 hours after the load was applied, deflections were recorded every 10 seconds, and then every hour.

During the tests, no cracks were observed near the supports or between the layers of BZM and SFRP. Cracks appeared only within the clean bending zone. Load-deflection curves were obtained and analysed. The maximum deflection in the middle of the span in the studied beams was less than 1/250 of the beam span length, which indicates the safety of the structure and the beam being in an elastic state with linear creep. The results obtained are the basis for the second stage of the experimental study, which will focus on the effect of nonlinear creep in such beams.

Thus, the paper presents the results of an experimental study of linear creep in two-layer reinforced concrete beams. A methodology for testing creep of reinforced concrete beams was developed. Special amplifying devices with lever systems were used to apply a long-term load to the test specimens. The experimental results showed that the previously proposed algorithm can be used to evaluate the effect of linear creep in two-layer reinforced concrete beams. The maximum deflection in the middle of the span of the tested beams was less than 1/250 of the span length, which indicates the safety of the structure and the beams being in an elastic state under the action of linear creep. The results obtained are the basis for the next stage of the experimental study, which will be devoted to the study of the effect of nonlinear creep in such beams.

Conclusions

Thus, reducing the use of cement and reducing the weight of concrete in bending reinforced concrete elements is an important task in modern construction. To solve this problem, various methods are being implemented, including the use of both removable and non-removable void formers, and the combination of several materials (e.g., heavy in the compressed zone and light in the tensile zone of concrete) for their mutually beneficial joint operation. The paper provides an overview of several experimental and theoretical studies in these areas, which substantiate the possibility and feasibility of reducing the strength of concrete in the tensile zone of bending reinforced concrete structures, and as a result, reducing the consumption of cement for the

preparation of concrete mix for structures, without pre-stressing the latter. The use of two- and multi-layer elements with porous aggregates can significantly improve sound and thermal insulation characteristics, as well as reduce the dead weight of structures, which leads to savings in materials, labour and financial resources. The right choice of material for each layer allows us to create structures with high performance characteristics.

References

1. Shmukler V.S. (2005). Evolutionist approach in rationalization of building structures Shmukler. *ISEC-03. Third International structural Engineering and construction Conference, Shunan (Japan)*

2. Мельник І.В., Сорохтей В.М., Кузик О.О. (2010). Монолітні плоскі залізобетонні перекриття з пінополістирольними вставками. *Вісн. Львів. терит. від-ня Акад. буд-ва України, 5* (10), 146-153.

3. Шмуклер В.С., Бугаєвський С.А., Нікулін В.Б., Ямкова Т.І. (2015). Вплив якісного та кількісного складу компонентів бетону на технологічні властивості само ущільнювальної бетонної суміші. *Зб. наук. пр. "Ресурсоекономні матеріали, конструкції, будівлі та споруди", 31*, 168-175.

4. Демчина Б.Г., Литвиняк О.Я., Давидюк О.В. (2011). Дослідження збірно-монолітних залізобетонних плит перекриття з використанням пінобетону. *Будівельні конструкції: міжвідомчий науково-технічний збірник наукових праць (будівництво), 74*: в 2-х книгах. Книга 1. 160–166.

5. Sohel K.M.A., Richard Liew J.Y. (2011). Steel-Concrete-Steel sandwich slabs with lightweight core - *Static performance. Engineering Structures*, 33(3), 981-992. [Електронний ресурс] - Режим доступу: http://www.sciencedirect.com/science/article/pii/S0141029610004918?via%3Dihub

6. Shams, A., Horstmann, M., Hegger, J. (2014). Experimental investigations on Textile-Reinforced Concrete (TRC) sandwich sections. *Composite Structures*, *118*, 643–653. [Електронний ресурс] - Режим доступу: http://linkinghub.elsevier.com/retrieve/pii/S0263822314003791

7. Lai T., Connor J.J., Veneziano D. (2020). Structural behavior of BubbleDeck slabs and their applicatiob to lightweight bridge decks. *Massachusetts Institute of Technology*; June 2020

8. Литвиняк О.Я. (2012). Дослідження на згин при монтажі та експлуатації збірно-монолітних залізобетонних плит перекриття з використанням пінобетону. *Науковий вісник будівництва: збірник наукових праць Харківського національного університету будівництва та архітектури, 69*, 153-160.

9. Шаленний В.Т., Щегула Р.В. (2022). Порівняльна ефективність монолітних перекриттів із вкладишами з картону, пластмаси та місцевих кам'яних матеріалів. *Будівництво та техногенна безпека. 24(76).* 63-70.

10. Бабій І.М, Коломійчук В.Г. (2019). Ефективні попередньо напружені монолітні залізобетонні перекриття з використанням незнімних вкладишів-порожниноутворювачів. *Бетон та залізобетон в Україні. 2.* 13-18.

11. Пушкарьов Б.А. (2023). Спосіб зниження витрат цементу під час виготовлення згинаних залізобетонних конструкцій без попереднього напруження. *Будівництво та техногенна безпека. 29(81),* 81-86.

1. Shmukler V.S. (2005). Evolutionist approach in rationalization of building structures Shmukler. *ISEC-03. Third International structural Engineering and construction Conference, Shunan (Japan)*

2. Melnyk I.V., Sorokhtey V.M. & Kuzyk O.O. (2010). Monolithic flat reinforced concrete slabs with expanded polystyrene inserts. *Bulletin of the Lviv Territorial Branch of the Academy of Civil Engineering of Ukraine, 5* (10), 146-153.

3. Shmukler V.S., Bugayevsky S.A., Nikulin V.B. & Yamkova T.I. (2015). Influence of the qualitative and quantitative composition of concrete components on the technological properties of self-compacting concrete mix. *Collection of scientific papers "Resource-efficient materials, structures, buildings and structures", 31*, 168-175.

4. Demchina B.G., Litviniak O.Y. & Davydiuk O.V. (2011). Investigation of precast monolithic reinforced concrete slabs using foam concrete. *Building structures: interdepartmental scientific and technical collection of scientific papers (construction), 74*: in 2 books. Book 1. 160-166.

5. Sohel K.M.A. & Richard Liew J.Y. (2011). Steel-Concrete-Steel sandwich slabs with lightweight core - *Static performance. Engineering Structures*, 33(3), 981-992. [Electronic resource] - Access mode: http://www.sciencedirect.com/science/article/pii/S0141029610004918?via%3Dihub

6. Shams, A., Horstmann, M. & Hegger, J. (2014). Experimental investigations on Textile-Reinforced Concrete (TRC) sandwich sections. *Composite Structures*, *118*, 643–653. [Electronic resource] - Access mode: http://linkinghub.elsevier.com/retrieve/pii/S0263822314003791

7. Lai T., Connor J.J. & Veneziano D. (2020). Structural behavior of BubbleDeck slabs and their applicatiob to lightweight bridge decks. *Massachusetts Institute of Technology*; June 2020

8. Litviniak O.Y. (2012). Bending tests during installation and operation of precast concrete slabs using foam concrete. *Scientific Bulletin of Construction: Collection of scientific papers of Kharkiv National University of Construction and Architecture, 69*, 153-160.

9. Shalenny V.T. & Shchegula R.V. (2022). Comparative efficiency of monolithic ceilings with liners made of cardboard, plastic and local stone materials. *Construction and technogenic safety. 24(76).* 63-70.

10. Babiy I.M. & Kolomiychuk V.G. (2019). Efficient prestressed monolithic reinforced concrete slabs using non-removable ones. hollow-forming inserts. *Concrete and reinforced concrete in Ukraine 2,* 13-18.

11. Pushkarev B.A. (2023). Method for reducing cement consumption when manufacturing flexible reinforced concrete structures without pre-stressin. *Construction and technogenic safety. 29(81),* 81-86.

12. Мазурак А., Ковалик І., Михайлечко В., Амброзяк П. (2015). Методика експериментальних досліджень залізобетонних елементів, підсилених торкретуванням, за різних рівнів навантажень. *Вісник Львівського національного аграрного університету Архітектура і сільськогосподарське будівництво 16,* 48-54.

13. Мазурак А.В., Калітовський В.М., Ковалик І.В. (2011). Методика експериментальних досліджень підсилених залізобетонних елементів за різних рівнів навантажень. *Вісник Львівського національного аграрного університету: архітектура і сільськогосподарське будівництво. 12.* 83 – 88.

14. Рутковська І.З., Рутковський З.М., Вознюк Л.І., Марущак А. (2008). Експериментальні дослідження тришарових конструкцій. *Вісник Національного університету "Львівська політехніка". 627.* 179-182.

15. Мазурак А.В., Калітовський В.М., Юхим М.Я., Мазурак Т.А. (2009). Методика експериментальних досліджень залізобетонних балок, виготовлених і підсилених торкретуванням. *Дороги і мости. Київ, Випуск 11.* 226-232.

16. Артюх В.Г., Санников І.В. (2007). Торкрет – бетон у цивільних будинках, що реконструюються. *Будівництво України, 3.* 11-13.

17. T.Q.K. Lam, T.M.D. Do, V.T. Ngo, T.T.N. Nguyen, D.Q. Pham. (2020). Concrete grade change in the layers of three-layer steel fibre reinforced concrete beams. *Journal of Achievements in Materials and Manufacturing Engineering, 102(1),* 16-29.

18. V.T. Ngo, T.Q. Khai Lam, T.M. Dung Do, T.C. Nguyen. (2019). Nano concrete aggregation with steel fibers:A problem to enhance the tensile strength of concrete, *E3S Web of Conferences 135,* 03001. https://doi.org/10.1051/e3sconf/201913503001

19. Wang, C., Shen, Y., Yang, R. & Wen, Z. (2017). Ductility and Ultimate Capacity of Prestressed Steel Reinforced Concrete Beams. *Hindawi Mathematical Problems in Engineering*, 6, 1467940. https://doi.org/10.1155/2017/1467940

20. V.T. Ngo, T.Q.K. Lam, T.M.D. Do, T.C. Nguyen. (2020). Increased plasticity of nano concrete with steel fibers, *Magazine of Civil Engineering 93/1* 27-34. https://doi.org/10.18720/MCE.93.3

21. T.Q. Khai Lam, D.D. Thi My, V.T. Ngo, T. Chuc Nguyen, T. Phuoc Huynh. (2020). Numerical simulation and experiment on steel fiber concrete beams. *Journal Physics: Conference Series 1425* 012007. https://doi.org/10.1088/1742-6596/1425/1/012007.

22. T.M.D. Do, T.Q.K. Lam. (2021). Design parameters of steel fiber concrete beams. *Magazine of Civil Engineering* 102/2.

23. I. Iskhakov, K. Holschemacher, S. Kaeseberg, Y. Ribakov. (2025). Methodology and Experimental Investigation of Linear Creep Behavior in Two-Layer Reinforced Concrete Beams. *Appl. Sci., 15(7),* 3456. https://doi.org/10.3390/app15073456

12. Mazurak A., Kovalyk I., Mihaylechko V. & Ambroziak P. Methods. (2015). Experimental experimental study concrete elements reinforced concrete spraying atdifferent levels of load. *Bulletin of the Lviv National Agrarian University. Architecture and Agricultural Construction, 16,* 48–54.

13. Mazurak A.V., Kalitovskiy V.M. & Kovalyk I.V. (2011). Methodology of experimental research on strengthened reinforced concrete elements under different load levels. *Bulletin of the Lviv National Agrarian University. Architecture and Agricultural Construction, 12,* 83–88.

14. Rutkovska I.Z., Rutkovskyi Z.M. & Voznyuk L.I., Marushchak A. (2008). Experimental studies of three-layer structures. *Bulletin of the National University "Lviv Polytechnic", 627,* 179–182.

15. Mazurak A., Kalitovsky V., Yuhim M. & Mazurak T. (2009). Technique of experimental research of reinforced beams manufactured and reinforced by guniting. *Roads and bridges. Kyiv,11.* 226-232.

16. Artiukh V.H. & Sannikov I.V. (2007). Shotcrete in renovated civil buildings. *Construction of Ukraine, 3,* 11–13.

17. T.Q.K. Lam, T.M.D. Do, V.T. Ngo, T.T.N. Nguyen & D.Q. Pham. (2020). Concrete grade change in the layers of three-layer steel fibre reinforced concrete beams. *Journal of Achievements in Materials and Manufacturing Engineering, 102(1),* 16-29.

18. V.T. Ngo, T.Q. Khai Lam, T.M. Dung Do & T.C. Nguyen. (2019). Nano concrete aggregation with steel fibers:A problem to enhance the tensile strength of concrete, *E3S Web of Conferences 135,* 03001. https://doi.org/10.1051/e3sconf/201913503001

19. Wang, C., Shen, Y., Yang, R. & Wen, Z. (2017). Ductility and Ultimate Capacity of Prestressed Steel Reinforced Concrete Beams. *Hindawi Mathematical Problems in Engineering*, 6, 1467940. https://doi.org/10.1155/2017/1467940

20. V.T. Ngo, T.Q.K. Lam, T.M.D. Do, T.C. Nguyen. (2020). Increased plasticity of nano concrete with steel fibers, *Magazine of Civil Engineering 93/1* 27-34. https://doi.org/10.18720/MCE.93.3

21. T.Q. Khai Lam, D.D. Thi My, V.T. Ngo & T. Chuc Nguyen, T. Phuoc Huynh. (2020). Numerical simulation and experiment on steel fiber concrete beams. *Journal Physics: Conference Series 1425* 012007. https://doi.org/10.1088/1742-6596/1425/1/012007.

22. T.M.D. Do & T.Q.K. Lam. (2021). Design parameters of steel fiber concrete beams. *Magazine of Civil Engineering* 102/2.

23. I. Iskhakov, K. Holschemacher, S. Kaeseberg & Y. Ribakov. (2025). Methodology and Experimental Investigation of Linear Creep Behavior in Two-Layer Reinforced Concrete Beams. *Appl. Sci., 15(7),*3456. https://doi.org/10.3390/app15073456

Збірник наукових праць. Галузеве машинобудування, будівництво
Academic journal. Industrial Machine Building, Civil Engineering
http://journals.nupp.edu.ua/znp
https://doi.org/10.26906/znp.2023.61.3552

UDC 622.24:691.327

Development of an energy-saving design for the feeding system of a concrete mixing plant

Bogdan Korobko [1], Oleksandr Levchenko [2], Rostyslav Rudyk [3]*

[1] National University «Yuri Kondratyuk Poltava Polytechnic» https://orcid.org/0000-0002-9086-3904
[2] National University «Yuri Kondratyuk Poltava Polytechnic» https://orcid.org/0009-0004-3191-7097
[3] National University «Yuri Kondratyuk Poltava Polytechnic» https://orcid.org/0000-0001-8386-977X
*Corresponding author E-mail: rostyslavrudyk@nupp.edu.ua

The study focuses on the development of an energy-saving design for concrete mixer mix components supply system to enhance efficiency and reduce environmental impact. The proposed changes to the schematic diagram include the implementation of separate hoppers with individual conveyors to optimize energy consumption and increase productivity. These modifications aim to improve energy efficiency, reduce material change time, and prevent congestion in the supply system, ultimately leading to enhanced productivity and streamlined production processes. This study highlights the importance of innovative design solutions in the feeding supply system of industrial plants to drive sustainability and efficiency improvements.

Keywords: concrete mixing plant, concrete mixer mix components supply system, energy efficiency, ecology, productivity, material change time, sustainability, concrete

Розробка енергозберігаючої конструкції системи живлення бетонозмішувальної установки

Коробко Б.О.[1], Левченко О. П.[2], Рудик Р.Ю.[3]*

[1,2,3] Національний університет «Полтавська політехніка імені Юрія Кондратюка»
*Адреса для листування E-mail: rostyslavrudyk@nupp.edu.ua

Виробництво бетону є важливою складовою будівельної промисловості, проте воно відоме своїми великими енергетичними витратами та негативним впливом на довкілля. У зв'язку з цим, дослідження системи живлення бетонозмішувальної установки має велике значення для підвищення сталості та зменшення впливу на навколишнє середовище. В статті проводяться дослідження, які спрямовані на оптимізацію виробничих процесів та зменшення споживання енергії в бетонозмішувальних установках. У роботі використовувалися моделювання та аналіз технічних параметрів конструкції бетонозмішувальної установки. Однією з ключових проблем, що виявлені, є неефективність системи живлення, що призводить до зайвого споживання енергії та втрат продуктивності. З метою вирішення цієї проблеми, запропоновано змінити принципову схему системи живлення, розташовуючи кожен бункер окремо із власним конвеєром. Результати дослідження показали, що запропоновані зміни сприяють підвищенню енергоефективності установки за рахунок мінімізації енерговитрат, підвищення ефективності процесу та зменшення ризику перешкод. Такі покращення можуть значно зменшити витрати енергії та покращити загальну продуктивність бетонозмішувальної установки. Висновки дослідження вказують на важливість постійного пошуку нових технологій та методів для зменшення енергоспоживання та покращення сталості виробництва. Запропоновані зміни можуть стати важливим кроком у напрямку створення екологічно чистих та енергоефективних установок для виробництва бетону, що відповідає сучасним вимогам сталого розвитку.

Ключові слова: бетонозмішувальний завод, система живлення, енергоефективність, екологія, продуктивність, час зміни матеріалу, стійкість, бетон

Introduction.

Nowadays, with the constant growth of the global construction sector and the tightening of environmental requirements, the development of energy-saving technologies is becoming an extremely urgent and important task. One of the key areas of improvement is the feeding systems of concrete mixing plants, which play an important role in the production of concrete for construction.

Concrete mixture is widely used in construction in the manufacture of various monolithic and prefabricated structures. This material is a homogeneous mass consisting of a viscous substance (cement), coarse and fine-grained fillers (crushed stone, sand), water, as well as

various additives that improve the properties of concrete. In each case, a careful calculation of the components is carried out, which must be observed when compiling the proportions [1].

The production process of concrete and mortar mixtures is a series of sequential mechanized and, mainly, automated operations: warehousing and storage of inert materials and cement; dosage of sand, gravel, water, chemical additives and pigments; mixing components; and transporting concrete to its destination [2].

The ever-increasing requirements for concrete quality and production efficiency, along with the need to reduce energy consumption and emissions of harmful substances into the air, require revolutionary changes in this area. Therefore, the purpose of this scientific study is to develop a new energy-saving design of the feeding supply system for concrete mixing plants, aimed at improving their efficiency and reducing the negative impact on the environment.

Review of the research sources and publications.

In recent times, a significant amount of research has been conducted in the field of concrete mixing plants and plants aimed at improving the quality and efficiency of concrete production. These researches include the development of new technologies, improvements in the processes of mixing and transporting concrete, as well as improvements in the designs of the equipment itself. However, among the large amount of researches, relatively little attention has been paid to the feeding supply system of the concrete mixing plant, which plays a key role in ensuring stable and effective mixing of concrete components.

In recent times, a significant amount of research has been conducted in the field of concrete mixing plants and plants aimed at improving the quality and efficiency of concrete production. These studies include the development of new technologies, improvements in the processes of mixing and transporting concrete, as well as improvements in the designs of the equipment itself. However, among the large amount of research, relatively little attention has been paid to the power system of the concrete mixing plant, which plays a key role in ensuring stable and effective mixing of concrete components.

Recent research on energy-efficient designs for concrete mixing plant feeding systems describes the use of modern, high-efficiency motors and control systems that optimize the operation of concrete mixing plants with minimal energy consumption [4].

A review of publications of modern methods and technologies aimed at improving energy efficiency in concrete mixing plants was carried out, in which various aspects were studied, such as the use of renewable energy sources, optimization of technological processes and the introduction of energy-saving technologies [6].

Studies have also shown the possibility of using innovative methods for optimizing processes, automating and improving the efficiency of concrete mixing plants [9].

Definition of unsolved aspects of the problem

Although there are works investigating the integration of renewable energies into concrete mixing plants [7], and more detailed research is needed to identify rational ways to use them and to address the technical and economic challenges of this process.

Detailed study of different technological processes impact on concrete mixing plants energy efficiency, as well as determining the rational parameters of these processes are very important to ensure efficient use of energy.

It is necessary to develop and implement the latest materials and technologies to improve the energy efficiency of concrete mixing plants, such as energy-saving drives and automation systems.

Problem statement

The purpose of this study is to conduct a comprehensive analysis of concrete mixing plants design in order to identify and solve unresolved problems that affect the energy efficiency of these plants, as a result of which to design feeding system, including the use of the latest technologies.

Basic material and results

The technological process of production of concrete mixtures and mortars at the modern level is a chain of interconnected mechanized and, in most cases, automated operations: warehouse processing of materials, including loading and unloading and stacking operations; transportation of components to the supply bins of the mixing unit; dosage of components; preparation (mixing) of the mixture; unloading of the finished mixture [11].

With the dismembered production technology, the dosed components are mixed on the road transport or in mixing plants located in the places of concrete laying.

Depending on the purpose, capacity and characteristics of consumer facilities, there are stationary and quickly relocated concrete plants, quickly relocated prefabricated plants and mobile mixing plants.

Stationary plants of continuous operation, produce ready-mixed concrete (mortar) for various consumers or for the plant of reinforced concrete prefabricated structures.

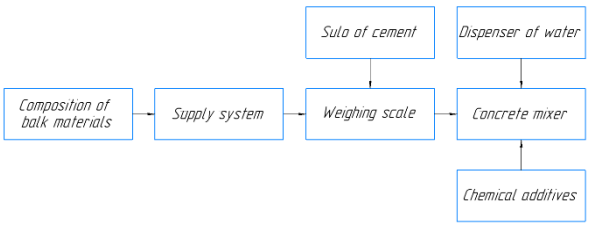

Figure 1 – Schematic diagram of a concrete mixing plant

Quickly relocated plants are built for the construction of specific facilities, taking into account their operation for several years. For better use, such plants should be able to quickly relocate to other facilities without high

costs for plant and dismantling of equipment and stationary structures.

Mobile concrete and mortar mixing plants are units mounted on trailers or consisting of blocks transported by vehicles. These plants are designed to serve concentrated objects.

The plant or plant includes: aggregate and cement warehouses with stacking machines and lifting and conveying equipment to feed them to the mixing department; mixing compartment with dosing equipment, consumable hoppers, mixing machines and devices for receiving the finished mixture and dispensing it to the consumer.

Concrete mixing and mortar mixing shops and plants are classified according to the following criteria: mode of operation - batch and continuous action; layout scheme - for high-rise and stepped. With the high-altitude scheme, the components are raised to their full height once, after which they move only under the influence of gravity during the entire technological cycle.

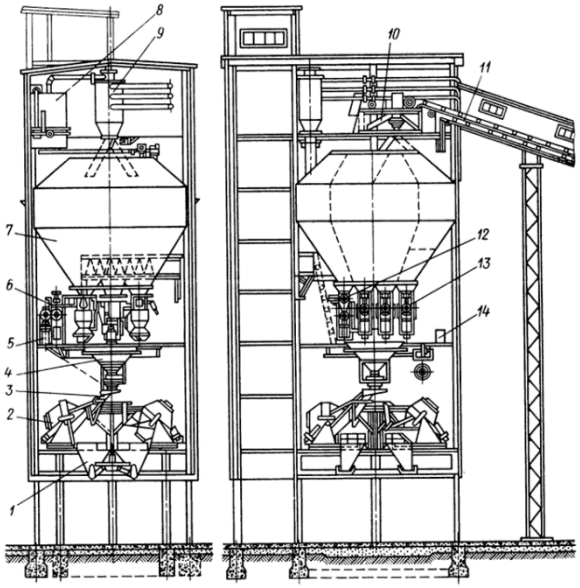

Figure 2 – Diagram of a concrete mixing unit with four concrete mixing units

With a two-stage layout scheme, the concrete mixture is sequentially lifted first into the consumable hoppers, then, after dosing, into the mixing machine.

Figure 2 shows a concrete mixing unit with four gravity concrete mixers, arranged in an elevation scheme [10]. The volume of the finished batch of each concrete mixer is 1600 liters.

Aggregates are fed from the warehouses by a conveyor belt 11 through a rotary funnel 10 to the compartments of the feed bins. Cement is fed by pneumatic transport to cyclone 8, from which it is sent through an air chute to hopper 7. The final air purification is carried out in the bag filter 9. From the consumable hoppers, the cement is poured through the batcher 12 and the aggregates through the batcher 13 into the collecting hopper 4 with a rotary funnel into the concrete mixer 2. Water through the dispenser 6 and liquid additives through the dispenser 5 flow directly into the rotary funnel through the pipeline.

The finished mixture from the concrete mixers is discharged into the dispensing hoppers 1. The operation of the equipment is controlled from the console 14, located in the dispenser compartment.

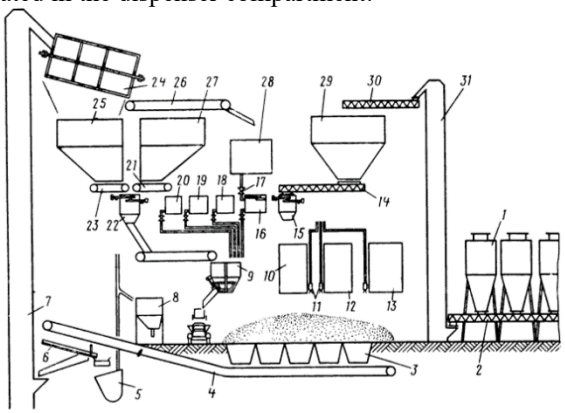

Figure 3 – Technological diagram of a concrete mixing unit with a turbulent mixer

Tower-type concrete mixing units with a layout similar to those of the concrete batching plant in question. Figure 3 shows the technological scheme for the preparation of mortar and concrete on an automated structural unit in which turbulent mixers are used. Cement from silos 1 by screw 2, elevator 31 and screw 30 is fed to hopper 29. From the hopper, the cement is fed by the feeder 14 to the batcher 15, from which it enters the mixer 9. Aggregates from warehouses 3 are fed by conveyor 4 to screen 6. The sifted sand is fed by the elevator 7 into the drum sand grinder 24 and then into the hopper 25. Large inclusions from the screen 6 are fed by the shaft hoist 5 into the waste bin 8. Crushed stone from the warehouse is transported by the same chain of machines and transport 26 to hopper 27 From the hoppers, the sand is fed by feeders 21 and 23 to the batcher 22 and further to the mixer. Water is supplied to the mixer from the tank 28 through the valve 17 and the dispenser 16. Lime from tank 13 and additives from tanks 12 and 10 are fed by pumps 11 to the corresponding dispensers 18, 19 and 20, from which they are drained into the mixer.

Figure 4 shows a diagram of a two-stage continuous concrete plant (SB-75 type), with a capacity of 30 m^3/h, designed for the preparation of concrete in open areas during the construction of roads, airfields, etc.

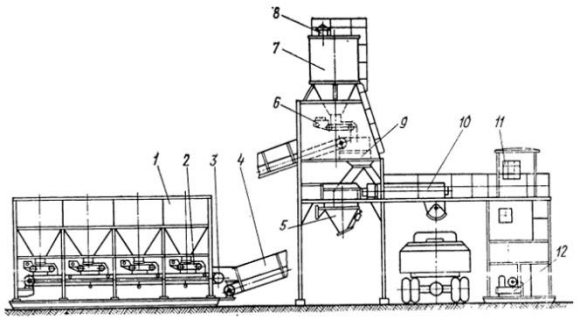

Figure 4 – Schematic diagram of a continuous concrete plant

The plant consists of three main units: a batching unit for aggregates, a mixing department with a cement hopper and a control unit. Aggregates from hoppers 1 are fed through continuous dispensers 2 through the conveyor 3 to the inclined conveyor 4 and the collecting hopper 9. Cement from cement trucks is sent to the hopper 7, equipped with a filter 8, and then to the collecting funnel with a batcher 6. The plant can produce the finished mixture by a continuous mixer 10, where water is supplied by a dosing pump 12 from a tank located under the control unit 11, or to ship separately dosed dry components and water to concrete mixer trucks. The unit has a cyclic calibration dispenser 5, mounted on a sliding frame.

The dosing unit of a plant or plant is one of the main units, it can be called a bulk material feeding system [14]. It consists of hoppers for temporary storage of material, dispensers and belt conveyors.

Hoppers for bulk materials belong to the main type of auxiliary equipment. The purpose of the hopper is to create an operational stock of materials for the smooth operation of production [15].

Consumable hoppers are designed so that they can contain the materials necessary for the preparation of the concrete mixture for 2-4 hours of operation. Usually, the stock of materials in consumable bins is taken to be equal: for aggregates - for 1-2 hours, for cement - 2-3 hours. The number of hoppers or its compartments is assigned to the development of the technological scheme of production and depends on the nomenclature of mixtures, the productivity of the line, the choice of the layout of the plant (one-, two-stage, and others). Usually their number is at least two for each type of material. The consumable hoppers are located above the dispensers and are equipped with gates at the outlets.

The design properties of concrete mixtures and concretes are ensured by dosing (measuring) their components with the required accuracy. This operation takes place with the help of dispensers. Dispensers can be volumetric and weight, batch and continuous, with manual, semi-automatic and automatic control. In modern conditions, automatic batch dispensers are used in most cases.

A batch weighing or volumetric weighing batch dispenser consists of a measuring device (a rectangular or more often cylindrical vessel with a pyramidal or conical lower part), a shutter and a weighing mechanism (device). Until recently, concrete mixing plants used weighers with a lever weighing mechanism, which was unreliable, quite complex and difficult to automate. Recently, weighers on load cells have been widely used, the design of which is very simple: the gauge is installed on load cells or suspended from load cells. The most commonly used strain gauges are resistance that varies depending on the deformations caused by gravity. The electrical signal is processed by the controller.

The use of strain gauges has made it possible to sequentially dose several materials with a single batcher, e.g. fine and coarse aggregates, different fractions of coarse aggregate, as they provide the required accuracy within the weighing range. In addition, it is possible to carry out weight dosing of bulk materials with the help of weighing conveyors-dosers.

The last component of the system is the belt conveyor, which feeds the metered material to the mixer.

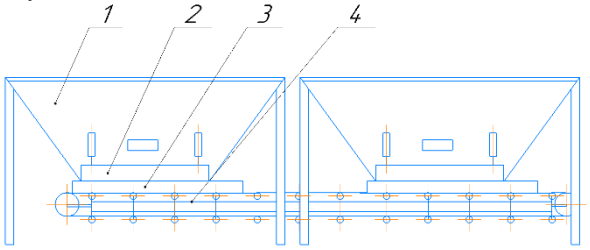

Figure 5 – Feeding supply system of the concrete mixing plant:
1 – receiving hopper; 2 – pneumatic shutter; 3 – measuring device; 4 – conveyor.

The feeding system consists of a belt conveyor, which is attached to the hoppers using load cells and is a weighing platform. Between the conveyor and the hoppers, there are meters for sand and gravel, the volume of which is equal to the required portion for one batch of concrete. The material is loaded into hoppers, then this material is dosed to prepare concrete. The operator gives a command and the hopper gates open one by one, through the pneumatic drive, the material enters the gauge and when the set weight is reached, the gate closes. The gauge and shutter are quite oversized elements, this is done in order to reduce the hanging of materials in the hopper and speed up dosing. Then the conveyor turns on and transports the material to the mixer. The conveyor drive must be powerful, since the gauges contain material for one batch. For example, if the mixer has a working volume of 0.5 m³, then the mass of bulk materials will be about 1000 kg. The conveyor will turn off when there is no material left in the gauges and on the belt. The disadvantages of this equipment are a large shutter, which significantly affects the error during weighing the material, a powerful and energy-consuming conveyor, vibration occurs during the operation of the equipment, which negatively affects the load cells and creates a large error in weighing and premature failure, as well as the need to free the conveyor belt from materials, which significantly affects the performance of the plant.

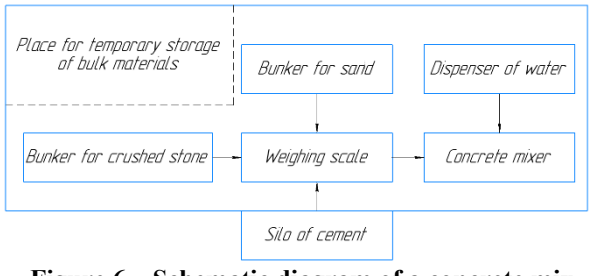

Figure 6 – Schematic diagram of a concrete mixing plant

It is proposed to change the design and schematic diagram of the feed system so that each hopper is located separately from each other and has its own conveyor. Weighing will take place in a separate gauge, which is

mounted on load cells or a weighing platform. The hopper of the feeder will be a gauge in which there are no gates, and a gate is installed in the discharge hole to regulate the supply of materials.

As a conclusion, the proposed system will have a number of advantages over the existing one.

During operation, vibration will not affect the weighing system, as it is located separately from the working units. There are no gates and gauges in the feeders, which greatly simplifies the design and reduces the loading height of the material with the same volume of hoppers. Although there will be several conveyors, they will be smaller and not as powerful. It will be possible, if necessary, to add material in any sequence and quantity, and there will always be material on the belt, which will allow instant dosing and significantly increase the productivity of the unit. With this layout, the system will be more compact, and when organizing a canopy to protect against precipitation, there will be a place for temporary storage of materials. Equally important is the fact that cement can be dosed using a single weighing system.

Conclusions

The results of the study of the energy efficiency of the concrete mixing plant design led to an important conclusion regarding the need for changes in the schematic diagram of the feeding supply system. The proposed changes provide for the location of each hopper separately from each other, each of which will have its own conveyor.

This new feeding system schematic diagram will help improve the energy efficiency of the plant in several ways. The isolated arrangement of hoppers and the use of separate conveyors will optimize the operation of the feeding system, avoid unnecessary energy consumption for transporting materials. Each hopper will be able to operate independently, which will help increase productivity and reduce the time to change the material being loaded.

The introduction of separate conveyors for each hopper will reduce the risk of congestion and interference in the feeding system, which will help to avoid wasting time and energy on solving such problems.

Therefore, the proposed changes in the design and schematic diagram of the feed system of the concrete mixing plant have significant potential to improve energy efficiency and optimize production processes. Their implementation can be an important step towards the creation of environmentally friendly and change-resistant concrete production plants.

References

1. Назаренко І.І., Туманська О.В. (2004). Машини і устаткування підприємств будівельних матеріалів: конструкції та основи експлуатації: Підручник.- К.: Вища шк., с. 590.

2. Сівко В.Й., Поляченко В.А. (2004). Обладнання підприємств промисловості будівельних матеріалів і виробів: Підручник. – К.: ТОВ «АВЕГА», с. 280.

3. Савенко В.Я., Словінська О.С., Каськів В.І., Петрович В.В. (2001). Проектування асфальтобетонних та цементобетонних заводів для потреб дорожнього будівництва. Посібник. Київ, 218 с.

4. Валовой О.І., Валовой М.О., Єрьоменко О.Ю. (2014). Нове обладнання і технології для виготовлення, транспортування і подачі бетону. Гірничий вісник, 97, 125-129.

5. Шпатакова О.Л (2019). Дослідження негативного впливу будівельного підприємства на навколишнє природне середовище. Економіка та управління підприємствами, 30 (69), 85-90
https://doi.org/10.32838/2523-4803/69-5-43

6. Шульгін Ю. В., Жнітов Я. В. (2015). Дослідження можливостей енергозбереження у технології виробництва залізобетону. Енергетичні та теплотехнічні процеси й устаткування. Вісник НТУ «ХПІ», 16 (1125), 157-161

7. Назукін Ю.М. (2013). Стан та перспективи розвитку підприємств з виробництва будівельних матеріалів. Науково-практичне видання «Незалежний аудитор», 5 (10), с. 59-63

8. Moonseo Park, Woo-Young Kim, Hyun-Soo Lee, Sangwon Han (2011). Supply chain management model for ready mixed concrete. Cutomation in Construction, 1 (20), Pages 44-55
https://doi.org/10.1016/j.autcon.2010.07.005

9. V. Deligiannis, S. Manesis (2008). Concrete batching and mixing plants: A new modeling and control approach

1. Nazarenko I.I., Tumanska O.V. (2004). Machines and equipment of building materials enterprises: designs and basics of operation: Textbook. - K.: Vyshcha shk., p. 590.

2. Sivko V.Y., Polyachenko V.A. (2004). Equipment of construction materials and products industry enterprises: Textbook. - K.: "AVEGA" LLC, p. 280.

3. Savenko V.Ya., Slovinska O.S., Kaskiv V.I., Petrovych V.V. (2001). Design of asphalt concrete and cement concrete plants for the needs of road construction. Manual. Kyiv, 218 p.

4. Valovoi O.I., Valovoi M.O., Eremenko O.Yu. (2014). New equipment and technologies for manufacturing, transporting and supplying concrete. Mining Bulletin, 97, 125-129.

5. Shpatakova O. L. (2019). Study of the negative impact of the construction enterprise on the natural environment. Economics and Enterprise Management, 30 (69), 85-90
https://doi.org/10.32838/2523-4803/69-5-43

6. Shulgin Yu. V., Zhnitov Ya. V. (2015). Study of energy saving possibilities in reinforced concrete production technology. Energy and heat engineering processes and equipment. Bulletin of NTU "KhPI", 16 (1125), 157-161

7. Nazukin Yu.M. (2013). The state and prospects of the development of construction materials production enterprises. Scientific and practical publication "Independent Auditor", 5 (10), p. 59-63

8. Moonseo Park, Woo-Young Kim, Hyun-Soo Lee, Sangwon Han (2011). Supply chain management model for ready mixed concrete. Cutomation in Construction, 1 (20), Pages 44-55
https://doi.org/10.1016/j.autcon.2010.07.005

9. V. Deligiannis, S. Manesis (2008). Concrete batching and mixing plants: A new modeling and control approach

based on global automata. Automation in Construction, 4 (17), 368-376
https://doi.org/10.1016/j.autcon.2007.06.001
10. Zhenyuan Liu, Yakun Zhang, Minghui Yu, Xiaolu Zhou (2017). Heuristic algorithm for ready-mixed concrete plant scheduling with multiple mixers. Automation in Construction, 84, 1-13
https://doi.org/10.1016/j.autcon.2017.08.013
11. Shangyao Yan, Weishen Lai, Maonan Chen (2008). Production scheduling and truck dispatching of ready mixed concrete. Transportation Research Part E: Logistics and Transportation Review, 1 (44), 164-179
https://doi.org/10.1016/j.tre.2006.05.001
12. Remon Fayek Aziz (2018). Statistical model for predicting and improving ready mixed concrete batch plants' performance ratio under different influences. Alexandria Engineering Journal, 3 (57), 1797-1809
https://doi.org/10.1016/j.aej.2017.06.016
13. Tian, X., Mohamed, Y., Abourizk, S. (2010). Simulation-based aggregate planning of batch plant operations. Canadian Journal of Civil Engineering, 10 (37), 1277-1288
DOI: 10.1139/L10-071
14. Тодавчич В. І.(2018). Чинники, що впливають на якість дозування. Наукові розробки молоді на сучасному етапі : тези доповідей XVII Всеукраїнської наукової конференції молодих вчених та студентів, Київ : КНУТД, с. 447-448.
15. Семенцов В. В. (2019). Теоретичне дослідження руху сипких матеріалів в бункерах. Вісник Харківського національного технічного університету сільського господарства, 205, с. 249-256.
16. Семенцов В. В. (2018). Розробка нових енергозберігаючих конструкцій дозаторів сипких матеріалів. Вісник Харківського національного технічного університету сільського господарства, 192, с. 227-233.
17. Ничеглод В. В., Бурмістенков О. П., Стаценко В. В. (2022). Дослідження впливу форми бункера на характер протікання порошкових сипких матеріалів. Технології та інжиніринг, 6(11), 42-51
https://doi.org/10.30857/2786-5371.2022.6.4
18. Лизан Х.О., Верескля Д.В., Федорів П.С. (2017). Дослідження Оптимальних Параметрів Бункерного Живильника. Матеріали VI Міжнародної науково-технічної конференції молодих учених та студентів, 204

based on global automata. Automation in Construction, 4 (17), 368-376
https://doi.org/10.1016/j.autcon.2007.06.001
10. Zhenyuan Liu, Yakun Zhang, Minghui Yu, Xiaolu Zhou (2017). Heuristic algorithm for ready-mixed concrete plant scheduling with multiple mixers. Automation in Construction, 84, 1-13
https://doi.org/10.1016/j.autcon.2017.08.013
11. István Kocserha, Ferenc Kristály (2010). Effects of Extruder Head's Geometry on the Properties of Extruded Ceramic Products. Materials Science Forum, Vol. 659, 499-504
doi:10.4028/www.scientific.net/MSF.659.499
12. Remon Fayek Aziz (2018). Statistical model for predicting and improving ready mixed concrete batch plants' performance ratio under different influences. Alexandria Engineering Journal, 3 (57), 1797-1809
https://doi.org/10.1016/j.aej.2017.06.016
13. Tian, X., Mohamed, Y., Abourizk, S. (2010). Simulation-based aggregate planning of batch plant operations. Canadian Journal of Civil Engineering, 10 (37), 1277-1288
DOI: 10.1139/L10-071
14. Todavchych V. I. (2018). Factors affecting the quality of dosing. Scientific developments of youth at the current stage: abstracts of reports of the XVII All-Ukrainian scientific conference of young scientists and students, Kyiv: KNUTD, p. 447-448.
15. Sementsov V. V. (2019). Theoretical study of the movement of loose materials in bunkers. Bulletin of Kharkiv National Technical University of Agriculture, 205, c. 249-256.
16. Sementsov V. V. (2018). Development of new energy-saving constructions of bulk materials dispensers. Bulletin of Kharkiv National Technical University of Agriculture, 192, p. 227-233.
17. Nycheglod V.V., Burmistenkov O.P., Statsenko V.V. (2022). Study of the influence of the shape of the hopper on the nature of the flow of powdery loose materials. Technologies and Engineering, 6(11), 42-51
https://doi.org/10.30857/2786-5371.2022.6.4
18. Lyzan H.O., Veresklya D.V., Fedoriv P.S. (2017). Study of the Optimal Parameters of the Bunker Feeder. Materials of the VI International Scientific and Technical Conference of Young Scientists and Students, 204

Збірник наукових праць. Серія: Галузеве машинобудування, будівництво
Academic journal. Series: Industrial Machine Building, Civil Engineering

http://journals.nupp.edu.ua/znp
https://doi.org/10.26906/znp.2023.61.3853

UDC 621.9.048

Calculation of optimal parameters for a vibratory finishing machine for decorative elements with an active working tool

Dmytro Buhrov [1]*, Tetiana Buhrova [2]

[1] National University «Yuri Kondratyuk Poltava polytechnic» https://orcid.org/0009-0000-4571-5147
[2] National University «Yuri Kondratyuk Poltava polytechnic» https://orcid.org/0000-0003-2690-4131

*Corresponding author E-mail: bugrov.dmitriy@gmail.com

The calculation of optimal parameters for a new design vibration installation with an active working body is proposed using numerical methods. By modeling the system as a mass-spring-damper system and applying harmonic Fourier analysis of the vibrations, a mathematical model of the dynamic interaction between the working body and the part was obtained, taking into account additional friction forces, the angle of inclination, and elastic and damping forces. The key determined parameters—phase shift between the vibrations of the working body, the part, and the abrasive. An example of calculating optimal parameters using the gradient descent method is provided. Based on the calculation results, comparative time graphs of the phase shift of vibrations of the part and the working body, as well as amplitude, were constructed.

Keywords: vibratory finishing, tumbling, active working tool, mathematical model of dynamic interaction between the working tool and workpiece in a vibratory machine, optimal parameters, phase shift of vibrations of the working tool and workpiece

Розрахунок оптимальних параметрів установки для віброабразивної обробки декоративних елементів з активним робочим органом

Бугров Д.Ю.[1*], Бугрова Т.М.[2]

[1,2] Національний університет «Полтавська політехніка імені Юрія Кондратюка»,
*Адреса для листування E-mail: bugrov.dmitriy@gmail.com

Запропоновано розрахунок оптимальних параметрів числовим методом віброустановки нової конструкції з активним робочим органом. Наведена нова принципова схема обладнання є модифікацією відомої УВВ-04, що містить керований механічний збуджувач кутових коливань, до якої введено додатково робочу камеру обробки з активним робочим органом, оберти якого регулюються окремим приводом. Методом моделювання системи як масово-пружинної демпферної системи та гармонійного Фур'є-аналізу коливань отримано математична модель динамічної взаємодії робочого органу і деталі, з врахуванням додаткових сил тертя, кутом нахилу, пружних і демпфуючих сил, що часто ігноруються в попередніх дослідженнях, і більш точно описує динамічні взаємодії у системі та дозволяє встановити шляхи оптимізації. Модель може бути розширена та вдосконалена з урахуванням конкретних вимог і особливостей оброблюваних деталей. Визначено ключові параметри - фазовий зсув між коливаннями робочого органу, деталі та абразиву. Наведено приклад розрахунку оптимальних параметрів методом чисельного розв'язання системи диференційних рівнянь за допомогою методу Рунге-Кутта. Запропоновано алгоритм визначення оптимальних параметрів з використанням методу градієнтного спуску. Цільова функція оптимізації включає мінімізацію фазового зсуву та амплітуди коливань робочого органу та деталі По результатам обчислень побудовано часові графіки залежностей величини фазового зсуву коливань деталі та робочого органу, амплітуди. Проведено їх порівняльний аналіз до і після оптимізації, який засвідчив досягнення мінімальних величин фазового зсуву коливань, максимальної амплітуди зі збереженням стійкості системи, синхронізацію коливань робочого органу і деталі. Це є передумовою забезпечення рівномірного контакту між робочим органом та деталлю, покращує передачу енергії, приводить до зменшення енерговитрат та собівартості вібротехнологічного процесу з підвищенням ресурсу міцності та надійності обладнання. Запропонований метод може бути використаний в прикладних задачах на виробництві.

Keywords: віброабразивна обробка, галтовка, активний робочий орган, математична модель динамічної взаємодії робочого органу і деталі віброустановки, оптимальні параметри, фазовий зсув коливань робочого органу і деталі

Introduction

Vibro-abrasive processing is a method that uses mechanical vibrations to treat parts to improve their quality. It is widely used in various industries, including the production of decorative elements, such as deburring after casting and mechanical processing of jewelry made from silver and gold, metal, ceramic (vases, figurines), and plastic interior items. Vibration installations with active working bodies ensure effective mechanical treatment of parts, improving the quality and productivity of processes. One of the key characteristics of such installations is their ability to generate high-frequency vibrations, which are transmitted to the treated materials through working bodies.

One of the main issues in using vibration installations is achieving system stability. Resonance phenomena that may occur during operation lead to significant vibration amplitudes, which can cause damage to working bodies and parts, as well as reduce processing efficiency. To avoid such phenomena, it is necessary to optimize system parameters such as vibration frequency, oscillation amplitude, and rotation speed of the working body. An example of calculating the optimal parameters of a vibration installation with an active working body is provided. The focus is on the mathematical modeling of the system, phase shift analysis, and studying the dynamic behavior of the working body and the treated parts. Special emphasis is placed on the treatment of small parts up to 15 mm, as they require a particular approach to selecting the geometric shapes and parameters of the working bodies. It is shown that the correct choice of vibration frequency and oscillation amplitude of the working body can significantly increase the productivity and stability of the vibration installation.

Review of the research sources and publications

Sofronas et al. were among the first researchers to develop a comprehensive model for the vibration processing process in 1979. They used a statistical tool known as the surface response methodology to study the effect of hardness, imprint width, processing time, abrasive media size, and vibration frequency on reducing the height of burrs, rounding edges, and reducing surface roughness.

Hashimoto, in defining the basic principles of vibration processing, proposed mathematical models using differential equations to calculate surface roughness and material removal. Hashimoto suggested that in the steady state, the vibration processing process has a constant material removal rate. He used two processing chambers with variable capacity, a vibration frequency of 21 Hz, and an amplitude of 5 mm for his experiments. The experimental results confirmed his mathematical models.

Naeini et al. developed a discrete element model (DEM) to simulate the motion of multiple spherical steel particles in a two-dimensional vibration system. DEM is used to simulate collisions and measure the velocities of particles, the working chamber, and the part. The DEM model is based on a linear contact model with the following parameters: normal and tangential stiffness (k), damping in the normal and tangential directions (β), and the coefficient of sliding friction (μ). It was noted that further increasing the accuracy of the model can be achieved by considering the stiffness and damping parameters in the normal and tangential directions as different rather than equal. Experimentally, it was found that the normal contact forces between the medium and the sensor were approximately 10 times higher than the tangential forces. It was established that vibration processing is based on such phenomena as plastic deformation from the impacts of the medium and material removal by abrasive particles due to the relative motion of the medium and the part.

Kumar et al. [4] developed a simple one-dimensional simulator for the vibration processing process. Titanium parts with different placements in the processing chamber were used to test material removal rates, surface roughness, and measure contact forces. During the study, it was found that surfaces located deeper in the abrasive medium and perpendicular to the vibrational motion demonstrated higher material removal rates. The flow of the medium can be imagined as layers—the medium deeper in the working chamber moves with the weight of the medium above it and thus strikes the part with greater force than the medium layer closer to the surface, leading to higher material removal rates.

In the work of Wang et al., a special sensor was developed to measure the normal contact forces between abrasive particles and the part in the working bowl-type processing chamber. Signal analysis from the force sensor using the Fourier series spectral decomposition method found that most of the energy transferred from the medium to the part occurred at the machine's operating frequency. Comparative results were obtained when the sensor was placed facing forward and backward on the surface of the part that rotated around the bowl. It was concluded that the amount of material removed from the workpiece by abrasive impacts was relatively constant for all surfaces of the part. Tests were also conducted with a fixed part, and it was found that the contact forces were higher compared to an unfixed part. Since the vibration processing time is significantly reduced in this case, fixation becomes increasingly relevant. It was also found that the average impact forces and average impulse showed an increasing trend with an increase in the size of the working chamber in a dry environment, while in a wet environment, this increase was insignificant. Wang et al. also noted that with a change in lubrication from dry to wet using a detergent, the quality of work decreased, and the medium's speed relative to the part also decreased, leading to the conclusion that the lubrication condition has a greater relative impact on the medium's speed than on the part's speed. The rigidity and roughness varied mainly depending on the degree of lubrication, the size of the medium, and its roughness. This is because plastic deformation with each impact depends on the interaction between the medium and the part.

One of the key studies [1] was conducted by Jia L. and Wang C. They investigated multi-frequency controlled synchronization of four induction motors in a vibration system using the fixed frequency ratio method. In their research, the authors found that the phase shift has a significant impact on the synchronization efficiency of the motors. Specifically, it was shown that proper phase shift adjustment allows for greater stability and efficiency of the system's operation, which is critical for industrial applications requiring high precision in part processing.

Blechman I.I. in his book [2] considers nonlinear dynamic effects in vibration mechanics and their applications. He developed a general approach to analyzing phase shifts in various types of vibration systems, including those used in industry. His work emphasizes the importance of accounting for nonlinear effects, which can significantly impact the system's behavior and stability.

The study by Andrievsky B. et al. [5] focuses on the creation of an educational-research complex for the study of vibration devices and processes. They found that the use of active working bodies in vibration installations allows achieving high accuracy and efficiency in part processing due to the control of phase shift and oscillation frequency.

Definition of unsolved aspects of the problem

However, most previous studies focused on individual parameters and did not consider a comprehensive approach to optimizing the entire system. This limited the ability to achieve maximum results, as the interaction between different parameters could affect the process efficiency. In particular, this pertains to the impact of phase shift between the oscillations of the working body and the part on processing efficiency and system stability.

Problem statement

Development of a methodology for determining the optimal parameters of a vibration unit with an active working body to ensure maximum processing efficiency of parts and maintain system stability. The main focus is on the analysis of phase shift between the oscillations of the working body and the part and its impact on system stability.

Basic material and results

Development of a methodology for determining the optimal parameters of a vibration unit with an active working body to ensure maximum processing efficiency of parts and maintain system stability. The main focus is on analyzing the phase shift between the oscillations of the working body and the part, and its impact on system stability.

Optimization in the context of vibratory abrasive processing refers to the process of adjusting and correcting system parameters, such as vibration frequency and amplitude, rotation speed of the working body, and the mass of the processed parts and abrasive, to achieve the best operational characteristics. The main goals of optimization may include:

Reducing the phase shift of oscillations to synchronize the movements of the working body and the processed parts, ensuring more effective interaction between them and improving surface processing quality.

Improving processing quality, reducing defects, and enhancing the surface finish of parts.

Increasing productivity, shortening processing time, and increasing the number of processed parts per unit of time.

Avoiding operation in resonance modes to prevent significant oscillation amplitudes that can lead to mechanical damage to the unit.

Enhancing reliability, allowing the unit to operate for extended periods without unstable modes or breakdowns.

In the context of vibration systems, processing accuracy is influenced by the following factors:

Dimensional tolerances. Accurate processing ensures that part dimensions meet specifications with minimal deviations.

Shapes, angles, and the mutual arrangement of surfaces must be precisely manufactured according to drawings. Suboptimal vibrations can lead to deformations or deviations from the specified geometric parameters.

Surface roughness and the repeatability of the technological process.

Algorithm for Selecting Optimal Parameters

1. Set Initial Values:

Establish initial values for the amplitude AAA, vibration frequency ω\omegaω, and angular rotation frequency.

2. Solve the System of Differential Equations:

Solve the system of differential equations for the mathematical model using the chosen initial parameters over a specified time interval with numerical methods (e.g., Runge-Kutta method).

3. Conduct Analysis:

Analyze the results by plotting the oscillations of the working body, the part, and the phase shift.

4. Apply Optimization Algorithm:

Use an optimization algorithm (e.g., gradient descent). The objective function for optimization includes minimizing the phase shift and the amplitudes of oscillations of the working body and the part. It can be represented as the sum of the quadratic deviations of phase shifts and amplitudes.

$$J(\theta) = \sum_{i=1}^{n} \left(\Delta\phi_i^2 + A_i^2 \right) \quad (1)$$

where $\Delta\phi_i$ - phase shift, A_i - amplitude of oscillations, n - number of data points

5. Repeat the Numerical Integration of the system of equations with the new parameter values.

6. Plot Graphs for the Optimized Parameters, compare them with the initial data. Perform an analysis and evaluation.

Consider the installation, the schematic diagram of which is shown in Fig. 1 [14]. The setup is based on a device with a controlled vibration exciter for angular oscillations [13], located in the laboratory of construction machinery at the Department of Industrial Engineering of "Poltava Polytechnic." The

working body performs a combined rotational and vibrational movement.

Let x(t) – be the position of the working body at time (t), $x_d(t)$ – be the position of the part at time (t), $x_a(t)$ – be the position of the abrasive at time (t).

The main parameters of the vibration setup are:

- m — mass of the working body
- m_d — mass of the processed parts
- m_a — mass of the abrasive
- k — stiffness coefficient of the spring connecting the working chamber to the frame
- k_d — elasticity coefficient of the workpiece
- k_a — elasticity coefficient of the abrasive
- c — damping coefficient of the working body
- c_d — damping coefficient of the parts
- c_a — damping coefficient of the abrasive
- A— amplitude of vibration oscillations
- ω— frequency of vibrations
- Ω— rotational frequency of the working element • μ — coefficient of friction
- g — acceleration due to gravity
- θ — angle of inclination of the installation
- ϕ — phase shift of vibrations between the part and the working tool

The mathematical model of the vibratory machine with an active working element is a key tool for analyzing and optimizing its parameters. Using Newton's second law, we can write the system of equations that describe the behavior of the system as follows:

$$\begin{cases} m\dfrac{d^2x}{dt^2} = mA\omega^2\sin(\omega t) - k(x - x_d) - c\left(\dfrac{dx}{dt} - \dfrac{dx_d}{dt}\right) \\ m_d\dfrac{d^2x_d}{dt^2} = mA\omega^2\sin(\omega t + \phi) + \mu m_d g\cos(\theta) + k(x - x_d) + c\left(\dfrac{dx}{dt} - \dfrac{dx_d}{dt}\right) - k_d x_d - c_d\dfrac{dx_d}{dt} \\ m_a\dfrac{d^2x_a}{dt^2} = k_a x_a + c_a\dfrac{dx_a}{dt} - k_d(x_d - x_a) - c_d\left(\dfrac{dx_d}{dt} - \dfrac{dx_a}{dt}\right) \end{cases} \quad (2)$$

where:

- $m\dfrac{d^2x}{dt^2}$ – inertial force of the working body
- $mA\omega^2\sin(\omega t + \phi)$ – the magnitude of the vibration force
- $m_d\dfrac{d^2x_d}{dt^2}$ – inertial force of the part
- $\mu m_d g\cos(\theta)$ – the friction force of the part due to the angle of inclination
- $c_d\dfrac{dx_d}{dt}$ – damping force acting on the part
- $k_d x_d$ – elastic force acting on the part.
- $c\left(\dfrac{dx}{dt} - \dfrac{dx_d}{dt}\right)$ – damping force of interaction with the working body
- $-k\left(x - x_d\right)$ – strength of elasticity of interaction with the working body.
- $m_a\dfrac{d^2x_a}{dt^2}$ – inertial force of the abrasive.
- $k_a x_a(t)$ – elastic strength
- $c_a\dfrac{dx_a}{dt}$ – damping force
- $k_d\left(x_d - x_a\right)$ – elastic force acting between the abrasive and the part

The resonant frequency is determined by the formula:

$$\omega_{res} = \sqrt{\frac{k}{m}} \quad (3)$$

where k– spring stiffness, m – the mass of the working body. This is the frequency at which the amplitude of the system's vibrations reaches its maximum. The optimal vibration frequency should be lower than the resonance frequency to avoid excessive vibration amplitudes and ensure the stable operation of the system

$$\omega_{opt} < \omega_{res} \quad (4)$$

The excitation force F_0 is selected to ensure the required vibration amplitude without overloading the system. Typically, the vibration amplitude for vibrosystems in the processing of small parts ranges from a few millimeters to several centimeters. This ensures effective contact between the working tool and the part without excessive wear or overloading the system.

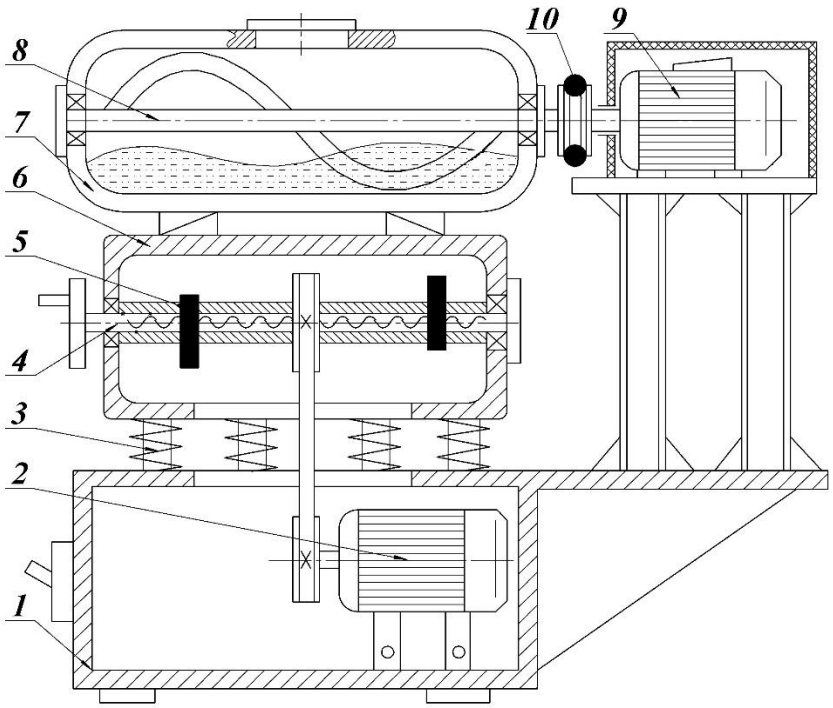

Figure 1 – Principal diagram of the vibro-abrasive processing setup:
1 – framework; 2 – vibration motor; 3 – spring; 4 – lead screw; 5 – debalances; 6 – frame;
7 – working chamber; 8 – active working element; 9 – working element motor; 10 - coupling

For this, the formula of the amplitude of oscillations in the harmonic mode is used:

$$A = \frac{F_0}{\sqrt{(k - m\omega^2)^2 + (c\omega)^2}} \quad (5)$$

where:
- A – amplitude of oscillations,
- ω – frequency of oscillations.

Selection of the Working Tool Shape

For processing small parts (up to 15 mm), it is essential to choose a working tool shape that ensures uniform treatment of the parts and minimizes system vibrations. Here are some possible shapes of working tools and their characteristics:

1. *Cylindrical Shape:*

Advantages: Simple to manufacture, good interaction with the parts.

Disadvantages: High vibration levels during operation, potential for uneven treatment.

Recommendations: Suitable for rough surface treatment where high precision is not required.2.

Conical Shape:

Advantages: Better load distribution, reduced vibration amplitude.

Disadvantages: Complex manufacturing, potential for parts to get stuck in sharp corners.

Recommendations: Optimal for medium complexity surface treatment, providing good stability.3.

Spherical Shape:

Advantages: Minimizes vibrations, ensures uniform load distribution, prevents parts from getting stuck.

Disadvantages: High manufacturing complexity.

Recommendations: Best choice for processing small parts requiring high precision.

Selection of the Working Tool Dimensions

1. Diameter of the Working Tool:

Recommendations: The diameter should be sufficient to ensure adequate contact area with the parts. An optimal diameter for parts up to 15 mm is 30-50 mm, which provides sufficient stability and uniform treatment.

2. Length of the Working Tool:

Recommendations: The length should correspond to the length of the working chamber to maximize the use of chamber space and ensure effective mixing of the parts.

3. Spiral Pitch (for Screw-Type Working Tools):

Recommendations: The spiral pitch should be chosen to ensure sufficient movement of parts along the axis of the working tool without imposing excessive loads on the system. The optimal spiral pitch for parts up to 15 mm is 20-30 mm.

Selecting a screw-type working tool will ensure a continuous flow of parts and abrasive along the working chamber, promoting uniform treatment, even load distribution on the parts, preventing localized force peaks, and facilitating intensive mixing.

Example of Numerical Calculation of Optimal Parameters

For the calculation example, let's consider the processing of ABS plastic parts, specifically decorative elements, with the goal of deburring, rounding sharp edges, and preparing the surface for painting. The abrasive medium used is ceramic granules. Below are the initial data and processing mode parameters:

- m — 2 kg
- m_d — 0,3 kg
- m_a — 1 kg
- k — 1000 N/m
- k_d — 500 N/m
- k_a — 300 N/m
- c — 10 Nc/m
- c_d — 5 Nc/m
- c_a — 3 Nc/m
- A— 0.002 m
- ω— 50 rad/s
- Ω—30 rad/s (287 RPM)
- μ — 0,1
- g — 9,81 m/s^2
- θ — 0 rad
- ϕ — 5 rad

We will perform the calculation of the main parameters of the setup, such as the vibration amplitude of the working tool and parts, and the phase shift, using the MathCAD software package. Then, the proposed gradient descent optimization algorithm will be applied to determine the optimal parameters.

In the graph shown in Fig. 2, it is observed that the amplitude of oscillations for both the working tool and the parts increased after optimization. This indicates an increase in the energy transmitted to the part, which enhances productivity, as the processing becomes more intense, removing more material per unit time. However, to maintain high processing accuracy in practice, it is essential to carefully control the amplitude and frequency of vibrations to avoid excessive impact on the quality of the manufactured parts.

The graph in Fig. 3 shows a reduction in the phase shift between the working tool and the part after optimization. This decreases relative movements, thereby improving processing accuracy. The phase shift can be further optimized by adjusting the stiffness and damping of the system.

1. The vibration amplitude A was increased from 0.002 m to 0.003 m.
2. The vibration frequency ω was increased from 50 rad/s to 55 rad/s.
3. The rotational frequency Ω was increased from 30 rad/s to 35 rad/s.
4. The spring stiffness k was increased from 1000 N/m to 1200 N/m to enhance force transmission efficiency and system stability.

Further experimental studies are necessary to validate the theoretical results obtained and to refine the mathematical model.

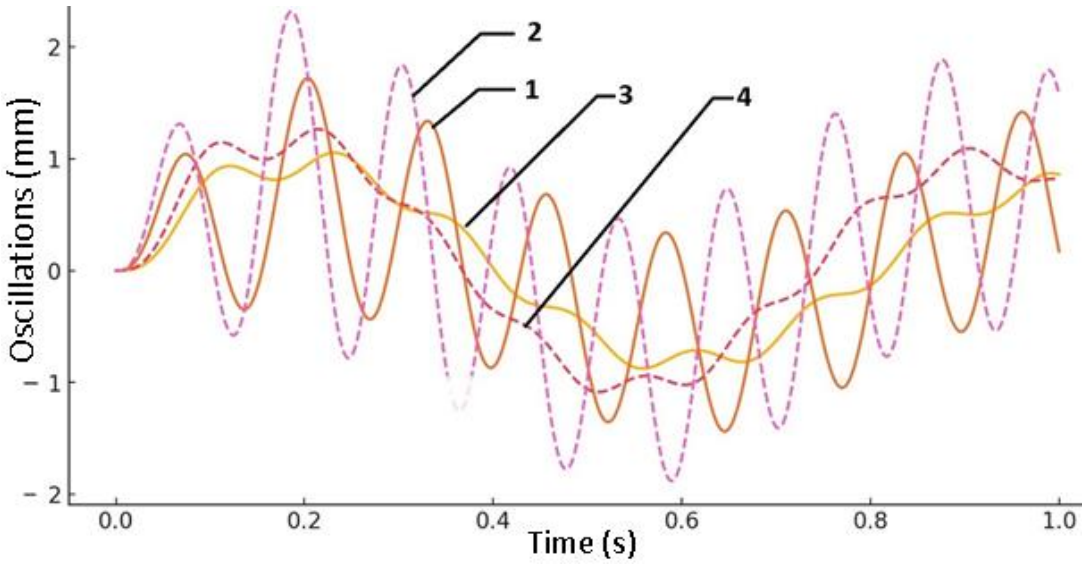

Figure 2 – The graph of oscillations based on the calculation results:
1 - workpiece before optimization; 2 - workpiece after optimization;
3 - working element before optimization; 4 - working element after optimization.

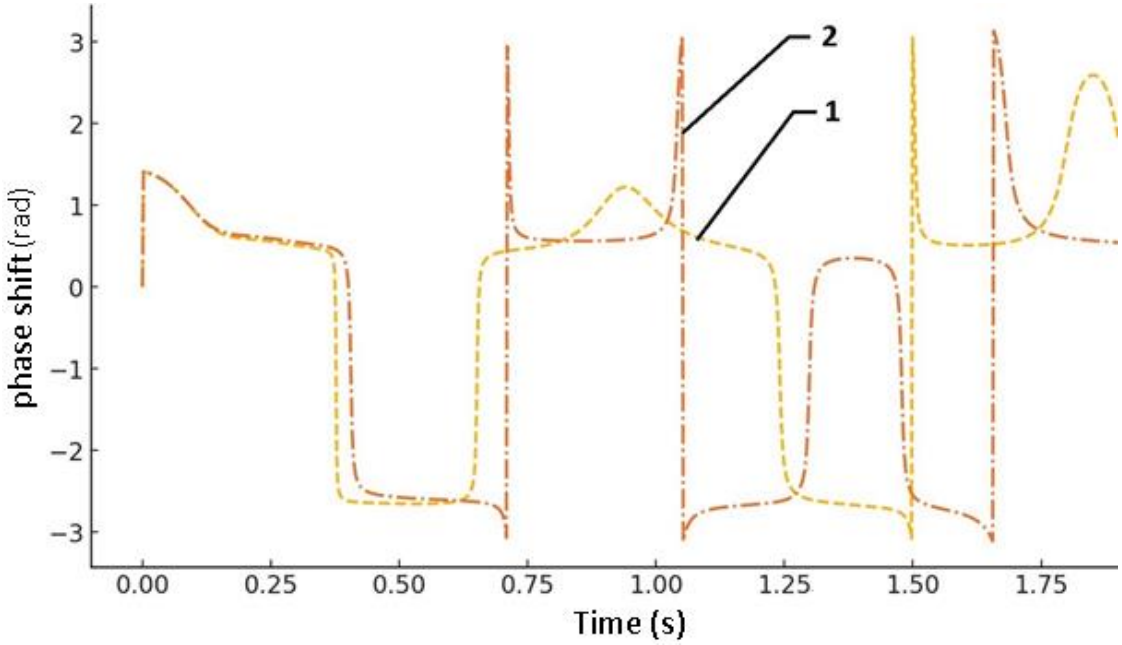

Figure 2 – The graph of the phase shift magnitude between the oscillations of the workpiece and the working element based on the calculation results: 1 - before optimization; 2 - after optimization.

Conclusions

Thus, the following has been established:

1. A mathematical model for analyzing the dynamic interaction between the working body and the workpiece in a vibro-abrasive machine has been proposed, taking into account frictional and damping forces. This allows consideration of all dynamic characteristics of the system and determination of the phase shift between the working body and the workpieces.

2. Precise adjustment of the optimal frequency and vibration amplitude parameters can be achieved through the use of numerical methods for integrating the system of differential equations in the model, combined with the application of optimization algorithms.

3. The constructed graphs based on the calculation results and their analysis demonstrated a reduction in the phase shift between the working body and the workpiece after optimization. This increases the accuracy of vibro-processing and improves the quality of the workpiece surfaces, while also reducing equipment wear.

4. Minimizing the phase shift between the working body and the workpiece reduces relative movements, thereby increasing processing accuracy. The phase shift can be optimized by adjusting the system's stiffness and damping.

5. Ensuring stable system operation without significant vibrational oscillations allows for maintaining high processing accuracy. Consistency in the frequency characteristics and amplitude contributes to precise processing

References

1. Jia, L., Wang, C., Liu, Z. (2023). Multifrequency controlled synchronization of four inductor motors by the fixed frequency ratio method in a vibration system. Scientific Reports, 13, 2467. https://doi.org/10.1038/s41598-023-29747-2

2. Blekhman, I.I. (2000). Vibrational Mechanics: Nonlinear Dynamic Effects, General Approach, Applications. World Scientific. https://doi.org/ 10.1142/3771

3. Zou, M., Fang, P., Hou, Y., Wang, Y., Hou, D., Peng, H. (2021). Synchronization analysis of two eccentric rotors with double-frequency excitation considering sliding mode control. Journal of Communication Nonlinear Science and Numerical Simulation, 92, 105458. https://doi.org/10.1016/j.cnsns.2021.105458

4. Khalil, H.K., Strangas, E.G., Jurkovic, S. (2009). Speed Observer and reduced nonlinear model for sensorless control of induction motors. IEEE Transactions on Control Systems Technology, 17(2), 327-339.. https://doi.org/10.1109/TCST.2008.2006697

1. Jia, L., Wang, C., Liu, Z. (2023). Multifrequency controlled synchronization of four inductor motors by the fixed frequency ratio method in a vibration system. Scientific Reports, 13, 2467. https://doi.org/10.1038/s41598-023-29747-2

2. Blekhman, I.I. (2000). Vibrational Mechanics: Nonlinear Dynamic Effects, General Approach, Applications. World Scientific. https://doi.org/ 10.1142/3771

3. Zou, M., Fang, P., Hou, Y., Wang, Y., Hou, D., Peng, H. (2021). Synchronization analysis of two eccentric rotors with double-frequency excitation considering sliding mode control. Journal of Communication Nonlinear Science and Numerical Simulation, 92, 105458. https://doi.org/10.1016/j.cnsns.2021.105458

4. Khalil, H.K., Strangas, E.G., Jurkovic, S. (2009). Speed Observer and reduced nonlinear model for sensorless control of induction motors. IEEE Transactions on Control Systems Technology, 17(2), 327-339.. https://doi.org/10.1109/TCST.2008.2006697

5. Andrievsky, B.R., Blekhman, I.I., Blekhman, L.I., Boikov, V.I., Vasil'kov, V.B., Fradkov, A.L. (2016). Education and research mechatronic complex for studying vibration devices and processes. Problems of Mechanical Engineering and Reliability of Machines, 4, 90-97

6. Hashemnia, K., Mohajerani, A., & Spelt, J. K. (2013). Development of a laser displacement probe to measure particle impact velocities in vibrationally fluidized granular flows. Powder Technology, 235, 940-952. https://doi.org/10.1016/j.powtec.2012.12.001

7. Hashimoto, F., Johnson, S. P., & Chaudhari, R. G. (2016). Modeling of material removal mechanism in vibratory finishing process. CIRP Annals, 65(1), 325-328. https://doi.org/10.1016/j.cirp.2016.04.011

8. Fleischhauer, E., Azimi, F., Tkacik, P., Keanini, R., & Mullany, B. (2016). Application of particle image velocimetry (PIV) to vibrational finishing. Journal of Materials Processing Technology, 229, 322-328. https://doi.org/10.1016/j.jmatprotec.2015.09.017

9. Mullany, B., Shahinian, H., Navare, J., Azimi, F., Fleischhauer, E., & Tkacik, P. (2017). The application of computational fluid dynamics to vibratory finishing processes. CIRP Annals, 66(1), 309-312. https://doi.org/10.1016/j.cirp.2017.04.087

10. Tian, Y. B., Zhong, Z. W., & Tan, S. J. (2016). Kinematic analysis and experimental investigation on vibratory finishing. The International Journal of Advanced Manufacturing Technology, 86(9-12), 3113-3121. https://doi.org/10.1007/s00170-016-8378-x

11. Kang, Y. S., Hashimoto, F., Johnson, S. P., & Rhodes, J. P. (2017). Discrete element modeling of 3D media motion in vibratory finishing process. CIRP Annals, 66(1), 313-316. https://doi.org/10.1016/j.cirp.2017.04.092

12. Serdyuk L. The controlled vibromachines / L. Serdyuk // Jubilee scientific conferens. University of architecture, civil ingineering and geodezy. – Sofia : UACIG, 2007. –P. 43 – 48.

13. Жигилій С. М. (2012) Дослідження динаміки дебалансного вала керованого віброзбуджувача УВВ-03 / С. М. Жигилій, К. С. Дяченко // Збірник наукових праць. Серія: Галузеве машинобудування, будівництво. – Полтава : ПолтНТУ, 2012. – Вип. 2 (32). – С. 159 – 164.

14. Коробко, Б.О., Бугров Д.Ю. (2024). Розробка конструкції установки для віброабразивної обробки поверхонь декоративних елементів з активним робочим органом. *Вібрації в техніці та технологіях*, 2024(1), 1-10. https://doi.org/10.37128/2306-8744-2024-1-1

5. Andrievsky, B.R., Blekhman, I.I., Blekhman, L.I., Boikov, V.I., Vasil'kov, V.B., Fradkov, A.L. (2016). Education and research mechatronic complex for studying vibration devices and processes. Problems of Mechanical Engineering and Reliability of Machines, 4, 90-97

6. Hashemnia, K., Mohajerani, A., & Spelt, J. K. (2013). Development of a laser displacement probe to measure particle impact velocities in vibrationally fluidized granular flows. Powder Technology, 235, 940-952. https://doi.org/10.1016/j.powtec.2012.12.001

7. Hashimoto, F., Johnson, S. P., & Chaudhari, R. G. (2016). Modeling of material removal mechanism in vibratory finishing process. CIRP Annals, 65(1), 325-328. https://doi.org/10.1016/j.cirp.2016.04.011

8. Fleischhauer, E., Azimi, F., Tkacik, P., Keanini, R., & Mullany, B. (2016). Application of particle image velocimetry (PIV) to vibrational finishing. Journal of Materials Processing Technology, 229, 322-328. https://doi.org/10.1016/j.jmatprotec.2015.09.017

9. Mullany, B., Shahinian, H., Navare, J., Azimi, F., Fleischhauer, E., & Tkacik, P. (2017). The application of computational fluid dynamics to vibratory finishing processes. CIRP Annals, 66(1), 309-312. https://doi.org/10.1016/j.cirp.2017.04.087

10. Tian, Y. B., Zhong, Z. W., & Tan, S. J. (2016). Kinematic analysis and experimental investigation on vibratory finishing. The International Journal of Advanced Manufacturing Technology, 86(9-12), 3113-3121. https://doi.org/10.1007/s00170-016-8378-x

11. Kang, Y. S., Hashimoto, F., Johnson, S. P., & Rhodes, J. P. (2017). Discrete element modeling of 3D media motion in vibratory finishing process. CIRP Annals, 66(1), 313-316. https://doi.org/10.1016/j.cirp.2017.04.092

12. Serdyuk L. The controlled vibromachines / L. Serdyuk // Jubilee scientific conferens. University of architecture, civil ingineering and geodezy. – Sofia : UACIG, 2007. – P. 43 – 48.

13. Zhygilii, S. M., & Dyachenko, K. S. (2012). Investigation of the dynamics of the unbalanced shaft of the controlled vibration exciter UVV-03. Collection of Scientific Works. Series: Industry Engineering, Construction, Poltava National Technical University, 2012, Issue 2 (32), pp. 159-164

14. Korobko, B.O., Bugrov, D.Yu. (2024). Development of a setup for vibratory abrasive treatment of surfaces of decorative elements with an active working tool. *Vibrations in engineering and technology*, 2024(1), 1-10. https://doi.org/10.37128/2306-8744-2024-1-1

Збірник наукових праць. Галузеве машинобудування, будівництво
Academic journal. Industrial Machine Building, Civil Engineering
http://journals.nupp.edu.ua/znp
https://doi.org/10.26906/znp.2023.61.3851

UDC 691.5:620.193.2

Analysis of equipment for thermoplastic molding artificial products of spatial form

Ivan Suchkov [1], Rostyslav Rudyk [2]*

[1] National University «Yuri Kondratyuk Poltava Polytechnic» https://orcid.org/0009-0002-9809-3681
[2] National University «Yuri Kondratyuk Poltava Polytechnic» https://orcid.org/0000-0001-8386-977X
*Corresponding author E-mail: rostyslavrudyk@nupp.edu.ua

The study explores the innovative use of recycled plastic in brick production in the construction industry in Ukraine. It examines the production process, including the collection and processing of plastic waste, and the formation of bricks using methods such as plastic molding and semi-dry pressing. The research emphasizes the importance of pressure distribution in screw presses for the compaction of clay in construction ceramics production and highlights the significance of vacuuming the molding mass for improving the quality of molded products. Plastic-brick products are found to offer advantages such as altered strength, improved insulation properties, and lighter weight. Comparing technological schemes, the semi-dry method of brick production is noted to have higher metal capacity and lower labor intensity compared to the plastic method. The study aims to enhance the efficiency and results of thermoplastic molding in the construction industry, contributing to sustainable construction practices and reducing environmental impact.

Keywords: ecology; energy efficiency; equipment; plastic; plastic-ceramic products; press; thermoplastic molding; pressure; brick; quality

Аналіз обладнання для термопластичного формування штучних виробів просторової форми

Сучков І. М.[1], Рудик Р. Ю.[2*]

[1,2] Національний університет «Полтавська політехніка імені Юрія Кондратюка»
*Адреса для листування E-mail: rostyslavrudyk@nupp.edu.ua

Будівельна галузь в Україні постійно розвивається, використовуючи сучасні технології та матеріали для підвищення стійкості та ефективності. Одне з таких нововведень передбачає використання переробленого пластику у виробництві цегли, пропонуючи багатообіцяюче рішення для боротьби з пластиковими відходами та сприяння переробці. Виробничий процес передбачає збір і переробку пластикових відходів, які потім змішуються з іншими компонентами та формуються в цеглу за допомогою таких методів, як формування пластику та напівсухе пресування. Ці методи мають явні переваги та недоліки, що впливає на загальну якість і властивості цегли. Критичним аспектом виробничого процесу є розподіл тиску в шнекових пресах, який відіграє ключову роль у пресуванні глини для виробництва будівельної кераміки. Проведено аналіз течії глини через прес на моделі в'язкопластичного матеріалу та розраховано характеристики шнека та формувальних тіл для визначення параметрів режиму роботи. Крім того, вакуумування формувальної маси визначено як вирішальний крок для підвищення якості формованих виробів. Отримані вироби з пластикової цегли демонструють ряд переваг, включаючи змінену міцність, покращені ізоляційні властивості та меншу вагу, що робить їх переконливою альтернативою традиційним цегляним матеріалам. Крім того, порівняння технологічних схем показує, що напівсухий спосіб виробництва цегли демонструє більшу металоємність і меншу трудомісткість на відміну від пластичного. Це дослідження має на меті зробити внесок у поточні зусилля щодо підвищення ефективності та результатів термопластичного формування в будівельній галузі. Досліджуючи інноваційне використання переробленого пластику у виробництві цегли та наголошуючи на важливості розподілу тиску та вакуумування в процесі формування, це дослідження спрямоване на просування екологічних методів будівництва та зменшення впливу на навколишнє середовище.

Ключові слова: екологія; енергоефективність; обладнання; пластик; пластико-керамічні вироби; прес; термопластичне формування; тиск; цегла; якість

Introduction.

The construction industry in Ukraine is one of the key sectors of the economy, which determines not only the socio-economic development of the country, but also contributes to the formation of modern infrastructure and maintains the stability of the national economy.

Technical progress and the introduction of innovations in the construction industry play an important role in ensuring high quality construction and energy efficiency of facilities.

One of the key trends in the construction industry is the active use of the latest building materials and technologies. Innovative building materials, such as high-strength concrete, environmentally friendly insulation materials and modern composite structures, ensure high strength and durability of structures.

The construction industry in Ukraine is constantly developing, using modern technologies and materials to achieve high quality and durability of construction projects. One of the key materials that is widely used is brick, which has the properties necessary for high-quality construction.

There are several basic methods of making bricks: plastic molding method (ceramic brick [7]) and semi-dry pressing method (silicate brick [8]). The plastic molding method is simpler in the technological process of making ceramic bricks. The method of producing bricks in this way is more economical and practical in our region, due to the use of local materials.

Today, a new innovative technology has emerged aimed at reducing the consumption of traditional building materials and the use of recycled plastic, which helps to reduce the negative impact on the environment [20].

Review of the research sources and publications.

Ukrainian and foreign researchers were engaged in research in the preparation of bricks using plastic, which made it possible to use plastic waste, which usually becomes a problem for the environment. The use of plastic in brick production can help reduce the amount of plastic waste and promote recycling.

Plastic-based brick manufacturing processes that use less energy compared to traditional brick production methods have also been described [6].

Studies have also shown that the use of plastic materials in construction can be an innovative solution that develops the construction technology industry. This can open up new possibilities for architectural solutions and structures, expanding the possibilities for the design and efficiency of buildings. The use of plastic in brick production can create a demand for recycled materials and contribute to the development of efficient recycling systems [17, 18].

Definition of unsolved aspects of the problem

It requires in-depth research on the properties and capabilities of new thermoplastic materials, namely the study of their resistance, mechanical characteristics and recycling capabilities.

There is insufficient theoretical justification for studies of the properties of plastics and their impact on the quality and strength of bricks and the types of plastic that are most suitable for use in bricks and can be combined with other materials.

It is also important to study and take into account production safety issues, as well as to determine the appropriate standards for thermoplastic molding. Consideration of the impact of thermoplastic molding on other production processes and the development of integrated approaches to production.

Problem statement

Research of promising technologies in the field of thermoplastic molding and their possible impact on production, analysis of modern brick forming equipment, including its specifications, efficiency and capabilities and the study of technological aspects and parameters, affecting the quality of thermoplastic molding, in order to improve efficiency and results.

Basic material and results

The production of plastic-ceramic products includes several key stages. The first stage is to collect and process the recycled plastic. Plastic waste is used, such as plastic bottles, bags, containers, and others. This plastic is placed in special containers and can be cleaned and shredded. The shredded plastic is mixed with other components such as sand, cement, water, and additional additives that improve strength and insulation properties. The resulting mixture is fed into special molds, which give the brick product the required shape and size. Products can be compressed or pressed to obtain the required density [16]. The formed bricks are subjected to a drying and hardening process, which can take place at room temperature or at elevated temperatures in special drying chambers or ovens [10]. Finished bricks are packed in bundles or on pallets for easy transportation and delivery to construction sites.

When assessing the plastic-ceramic mass's ability to form, first of all, the quantitative relationships between the solid, liquid and gaseous phases of the mixture are considered. The liquid phase (water) is an essential component of the ceramic mass for all practically used molding methods. Water, on the one hand, tightens clay particles, on the other hand, causes significant mobility of clay particles, providing them with the ability to slide relative to each other. The required amount of the liquid component for the formation process in one way or another depends on many different factors: the method of formation, the mineral composition of the clay component, its amount in the plastic-ceramic mass, the content of the air component, etc. One of the main requirements for the formed semi-finished plastic and ceramic product is a sufficient and constant degree of its compaction, which is characterized by an indicator of relative density or porosity, which largely determines the behavior of the semi-finished product in drying and especially in firing.

To assess the quality of the semi-finished product, not only the density values are important, but also its uniformity in different parts of the body of the formed product. Insufficient even density of the semi-finished product leads to unequal shrinkage during sintering, accompanied by deformation and even cracking [5].

This indicator is decisive for transportation, processing, installation of the semi-finished product in dryers and furnaces without damage and violation of its integrity.

The main requirements proposed for the semi-finished product after its formation also include the absence of structural defects – internal cracks, sinks and the absence of significant internal stresses, which in the process of subsequent technological operations can cause the formation of various defects and destruction of the finished product.

Based on these technical and economic requirements for the semi-finished product, as well as taking into account the physical and mechanical properties of the feedstock, it is possible to choose one or another method of forming the semi-finished product. In the production of building ceramics, the following methods are most common: plastic molding from masses with a moisture content of 14...20%, pressing from powdered masses with a moisture content of 5... 7% and casting of semi-finished products in gypsum molds from foundry masses with a moisture content of 30... 33%.

There are several ways in which plastic-ceramic mass is processed and products are formed. Based on the properties of the initial raw materials and the type of products that are manufactured, there are plastic and semi-dry methods.

Semi-dry pressing is based on pressing individual bricks from raw materials in the form of powder with a moisture content of 7...12% by sealing in closed molds. The low moisture content of the raw material with this method makes it possible to combine drying with firing in some complexes.

The advantages of semi-dry pressing are the ability to deploy the production of sufficiently high-quality bricks using clay raw materials of low conditions. The energy consumption for drying the loose clay before molding is much less than for the gentle drying of the wet raw material of plastic molding.

The main disadvantage, organically inherent in the method of semi-dry molding, is associated with the granular structure of raw materials and bricks, which loses in the homogeneity of plastic molded bricks. Quality indicators of semi-dry molded bricks (strength, frost resistance, durability), meeting the requirements of the standards, still have a significantly lower maximum limit. An inherent defect in semi-dry pressing of ceramic products is delamination cracks, which are located perpendicular to the pressing force. The main reasons for the appearance of such cracks are the growth of pressed air, segregation of the press powder when it is poured into the mold and elastic deformations of clay particles.

Plastic molding is characterized by the extrusion of solid timber and cutting it with strings into individual bricks. To implement this method, the raw material is prepared for formation in the form of a plastic charge with a moisture content of 17...25%, capable of defect-free extrusion, which is performed, as a rule, on screw presses. Depending on the pressure required for extrusion, a distinction is made between the so-called soft (pressure up to 1.6 MPa), semi-rigid (pressure 1.6...2.5 MPa) and rigid (pressure 2.5...4.0 MPa) extrusion. The power of the press motors also increases approximately in proportion to the pressure. Such presses are called belt presses, because they cut a beam (strip), which is then cut into products of the required size.

The main goal of the powder pressing process is to obtain the maximum pressing density. This indicator has the main impact on the completeness of the physicochemical processes in the mass during firing of products, as well as on the quality of the final product. It is for this reason that in the production of plastic-ceramic tiles, the insufficient density of the semi-finished product causes increased shrinkage, and therefore an increase in firing defects – cracks, warping, etc.

Uneven pressing also has a negative value. The main reasons for this may be the loss of pressure on the passage of friction against the walls of the mold, the dissimilar ratio between the depth of the layering and the thickness of the semi-finished product in different parts of the product, in addition, there may also be filling individual sections of the mold with powder of different granular composition and moisture content. A positive effect on the quality of pressing is made by stepped or repeated pressing, in which the die presses on the powder with the stages of unloading, namely, after a certain period of pressure, the die rises slightly and the pressing is released from the pressing pressure. This technique allows you to remove air from the presses as much as possible, causes less uneven density with a significantly lower maximum pressure than with one-stage pressing.

Presses that are used for plastic molding in relation to the design of the pressing device are divided into piston and screw presses [4].

The reciprocating press is simple in design and contains forming organs such as a press head with cavity formers, a mouthpiece and a cyclic operating piston blower. The cycle of operation of the piston blower consists of the working stroke for compaction of clay and extrusion of the beam and the return stroke to the original position after the next portion of clay [10]. The hydraulic piston drive allows to obtain significant pressure sufficient for rigid brick formation, and also ensures high piston speed in its reverse stroke and pre-sealing stroke, when the resistance force of the piston movement is negligible. Pauses in extrusion reduce productivity but significantly facilitate the cutting of fixed timber. It is advisable to use a reciprocating press in parallel with a powerful screw press as part of complexes for the production of facing bricks for the formation of relatively small batches of shaped bricks and other products of a wide range of shapes and sizes. In this version, the powerful screw press is used as efficiently as possible, without wasting time on frequent changeovers.

Screw presses use the principle of working with a screw shaft or screw squeeze, which moves plastic-ceramic raw materials and compresses them into a mold to obtain the desired shape and size of the product.

The blade of screw presses can be one-, two- and three-pass (Figure 1). Single-pass squeeze blades provide high press productivity and lower specific energy consumption for pressing. A press with a two-stroke squeeze blade has a much better pressing quality than a press with a single-pass blade, however, all other things

being equal, the performance is less and the specific energy consumption is greater. Three-pass blades with and without overlap are rarely used due to a sharp decrease in the productivity of the press.

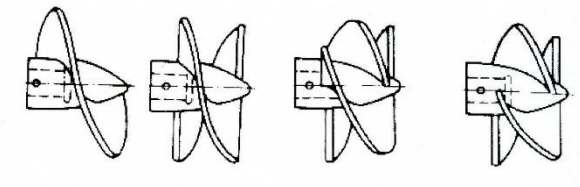

Figure 1 – Designs of pressing screw shaft blades

Belt screw presses are designed for the production of plastic-ceramic products with a moisture content of 14...25%. Also, according to technological characteristics, they are divided into presses with vacuuming and presses without vacuuming of plastic-clay mass. By design – for presses with discontinuous screw blades and for presses with cylindrical, stepped or conical bodies [3].

The speed of axial movement of the mass in the press cylinder is uneven: it is almost zero in the screw hub and maximum at the inner surface of the housing. As a result, in the mass moved in the press body, delaminations occur parallel to the axis of the press. With the further advancement of the mass in the press head, its individual sections also move at different speeds due to frictional forces along the outer perimeter of the mass beam, as well as the rotational motion, which continues partially, the mass and filling with it of the space previously occupied by the hub of the screw. As a result of such a complex movement of the mass, which depends on a large number of factors and is basically not suitable for theoretical calculation, the bar at the exit from the mouthpiece does not have a homogeneous structure, but is a sequential layering of empty cones of mass nested within each other.

To reduce and eliminate these shortcomings of plastic molding in screw presses of continuous action, it is necessary to observe the following technological parameters and measures: careful preparation of the plastic mass for the pressing operation; decrease in retention (in %) of the dusty part of the fireclay component of the mass; lengthening of the press head by inserting an intermediate ring 100...200 mm long between the body and the press head, reducing the gap between the screw blades and the press body to 2...4 mm; installation of peeling knives in the intermediate ring or head of the press; reducing the speed of the screw shaft to 20... 30 rpm; some increase in the moisture content of the mass.

Prior to the output of the timber formation and depending on the design, the presses are divided into vertical and horizontal. They are used in the production of special fine ceramics, building bricks, strip tiles, hollow ceramic blocks, socketless and drainage sewer pipes.

The screw aggregate press contains a press, a vacuum chamber and a mixer. Mixing the clay should take place without sucking in air. In this way, a screw and a working body are added to the paddle mixer to give resistance to the movement of the clay and its crushing by a grate or knives and cones [2]. While the pressure of the clay in the screw-sealed ring may be sufficient to maintain a high level of vacuum, it should not be excessive to reduce wear and energy intensity.

The press, which contains the forming organs, the screw blower (mouthpiece with cavity formers) and the press head, performs the main forming process.

The pressing process demonstrates the change in pressure in different areas of the auger, as shown in the Fig. 2. The highest pressure observed in the area of the mixer screw end blade is 0.4–0.5MPa. This is significantly less than the pressure of the main screw. Loading, pre-compaction, pressure build-up, and forming are all parts of the main screw. In the first section, the screw is filled with cut clay. During transportation, it constantly sucks out air, starting from the moment it falls. There's no pressure at this point, and it shouldn't be. In this region, the screw capacity must exceed the maximum possible with power fluctuations [1].

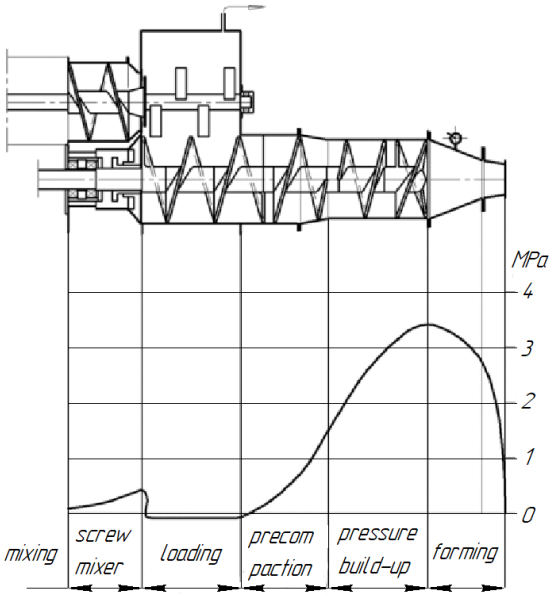

Figure 2 – Pressure distribution in the screw press

In the next part, preliminary compaction begins, and when the clay has already filled the entire turn-to-turn channel of the screw, air is squeezed out of the pores into the vacuum chamber. Reducing the channel area with auger taper and auger pitch helps to speed up compaction.

The increase in pressure is carried out by a screw in the following area. The presence of knives helps to stop the clay from turning along with the screw, in the gaps of the auger blades in this area. The pressure in the clay in the zones of action of the knives is balanced at a level sufficient to overcome the resistance of the forming organs. This means that when the supply fluctuates, these areas also help prevent overpressure inside the screw. Clay flows unevenly through the interturn channel of the auger. It flows faster in the periphery than in the hub. The cross-section that passes through the end blade at the inlet to the press head has the highest pressure. The level of this pressure is determined by the

pressure losses that occur during the passage of clay through the channels of the organs that are being formed.

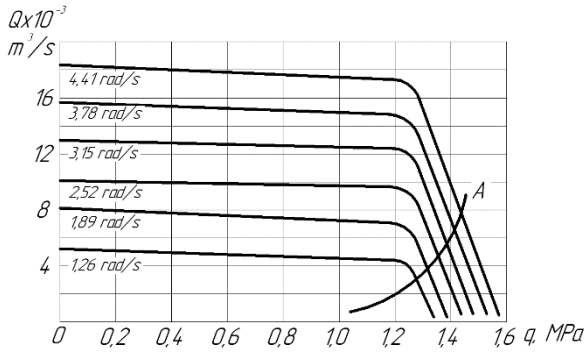

Figure 3 – Characteristics (performance as a function of pressure) of the screw and molding bodies at variable frequency

The new methods for measuring the pressure and capacity of the screw press are similar to those for aerodynamic and hydraulic systems. This method focuses on the interaction of the supercharger and the forming organs together, which means that their characteristics is $Q=f(q)$, i.e., the dependence of performance Q on pressure q. Figure 3 shows the characteristics of the screw at variable angular velocity (1.26 to 4.41 s^{-1}), as well as the characteristics of the forming organs (curve A). The operating mode parameters, Q_p and q_p, are identified as the points of intersection of the curves.

Models of Shvedov-Bingam visco-plastic material are used to describe the flow of clay through auger channels and forming organs:

$$\tau = \tau_0 + \mu \cdot \frac{dU}{dy} \quad (1)$$

where τ and τ_0 – effective and maximum stress shear;
μ – material viscosity;
$\frac{dU}{dy} = \gamma$ – velocity gradient.

This model demonstrates a class of materials in which the stress is proportional to the velocity gradient, as in a classical Newtonian fluid, but the flow begins only after the maximum shear stress is reached τ_0. In the clays used to make building ceramics using the plastic molding method, there is a feature known as the viscosity anomaly. Its essence lies in the fact that shear stress, or effective viscosity $\mu_e = f(\gamma)$, decreases significantly as the velocity gradient increases, rather than remaining constant [1]. The rheological curve, which is a mathematical description of dependence, has the form:

$$\mu_e = \mu_0 \cdot (\gamma)^{-\psi} \quad (2)$$

where ψ – the flow index, which depends in logarithmic coordinates on the angle of inclination of the rheological curve to the abscissa axis;

μ_0 – consistency index is an indicator that determines the effective viscosity at a unit velocity gradient, H·s/m^2.

A complex equation that describes the properties of a screw takes into account the leakage of clay through the gaps between the screw and the cylinder jacket and through the turn-to-turn channel:

$$Q_{шн} = Q_{пр} - Q_{зв} - Q_{вит} \quad (3)$$

where $Q_{шн}$ – supercharger performance;
$Q_{пр}$ – direct flow, which occurs due to the pushing ability of the main front surfaces of the screw;
$Q_{зв}$ – the backflow that occurs when the forward flow is restrained;
$Q_{вит}$ – outflow through the gaps.

The characteristics of the forming organs (curve A in Figure 3) are calculated as $q=f(Q)$, moreover, the total pressure q_Σ is equal to the sum of the pressure losses in the press head $q_{гол}$ and mouthpieces $q_{мун}$: $q_\Sigma = q_{гол} + q_{мун}$. Each loss is calculated using the formula:

$$q_{гол}(q_{мун}) = \mu \cdot \frac{Q}{K_г} \quad (4)$$

where $K_г$ – A coefficient that describes the shape of a flow channel and is calculated using formulas for cylindrical, conical, slit, and wedge-shaped channels.

Effective viscosity μ_e for each channel, find by a chart $\mu_e = f(\gamma)$ after calculating the velocity gradient for each channel.

It should be noted that the rheological characteristics of different clays differ significantly from each other. In addition, experiments with the calculation of rheological curves on piston rheometers are quite complex and require special equipment [13]. For this reason, simplified methods for calculating screw presses are used in design practice.

Vacuuming molding is one of the best ways to improve the quality of molded products. As you know, the presence of air in the mass reduces the strength and molding properties of the ceramic mass due to the breaking of bonds between individual grains of clay minerals and water molecules. The presence of air in the ceramic mass also reduces the process of disaggregation of clay particles, reduces the molding ability of the mass, and leads to uneven compaction during molding, which leads to the formation of microcracks in the formed product. Stable vacuum, which depends on uniform press feed, as well as the power and reliability of the vacuum pumps, is important for effective vacuuming.

Unlike ordinary bricks, the characteristics of plastic-brick products differ and have a number of advantages. Plastic-brick products may have altered strength compared to traditional bricks depending on the type of plastic and the ratio of components in the mixture.

Plastic-brick products have better insulation properties, especially if they contain polystyrene foam, which helps to improve the energy efficiency of buildings and reduce heating and air conditioning costs.

Also, plastic-brick products are lighter compared to traditional bricks, which makes it easier to transport and process on the construction site.

The semi-finished product, which is pressed on vacuum presses, is not fully formed and undergoes pressing again on a pre-pressing press to give the semi-finished product the correct shape, as well as the necessary strength. At the same time, there are ancillary costs, which is inappropriate nowadays.

Comparing the technological schemes for the production of bricks by plastic and semi-dry methods of mass preparation, it should be noted that with almost the same indicators of energy consumption, the indicators of metal consumption of semi-dry pressing plants are about three times higher, and the labor intensity of making one thousand bricks is 30% lower compared to the semi-dry method.

Conclusions

The construction industry in Ukraine is adopting innovative technologies such as using recycled plastic to make bricks, tackling plastic waste, and promoting recycling. The production process involves collecting and recycling plastic waste, mixing it with other components, and shaping bricks using methods such as plastic molding and semi-dry pressing. To improve the quality of bricks, various equipment is used, for example, reciprocating and screw presses. The study aims to improve the efficiency and results of thermoplastic casting in the construction industry. In addition, the study highlights the importance of pressure distribution in screw presses to compact clay in the production of building ceramics. Vacuuming of the molding mass is emphasized as crucial for improving the quality of molded products. Plastic brick products have advantages such as altered strength, better insulation properties, and lighter weight. Comparing technological schemes, the semi-dry method of brick production has a higher metal consumption and less labor intensity compared to the plastic one. Overall, the study highlights the potential of recycled plastic bricks in promoting sustainable construction practices and reducing environmental impact.

References

1. Савченко О.Г. (2006). *Обладнання комплексів для виробництва будівельних дрібноштучних стінових виробів*. Х.: Тимченко. – 416 с.

2. Болотських М.С., Ємельянова І.А., Савченко А.Г. (1994) *Машини для будівельно-монтажних робіт: Довідник*. – К.: Будівельник. – 342 с.

3. Болотських М.С., Федоров Г.Д., Савченко А.Г., Крот А.Ю.(2001) Виробництво цегли із шлаку з використанням барабанно-валкового активатора. Будівельні матеріали та вироби. Всеукр. науково-техн. журнал. – Київ, 4, 27-28.

4.Назаренко І.І. (1999). Машини для виробництва будівельних матеріалів: Підручник. – К.: КНУБА, 488 с.

5. Федоров Г.Д., Савченко О.Г. (1998). Аналіз схем підготовки прес-порошку під час підготовки керамічної цегли. Науковий вісник будівництва. ХДТУБА ХОТВ АБУ, 3, 104-105.

6. Франківський А.А., Рунова Т.В., Свінцицкий Р.Л., Пліс А.В. (1997). Високоякісна керамічна продукція та енергозбереження – головні цілі модернізації цегельного виробництва в Україні. Будівництво України, 6, 13-16.

7. ДСТУ Б В.2.7-61:2008 (2009). Будівельні матеріали. Цегла та камені керамічні, рядові та лицьові. Технічні умови. Київ: Мінрегіонбуд України

8. ДСТУ Б В.2.7-80:2008 (2009). Будівельні матеріали. Цегла та камені силікатні. Технічні умови. Київ: Мінрегіонбуд України

9. Величко Ю.М., Племянніков М.М., Яценко А.П., Корнілович Б.Ю.(2016). Хімія і технологія кераміки. Високотемпературні процеси: навчальний посібник. К.: «Освіта України»

10. Kocserha I., Kristály F. (2010). Effects of Extruder Head's Geometry on the Properties of Extruded Ceramic Products. Materials Science Forum, Vol. 659, 499-504 https://doi:10.4028/www.scientific.net/MSF.659.499

11. Constantine Sikalidis, Manassis Mitrakas (2006). Utilization of Electric Arc Furnace Dust as Raw Material for the Production of Ceramic and Concrete Building Products. Journal of Environmental Science and Health, 9 (41),

1. Savchenko O.G. (2006). Equipment for complexes for the production of construction small-scale wall products. Kh.: Tymchenko. - 416 p.

2. Bolotskikh M.S., Yemelyanova I.A., Savchenko A.G. (1994) Machines for construction and assembly work: Handbook. - K.: Builder. - 342 p.

3. Bolotskikh M.S., Fedorov G.D., Savchenko A.G., Krot A.Yu. (2001) Production of bricks from slag using a drum-roll activator. Building materials and products. All-Ukrainian scientific and technical magazine. - Kyiv, 4, 27-28.

4. Nazarenko I.I. (1999). Machines for the production of building materials: Textbook. - K.: KNUBA, 488 p.

5. Fedorov G.D., Savchenko O.H. (1998). Analysis of schemes for the preparation of pressed powder during the preparation of ceramic bricks. Scientific bulletin of construction. HDTUBA HOTV ABU, 3, 104-105.

6. Frankivskyi A.A., Runova T.V., Svintsytskyi R.L., Plis A.V. (1997). High-quality ceramic products and energy saving are the main goals of modernization of brick production in Ukraine. Construction of Ukraine, 6, 13-16.

7. DSTU B V.2.7-61:2008 (2009). Building materials. Bricks and stones are ceramic, ordinary and facing. Specifications. Kyiv: Ministry of Regional Construction of Ukraine

8. DSTU B V.2.7-80:2008 (2009). Building materials. Bricks and silicate stones. Specifications. Kyiv: Ministry of Regional Construction of Ukraine

9. Velychko Y.M., Plemyannikov M.M., Yatsenko A.P., Kornilovych B.Yu. (2016). Chemistry and technology of ceramics. High-temperature processes: a study guide. K.: "Education of Ukraine"

10. Kocserha I., Kristály F. (2010). Effects of Extruder Head's Geometry on the Properties of Extruded Ceramic Products. Materials Science Forum, Vol. 659, 499-504 https://doi:10.4028/www.scientific.net/MSF.659.499

11. Constantine Sikalidis, Manassis Mitrakas (2006). Utilization of Electric Arc Furnace Dust as Raw Material for the Production of Ceramic and Concrete Building Products. Journal of Environmental Science and Health, 9 (41),

1943-1954
https://doi.org/10.1080/10934520600779240
12. A.A Adekunle (2021). Characteristics of earth bricks produced with partial replacement of laterite with plastic, ceramic tiles and glass for sustainable management of the environment. Journal of Advanced Education and Sciences; 1(1):17-22
13. Wolfgang Gleißle, Jan Graczyk, Hans Buggisch (1993). Rheological Investigation of Suspensions and Ceramic Pastes: Characterization of Extrusion Properties. KONA Powder and Particle Journal, 11, 125-137
https://doi.org/10.14356/kona.1993015
14. F Kolenda, P Retana, G Racineux, A Poitou (2003). Identification of rheological parameters by the squeezing test. Powder Technology, 1-3 (120), 56-62
https://doi.org/10.1016/S0032-5910(02)00227-9
15. Aleko, V.A. (2003). Electric Heating of Ceramic Mixture in Molding. Glass and Ceramics 60, 246–247. https://doi.org/10.1023/A:1027355629336
16. Bandieira, M., Zat, T., Schuster, S.L., Justen L. H., Weide H., Rodríguez E. D. (2021). Water treatment sludge in the production of red-ceramic bricks: effects on the physico-mechanical properties. Mater Struct 54, 168.
https://doi.org/10.1617/s11527-021-01764-0
17. Sanchez Soloaga, I., Oshiro, A., & Positieri, M. (2014). The use of recycled plastic in concrete. An alternative to reduce the ecological footprint. Revista De La Construcción. Journal of Construction, 13(3), 19–26
18. P.O. Awoyera, A. Adesina (2020). Plastic wastes to construction products: Status, limitations and future perspective. Case Studies in Construction Materials, 12
https://doi.org/10.1016/j.cscm.2020.e00330
19. Paul O. Awoyera ,Julius M. Ndambuki ,Joseph O. Akinmusuru, David O. Omole (2016). Characterization of ceramic waste aggregate concrete. HBRC Journal, 3 (14), 282-287
https://doi.org/10.1016/j.hbrcj.2016.11.003
20. Sheelan M. Hama, Nahla N. Hilal (2017). Fresh properties of self-compacting concrete with plastic waste as partial replacement of sand. International Journal of Sustainable Built Environment, 2 (6), 299-308
https://doi.org/10.1016/j.ijsbe.2017.01.001

1943-1954
https://doi.org/10.1080/10934520600779240
12. A.A Adekunle (2021). Characteristics of earth bricks produced with partial replacement of laterite with plastic, ceramic tiles and glass for sustainable management of the environment. Journal of Advanced Education and Sciences; 1(1):17-22
13. Wolfgang Gleißle, Jan Graczyk, Hans Buggisch (1993). Rheological Investigation of Suspensions and Ceramic Pastes: Characterization of Extrusion Properties. KONA Powder and Particle Journal, 11, 125-137
https://doi.org/10.14356/kona.1993015
14. F Kolenda, P Retana, G Racineux, A Poitou (2003). Identification of rheological parameters by the squeezing test. Powder Technology, 1-3 (120), 56-62
https://doi.org/10.1016/S0032-5910(02)00227-9
15. Aleko, V.A. (2003). Electric Heating of Ceramic Mixture in Molding. Glass and Ceramics 60, 246–247. https://doi.org/10.1023/A:1027355629336
16. Bandieira, M., Zat, T., Schuster, S.L., Justen L. H., Weide H., Rodríguez E. D. (2021). Water treatment sludge in the production of red-ceramic bricks: effects on the physico-mechanical properties. Mater Struct 54, 168.
https://doi.org/10.1617/s11527-021-01764-0
17. Sanchez Soloaga, I., Oshiro, A., & Positieri, M. (2014). The use of recycled plastic in concrete. An alternative to reduce the ecological footprint. Revista De La Construcción. Journal of Construction, 13(3), 19–26
18. P.O. Awoyera, A. Adesina (2020). Plastic wastes to construction products: Status, limitations and future perspective. Case Studies in Construction Materials, 12
https://doi.org/10.1016/j.cscm.2020.e00330
19. Paul O. Awoyera ,Julius M. Ndambuki ,Joseph O. Akinmusuru, David O. Omole (2016). Characterization of ceramic waste aggregate concrete. HBRC Journal, 3 (14), 282-287
https://doi.org/10.1016/j.hbrcj.2016.11.003
20. Sheelan M. Hama, Nahla N. Hilal (2017). Fresh properties of self-compacting concrete with plastic waste as partial replacement of sand. International Journal of Sustainable Built Environment, 2 (6), 299-308
https://doi.org/10.1016/j.ijsbe.2017.01.001

Збірник наукових праць. Серія: Галузеве машинобудування, будівництво
Academic journal. Industrial Machine Building, Civil Engineering
http://journals.nupp.edu.ua/znp
https://doi.org/10.26906/znp.2023.61.3868

UDC 622.273

Improvement of the industrial extraction method of methane homologues

Mykhailo Pedchenko [1]*, Larysa Pedchenko [2], Nazar Pedchenko [3], Vasyl Savyk [4]

[1] National University «Yuri Kondratyuk Poltava Polytechnic» https://orcid.org/0000-0003-1409-8523
[2] National University «Yuri Kondratyuk Poltava Polytechnic» https://orcid.org/0000-0002-3279-8649
[3] National University «Yuri Kondratyuk Poltava Polytechnic» https://orcid.org/0000-0002-0018-4482
[4] National University «Yuri Kondratyuk Poltava Polytechnic» https://orcid.org/0000-0002-0706-0589
*Corresponding author E-mail: pedchenkomm@ukr.net

Absorption processes are one of the main ones in the preparation of hydrocarbon gases. However, in connection with a decrease in the pressure of the input gas, a number of facilities for the preparation of industrial products cannot provide the necessary technological regime and therefore require reconstruction. A typical example is the installation of low-temperature absorption at the main facilities «Solokha» of the gas industry management «Poltavagasvydobuvannya» where there is a decrease in the efficiency of the separation process of natural and oil gases. According to the results of analytical studies, to eliminate the indicated shortcoming, a variant of the reconstruction of the ULTA MF «Solokha» is proposed, which involves the use of a scheme with preliminary saturation of the regenerated absorbent. This will increase the extraction rate of components by 21.96%.

Keywords: low-temperature absorption, a wide fraction of light hydrocarbons, pre-saturation of the absorbent

Удосконалення методу промислового вилучення гомологів метану

Педченко М.М.[1]*, Педченко Л.О.[2], Педченко Н.М.[3], Савик В.М.[4]

[1,2,3,4] Національний університет «Полтавська політехніка імені Юрія Кондратюка»
*Адреса для листування E-mail: pedchenkomm@ukr.net

Процеси абсорбції є одними з основних при підготовці природного і супутнього нафтового газів. Застосування схем низькотемпературної абсорбції дає змогу забезпечити високе вилучення компонентів С3+ з вуглеводневих газів при порівняно помірному охолодженні технологічних потоків. Однак, у зв'язку зі зниженням тиску вхідного газу, ряд об'єктів підготовки промислової продукції не можуть забезпечити необхідний технологічний режим і тому потребують реконструкції. Типовим прикладом є установка низькотемпературної абсорбції (УНТА) на головних спорудах (ГС) «Солоха» газопромислового управління «Полтавагазвидобування». При роботі установки абсорбції під середнім і високим тиском разом з пропаном і вищими вуглеводнями абсорбентом поглинається також значна кількість метану і етану. У результаті розвиток процесу може лімітуватися за деякими компонентами внаслідок термодинамічної рівноваги. Отже, поглинання небажаних компонентів в абсорбері спричиняє підвищення середньої температури абсорбції та несприятливого формування профілю температур по висоті апарата. Наслідком цього є зниження ефективності процесу розділення природних і нафтових газів. За результатами аналітичних досліджень для усунення вказаного недоліку запропоновано варіант реконструкції УНТА ГС «Солоха», який передбачає застосування схеми з попереднім насиченням регенерованого абсорбенту. В такій схемі контакт сирого газу і насиченого абсорбенту здійснюється в холодильнику сирого газу при нижчій температурі, ніж в абсорбері. Попереднє насичення регенерованого абсорбенту сухим газом дозволяє підвищити глибину вилучення цільових компонентів з газу в абсорбері. У цьому холодильнику одночасно конденсується частина важких вуглеводнів, що призводить до зниження тепла абсорбції в абсорбері. Завдяки попередньому насиченню абсорбенту метаном, в самому абсорбері відбувається вилучення з газу в основному цільових вуглеводнів. Застосування вузла насичення регенерованого абсорбенту інертними компонентами дозволить мінімізувати наслідки зниження тиску вхідного газу і підвищити рівень вилучення компонентів широкої фракції легких вуглеводнів (ШФЛВ) на 21,96 % (в т. ч. пропану на 22,05 %, бутанів на 30,75 %). При цьому рівень вилучення досягне проектного.

Ключові слова: низькотемпературна абсорбція, широка фракція легких вуглеводнів, попереднє насичення абсорбенту

Introduction

Absorption processes are one of the main ones in the preparation of natural and associated petroleum gases. Absorption schemes, in addition to general nodes (modules) of separation, compression and drying of gas, have absorption and desorption modules [1].

The use of LTA schemes makes it possible to ensure a high extraction of propane from petroleum gases with

relatively moderate cooling of process flows: on LTA installations, to extract 90-95% of propane, it is enough to have a refrigeration cycle with an isotherm of minus 30-38 °C [2]. At low-temperature condensation (LTC) installations, this requires an isotherm of minus 80-85 °C [3, 4].

Light absorbents (molecular weight 80-140) are used at LTA installations, their specific consumption is usually no more than 1-1.5 l/m^3. In combination with other measures, this made it possible to increase the degree of extraction of commercial products at the gas processing plant (GPP) and reduce the specific costs of gas processing by 25-50% (compared to the costs of conventional oil absorption plants) [5-8].

However, during absorption, the absorbent and the gas are heated due to the released heat, and the temperature of the absorbent is higher than the temperature of the gas, since the heat is directly transferred to the absorbent, and the gas is heated only due to the heat exchange between it and the absorbent [8, 9].

Peculiarities of the technological regime of the ILTA of the main facilities (MF) «Solokha»

The gas at the outlet of the ILTA installation must meet the dew point requirements for water and hydrocarbons. However, the pressure of the inlet stream is currently at the lower level permissible for the implementation of the process at the required level. It will be quite logical to envisage the option of its reconstruction with (preliminary saturation of the absorbent with an inert gas).

At ILTA (MF) «Solokha», pre-dried gas under a pressure of 2.2-2.4 MPa and at a temperature of minus 11.6 °C enters two absorbers working in parallel (130,000 m^3/h). Although according to the regulations, this pressure should have been 4 MPa [10]. The ILTA installation allows to increase the extraction rate of C_{3+} higher hydrocarbons in the form of a broad fraction of light hydrocarbons (BFLH) by 80% (63 thousand tons per year, although the absolute value of propane extraction is only 27% of its content in raw gas).

The existing sheme of low-temperature absorption at the main facilities «Solokha» JSC «Ukrgazvydobuvannya» is shown in Fig. 1. In Tables 1 and 2. the composition of the input gas and adsorbent of ILTA at the main facilities «Solokha», respectively, is given.

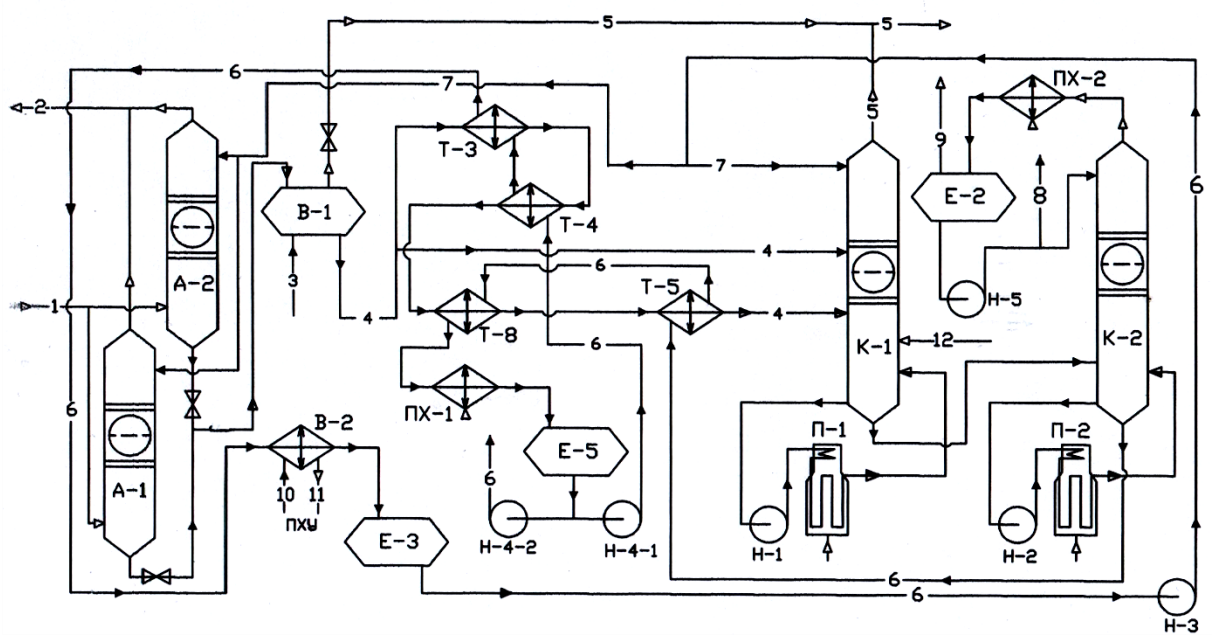

Figure 1 – **Scheme of low-temperature absorption of MF «Solokha»** [10]**:**
A-1, A-2 - absorbers; K-1 – absorption-evaporation column; K-2 – desorber; B-1 – weathering agent;
T-3, T-4, T-5, T-8 – recuperative heat exchangers; P-1, P-2 – ovens; E-3, E-5 – collection tanks;
E-2 – irrigation capacity; H-1, H-2, H-3, H-4-1, H-4-2, H-5 – pumps; B-2 – propane vaporizer of ACI;
AC-1, AC-2 – air coolers; 1 – raw gas; 2 – dry gas; 3 – feeding with an absorbent; 4 – saturated absorbent;
5 – deethanization and weathering gas for own needs; 6 – regenerated absorbent; 8 – BFLH;
9 – blowing gas to the torch; 10 – liquid propane; 11 – propane vapors;
12 – refueling with the vapor phase from the absorbent preparation unit

Table 1 – Characteristics of the input and output gas of ILTA (%) [10]

Components	Raw natural gas in ILTA	Commodity dry gas in ILTA	Low pressure for own	Propane technical
N_2	1.112	1.582	0.287	
CH_4	88.67	89.475	59.71	
CO_2	2.477	2.396	5.923	
C_2H_6	5.037	5.125	31.62	1.232
C_3H_8	1.791	1.087	2.043	89.70
Iso-butane	0.201	0.09	0.127	5.265
n-butan	0.421	0.168	0.179	3.756
neopentane	0.005	0.02	0.001	0.006
iso-pentan	0.087	0.03	0.02	0.031
n-pentan	0.082	0.023	0.015	0.012
Fract. to 60 °C	0	0.002	0.007	10^{-4}
Fractю 60-80 °C	0	0.002	0.012	-
Fract. 80-100 °C	0.089	0.009	0.010	-
Fract. 100-120°C	0.015	0.007	0.027	-
Fract. 120-150°C	0.017	0.003	0.013	-
Fract. 150-160°C	-	0.0003	0.001	-
Fract. 160-180°C	-	0.0001	$7 \cdot 10^{-4}$	-
Fract. 180-200°C	-	$2 \cdot 10^{-5}$	$2 \cdot 10^{-4}$	-
Fract. 200-230°C	-		$2 \cdot 10^{-5}$	-
M_{aver}, kg/mol	18.54	18.08	22.95	45.2
Density, kg/m^3	0.746	0.728	0.924	503.8

Table 2 – Characteristics of absorbents of the ILTA installation [10]

Components	Regenerov. absorbent	Saturated absorbent	Absorbent with IPA (light)
N_2	-	1.25	$6 \cdot 10^{-5}$
CH_4	-	0.002	0.006
CO_2	-	0.004	0.007
C_2H_6	$6 \cdot 10^{-5}$	0.59	0.1
C_3H_8	0.04	7.64	0.85
Iso-butane	0.13	1.98	0.99
n-butan	0.57	3.98	2.15
neopentane	0.01	0.04	0.02
iso-pentan	1.07	1.52	2.36
n-pentan	1.39	1.62	2.99
Fract. to 60 °C	0.83	0.86	4.49
Fract. 60-80 °C	2.03	1.86	6.68
Fract. 80-100 °C	4.87	4.25	9.57
Fract. 100-120 °C	21.36	18.41	17.79
Fract. 120-150 °C	32.62	27.71	26.87
Fract. 150-160 °C	8.08	6.82	6.94
Fract. 160-180 °C	10.07	8.48	10.5
Fract. 180-200 °C	6.79	5.71	6.82
Fract. 200-230 °C	3.88	3.25	0.83
Fract. 230-250 °C	2.83	2.37	0.02
Fract. 250-270 °C	3.44	2.88	0.01
Fract. 270-290 °C	0.01	0.008	0
Fract. 290-320 °C	0.008	1.26	0
Fract. 320-250 °C	0.003	0.002	0
Fract. > 350 °C	0.0007	0.004	0
M_{aver}, kg/mol	121.03	81.43	110.88
Density kg/m^3	755.11	623.49	716.89

Insufficient pressure, as well as the limited capabilities of the propane refrigeration plant for cooling the absorbent and gas complicate the process of absorption of C_{3+} higher in the absorbers and further affect the parameters of the processes of deethanization and regeneration of the absorbent. As practice shows, the disadvantages of the absorption process under such conditions are especially noticeable when the ambient temperature rises above 20-25 °C. At the same time, the temperature of the gas at the entrance to the LTA rises to minus 18 – minus 15 °C, the temperature of the regenerated absorbent when fed to the absorber to minus 10 – minus 8 °C. During this period, the production indicators of BFLH decrease by an average of 30% – from 120-140 to 90-100 t/day (although the design capacity of the installation is 200 t/day).

From Table 3 [10], which presents a verification calculation of the absorption of ILTA MF «Solokha» (theoretically possible), namely from the liquid plate enthalpy (absorption occurs in the liquid, and therefore the main release of energy) and the average temperature on each of the eight theoretical plates (the temperature difference between the first and second and second and third plates is 1.7 °C, while between the third and fourth, fourth and fifth plates is only 1.2 °C), it can be concluded that the majority of heat is in the upper part of the absorber is released during the absorption of methane and ethane.

At a given pressure and average temperature on the plates, the value of the phase equilibrium constant shifts towards the opposite process – desorption (Fig. 2).

The level of extraction of propane, as the main target component of the process (39% according to the regulations of the installation and 27% in real conditions), which can be seen from the difference in its content in the gas at the entrance and at the exit from the installation (Table 4), is hardly acceptable from the point of view of profitability in general for absorption processes and even more so for low-temperature absorption with significant costs for obtaining cold.

Table 3 – Verification calculation of absorption (one absorber), pressure 2.2 MPa [10]

№ theoretical plate	Temperature °C	Flows, kmol/h		Enthalpy, kcal/kmol		Flows, kg/h		Density, kg/m^3	
		gas	liquid	gas	liquid	gas	liquid	gas	liquid
1	-5.9	2586.5	256.43	2025.62	-4617.29	47166.5	27332.09	19.32	761.53
2	-7.6	2638.4	263.51	22010.98	-4593.87	48498.56	27576.14	19.66	760.12
3	-9.3	2645.5	268.26	1995.25	-4605.64	48743.76	27737.64	19.88	759.73
4	-10.7	2650.3	272.46	1981.9	-4613.07	48907.3	27884.51	20.05	759.36
5	-11.9	2654.6	276.88	1970.34	-4610.16	49056.77	28047.08	20.21	758.77
6	-13.1	2659.2	282.56	1959.41	-4590.83	49222.14	28270.35	20.35	757.69
7	-14.5	2664.9	292.32	1947.22	-4533.86	49447.88	28685.97	20.57	755.35
8	-16.5	2674.7	321.42	1929.43	-4328.68	49865.15	30074.02	20.90	747.77

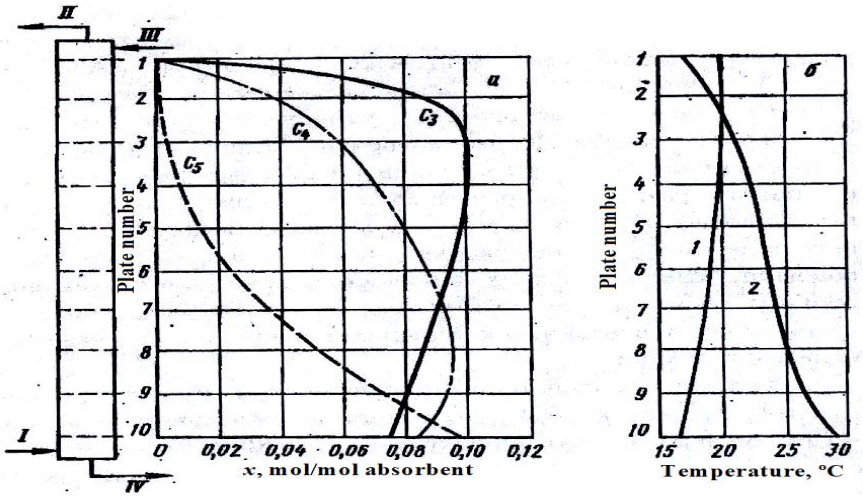

Figure 2 – Dynamics of changes in the height of the absorption apparatus [5]:
a – the content of saturated components in the absorbent; b – flow temperatures; And – raw gas;
II – dry gas; III – regenerated absorbent; IV – saturated absorbent; 1 – gas; 2 – absorbent.

Table 4 – Material balance of ILTA MF «Solokha» with a gas productivity of 130,000 m^3/h before reconstruction

Compositions	gas inlet		withdrawal	Dry gas output		Withdrawal of BFLH		
	% mol.	g / m^3	% mol.	% mol.	g/m^3	g/m^3	t/h	t/day
C_3	1.791	43.0	35.56	1.14	27.71	15.29	1.9875	47.70
$\sum C_4$	0.701	17.7	55.86	0.16	7.81	9.89	1.2858	30.86
$\sum C_5$	0.179	5,40	100	0	0	5.40	0.7021	16.85
$\sum C_{6+}$	0.05	1.88	100	0	0	1.88	0.2438	5.85
$\sum CO_2, CH_4, C_2H_6$	-	-	-	-	-	-	-	3.48
$\sum$	2.72	67.98	47.74	1.30	35.52	32.46	4.2192	104.74

Review of the research sources and publications

Currently, the following technological schemes of absorption plants are used:

– absorption with partial evaporation of light hydrocarbons;

– absorption with recirculation of non-condensed gases;

– two-stage absorption;

– absorption with preliminary saturation of the regenerated absorbent.

Absorption with partial evaporation of light hydrocarbons involves heating the bottom of the column in order to partially evaporate methane (and sometimes ethane). At the same time, partial desorption of propane and heavier hydrocarbons occurs. Devices in which this

process is implemented are called absorption-evaporation columns (AECs). At present, technological schemes of almost all absorption plants include AEC.

During the operation of the absorption unit under medium and high pressure, along with propane and higher hydrocarbons, the absorbent also absorbs a significant amount of methane and ethane. This complicates the desorption scheme. Due to the high pressure of the saturated vapor of the products at the top of the column, their condensation is difficult, since low temperatures are required.

At a number of gas processing plants, schemes with recirculation of residual gases. However, it is difficult to determine the optimal operating parameters of such an installation. On the one hand, it is desirable to carry out demethanization of the saturated absorbent under high pressure in order to reduce the load on the compression of the residual gas, on the other hand, increasing the pressure increases the metal capacity of the column and heat consumption for the regeneration of the absorbent.

In the LTA process, a number of issues arise when using a light absorbent: the removal of the absorber with gas increases both due to its dissolution in the gas and due to removal in the form of small droplets. To reduce the losses of the absorber with dry gas, two-stage absorption schemes are used: a light absorbent is fed to the first stage, and a relatively heavy one to the second stage of absorption. Multi-stage absorption schemes with different temperatures and pressures at individual stages are also used.

It is known that the process of absorption of hydrocarbon gases takes place with the release of heat – the greatest exothermic effect is observed in the upper and lower parts of the absorber, because the main mass of methane and ethane is absorbed at the top, and butane and heavier hydrocarbons are absorbed at the bottom. During the processing of oil gas of medium «fatness» ($C_{3+higher}$ = 300 g/m^3), more methane and ethane are absorbed in the absorber than propane and heavier hydrocarbons (in moles). And this means that the removal of unwanted components (methane and ethane) causes more heat release than the absorption of high molecular target hydrocarbons, since methane and ethane have higher heats of absorption at the operating pressures of the processes. The profile of the change in propane concentration, for example, is formed by the height of the apparatus so that sometimes in the middle part of the absorber propane desorption begins from the absorbent flowing from the higher plates (Fig. 2).

Accordingly, under these conditions, the development of the process may be limited by some components due to thermodynamic equilibrium. Therefore, probably, increasing the number of real plates in the absorber (more than 25-30) does not contribute to increasing the efficiency of the process. Therefore, in the conditions of the adiabatic regime, the absorption of unwanted components in the absorber causes an increase in the average temperature of absorption and an unfavorable formation of the temperature profile along the height of the device and, as a result, is one of the reasons for reducing the efficiency of the separation process of natural and petroleum gases.

The analysis of the temperature distribution along the height of the absorbers at different installations showed that the intensity of the heating of the absorbent is greater in the upper and lower parts of the apparatus, since the main amount of methane and ethane is absorbed at the top of the column, while the dissolution of butanes and pentanes occurs on the lower plates. Therefore, it is advisable to remove the maximum amount of heat of the dissolution process in intermediate refrigerators installed at the top and bottom of the absorber. However, schemes with intermediate refrigerators have a number of disadvantages: the presence of blind plates in the absorber, the difficulty of accurately choosing the place of introduction of the cooled absorbent, low heat transfer coefficients.

To eliminate the indicated shortcomings, it is possible to use schemes with preliminary degasification of raw gas and saturation of the regenerated absorbent. Pre-saturation of the regenerated absorbent with dry gas makes it possible to increase the depth of extraction of the target components from the gas in the absorber, since in this scheme the contact of raw gas and saturated absorbent is carried out in the refrigerator of raw gas at a lower temperature than in the absorber. In this refrigerator, at the same time, a part of heavy hydrocarbons condenses, which leads to a decrease in the heat of absorption in the absorber. Due to the pre-saturation of the absorbent with methane, mainly target hydrocarbons are extracted from the gas in the absorber itself. On the basis of calculations, it was found that the lower the content of heavy hydrocarbons in raw gas, the greater the negative impact of residual components in the regenerated absorbent on the depth of their extraction [8, 9].

Increasing the absorption pressure reduces the negative impact of residual components. For example, at pressures of 1.5 and 3 MPa and 15 °C, the presence of 1% (wt.) propane and butane in the regenerated absorbent reduces the extraction of propane in the first case by 15%, and in the second by 10%, butane by 5 and 3, respectively. 5% in comparison with the mode in which complete evaporation of the absorbent would be carried out [11, 12].

First of all, three pre-saturation schemes are used. The first option (Fig. 3) – the regenerated absorbent is mixed with dry gas of the absorption-evaporation column 4 and enters the propane evaporator 5 together with it. As a result of the contact of these flows, the regenerated absorbent is saturated with light hydrocarbons with the simultaneous removal of heat of absorption. After that, the saturated (ballast) regenerated absorbent is separated from the free gas in the separator 6 and fed to the upper plate of the absorber and AEC.

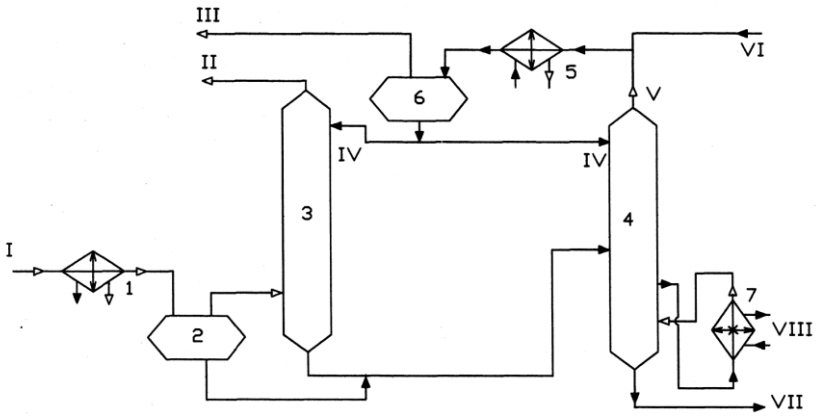

Figure 3 – Schematic diagram of the absorption unit with pre-saturation of the regenerated absorbent with dry AEC gas (option I):
1, 5 – propane evaporators; 2, 6 – separators; 3 – absorber; 4 – AEC; 7 – reboiler; And – raw gas;
II – dry gas; III – dry gas after preliminary saturation of the regenerated absorbent;
|IV – regenerated absorbent after previous saturation; V – dry gas AEC;
VI – regenerated absorbent; VII – deethanized saturated absorbent; VIII – coolant

The second option (Fig. 4) – the regenerated absorbent is mixed with dry AEC gas 4 and enters the propane evaporator 5 together with it. As a result of the contact of these streams, the absorbent is saturated with light hydrocarbons with the simultaneous removal of the heat of absorption. After separating this mixture in the separator 6, the saturated absorbent is divided into two streams – one is directed to the upper plate of the AEC, the other is mixed with the dry gas of the absorber and enters the propane evaporator 7. As a result, the absorbent is additionally saturated with light hydrocarbons. After the evaporator 7, the mixture of gas and absorbent enters the separator 8, from which the saturated regenerated absorbent is fed to the upper plate of the absorber 3, and the dry gas is sent to consumers.

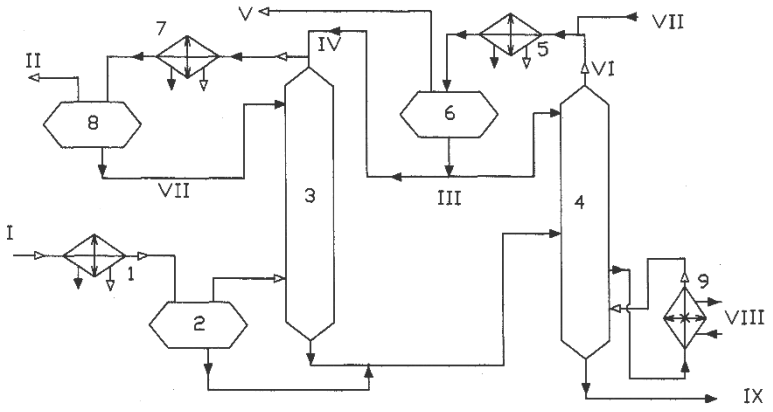

Figure 4 – Basic technological scheme of the absorption unit with preliminary saturation of the regenerated absorbent with dry gas of the absorber and dry gas of AEC (II variant):
1, 5, 7 – propane evaporators; 2, 6, 8 – separators; C – absorber; 4 – AEC; 9 – reboiler; I - raw gas;
II – dry gas after preliminary saturation of the regenerated absorbent;
III – regenerated absorbent after the pre-saturation node; IV, V, VI – dry gas;
VII – regenerated absorbent; VIII – coolant; IX – deethanized saturated absorbent

The third option (Fig. 5) – one stream of regenerated absorbent is saturated with light hydrocarbons as a result of mixing with dry gas of absorber C, after cooling in propane evaporator 7 and separation from gas in separator 8, it is fed to the upper plate of absorber 3. The second stream of regenerated absorbent is saturated with light hydrocarbons as a result of mixing with dry gas of the absorption-evaporation column 4 and after cooling in the propane evaporator 5 and separation from the gas in the separator 6 is fed to the upper plate of the absorption-evaporation column 4.

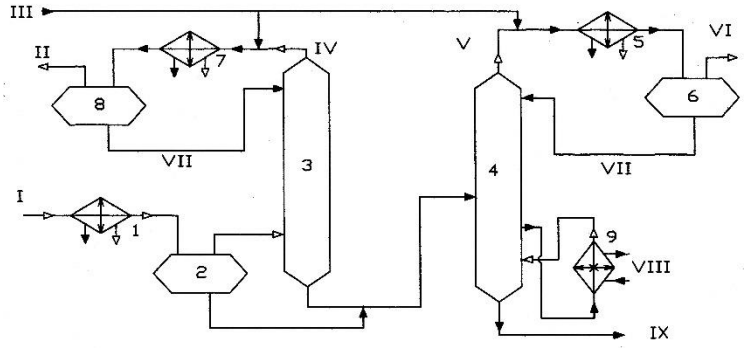

Figure 5 – Basic technological scheme of the absorption unit with preliminary saturation of the regenerated absorbent with dry gas of the absorber and dry gas of AEC (III variant):
1,5, 7 – propane evaporators; 2, 6, 8 – separators; C – absorber; 4 – AEC; 9 – reboiler; I – raw gas; II – dry gas of the absorber after preliminary saturation of the regenerated absorbent; III – regenerated absorbent; IV, V – dry gas; VI – dry AEC gas after pre-saturation of the regenerated absorbent; VII – regenerated absorbent after previous saturation; VIII – coolant IX – deethanized saturated absorbent

The installation uses two absorbents: light - with a molecular weight of 100 and heavy - with a molecular weight of 140.

In fig. 6 shows the technological diagram of the LTA installation with the absorbent pre-saturation unit of the gas processing plant designed for the extraction of ethane and heavier hydrocarbons from natural gas (Alvin, USA). [8]. A gasoline fraction with a molecular weight of 100 is used as an absorbent.

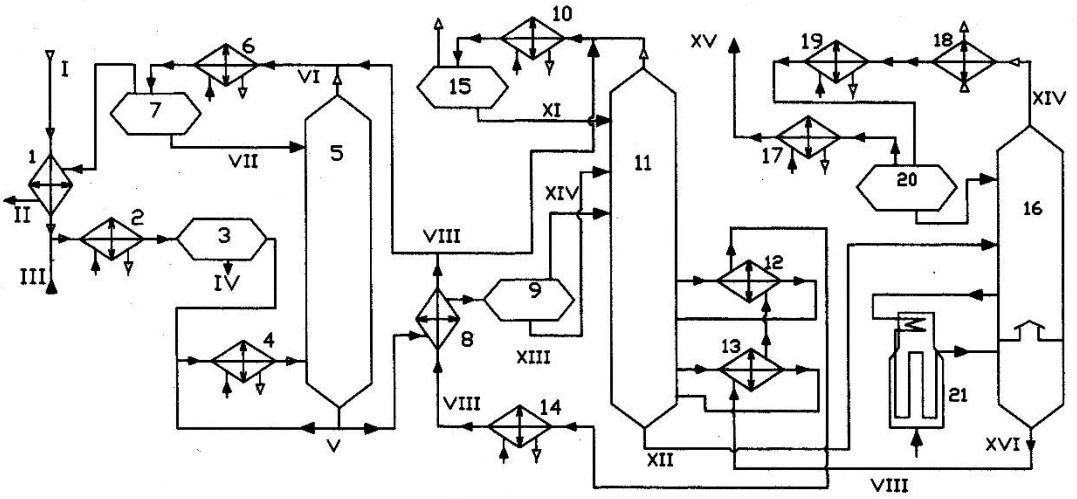

Figure 6 – Technological scheme of the LTA gas processing plant, designed for the extraction of C^{2+} HIGHER hydrocarbons from natural gas:
1, 8, 12, 13 – recuperative heat exchangers; 2, 4, 6, 10, 14, 17, 19 – propane vaporizers; Z, 7, 15 – separators; 5 – absorber; 9 – evaporator-separator; 11 – AEC; 16 – desorber; 18 – air cooler; 20 – reflux capacity; 21 – stove; 1 – raw gas; 11 – dry gas of the absorber after the assembly of pre-saturation of the regenerated absorbent with light hydrocarbons; II I – ethylene glycol solution; IV – hydrated ethylene glycol; V – saturated absorbent; VI – dry gas; VII – regenerated absorbent saturated with light hydrocarbons; VIII – regenerated absorbent; IX – dry gas; X – dry gas of AEC after pre-saturation of the regenerated absorbent with light hydrocarbons; XI – regenerated absorbent saturated with light hydrocarbons; XII – demethanized saturated absorbent; XIII – saturated partially degassed absorbent; XIV – gas; XV is a broad fraction of C_{2+} higher hydrocarbons

Definition of unsolved aspects of the problem

However, in connection with a decrease in the pressure of the input gas, a number of facilities for the preparation of industrial products cannot provide the necessary technological regime and therefore require reconstruction. A typical example is the installation of low-temperature absorption (ILTA) at the main facilities (MF) «Solokha» of the gas industry management JSC «Ukrgazvydobuvannya». During the operation of the

absorption unit under medium and high pressure, along with propane and higher hydrocarbons, a significant amount of methane and ethane is also absorbed by the absorbent. As a result, the development of the process may be limited by some components due to thermodynamic equilibrium. Therefore, the absorption of unwanted components in the absorber causes an increase in the average absorption temperature and an unfavorable formation of the temperature profile along the height of the device. The consequence of this is a decrease in the efficiency of the process of separation of natural and oil gases

Problem statement

Therefore, the extraction of light hydrocarbons from the gas by a regenerated absorbent outside the absorber with the simultaneous removal of heat of absorption makes it possible to reduce the release of heat in the upper part of the apparatus and, as a result, to increase the degree of extraction of target hydrocarbons from the gas or to reduce the specific consumption of the absorbent with an unchanged degree of extraction of commercial products.

Calculation studies of the described schemes in relation to the conditions of a typical installation showed that with «average» gas fat content and low flow temperature (minus 37 °C), the extraction of propane is ensured in the first case by 76%, in the second by 83% and in the third by 91% (removal of butanes and heavier hydrocarbons was in all cases about 100%). Experience shows the possibility of reducing the specific absorbent consumption due to this measure by 20%.

Thus, the extraction of light hydrocarbons from the gas by a regenerated absorbent outside the absorber with the simultaneous removal of the heat of absorption allows to reduce the release of heat in the upper part of the apparatus and, as a result, to increase the degree of extraction of target hydrocarbons from the gas or to reduce the specific consumption of the absorbent with an unchanged degree of extraction of commercial products.

Basic material and results

Taking into account the fact that the existing LTA installation lacks technological solutions for removing excess heat along the height of the absorber or preventing its release in the absorber due to the pre-saturation of the regenerated absorbent with inert components (methane, ethane) and removal of excess heat before it is fed to the absorber, it should be optimized first of all, the temperature regime of the absorber. Based on the availability of a resource of inert components (self-needs gas consisting of the deethanization gas of the K-1 column and the weathering gas of the aerator B-1 (Fig. 1)), it is advisable to supplement the ILTA scheme with a node for saturating the regenerated absorbent with gas for own needs.

Figure 7 shows the ILTA scheme supplemented with the node of saturation of the regenerated absorbent.

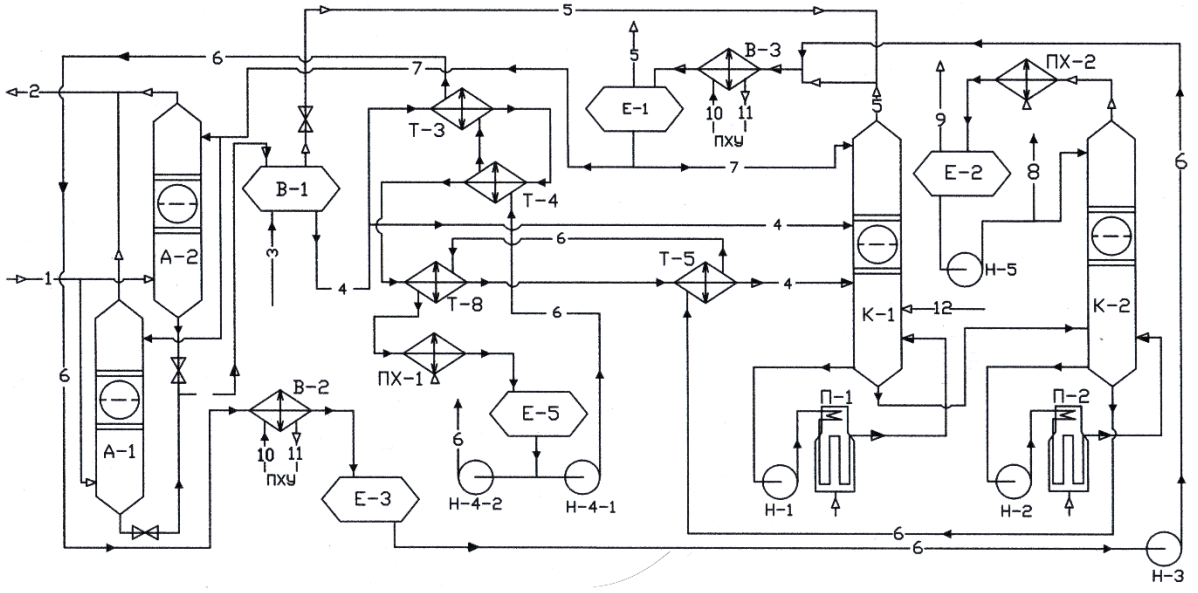

Figure 7. – Scheme of the ILTA with the node of saturation of the regenerated absorbent:

A-1, A-2 – absorbers; K-1 – absorption-evaporation column; K-2 – desorber; B-1 – weathering agent; T-3, T-4, T-5, T-8 – recuperative heat exchangers; P-1, P-2 – ovens; E-3, E-5 – collection tanks; E-2 – irrigation capacity; E-1 – separator; H-1, H-2, H-3, H-4-1, H-4-2, H-5 – pumps; B-2, B-3 – propane vaporizers of ACI; AC-1, AC-2 – air coolers; 1 – raw gas; 2 – dry gas; 3 – feeding with an absorbent; 4 – saturated absorbent; 5 – deethanization and weathering gas for own needs; 6 – regenerated absorbent; 7 – pre-saturated absorbent; 8 – BFLH; 9 – blowing on a torch; 10 – liquid propane; 11 – propane vapors; 12 – refueling with the vapor phase from the absorbent preparation unit

The process is implemented as follows. Gas from the LTS installation with a pressure of 2.2 MPa and a temperature of minus 21 °C in the amount of 130,000 m^3/h enters the lower part of two absorbers A-1 and A-2, irrigated with regenerated and cooled to a temperature of minus 11.6 °C absorbent.

The absorption process is accompanied by the release of heat (heating of the absorbent from minus 11.6 ºC to minus 10 ºC, and the gas from minus 21 to 5.9 ºC).

The absorbent, saturated with BFLH, with a temperature of minus 10 ºC and a pressure of 2.2 MPa is throttled from the absorbers to 1.6 MPa in the air conditioner B-1. As a result of the throttle effect, the absorbent temperature drops to minus 16.9 ºC.

In the weathering device B-1, weathering gases (methane, ethane) are desorbed from the absorbent, which, through the regulating valve, are sent to the gas collector for its own needs. The degassed absorbent is sent from it in two streams to the K-1 deethanization column as feed. One stream with a temperature of minus 16.9ºC (about 25% of the total feed) is supplied as a «cold» feed to the 30 plate of the column. The second flow is heated in heat exchangers T-3, T-4, T-8 and T-5 to a temperature of 200 ºC by the flow of hot regenerated absorbent coming from the cube of column K-2 and sent as «hot» feed to plate 36 of column K-1.

As irrigation, regenerated, pre-saturated and cooled to a temperature of minus 11.6 ºC absorbent is supplied to the first plate from the separator of the pre-saturation unit of the regenerated absorbent, maintaining the temperature of the top of the column to 10 ºC. The heating of the liquid in the cube up to 170 ºC is ensured by the circulation of the cube liquid according to the scheme: «cube column K-1 – pump H-1 – condensate heating furnace P-1 – cube column K-1».

In the K-1 column, light components (methane, ethane) are separated from the absorbent. The deethanization gases from the top of the K-1 column together with the weathering gas from the B-1 weatherer pass through the regenerated absorbent saturation node into the fuel gas system.

The deethanized absorbent with a temperature of 185ºC and a pressure of 1.6 MPa is fed from the bottom of the K-1 column as feed to the K-2 absorbent regeneration column on a 36 plate.

In the K-2 column, the cubic residue of the K-1 column is separated into the regenerated absorbent and the HFLV extracted from the gas, which comes out in the form of a vapor phase from the upper part of the column, condenses in the AC-2 air coolers and enters the reflux tank at a temperature of 45-50°C E-2.

The pressure of 1.4 MPa in the K-2 column is maintained by changing the degree of condensation of BFLH in the air cooler AC-2.

From the reflex tank E-2, a part of broad fraction of light hydrocarbons (BFLH) is supplied in the form of irrigation to the first plate K-2, the rest is removed from the installation as a target product. The regenerated absorbent from the bottom of the column K-2 is successively cooled in the heat exchangers T-5 and T-8 by the flow of saturated absorbent and in the air cooling apparatus X-1 to a temperature of 50 ºC and enters the tank E-5.

The regenerated absorbent from tank E-5 is sequentially cooled in the pipe space of heat exchangers T-4 and T-3 with saturated absorbent, in the pipe space of evaporator B-2 with boiling propane (to a temperature of minus 11.6 ºC) and enters the buffer tank E-3.

The cooled regenerated absorbent from the E-3 tank is pumped by the H-3 pump through the pre-saturation unit, which consists of the B-3 propane evaporator and the E-1 separator. This is where it is saturated with deethanization gas and weathering, removal of heat of absorption (methane and ethane) and separation of the gas from the absorbent. After the saturation node, the gas enters the gas system of its own needs, and the pre-saturated absorbent with a temperature of minus 11.6 ºC is divided into two streams, the first flows into absorbers A-1 and A-2, the second – into the deethanization column – as irrigation.

Absorption calculation

At the moment, the supply of regenerated absorbent to ILTA is limited by the capacity of the ACI and is 511 kmol/h. In the variant of pre-saturation of the regenerated absorbent, its amount increases from 511 to 584 kmol/h (by 14.4%) (Table 5). At the same time, absorption will receive 468 kmol/h instead of 409 kmol/h before reconstruction. Due to the reduction of the average absorption temperature to the regulatory level (minus 15 ºC), the installation will reach the design level of extraction of BFLH (from 100 – 110 t/day to 150 t/day) (Table 6).

Conclusions

The application of the saturation of regenerated absorbent with inert components at the low-temperature absorption instalation of MF «Solokha» will allow to minimize the consequences of reducing the pressure of the inlet gas and increase the level of extraction of the components of BFLH by 21.96 % (including propane by 22.05 %, butanes by 30.75 %). At the same time, the extraction level will reach the design level.

The proposed version of the reconstruction of the installation involves supplementing the existing technological scheme with standard equipment, analogues of which are already used at the enterprise (propane evaporator, separator and mixing unit). Deethanization and weathering gases of the saturated absorbent act as raw materials for pre-saturation of the regenerated absorbent. Their consumption in conditions critical for the implementation of low-temperature absorption (reduced pressure and elevated temperature) increases 1.5-2 times.

Table 5 – Calculation of the saturation node of the regenerated absorbent (under existing conditions)

Component	*M*	Regenerated absorbent, T=-11.6 ºC				Weathering gas K-1: T=-5.6 ºC, P=1.6 MPa			
		mol/ mol	kg/ kmol	kmol/ h	kg/h	mol/ mol	kg/ kmol	kmol/ h	kg/h
N_2	28.01	0	0	0	0	0.001	0.036	0.152	4.258
CH_4	16.04	0	0	0	0	0.55	8.795	65.613	1052.43
CO_2	44.01	0	0	0	0	0.08	3.571	9.709	427.293
C_2H_6	30.07	0.00003	0.001	0.0153	0.4612	0.354	10.64	42.341	1273.19
C_3H_8	44.09	0.00736	0.325	3.7630	165.91	0.010	0.429	1.163	51.277
Iso-butane	58.1	0.00809	0.470	4.1362	240.31	0.001	0.066	0.136	7.902
n-butan	58.1	0.02322	1.349	11.872	689.75	0.002	0.128	0.264	15.338
iso-pentan	72.1	0.01805	1.301	9.2285	665.38	0.001	0.047	0.077	5.552
n-pentan	72.1	0.02590	1.867	13.242	954.75	0.001	0.048	0.080	5.768
Fr. to 80ºC	85.7	0.0493	4.224	25.201	2159.7	0.001	0.046	0.060	5.142
80-100 ºC	98.8	0.0830	8.200	42.436	4192.7	0	0.027	0.033	3.260
100-130 ºC	110.1	0.1574	17.329	80.47	8859.7	0	0.020	0.022	2.422
130-160 ºC	125.9	0.1530	19.266		9850.5	0	0.006	0.005	0.630
160-180 ºC	140.1	0.18348	25.706	93.809	13142.6	0	0.003	0.002	0.280
180-200 ºC	152.8	0.2008	30.676	102.64	15684		0.002	0.001	0.153
200-240 ºC	172.6	0.072	12.49	36.98	6383.1				
240-290 ºC	205.7		2.983	7.414	1525.0				
290-330 ºC	242.5	0.003	0.783	1.651	400.5				
>330 ºC	305.1	0.00034	0.104		53.037				
∑	-	1.000	127.07	511.28	64967.3	1.00	23.86	119.66	2854.90

Continuation of Table 5

Component	*M*	*Ki*	***Ai***	**φi**	1- **φi**	Dry gas	Pre-saturation of the absorbent	
						V1,i	***LN,i***	
		P= 1.6 MPa, T= -10 ºC				kmol/h	kmol/h	mol/mol
N_2	28.01	32.0	0.24	0.59	0.406	0.062	0.090	0.0015
CH_4	16.04	9.5	0.80	0.45	0.55	36.087	29.526	0.05049
CO_2	44.01	2.9	2.62	0.72	0.28	2.719	6.990	0.1195
C_2H_6	30.07	1.5	5.07	0.83	0.17	7.198	35.158	0.06012
C_3H_8	44.09	0.42	18.10	0.95	0.05	0.058	4.868	0.00832
Iso-butane	58.1	0.17	44.71	0.99	0.01	0.001	4.271	0.00730
n-butan	58.1	0.11	69.09	1.0	0	0	12.136	0.02075
iso-pentan	72.1	0.042	181.0	1.0	0	0	9.306	0.01591
n-pentan	72.1	0.035	217.0	1.0	0	0	13.322	0.02278
Fr. to 80 ºC	85.7	0.0108	704.0	1.0	0	0	25.261	0.04319
80-100 ºC	98.8	0.0039	1949.0	1.0	0	0	42.469	0.07262
100-130 ºC	110.1	0.0017	4471.0	1.0	0	0	80.492	0.13764
130-160 ºC	125.9	0.0007	10857.0	1.0	0	0	78.245	0.13380
160-180 ºC	140.1	0.0004	19000.0	1.0	0	0	93.811	0.16041
180-200 ºC	152.8	0.0002	38000.0	1.0	0	0	102.645	0.17552
200-240 ºC	172.6						36.981	0.06324
240-290 ºC	205.7						7.413	0.01268
290-330 ºC	242.5						1.651	0.00282
>330 ºC	305.1						0.174	000030
∑	-					46.12489	584.81	10

Table 6 – Calculation of the absorber operation with the absorbent saturation unit

Component	*M*	Regenerated absorbent, T=-11.6 ºC				Dry gas, T=-21 ºC, P=2.2 MPa			
		mol/ mol	kg/ kmol	kmol/ h	kg/h	mol/ mol	kg/ kmol	kmol/ h	kg/h
N_2	28.01	0	0.004	0.04	1.01	0.014	0.401	38.69	1083.8
CH_4	16.04	0.050	0.810	11.81	189.49	0.864	13.864	2337.03	37485.9
CO_2	44.01	0.012	0.526	2.80	123.10	0.031	1.349	82.87	3647.2
C_2H_6	30.07	0.060	1.808	14.07	423.01	0.059	1.774	159.53	4797.0
C_3H_8	44.09	0.008	0.367	1.95	85.87	0.022	0.988	60.57	2670.4
Iso-butane	58.1	0.007	0.424	1.71	99.28	0.003	0.145	6.76	392.7
n-butan	58.1	0.021	1.206	4.86	282.12	0.005	0.261	12.17	706.9
iso-pentan	72.1	0.016	1.147	3.72	268.45	0.001	0.072	2.70	195.0
n-pentan	72.1	0.023	1.642	5.33	384.32	0.001	0.058	2.16	156.0
Fract. to 80 ºC	85.7	0.043	3.702	10.11	866.19	0.000	0.030	0.95	81.1
80-100 ºC	98.8	0.073	7.175	16.99	1678.86	0.000	0.013	0.35	34.7
100-30ºC	110.1	0.138	15.154	32.21	3545.89	0.000	0.002	0.05	5.95
130-60ºC	125.9	0.134	16.845	31.31	3941.60				
160-80ºC	140.1	0.160	22.474	37.54	5258.70				
180-00ºC	152.8	0.176	26.819	41.07	6275.48				
200-240C	172.6	0.063	10.915	14.80	2554.03				
240-290 ºC	205.7	0.013	2.608	2.97	610.16				
290-330 ºC	242.5	0.003	0.685	0.66	160.23				
>330 ºC	305.1	0	0.091	0.07	21.22				
∑	-	1.000	114.40	233.99	26769.03	1.000	18.957	2703.83	51256.5

Continuation of Table 6

Component	*M*	***K****i* -15,5ºC	***A****i*	φi	1- φi	Dry gas	Saturated absorbent	
						V*1,i* *k*mol/h	***L****N,i* kmol/h	$G_{abs.}$ kg/h
N_2	28.01	30.0	0.003	0.003	0.997	38.576	0.52	4.259
CH_4	16.04	7.0	0.013	0.013	0.987	2307.014	41.828	670.920
CO_2	44.01	2.8	0.032	0.032	0.968	80.212	5.458	240.198
C_2H_6	30.07	1.19	0.076	0.076	0.924	147.474	26119	785.40
C_3H_8	44.09	0.31	0.290	0.290	0.710	43.002	19.512	860.28
Iso-butane	58.1	0.13	0.790	1.000	0	0	8.468	492.02
n-butan	58.1	0.08	0.773	1.000	0	0	17.023	989.04
iso-pentan	72.1	0.03	0.692	1.000	0	0	6.427	463.40
n-pentan	72.1	0.025	0.605	1.000	0	0	7.493	540.28
Fraction to 80 ºC	85.7	0.008	0.306	1.000	0	0	11.054	947.29
80-100 ºC	98.8	0.0027	0.110	1.000	0	0	17.344	1713.59
100-130ºC	110.1	0.0013	0.001	1.000	0	0	32.260	3551.85
130-160ºC	125.9						31.307	394160
160-180ºC	140.1						37.535	5258.70
180-200ºC	152.8						41.070	6275.48
200-240ºC	172.6						14.797	2554.03
240-290ºC	205.7						2.966	610.16
290-330ºC	242.5						0.661	160.24
>330 ºC	305.1						0.070	21.22
∑	-	-	-	-	-	2586.96	321.54	30079.93

This actualizes the problem of its more efficient use, increases the pressure in the gas system of own needs and leads to non-productive emissions of valuable raw materials through the safety valves for combustion in the flare system. However, in the case of using these gases for pre-saturation of the absorbent, about 19% of the low-pressure gas is absorbed and returned to the process. As a result, the percentage of marketable products (BFLH and dry gas) is increasing.

Table 7- 9 shows the material balance of absorption.

Table 7 – Calculation of extraction coefficients

Component	Absorption, T=21.1 °C, P=1.58MPa			Desorption, T=153 °C, P=1.61MPa		
	Ki at 21 °C	***Ai***	**φ'**i	***K'***i	***S'i***	**φ''**i
N_2	40.000	0.019	0.019	60.0	9.9740	1.0
CH_4	10.000	0.077	0.077	17.3	2.8758	1.0
CO_2	8.200	0.094	0.094	18.25	3.0338	1.0
C_2H_6	2.000	0.385	0.385	6.8	1.1304	0.88
C_3H_8	0.642	1.200	0.95	3.85	0.64	0.64
Iso-butane	0.270	2.855	1.0	2.2	0.3657	0.36571
n-butan	0.160	4.817	1.0	1.9	0.3158	0.31584
iso-pentan	0.080	9.635	1.0	1.05	0.17455	017455
n-pentan	0.060	12.846	1.0	0.93	0.1546	0.15460
Fraction up to 80 °C	0.024	32.115	1.0	0.56	0.0931	0.09309
80-100 °C	0.009	85.640	1.0	0.3	0.0499	0.0499
100-130 °C	0.005	154.152	1.0	0.186	0.0309	0.03092
130-160 °C	0.003	296.446	1.0	0.093	0.0155	0.0155
160-180 °C	0.001	7707.600	1.0	0.052	0.0086	0.0086
180-200 °C	0	2569.200	1.0	0.0295	0.0049	0.00490
200-240 °C	0	7707.600	1.0	0.0165	0.0027	0.00274
240-290 °C	0		1.0	0.0083	0.00138	0.0014
290-330 °C	0		1.0	0.0046	0.00076	0.00077
>330 °C	0		1.0	0.0022	0.00037	0.00037

Table 8 – Material balance of ILTA MF «Solokha» after reconstruction with a «raw» gas productivity of 130,000 m³/h

Component	Gas inlet in ILTA		Degree withdrawal	Entrance		Withdrawal of BFLH		
	% mol.	g / m³	% mol.	% mol.	g/m³	g/m³	t/h	t/day
C_3	1.791	43.0	57.61	0.759	18.23	24.77	3.2204	77.29
$\sum C_4$	0.701	17.7	86.61	0.094	2.37	15.33	1.9925	47.82
$\sum C_5$	0.179	5.40	100	0	0	5.40	0.7021	16.85
$\sum C_{6+}$	0.05	1.88	100	0	0	1.88	0.2438	5.85
$\sum CO_2, CH_4, C_2H_6$	-	-	-	-	-	-	-	7.35
$\sum$	2.72	67.98	69.70	0.853	20.6	47.38	6.1588	155.16

Table 9 – Results of the introduction of the node of saturation of the regenerated absorbent with inert components

Component	Withdrawal of BFLH						Difference		
	after reconstruction			before reconstruction					
	g/m³	t/day	% mol.	g/m³	t/day	%mol.	g/m³	t/day	% mol.
C_3	24.77	77.29	57.61	15.29	47.70	35.56	+9.48	+29.59	+22.05
$\sum C_4$	15.33	47.82	86.61	9.89	30.86	55.86	+5.44	+16.96	+30.75
$\sum C_5$	5.40	16,85	100	5,40	16,85	100	-	-	-
$\sum C_{6+}$	1.88	5.85	100	1.88	5.85	100	-	-	-
$\sum CO_2, CH_4, C_2H_6$	-	7.35	-	-	3.48	-	-	+3.87	-
$\sum$	47.38	155.16	69.70	32.46	104.74	47.74	+14.92	+50.42	+21.96

References

1. Farnoosh Allahdinian Hesaroeieh, Sina Mosallanezhad, Mohammad Reza Rahimpour (2024). 4 - Refrigeration process for condensate recovery from natural gas. Advances in Natural Gas: Formation, Processing, and Applications. Volume 5: Natural Gas Impurities and Condensate Removal Editor(s): Mohammad Reza Rahimpour, Mohammad Amin Makarem, Maryam Meshksar, *Elsevier,* 2024, pp. 65-91, ISBN 9780443192234, https://doi.org/10.1016/B978-0-443-19223-4.00012-7

2. Chapter 10 - Natural gas liquids recovery. Handbook of Natural Gas Transmission and Processing Editor(s): Saeid Mokhatab, William A. Poe, James G. Speight. *Gulf Professional Publishing*, 2006, pp. 365-400, ISBN 9780750677769. https://doi.org/10.1016/B978-075067776-9/50015-4

3. Olsen C., Kozman T. A., Lee J., Yuvamitra K. (2012). A Comparative Study of Natural Gas Liquids Recovery Methods. *Distributed Generation & Alternative Energy Journal*, 27(2), 42–55. https://doi.org/10.1080/21563306.2012.10505411

4. Kokkinos Nikolaos C., Zachos Dimitrios K. (2023). C_{3+} Hydrocarbon Removal for Natural Gas Pretreatment (book chapter). *Reference Module in Chemistry, Molecular Sciences and Chemical Engineering. Elsevier* (2023). ISBN 9780124095472, https://doi.org/10.1016/B978-0-443-15740-0.00005-7

5. Топільський П.І. (2001). *Переробка нафтових і природних газів.* – Львів: НУ «Львівська політехніка», 212 с.

6. Mokhatab, S., Poe, W.A., and Mak, J.Y., *Handbook of Natural Gas Transmission and Processing: Principles and Practices,* Amsterdam: Gulf Professional, 2015, 3rd ed.

7. Getu, M., Mahadzir, S., Long, N.V.D., and Lee, M., Techno-economic analysis of potential natural gas liquid (NGL) recovery processes under variations of feed compositions, *Chem. Eng. Res. Des.*, 2013, vol. 91, no. 7, pp. 1272–1283. https://doi.org/10.1016/j.cherd.2013.01.015

8. Saeid Mokhatab, John Y. Mak, William A. Poe (2019) Handbook of Natural Gas Transmission and Processing Principles and Practices. *Gulf Professional Publishing,* 830 p. ISBN 978-0-12-815817-3, https://doi.org/10.1016/C2017-0-03889-2

9. Jaubert, J.-N. and Mutelet, F., VLE predictions with the Peng–Robinson equation of state and temperature dependent k ij calculated through a group contribution method, Fluid Phase Equilib., 2004, vol. 224, no. 2, pp. 285–304. https://doi.org/10.1016/j.fluid.2004.06.059

10. Звіт про науково-дослідну роботу: «Аналіз пропозицій по реконструкції установки НТА ГС «Солоха», визначення сировинної бази, проведення промислових технологічних досліджень на установці з метою встановлення ефективного режиму її експлуатації». Тема 35. 424/2001 – 2001. УкрНДІГазу, 2001, – 185 с.

11. Клименко А.П. (1964). *Поділ природних вуглеводневих газів.* –. Київ:Техніка, 379 с.

12. Бучинський А.К., Коваленко В.С. (2004). *Основи технології та техніки абсорбційних процесів; Укр. держ. хім.-технол. ун-т.* – Д.: УДХТУ, 216 с.

1. Farnoosh Allahdinian Hesaroeieh, Sina Mosallanezhad, Mohammad Reza Rahimpour (2024). 4 - Refrigeration process for condensate recovery from natural gas. Advances in Natural Gas: Formation, Processing, and Applications. Volume 5: Natural Gas Impurities and Condensate Removal Editor(s): Mohammad Reza Rahimpour, Mohammad Amin Makarem, Maryam Meshksar, *Elsevier*, 2024, pp. 65-91, ISBN 9780443192234, https://doi.org/10.1016/B978-0-443-19223-4.00012-7

2. Chapter 10 - Natural gas liquids recovery. Handbook of Natural Gas Transmission and Processing Editor(s): Saeid Mokhatab, William A. Poe, James G. Speight. *Gulf Professional Publishing*, 2006, pp. 365-400, ISBN 9780750677769. https://doi.org/10.1016/B978-075067776-9/50015-4

3. Olsen C., Kozman T. A., Lee J., Yuvamitra K. (2012). A Comparative Study of Natural Gas Liquids Recovery Methods. *Distributed Generation & Alternative Energy Journal*, 27(2), 42–55. https://doi.org/10.1080/21563306.2012.10505411

4. Kokkinos Nikolaos C., Zachos Dimitrios K. (2023). C_{3+} Hydrocarbon Removal for Natural Gas Pretreatment (book chapter). *Reference Module in Chemistry, Molecular Sciences and Chemical Engineering. Elsevier* (2023). ISBN 9780124095472, https://doi.org/10.1016/B978-0-443-15740-0.00005-7

5. Topilsky P.I. (2001). *Processing of petroleum and natural gases*. Lviv: NU «Lviv Polytechnic», 212 p.

6. Mokhatab, S., Poe, W.A., and Mak, J.Y., *Handbook of Natural Gas Transmission and Processing: Principles and Practices,* Amsterdam: Gulf Professional, 2015, 3rd ed.

7. Getu, M., Mahadzir, S., Long, N.V.D., and Lee, M., Techno-economic analysis of potential natural gas liquid (NGL) recovery processes under variations of feed compositions, *Chem. Eng. Res. Des.*, 2013, vol. 91, no. 7, pp. 1272–1283. https://doi.org/10.1016/j.cherd.2013.01.015

8. Saeid Mokhatab, John Y. Mak, William A. Poe (2019) Handbook of Natural Gas Transmission and Processing Principles and Practices. *Gulf Professional Publishing,* 830 p. ISBN 978-0-12-815817-3, https://doi.org/10.1016/C2017-0-03889-2

9. Jaubert, J.-N. and Mutelet, F., VLE predictions with the Peng–Robinson equation of state and temperature dependent k_{ij} calculated through a group contribution method, *Fluid Phase Equilib.*, 2004, vol. 224, no. 2, pp. 285–304. https://doi.org/10.1016/j.fluid.2004.06.059

10. Report on scientific and research work: «Analysis of proposals for the reconstruction of the ULTA MF «Solokha», determination of the raw material base, industrial technological research at the installation in order to establish an effective mode of its operation». Topic 35. 424/2001 – 2001. UkrRIGaz, 2001, – 185 p.

11. Klymenko A.P. (1964). *Separation of natural hydrocarbon gases*. -. Kyiv: Technyka, 379 p.

12. Buchynskyi A.K., Kovalenko B.C. (2004). *Basics of technology and techniques of absorption processes; Ukraine state chemical and technological Univ*. – D.: USChTU, 216 p.

Збірник наукових праць. Галузеве машинобудування, будівництво
Academic journal. Industrial Machine Building, Civil Engineering
http://journals.nupp.edu.ua/znp
https://doi.org/10.26906/znp.2023.61.3874

UDC 666.97.033.16

Loaders for Concrete Compaction

Mykola Nesterenko [1*], Olexandr Panfilov [2], Maxim Pyrlyk [3]

[1] National University «Yuri Kondratyuk Poltava Polytechnic» https://orcid.org/0000-0002-4073-1233
[2] National University «Yuri Kondratyuk Poltava Polytechnic» https://orcid.org/0009-0007-2917-0328
[3] National University «Yuri Kondratyuk Poltava Polytechnic» https://orcid.org/0009-0006-1343-9516

*Corresponding author E-mail: nesterenkonikola@gmail.com

The article presents a comprehensive analysis of load applicator designs used in the compaction technologies of stiff and lightweight concrete mixtures. The role of loading is revealed as one of the key factors influencing the effectiveness of forming products made from concrete with a low water-to-cement ratio. The main operating principles of load applicators are described, which apply additional force to the concrete mixture in combination with vibrational loading. A classification of load applicators is provided based on design features and energy source: inertial, non-inertial, pneumatic, and vibratory load applicators. Special attention is given to combined devices that integrate vibrational and impulse action on concrete. The study summarizes research findings that confirm the advantages of combined compaction, particularly when using pneumatic load applicators with adjustable pressure. It has been established that the use of active load applicators allows for a reduction in cement consumption by up to 30%, a decrease in product forming time by up to 50%, improved compaction uniformity along the height, and enhanced surface quality. An original design of an active load applicator with a vibration exciter and impact elements is proposed, providing impulse compaction with adjustable pressure and frequency. The main unresolved aspects of the problem are identified — the lack of unified methodologies for calculating loading parameters, insufficient adaptability of designs to changes in product geometry and concrete mixture properties. The feasibility of developing intelligent controlled load applicators capable of adapting to forming conditions is substantiated to improve the efficiency of reinforced concrete product manufacturing.

Keywords: concrete mixture, compaction, load applicator, vibration, combined compaction, vibratory load applicator, pneumatic loading, lightweight concrete, energy efficiency.

Привантажувачі для ущільнення бетонів

Нестеренко М.М. [1*], Панфілов О.І. [2], Пирлик М.О. [3]

[1,2,3] Національний університет «Полтавська політехніка імені Юрія Кондратюка»
*Адреса для листування E-mail: nesterenkonikola@gmail.com

У статті виконано комплексний аналіз конструкцій привантажувачів, які застосовуються в технологіях ущільнення жорстких і легких бетонних сумішей. Розкрито роль привантаження як одного з ключових факторів, що впливає на ефективність формування виробів із бетонів з низьким водоцементним відношенням. Описано основні принципи дії привантажувачів, які реалізують додаткову силову дію на бетонну суміш у поєднанні з вібраційним навантаженням. Наведено класифікацію привантажувачів за конструктивними ознаками та джерелом енергії: інерційні, безінерційні, пневматичні, вібропривантажувачі. Особливу увагу приділено комбінованим пристроям, які поєднують вібраційний та імпульсний вплив на бетон. Узагальнено результати досліджень, що підтверджують переваги комбінованого ущільнення, зокрема з використанням пневматичних привантажувачів із регульованим тиском. Встановлено, що застосування активних привантажувачів дозволяє зменшити витрати цементу до 30 %, скоротити час формування виробу до 50 %, покращити однорідність ущільнення по висоті та підвищити поверхневу якість. Запропоновано оригінальну конструкцію привантажувача активної дії із віброзбуджувачем та ударними елементами, що забезпечує імпульсне ущільнення із регульованим тиском і частотою. Визначено основні нерозв'язані аспекти проблеми — відсутність уніфікованих методик розрахунку параметрів привантаження, недостатня адаптивність конструкцій до змін геометрії виробів та властивостей бетонних сумішей. Обґрунтовано доцільність розроблення інтелектуальних керованих привантажувачів з можливістю адаптації до умов формування для підвищення ефективності виробництва залізобетонних виробів.

Ключові слова: бетонна суміш, ущільнення, привантажувач, вібрація, комбіноване ущільнення, вібропривантажувач, пневмопривантаження, легкі бетони, енергоефективність.

Introduction

Loaders as elements of vibration equipment play a key role in the compaction process of stiff and low-workability concrete mixtures, which are widely used in the production of precast reinforced concrete products. Compaction is the factor that determines the main physical and mechanical properties of the final product—strength, density, frost resistance, crack resistance, and durability. Under construction conditions, where quality requirements and the productivity of technological processes are constantly increasing, the need arises for more efficient compaction methods than traditional vibration techniques [1, 2, 5].

The use of loaders in combination with vibrational loading is particularly relevant, as it allows the water-cement ratio to be reduced, prevents segregation of the mixture, and ensures uniform compaction throughout the entire volume of the form. Due to the additional static or dynamic pressure, loaders facilitate the active expulsion of air and compaction of the granular structure of the mixture, which, in turn, improves the quality and strength of concrete products [3].

Depending on their structural design and operating principle, loaders are classified into inertial, non-inertial, pneumatic, and vibratory types, among others. Each type has its own application features, advantages, and limitations, which necessitate a thorough analysis in the context of forming technologies. Combined compaction modes, in which vibration is combined with active loading—pneumatic, mechanical, or impulse—are especially effective.

Given the diversity of product types, the properties of concrete mixtures, and performance requirements, a systematic analysis of existing loader designs and their impact on compaction efficiency is of significant importance.

Definition of unsolved aspects of the problem

Despite the availability of various technical solutions for loading concrete mixtures during compaction, there remain a number of unresolved issues related to both the structural improvement of loaders and their classification by operating principle, type of loading, and intended function.

A significant portion of existing loader designs feature fixed geometric and load parameters, which limits their applicability for products of varying shapes and sizes. Adaptive, modular, or universal designs capable of automatically adjusting the force, direction, or point of load application have yet to become widespread or standardized in serial production.

Many existing designs also lack technical solutions for precise synchronization between the loader’s action and the operation mode of the vibration exciter (in terms of frequency, phase, and direction). This limits the effectiveness of combined compaction modes, where the synchronization of impact and vibration is critically important for forming a homogeneous concrete structure.

Basic material and results

One of the key stages in the production of reinforced concrete products is the compaction of the concrete mixture. Particular attention must be paid to low-workability and stiff concrete mixtures, for which traditional compaction methods based solely on vibration often prove to be insufficiently effective [4, 7]. In such cases, it is advisable to combine vibrational impact with additional static pressure, which is implemented through the use of loaders. This approach significantly increases the degree of mixture compaction, reduces forming time, and improves the uniformity of the product structure.

Loaders perform the function of applying additional pressure to the concrete mixture during vibration. This promotes the intensification of the compaction process by reducing viscosity, preventing segregation, and accelerating air expulsion. Critical parameters in this context include the magnitude of the pressure applied to the mold surface, the frequency and amplitude of vibrations, all of which must correspond to the physical and mechanical properties of the concrete mixture.

Studies show that the application of combined effects—vibration and loading—can increase the early (24-hour) strength of concrete by 130–200% compared to traditional pressing. This improvement is attributed to denser particle packing, reduced void content, and enhanced development of molecular bonding forces. In particular, vibropressing technology with a loader is successfully used in the production of paving slabs, curb stones, and wall blocks made from stiff concrete mixtures with workability of 40–50 seconds under a pressure of 5–10 kPa.

Depending on the compaction conditions and the properties of the concrete mixture, loaders can serve various functions—from stabilizing the mixture's position in the mold to initiating additional particle movement. For example, in the case of heavy stiff concrete, loading facilitates intensive air expulsion, while in the compaction of lightweight concretes with porous aggregates, it helps prevent segregation. Therefore, it is a relevant task to adapt the type of loader to the specific technological process and material type.

In the compaction of polystyrene concrete, which exhibits high damping properties, the effectiveness of traditional vibrocompaction is significantly reduced. Under such conditions, the use of combined loaders (e.g., pneumatic loading in conjunction with vibration) enables a substantial increase in density and strength while reducing cement consumption. Research findings indicate that the application of variable pressure throughout the compaction cycle not only ensures uniform mixture distribution but also reduces internal stresses in the product after hardening.

Given the wide range of concrete products, the universality of loaders is also of great importance. Modular designs with easily replaceable sections, variable shield geometries, universal mountings, and adjustable stiffness of elastic elements allow for rapid reconfiguration of equipment for new products without significant time and resource costs. This is especially

important for small and medium-sized manufacturers, where equipment flexibility directly affects production efficiency.

An important criterion for selecting a loader remains the energy efficiency of the compaction process. It has been established that, at the same degree of compaction, energy consumption for systems with vibratory loading can be 20–30% lower compared to traditional vibration-only methods, particularly when compacting heavy or low-workability mixtures. This is due to reduced energy losses from oscillations of massive formwork elements and stabilization of vibration modes.

Structurally, loaders can be implemented as movable frames, loading plates, or mechanical or pneumatic systems that provide controlled pressure on the surface of the concrete mixture. The most common are vertical loaders, which act on the top part of the form, ensuring uniform pressure distribution across the surface. When combined with vibrating platforms or vibrating tables, loaders may be integrated into a common kinematic scheme.

In industrial conditions, the effectiveness of loaders is determined not only by the pressure applied but also by the precision of synchronization with the vibration mode. The best results are achieved using multi-frequency compaction, where the vibrating table operates at 55 Hz and the loader at 75–150 Hz.

Such a mode contributes to reduced energy consumption, improved uniformity of compaction, and significantly shortened forming time.

Despite the widespread adoption of loaders in production, a unified methodology for calculating their parameters is still lacking. Existing theoretical approaches show significant discrepancies in assessing the optimal pressure, creating difficulties in implementing such systems in new technological lines. This highlights the need for further research aimed at harmonizing loader parameters with the characteristics of the concrete mixture, the product geometry, and the vibration compaction modes.

In the practice of manufacturing concrete and reinforced concrete products, loaders have gained widespread use due to their ability to provide additional force on the mixture during vibrocompaction. They can be designed as devices that replicate the shape of the product in plan view and operate based on mass, elastic elements, or controlled pressure. According to their mode of action, they are classified as passive or active.

Passive loaders, which do not have built-in sources of oscillation, apply pressure using gravity or elastic systems. The simplest type is the inertial loader, in which compaction occurs under the weight of the structure itself. These are effective for small-batch production, for example, in the manufacture of cinder blocks or wall stones. However, their disadvantages include limited productivity, manual feeding, and the inability to precisely control the applied pressure.

Another type is the non-inertial loader, in which the additional pressure is applied by a mass that does not participate in oscillations but transmits the load through elastic elements.

These systems may use either rigid or pneumatic springs. In such two-mass systems, periodic impact between the loader components is possible, which further enhances the compaction effect. However, to achieve stable impacts, it is necessary to precisely adjust the spring stiffness according to the height of the product and the nature of oscillations.

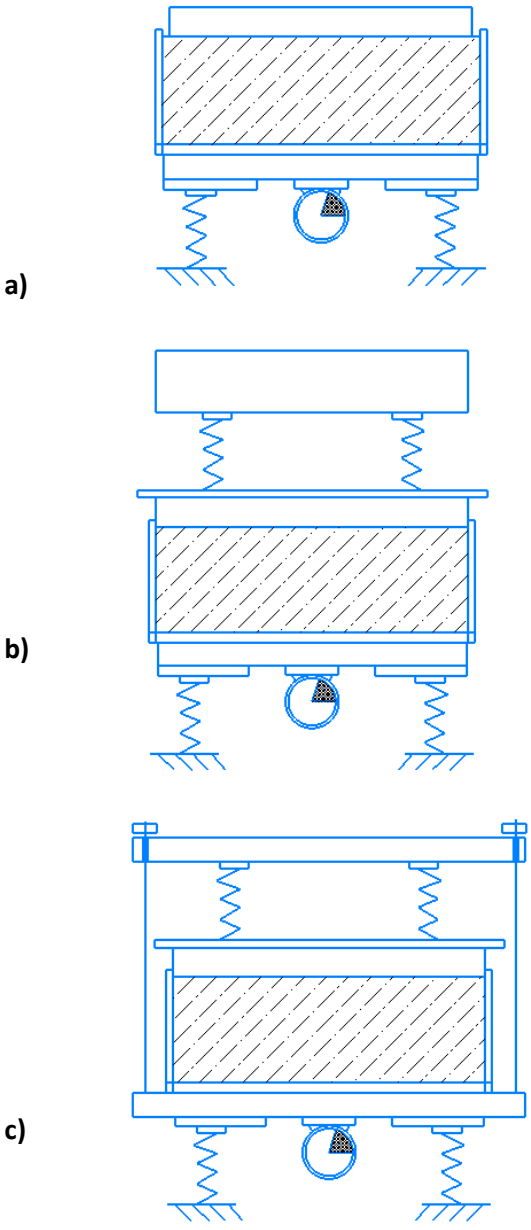

Figure 1 – Passive Loaders:
a) inertial loader; b) inertial loader with an additional spring-loaded mass; c) inertial loader with a spring-loaded pressing system

Active loaders are equipped with vibration exciters and provide not only static pressure but also dynamic action (vibrational or impact) on the concrete mixture. This allows for a significant intensification of the compaction process and improved structural uniformity, particularly for products with complex geometries.

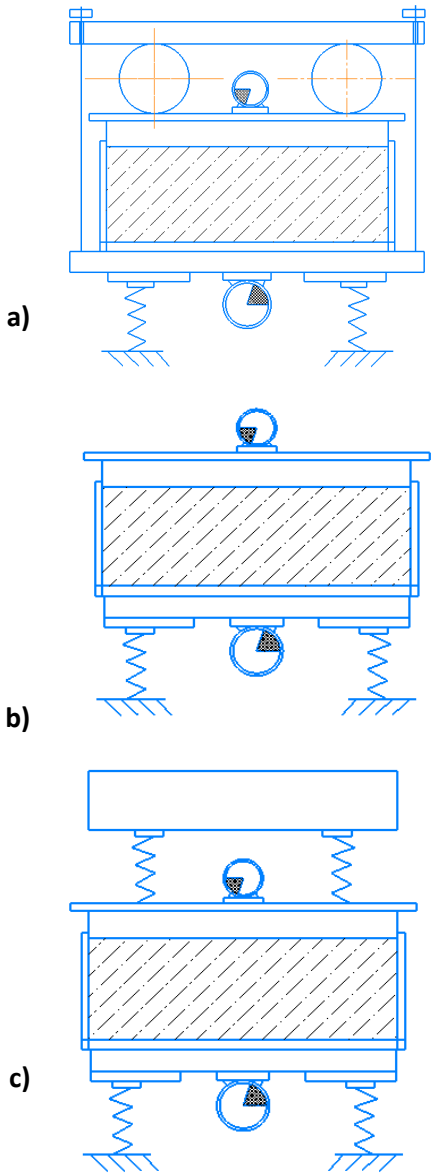

Figure 2 – Active Loaders:
a) pneumatic loader with vibration exciter;
b) inertial active loader with vibration exciter;
c) inertial active loader with additional spring-loaded mass and vibration exciter

Among active-type designs, special attention is given to pneumatic loaders, in which pressure on the mixture is generated by inflatable rubber bladders filled with air. Such systems enable effective compaction of both the external and internal surfaces of the product. For example, in the production of pipes or hollow elements, the bladders are installed on internal core formers, creating uniform pressure on the concrete from all sides. According to research, this technology can reduce cement consumption by up to 25%, cut hardening time nearly in half, and decrease the need for thermal curing.

Particular mention should be made of combined compaction systems, where pneumatic loading is used in conjunction with vibration applied both from the top and the bottom [5]. This ensures uniform compaction throughout the entire volume, reduces the risk of segregation, and enables efficient processing of stiff mixtures with a low water-cement ratio.

The design of an active loader equipped with a vibration exciter and impact elements (Figure 3) enables the generation of additional impulses on the compacted mixture. This design is based on the results of the study [8].

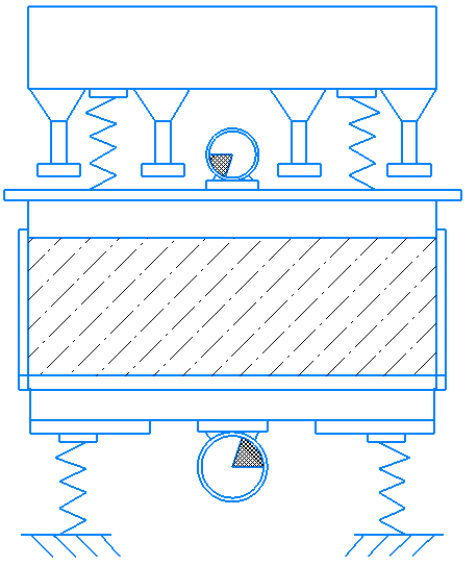

Figure 3 – Active loader with vibration exciter and impact elements

Thus, concrete compaction loaders offer a wide range of structural solutions, each oriented toward a specific product type, concrete mixture properties, and production conditions. The most promising among them are combined systems that integrate vibrational impact with controlled loading. Their implementation enables improved strength and density of products, reduced cement consumption, increased productivity, and consistent product quality with significantly lower energy consumption.

In the context of compacting stiff and lightweight concrete mixtures, pneumatic loaders hold a special place due to their high efficiency enabled by continuous pressure adjustment during the forming process. Studies [5, 6] have shown that when compacting lightweight concrete using pneumatic loading for 30–40 seconds, the strength increases initially, then stabilizes, and eventually begins to decline. This indicates the necessity to optimize both the duration and dynamic control of pressure during compaction, especially at the final stage of forming.

Experimental results [5] also indicate a significant increase in strength (up to 50%) when combining variable vibration modes with non-inertial loading, compared to compaction without loading. The main advantages of pneumatic bladder-type loaders are reduced structural metal consumption, quick adjustment of compaction modes, and minimized human influence. This is particularly important for serial production of components with varying heights or complex geometries.

Active vibro-loaders equipped with autonomous vibration exciters are widely used and operate in coordination with vibrating platforms. These systems provide a dual-factor effect on the concrete mixture: bottom vibration (via vibrating table) and top vibration (via loader), with the ability to independently adjust the frequency of each vibration source. As a result, so-called dual-frequency compaction is achieved, which, according to research [3, 8, 9], is the most effective method for attaining maximum concrete density and strength.

The practical implementation of such solutions is realized in serially produced vibro-loaders of the SMZh-849 and SMZh-852 types, used both in automated lines and stationary posts. However, one of the drawbacks of these systems is the fixed geometry of the contact surface, which limits their versatility. To overcome this limitation, some designs [9] include shields composed of independent sections, each of which can move separately. This allows the loader to adapt to the shape of any product without replacing the main unit.

We propose a design of an active-type loader equipped with a vibration exciter, impact elements, and an additional mass.

This loader consists of two plates:

1 – the lower plate, which rests on the concrete mixture and has a vibration exciter (3) mounted on it;

2 – the upper plate, connected to the lower plate through guide elements (4) with spring elements (5).

On the underside of the upper plate, impact elements (6) are installed with threaded height adjustment.

Additionally, the system allows for adjustment of the added weight (7) to fine-tune the loader's operating mode.

Summarizing the advantages of active vibro-loaders, the following key points should be noted:

– Capability to form products from stiff concrete mixtures without the need for excessive pressure;

– Implementation of dual-frequency compaction to enhance efficiency;

– Reduced energy consumption through localized vibrational impact;

– Improved uniformity of compaction and surface quality of products.

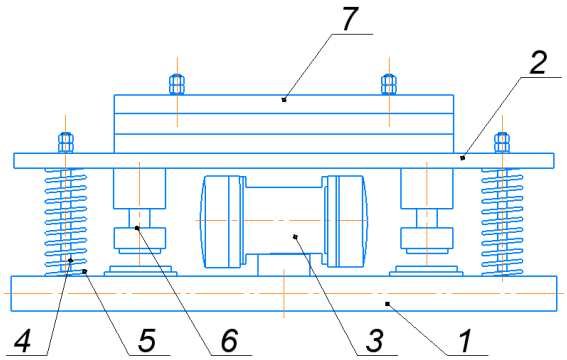

Figure 4 – Design of active loader with vibration exciter, impact elements, and additional mass

Conclusions

The designs of loaders used for the compaction of concrete and lightweight concrete mixtures were analyzed, and it was established that the most effective are combined devices that integrate vibrational impact with controlled loading on the mixture.

It was determined that active vibro-loaders particularly pneumatic and impact-vibration types provide enhanced homogeneity of the concrete structure, reduce cement consumption by 15–30%, and shorten the compaction cycle duration by up to 50%.

A design of an active-type loader equipped with a vibration exciter, impact elements, and adjustable mass was proposed. This design allows for the compaction mode to be adapted to specific types of concrete mixtures and product geometries.

References

1. Nazarenko I., Diachenko O., Pryhotskyi V. & Nesterenko M. (2021). Structural analysis of vibration platform for panel units forming and consideration of its utilizing options. *Academic Journal. Industrial Machine Building, Civil Engineering*. 1(56). 37-42 https://doi.org/10.26906/znp.2021.56.2505

2. Маслов, О., Саленко, Ю., & Маслова, Н. (2011). Дослідження взаємодії вібруючої плити з цементобетонною сумішшю. *Вісник КНУ імені Михайла Остроградського*, (2/201 (67), ч. 1), 93–98.

3. Маслов, О. Г., Саленко, Ю. С., Жовтяк, І. І., Вакуленко, Р. А., & Дятловська, В. Л. (2020). Дослідження вібраційного органу для ущільнення бетонних сумішей з віброімпульсними коливаннями. *Вісник Кременчуцького національного університету імені Михайла Остроградського,* (5–6), 139–146. https://doi.org/10.30929/1995-0519.2020.5-6.139-146

4. Назаренко, І. І. (2010). *Прикладні задачі теорії вібраційних систем* (2-е вид.). Київ. 440 с.

1. Nazarenko I., Diachenko O., Pryhotskyi V. & Nesterenko M. (2021). Structural analysis of vibration platform for panel units forming and consideration of its utilizing options. *Academic Journal. Industrial Machine Building, Civil Engineering*. 1(56). 37-42 https://doi.org/10.26906/znp.2021.56.2505

2. Maslov, O., Salenko, Yu., & Maslova, N. (2011). Study of the interaction between a vibrating plate and a cement concrete mixture. *Bulletin of Kremenchuk Mykhailo Ostrohradskyi National University*, (2/201 (67), Part 1), 93–98.

3. Maslov, O. H., Salenko, Yu. S., Zhovtiak, I. I., Vakulenko, R. A., & Diatlovska, V. L. (2020). Study of a vibration device for compacting concrete mixtures with vibro-impulse oscillations. *Bulletin of Kremenchuk Mykhailo Ostrohradskyi National University*, (5–6), 139–146. https://doi.org/10.30929/1995-0519.2020.5-6.139-146

4. Nazarenko, I. I. (2010). *Applied problems of the theory of vibration systems* (2nd ed.). Kyiv. 440 p.

5. Давиденко, Ю. О. (1999). *Розробка та дослідження керованої віброплощадки для ущільнення легких бетонів* (Дис. канд. техн. наук). Полтава. 181 с.

6. Демченко, С. В. (2022). Вплив параметрів вібрації на міцність бетону. *Ресурсоекономні матеріали, конструкції, будівлі та споруди,* (55), 89–94.

7. Дєдов, О. П. (2010). Розповсюдження плоских хвиль напруження в пружно-пластичному середовищі під дією силового навантаження. *Техніка будівництва*, (25), 6–73.

8. Нестеренко, М. М. (2008). *Привантажувач для додаткового формування залізобетонних вир* (Пат. № 33705, Україна). Бюл. № 14.

9. Назаренко, І. І., Смірнов, В. М., Фомін, А. В., Свідерський, А. Т., Костенюк, О. О., Дєдов, О. П., & Зухба, А. Г. (2010). *Основи теорії взаємодії робочих органів будівельних машин із напружено-деформованим середовищем* (за ред. І. І. Назаренка). Київ: МП Леся. 216 с.

5. Davydenko, Yu. O. (1999). *Development and investigation of controlled vibration platform for compaction of lightweight concrete* (PhD thesis). Poltava. 181 p.

6. Demchenko, S. V. (2022). Influence of vibration parameters on the strength of concrete. *Resource-Saving Materials, Structures, Buildings and Constructions*, (55), 89–94..

7. Diedov, O. P. (2010). Propagation of plane stress waves in an elastic–plastic medium under force loading. *Construction Engineering*, (25), 6–73.

8. Nesterenko, M. M. (2008). Load applicator for additional forming of reinforced concrete products. (Patent No. 33705). Ukraine. Retrieved from https://uapatents.com

9. Nazarenko, I. I., Smirnov, V. M., Fomin, A. V., Sviderskyi, A. T., Kostenyuk, O. O., Diedov, O. P., & Zukhba, A. H. (2010). Fundamentals of the theory of interaction of working bodies of construction machines with stress-strain medium. Kyiv: MP Lesia. 216 p.

Збірник наукових праць. Галузеве машинобудування, будівництво
Academic journal. Industrial Machine Building, Civil Engineering
http://journals.nupp.edu.ua/znp
https://doi.org/10.26906/znp.2023.61.3864

UDC 622.276.72

Justification for the Choice of a Modeling Scheme for the Hydrocarbon Preparation Process for Transportation Using Supersonic Separation

Tetiana Nesterenko [1*], Mykola Nesterenko [2], Oleksandr Shevchenko [3], Oleksii Omelchenko [4]

[1] National University «Yuri Kondratyuk Poltava Polytechnic» https://orcid.org/0000-0002-2387-8575
[2] National University «Yuri Kondratyuk Poltava Polytechnic» https://orcid.org/0000-0002-4073-1233
[3] National University «Yuri Kondratyuk Poltava Polytechnic» https://orcid.org/0009-0005-0478-7060
[4] National University «Yuri Kondratyuk Poltava Polytechnic» https://orcid.org/0009-0001-8225-2089
*Corresponding author: tnesterenko2021@gmail.com

A study was conducted to select a modeling scheme for the process of preparing hydrocarbons for transportation by supersonic separation. Modeling was performed in the HYSYS environment, which allowed obtaining optimal parameters for effective removal of moisture and heavy hydrocarbons. The influence of pressure and temperature changes on the efficiency of heavy hydrocarbon extraction was analyzed. The most effective modeling scheme was selected, which provides high prediction accuracy. The results obtained can be used for further optimization of gas purification technological processes and their adaptation to industrial applications.

Keywords: supersonic separation, natural gas, modeling, associated formation water, hydrocarbon preparation.

Обґрунтування вибору схеми моделювання процесу підготовки вуглеводнів до транспортування методом надзвукової сепарації

Нестеренко Т.М.[1]*, Нестеренко М.М.[2], Шевченко О.О.[3], Омельченко О.Ю.[4]

[1,2,3,4] Національний університет «Полтавська політехніка імені Юрія Кондратюка»
*Адреса для листування E-mail: tnesterenko2021@gmail.com

Проведено аналіз методів підготовки вуглеводнів до транспортування та обґрунтовано вибір схеми моделювання процесу надзвукової сепарації. Ця технологія дозволяє ефективно видаляти вологу, важкі вуглеводні та CO_2, що значно покращує якість газу та зменшує негативний вплив на довкілля. Виконано чисельне моделювання в програмному середовищі HYSYS, яке дозволило отримати оптимальні параметри процесу. Досліджено вплив ключових факторів, таких як тиск, температура та швидкість потоку, на ефективність сепарації. Отримано залежності, що демонструють, що збільшення тиску до 12,5 МПа підвищує ефективність процесу, однак подальше його зростання не дає значного покращення. Проведено порівняльний аналіз двох схем моделювання, в результаті якого досягнуто вибору оптимальної моделі, що забезпечує високу точність прогнозування та мінімізує обчислювальні витрати. Визначено, що запропонована схема дозволяє найбільш точно відтворити фізичні процеси, які відбуваються в надзвуковому сепараторі, включаючи розширення потоку, фазовий перехід, розділення рідкої та газової фаз і дифузію. Проаналізовано обмеження сучасних моделей, зокрема їхню чутливість до рівноважних припущень. Встановлено, що для підвищення точності прогнозів необхідні подальші удосконалення методів моделювання, оскільки реальний процес є нерівноважним. Досягнуто висновку, що використання надзвукового сепаратора може значно підвищити ефективність підготовки природного газу та забезпечити додаткове вилучення конденсату. Отримані результати можуть бути використані для подальшої оптимізації технологічних процесів очищення газу та їхньої адаптації до промислового застосування.

Ключові слова: надзвукова сепарація, природний газ, моделювання, супутньо-пластова вода, підготовка вуглеводнів

Introduction

Efficient hydrocarbon feedstock preparation is a crucial stage in the technological processes of the oil and gas industry. One of the promising methods for enhancing the separation efficiency of gas-liquid mixtures is supersonic separation, which provides high-speed and selective removal of undesirable impurities such as moisture, condensate, and solid particles.

The successful implementation of supersonic separation requires a thorough selection and justification of the modeling scheme, taking into account the thermodynamic and hydrodynamic characteristics of the flow, phase state changes of the components, and the influence of key parameters such as pressure, temperature, and gas flow velocity.

Despite the significant potential of supersonic separation technology, its practical application is often limited by the complexity of process modeling and the lack of standardized approaches to predicting separation efficiency under different operating conditions. The choice of a s grounded modeling scheme is essential for optimizing equipment design, improving energy efficiency, and ensuring the stability of the separation process. Therefore, this study aims to address these challenges by providing a justification for selecting an appropriate modeling scheme for hydrocarbon feedstock preparation using supersonic separation.

Review of the research sources and publications

The study of hydrocarbon preparation processes involving supersonic separation technology is rapidly evolving, as reflected in modern scientific publications. The main focus is on modeling this process, optimizing the design of supersonic separators, and integrating them into real technological chains.

In study [1], a Unit Operation Extension (UOE) was developed for use in the HYSYS environment, enabling effective modeling of supersonic separation processes. Specifically, the study examined in detail the processes of dehydration, heavy hydrocarbon fraction removal, and decarbonization in high-carbon-content natural gas.

A similar approach was applied in study [2], where an HYSYS model was developed to simulate the operation of a supersonic separation module. This research proposed a design solution that ensures stable nozzle performance even under varying inlet pressure or gas composition. In particular, it was demonstrated that the system can maintain the dew point with a deviation of no more than ±2.5 °C from the established criteria, even with inlet pressure variations of ±18%. The impact of natural gas composition changes was also analyzed, confirming the system's high stability under such fluctuations. The computational scheme of the supersonic separation process is presented in figure 1.

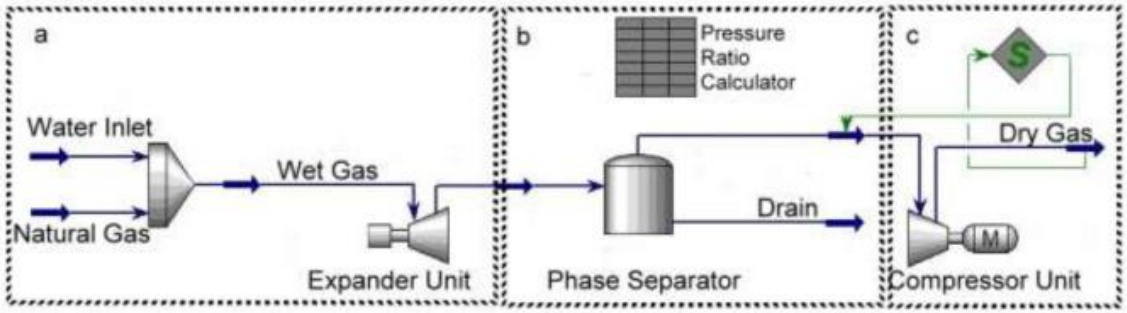

Figure 1 – Calculation scheme

In addition to its use in natural gas dehydration and heavy hydrocarbon removal, supersonic technology has significant potential for industrial application. One of its important applications is decarbonization, i.e. the extraction and utilization of CO2 from gas mixtures with a high carbon concentration, such as natural gas or exhaust gases from internal combustion engines. Effective reduction of CO2 emissions using this technology opens up opportunities not only to reduce environmental risks, but also to provide economic benefits through further storage and use of carbon dioxide. Research activities in the field of supersonic separation cover numerous aspects: experimental studies of flow properties, mechanisms of intraphase transition condensation, as well as structural features of devices. In particular, eddy flows [3], diffusion recovery processes [4], dehydration efficiency of separation tubes [5] and optimization of nozzle designs using CFD (computational fluid dynamics) [6] have been studied.

Other examples include the study of methods for modeling such processes using software such as UniSim Design [7] and HYSYS [8], which allow for increased accuracy in estimating the efficiency of separation tubes at the design stage. In [9], a one-dimensional model of a supersonic tube was proposed, which significantly reduces the computational complexity during the initial design.

Definition of unsolved aspects of the problem

Although substantial advancements have been made in this field, a range of persistent challenges continues to demand attention. One notable issue is the heavy reliance of the technology on accurate modeling to achieve optimal performance. Currently, there is an absence of a clearly established or universally accepted computational framework capable of adequately representing the complexities involved in the supersonic separation process. This gap highlights the pressing need for more focused and in-depth research efforts to address these limitations and enhance our understanding in this area.

Problem statement

The operation of the separation equipment can be simulated using modern software. However, since the 3S separator is a non-standard separation equipment, it is necessary to substantiate the model of the supersonic separation process by comparing the simulation results for different model variants.

Basic material and results

The literature review examined various schemes used for simulation. Two main schemes for simulating the 3S separator process were selected for comparison (Fig. 2, 3).

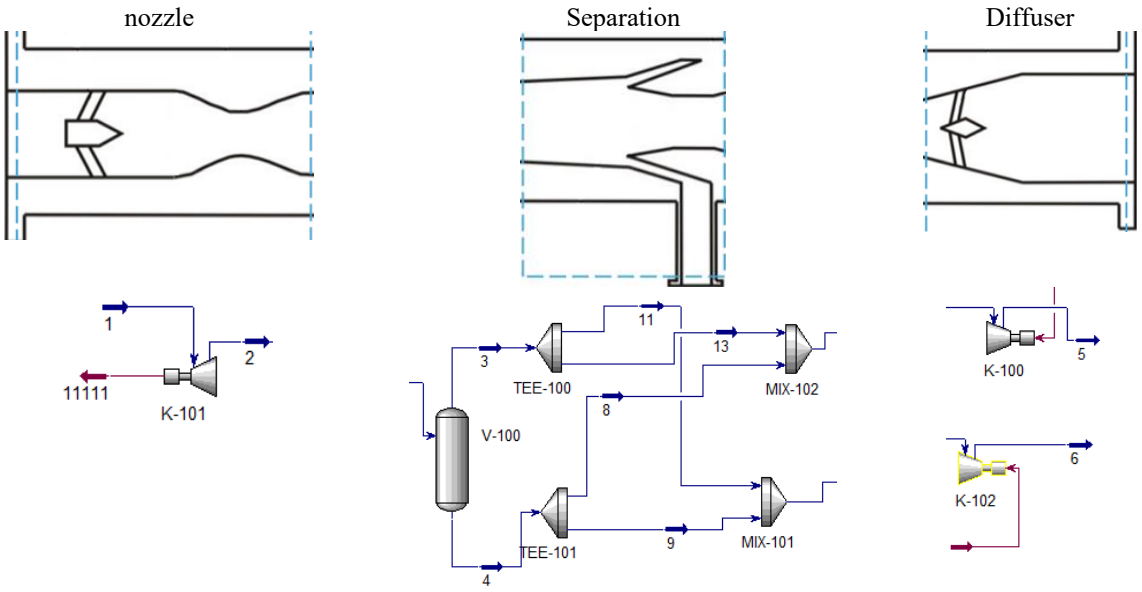

Figure 2 – Equivalent circuit of a supersonic separator in HYSYS (option 1)

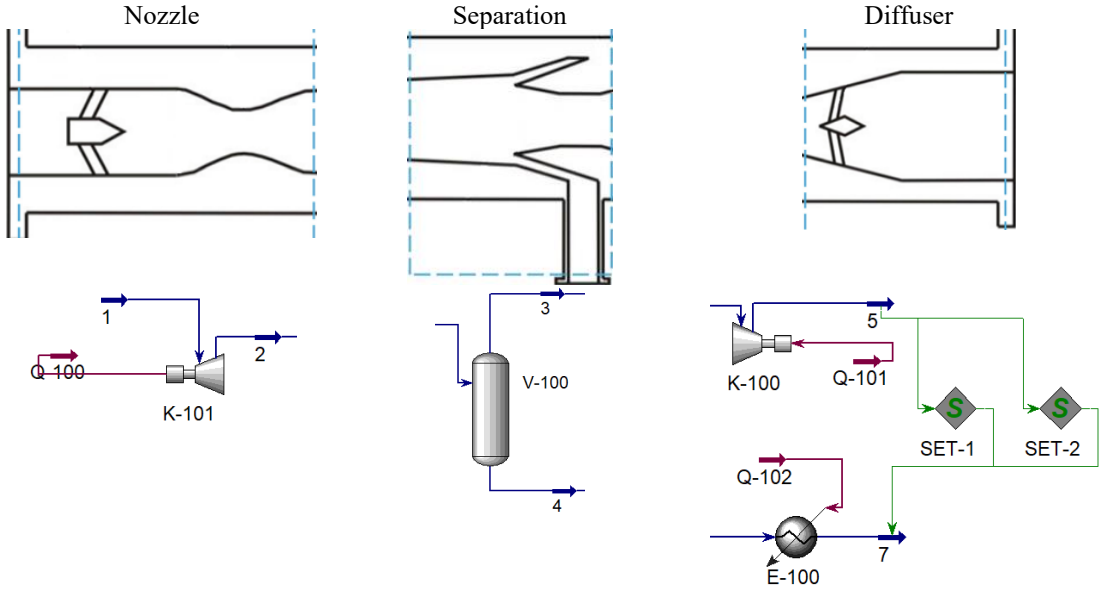

Figure 3 – Equivalent circuit of a supersonic separator in HYSYS (option 2)

The functional stages of liquefaction, separation and diffusion in a supersonic gas separator require replacement by equivalent processes and simplification in the HYSYS software used for modeling.

Particular attention should be paid to the fact that the two separated liquid streams in a real supersonic separator are not completely pure gas or liquid. Therefore, it is necessary to simulate the procedure of redistribution and recombination of these streams in certain proportions in order to reproduce the real efficiency of the supersonic separator as accurately as possible. Subsequently, two redistributed streams are obtained at the output. Based on the principles of operation of the supersonic separator and the functionality of the modules in HYSYS, the following scheme can be considered an optimal equivalent model.

In the first section (nozzle), the compressed gas expands adiabatically, as a result of which the flow velocity reaches supersonic values, and the temperature and pressure decrease sharply. This promotes phase transition and condensation in the target components. The role of this stage is played by the expansion module, which forms the effect of cooling and liquefaction of important components. In the second stage, the formed high-energy gas-liquid flow is directed to the separation section, where the droplets are separated through the side outlet. The equivalence of this phase is ensured by a modular combination of a separator, tees and mixers. After the separation of the two-phase mixture, the dry gas is directed to the diffusion segment, where its speed decreases, and the pressure and temperature increase. In the simulation, this process is reproduced using a compressor module, ensuring the restoration of

the physical parameters of the gas at the end of the diffusion section.

In the process of modeling supersonic separation in HYSYS, several assumptions are introduced to simplify the calculations and more accurately reflect the results.

For physical properties, the Peng-Robinson equation of state (PR EOS) is used, which is suitable for gas preparation. A stable flow regime within the supersonic separator is taken into account as a basic assumption.

The separator throughput is set to 100 kg/h, which exceeds the minimum critical value for stable operation.

For the treatment of humid air, the flow distribution coefficients in the gas-phase and liquid-phase tees are set to 0.7 + 0.3 and 0.32 + 0.68, respectively. In the case of natural gas, these figures change to 0.75 + 0.25 and 0.002 + 0.998.

The flow within the entire separator is assumed to be adiabatic. For equivalent modeling, the adiabatic efficiency of the compressor and expander is set to 99%.

The construction of the equivalent module is aimed at minimizing energy losses due to the impact of shock waves and secondary gasification of condensate.

The pressure and temperature at the outlet of the nozzles are considered critical parameters that have a direct impact on the quality of component separation. Thus, the proposed model in HYSYS allows for a fairly accurate reproduction of the functional stages of a supersonic gas separator and provides the necessary flexibility for laboratory or industrial applications. [5].

The modeling working environment is equipped with all the necessary components to solve the task. It includes raw material components, material and energy flows, technological equipment, process control and regulation tools, as well as logical operations and utilities. The Peng–Robinson equation of state was chosen as the thermodynamic method in the modeling. For the correct implementation of the 3S separator device model using standard tools, it is necessary to reflect three key physical processes occurring in the device: – expansion of the gas input flow with its subsequent cooling; – separation of the resulting gas condensate flow into gas and gas-liquid fractions; – compression of the separated gas flow after separation.

It is also necessary to make a reservation that the software environment gives the most accurate results when modeling equilibrium processes. Since the process occurring in the supersonic separator is non-equilibrium, this method of modeling is considered as a first approximation to the actually occurring processes. To justify the choice of the model type, a study was conducted for weathering gas. The study was conducted for both models. Model options 1, 2 (Fig. 4,5).

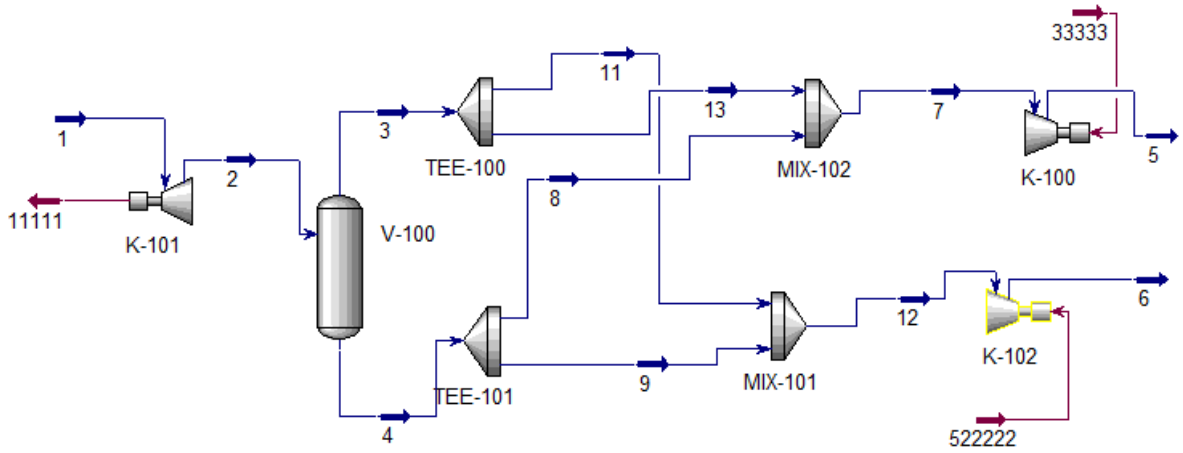

Figure 4– Option 1 of the separation process modeling

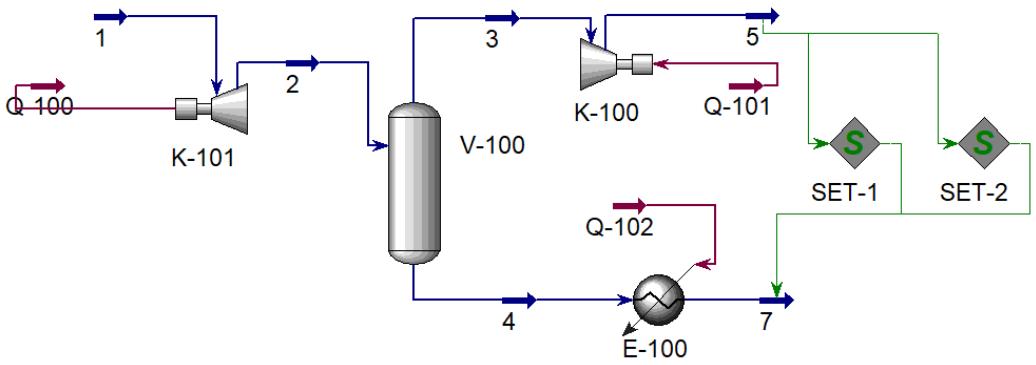

Figure 5 – Option 1 of the separation process modeling

The influence of pressure on the extraction of target components. For the raw material stream, the dependence of the extraction of the C3 + fraction (% wt.) Into the condensed phase of the gas-liquid flow (gas– liquid phase) on the pressure at the inlet to the 3S– separator in the range of 7–15 MPa in 1 MPa increments at a raw material temperature of +10 ° C was studied. The results of the studies for the two options are shown in the

figures 6-9. For options 1 and 2, the data obtained during the study on the dependence of the extraction of the C3 + fraction on the pressure of the raw material allow us to conclude that in the considered pressure range, the extraction of the target components increases non-linearly. At a pressure of 12.5 MPa, the content of the C3 + fractions practically does not change. This is confirmed by Fig. 8, in which the mass of condensate per year, starting from a pressure of 12.5 MPa, almost does not change. The dew point temperature for moisture and hydrocarbons of the extracted gas meets the requirements of the Code of the Gas Transportation System of Ukraine. For all considered raw material flows, the deviation of the graphs from linearity is insignificant. It should also be noted that temperature, unlike pressure, has an anti-battery effect on the yield of the liquefied product. Therefore, it can be stated that both schemes show convergent results, since the nature of the distribution is the same. Further use is possible for both option 1 and option 2. We choose scheme 1 for further modeling, since it has fewer components.

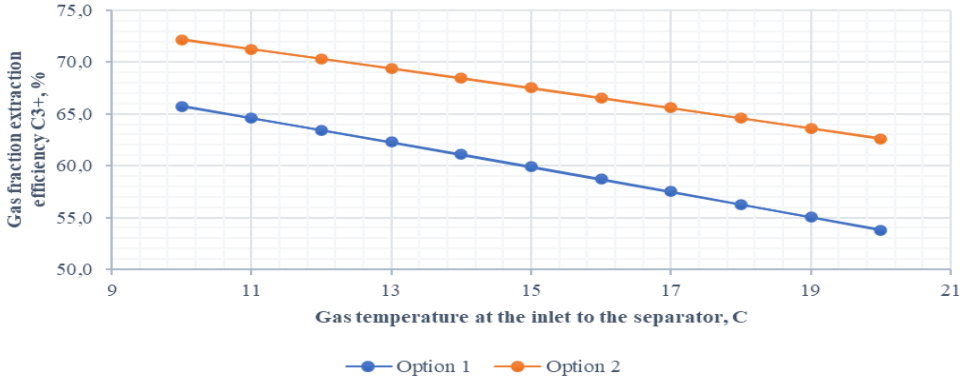

Figure 6 – Extraction of target components C3 + from the pressure at the inlet to the apparatus at P = 10 MPa

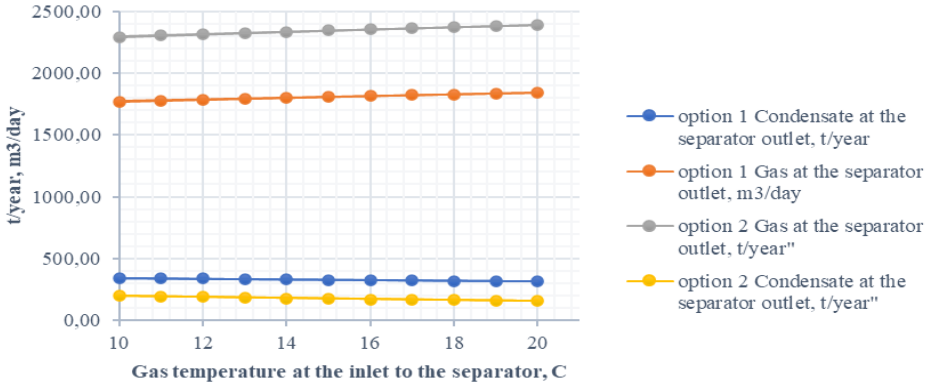

Figure 7 – Gas and condensate extraction at the pressure at the inlet to the apparatus at P = 10 MPa

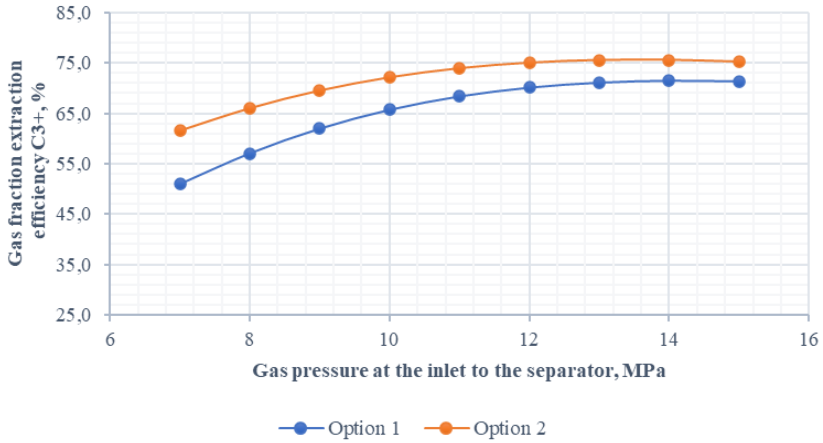

Figure 8 – Extraction of target components C3 + from the pressure at the inlet to the apparatus at Tc = 283 K

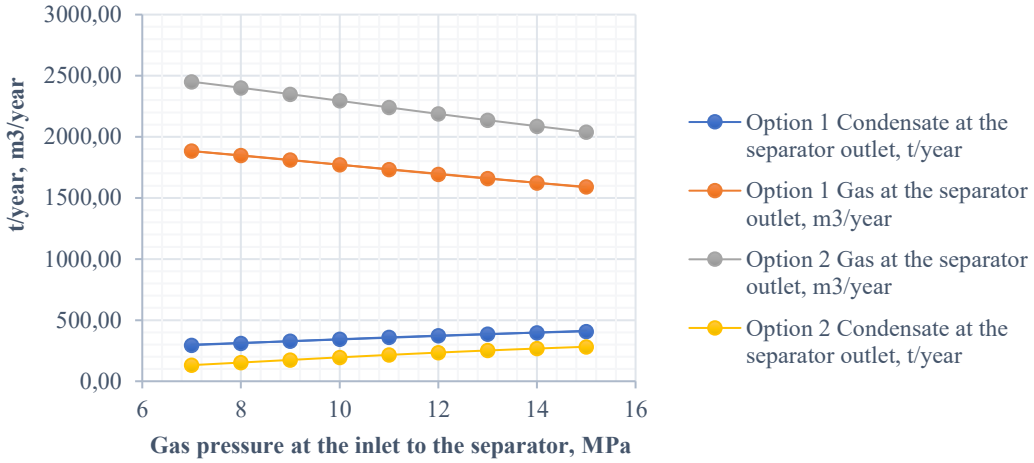

Figure 9 – Gas and condensate extraction at the pressure at the inlet to the apparatus at Tc = 283 K

The object of modeling was chosen as the hydrocarbon preparation system at the gas condensate field. It has a capacity for: gas – 2 million m^3/day, gas condensate – 150 t/day, formation water – 52 t/day.

The component composition of the gas is given in Table 1.

Table 1 − Component composition of hydrocarbons

Name and chemical formula		Component content, % vol.
Methane	CH_4	86,607
Ethane	C_2H_6	5,739
Propane	C_3H_8	1,253
i-Butane	iC_4H_{10}	0,154
n-Butane	$нC_4H_{10}$	0,198
neo-Pentane	$neoC_5H_{12}$	0,007
i-Pentane	iC_5H_{12}	0,063
n-Pentane	$нC_5H_{12}$	0,041
Hexane+higher	C_6H_{14}+	0,204
Oxygen	O_2	0,000
Nitrogen	N_2	0,240
Carbon dioxide	CO_2	4,494

The process of gas and condensate preparation at the installation for further transportation includes: gas collection at the unit of the input threads of the installation; gas separation at the input separators of the first stage, pre-cooling at recuperative heat exchangers (for gas from high-pressure wells) throttling and separation at low-pressure separators of the second stage, heating at recuperative heat exchangers (for gas from high-pressure wells) before feeding into the main gas pipeline; separation of gas condensate from associated formation water from condensate in the dehydrator1; final separation of associated formation water from gas condensate in the dehydrator B-1; degassing of gas condensate in the degasser B-2; final degassing of condensate on the ladder and in condensate storage tanks.

Gas preparation is carried out on two technological lines (high-pressure and low-pressure) with a total design capacity of 2 million m^3/day. Additionally, a measuring technological line with a capacity of 300-600 thousand m^3/day is provided for the performance study of wells.

The gas-water-condensate mixture from the production wells of the gas condensate field is supplied to the unit of the input threads of the installation using gas pipelines-loops, where the technological mode of operation of the "formation-well-loop" system is set using regulating fittings. Also, at the input string node, gas (wells) is distributed into high-pressure and low-pressure technological lines or to a measurement line for performance monitoring.

The gas obtained as a result of the technological process is sent to the commercial metering unit and then transported to the gas pipeline connecting to the main gas pipeline.

The condensate obtained after stabilization to atmospheric pressure and separated from the sub-product water is shipped from the condensate park tanks to tanker trucks.

The associated formation water, which was separated from the condensate as a result of the technological process, is sent via a bypass to the formation water storage tank. The results of the calculation using a supersonic separator are shown in Figure 10.

The figure shows the input parameters of the gas along 3 lines and shows the parameters of the prepared gas, winding gas, condensate and formation water.

The ventilation gas at the installation can be utilized immediately: from the separator of another stage it is directed to the low side of the ejector, from the degasser tank the condensate is sent to the compressor, also when necessary. It is possible to direct the ventilated gas from the separator to another stage and from the degasser tank to the condensate to the compressor or ejector.

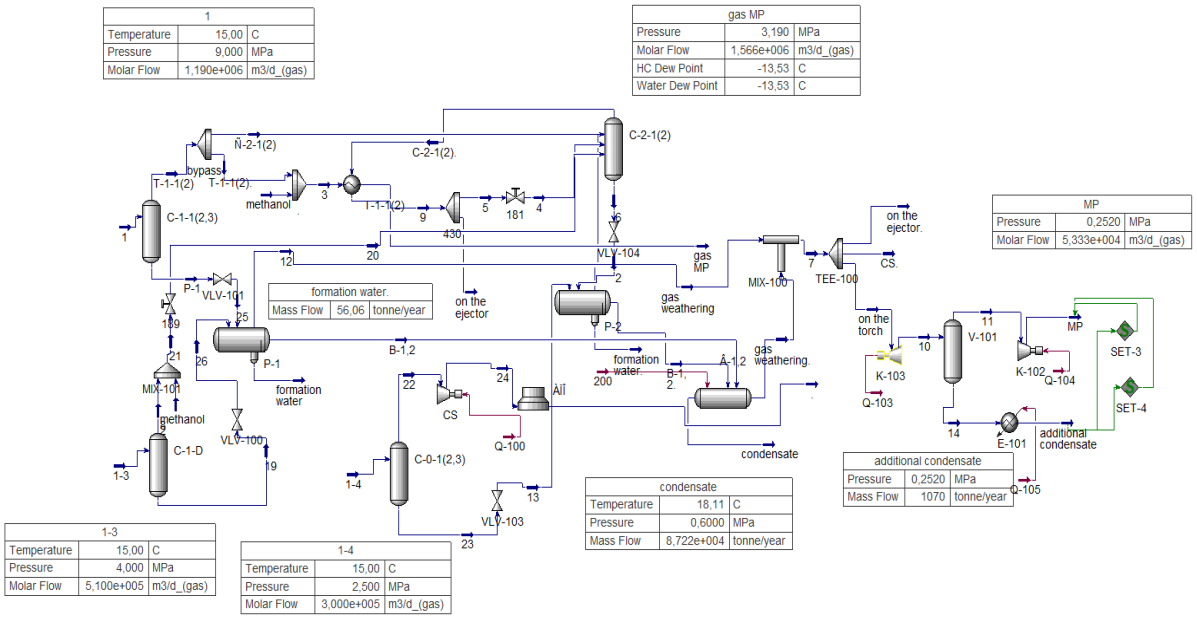

Figure 10 – Equivalent calculation scheme of a complex gas preparation installation

Also, when connecting to the compressor, it is possible to direct the gas supply to the power gas separator. Whenever there is a supply of gas, excess gas from the gas separator is discharged to the flare. It is advisable to install a supersonic separator at the installation, and if there is a presence of winding gas, direct it not to the torch, but to this separator. The results of modeling an improved scheme for the preparation of carbohydrates are shown in Figure 4.3. It can be seen that additional condensate of 1070 t/year was recovered, but not much was recovered, and gas can also be supplied to the supersonic separator, which is sent to the propane refrigeration unit of another gas treatment unit. After supersonic separation of the gas, this gas is determined by the dew point temperatures of the liquid and carbohydrates.

Conclusions

The simulation of the supersonic separation process was performed in the HYSYS environment, which allowed obtaining optimal parameters for the extraction of heavy hydrocarbons from natural gas. The effect of pressure on the efficiency of the separation of target components was studied. Data were obtained that when the pressure was increased to 12.5 MPa, the efficiency of the process increases, however, a further increase in pressure does not provide significant advantages. A comparative analysis of two modeling schemes was carried out, as a result of which the optimal option was selected, which has fewer components and provides sufficient prediction accuracy.

The limitations of existing models were analyzed, in particular their sensitivity to equilibrium assumptions. Using the example of an existing gas preparation plant, it was proven that the use of a supersonic separator contributes to increasing the efficiency of natural gas preparation and additional condensate extraction. The results obtained can be used to further improve natural gas purification technologies and their adaptation to industrial application.

References

1. Niknam, P. H., Mortaheb, H. R., & Mokhtarani, B. (2017). Optimization of dehydration process to improve stability and efficiency of supersonic separation. *Journal of Natural Gas Science and Engineering*, *43*, 90–95. https://doi.org/10.1016/j.jngse.2017.03.017
2. Lai, X.-y., Jiang, W.-m., Chen, J.-n., Ru, Y.-p., Hu, W.-l., & Wang, S.-t. (2021). Process Simulation Investigation of Purification and Deacidification in Supersonic Separation Process for Natural Gas Treatment. У *Proceedings of the International Petroleum and Petrochemical Technology Conference 2020* (с. 266–284). Springer Singapore. https://doi.org/10.1007/978-981-16-1123-0_27

1. Niknam, P. H., Mortaheb, H. R., & Mokhtarani, B. (2017). Optimization of dehydration process to improve stability and efficiency of supersonic separation. *Journal of Natural Gas Science and Engineering*, *43*, 90–95. https://doi.org/10.1016/j.jngse.2017.03.017
2. Lai, X.-y., Jiang, W.-m., Chen, J.-n., Ru, Y.-p., Hu, W.-l., & Wang, S.-t. (2021). Process Simulation Investigation of Purification and Deacidification in Supersonic Separation Process for Natural Gas Treatment. У *Proceedings of the International Petroleum and Petrochemical Technology Conference 2020* (с. 266–284). Springer Singapore. https://doi.org/10.1007/978-981-16-1123-0_27

3. Jiang, W., Bian, J., Wu, A., Gao, S., Yin, P., & Hou, D. (2018). Investigation of supersonic separation mechanism of CO2 in natural gas applying the Discrete Particle Method. *Chemical Engineering and Processing - Process Intensification*, *123*, 272–279. https://doi.org/10.1016/j.cep.2017.11.019
4. Shooshtari, S. H. R., & Shahsavand, A. (2018). Optimal operation of refrigeration oriented supersonic separators for natural gas dehydration via heterogeneous condensation. *Applied Thermal Engineering*, *139*, 76–86. https://doi.org/10.1016/j.applthermaleng.2018.04.109
5. Cao, X., & Yang, W. (2015). The dehydration performance evaluation of a new supersonic swirling separator. *Journal of Natural Gas Science and Engineering*, *27*, 1667–1676. https://doi.org/10.1016/j.jngse.2015.10.029
6. Bian, J., Cao, X., Yang, W., Edem, M. A., Yin, P., & Jiang, W. (2018). Supersonic liquefaction properties of natural gas in the Laval nozzle. *Energy*, *159*, 706–715. https://doi.org/10.1016/j.energy.2018.06.196
7. Machado, P. B., Monteiro, J. G. M., Medeiros, J. L., Epsom, H. D., & Araujo, O. Q. F. (2012). Supersonic separation in onshore natural gas dew point plant. *Journal of Natural Gas Science and Engineering*, *6*, 43–49. https://doi.org/10.1016/j.jngse.2012.03.001
8. Arinelli, L. d. O., Teixeira, A. M., de Medeiros, J. L., & Araújo, O. d. Q. F. (2019). Supersonic separator for cleaner offshore processing of natural gas with high carbon dioxide content: Environmental and economic assessments. *Journal of Cleaner Production*, *233*, 510–521. https://doi.org/10.1016/j.jclepro.2019.06.115
9. Alnoush, W., & Castier, M. (2019). Shortcut modeling of natural gas supersonic separation. *Journal of Natural Gas Science and Engineering*, *65*, 284–300. https://doi.org/10.1016/j.jngse.2019.03.004

3. Jiang, W., Bian, J., Wu, A., Gao, S., Yin, P., & Hou, D. (2018). Investigation of supersonic separation mechanism of CO2 in natural gas applying the Discrete Particle Method. *Chemical Engineering and Processing - Process Intensification*, *123*, 272–279. https://doi.org/10.1016/j.cep.2017.11.019
4. Shooshtari, S. H. R., & Shahsavand, A. (2018). Optimal operation of refrigeration oriented supersonic separators for natural gas dehydration via heterogeneous condensation. *Applied Thermal Engineering*, *139*, 76–86. https://doi.org/10.1016/j.applthermaleng.2018.04.109
5. Cao, X., & Yang, W. (2015). The dehydration performance evaluation of a new supersonic swirling separator. *Journal of Natural Gas Science and Engineering*, *27*, 1667–1676. https://doi.org/10.1016/j.jngse.2015.10.029
6. Bian, J., Cao, X., Yang, W., Edem, M. A., Yin, P., & Jiang, W. (2018). Supersonic liquefaction properties of natural gas in the Laval nozzle. *Energy*, *159*, 706–715. https://doi.org/10.1016/j.energy.2018.06.196
7. Machado, P. B., Monteiro, J. G. M., Medeiros, J. L., Epsom, H. D., & Araujo, O. Q. F. (2012). Supersonic separation in onshore natural gas dew point plant. *Journal of Natural Gas Science and Engineering*, *6*, 43–49. https://doi.org/10.1016/j.jngse.2012.03.001
8. Arinelli, L. d. O., Teixeira, A. M., de Medeiros, J. L., & Araújo, O. d. Q. F. (2019). Supersonic separator for cleaner offshore processing of natural gas with high carbon dioxide content: Environmental and economic assessments. *Journal of Cleaner Production*, *233*, 510–521. https://doi.org/10.1016/j.jclepro.2019.06.115
9. Alnoush, W., & Castier, M. (2019). Shortcut modeling of natural gas supersonic separation. *Journal of Natural Gas Science and Engineering*, *65*, 284–300. https://doi.org/10.1016/j.jngse.2019.03.004

Зміст

CONTENTS